KFA

KERNFORSCHUNGSANLAGE JÜLICH GmbH

Projektleitung Energieforschung
International Energy Agency IEA

Implementing Agreement for Co-Operation in the Development of Large Scale Wind Energy Conversion Systems

Second Meeting of Experts - Control of LS-WECS and Adaption of Wind Electricity to the Network

Organised by
Project Management for Energy Research (PLE)
of the Nuclear Research Establishment Jülich (KFA)
on behalf of the
Federal Minister of Research and Technology

Jül - Spez - 40
Juli 1979
ISSN 0343-7639

Als Manuskript gedruckt

Spezielle Berichte der Kernforschungsanlage Jülich - Nr. 40

Projektleitung Energieforschung Jül - Spez - 40

Zu beziehen durch: ZENTRALBIBLIOTHEK der Kernforschungsanlage Jülich GmbH,
Jülich, Bundesrepublik Deutschland

Implementing Agreement for Co-Operation in the Development of Large Scale Wind Energy Conversion Systems

Second Meeting of Experts - Control of LS-WECS and Adaption of Wind Electricity to the Network

Organised by
Project Management for Energy Research (PLE)
of the Nuclear Research Establishment Jülich (KFA)
on behalf of the
Federal Minister of Research and Technology

Scientific Coordination:
R. Meggle (MBB München) and R. Windheim (PLE KFA)

CONTENTS

Experiences with the 200 keV GEDSER wind turbine induction generation scheme

by

C.J. Christensen, Risø

Talk held at the
meeting on control of LS-WECS and adaption of
wind electricity to the network
of the
expert committee on the Development of Large-
Scale Wind Energy Conversion Systems.

Copenhagen, April 3rd 1979.

The full text of this paper was not available.

GEDSER MILL

3 wings (stiff, stall regulated)

Induction generator

Slip 1% at 200 kW

Transmission: 2-step chain drive

Rotor speed 0.5 rps

Generator speed 12.5 rps

Automatic on grid

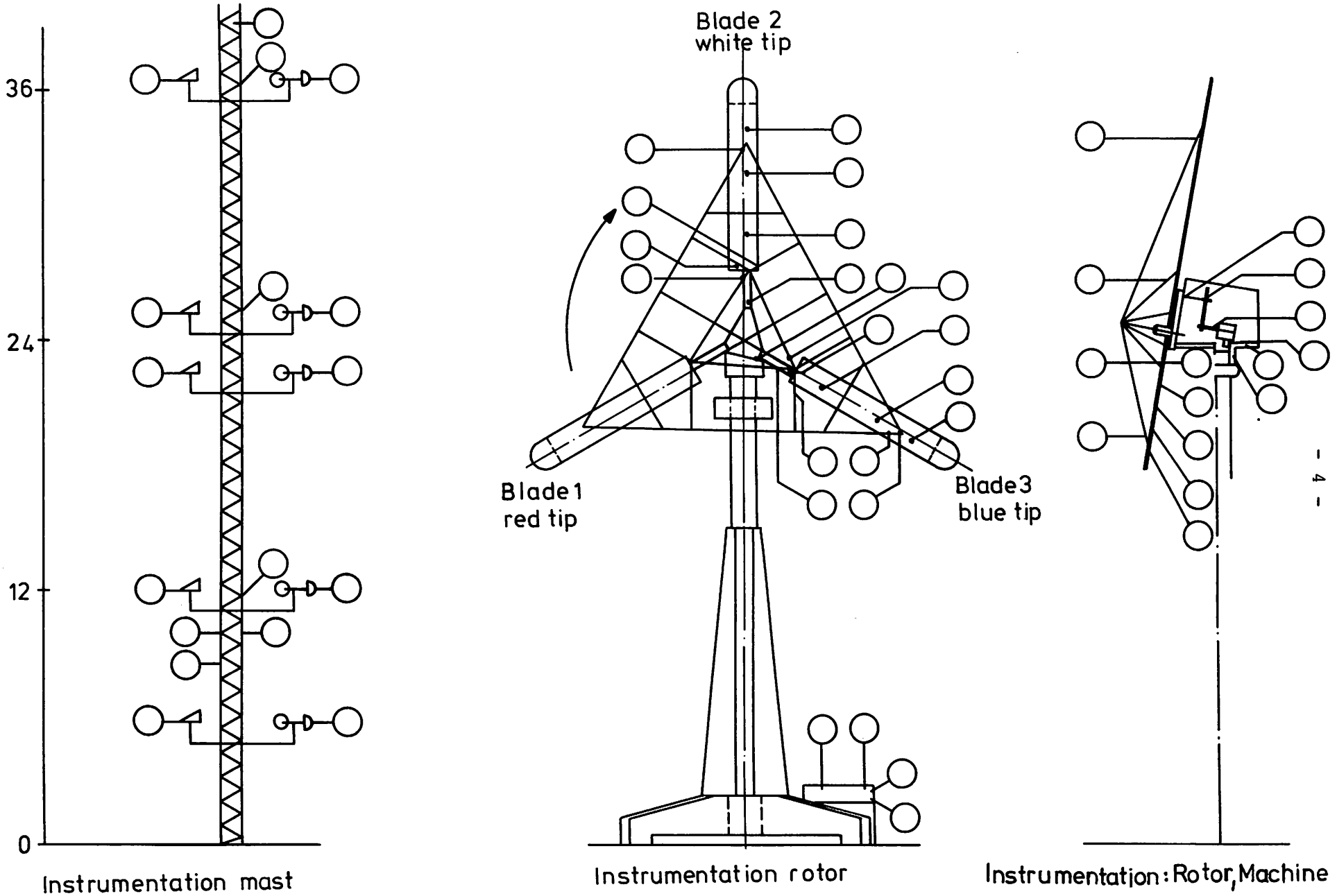

○ SENSOR LOCATIONS FOR THE ENTIRE INSTRUMENTATIONS. SCHEMATIC

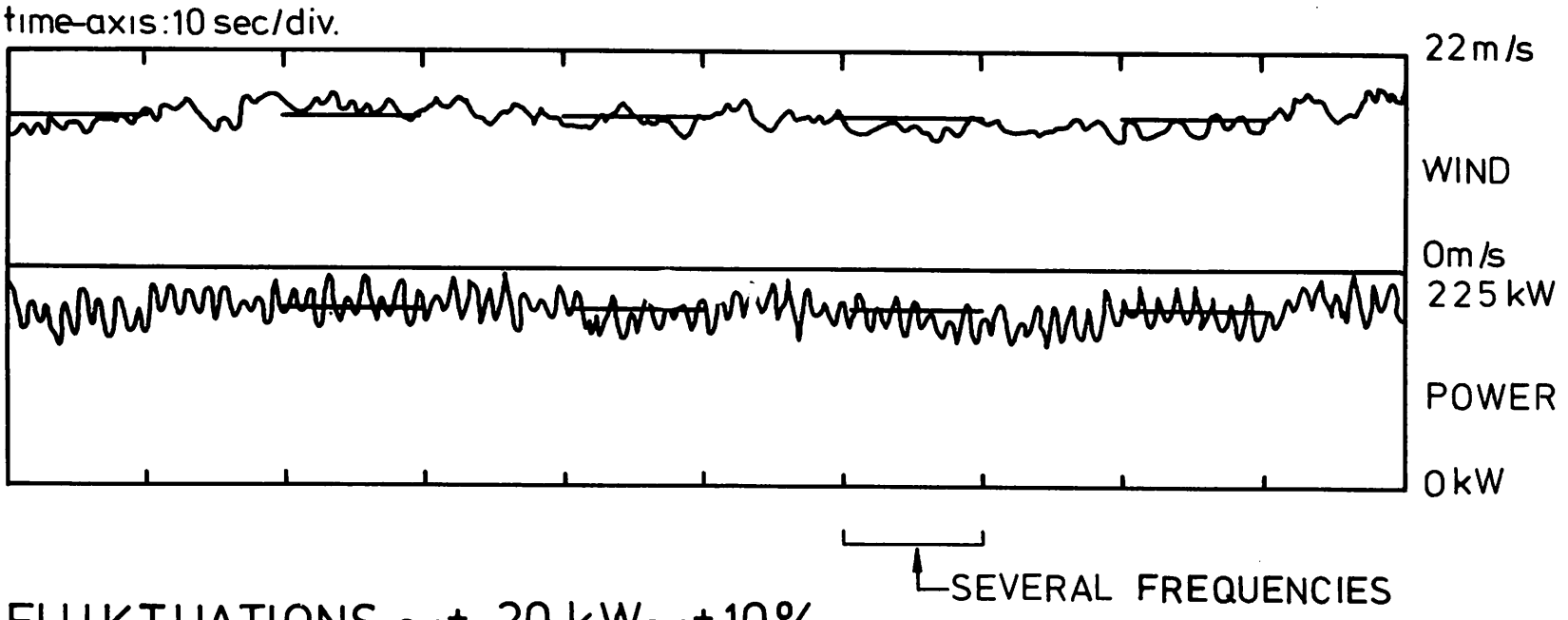

FLUKTUATIONS ~± 20 kW~±10%

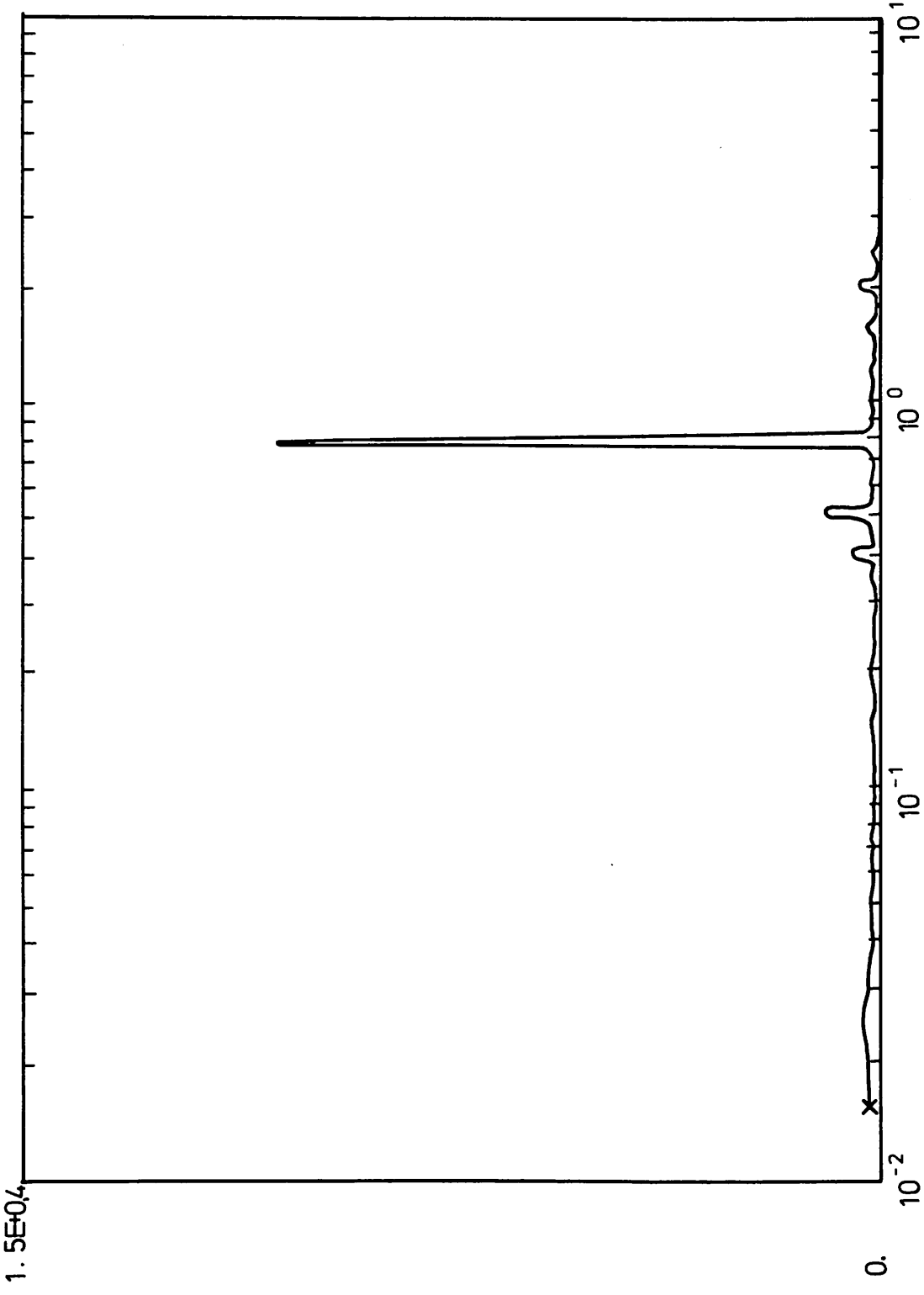

POWER,FREQUENCY SPECTR.(HIGH WIND)

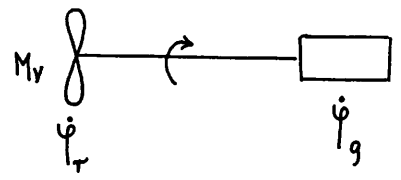

$$s = \frac{\dot\varphi - \omega_0}{\omega_0}$$

$$M_V = I\,\ddot\varphi_r + M_r ; \qquad M_r = K_\downarrow\,(\varphi_r - \varphi_g)$$

$$\boxed{\frac{M_V}{\omega_0} = I\left[\frac{\ddot M_r}{K\omega_0} + \dot s_g\right] + \frac{M_r}{\omega_0}} \leftarrow \frac{\dot M_r}{\omega_0} = K\,(s_r - s_g)$$

Assume: $M_r = A_c \cdot s_g$

A_c complex, indep. of t.

$$\boxed{\ddot s_g + \frac{k\,\omega_0}{A_c}\,\dot s_g + \frac{K}{I}\,s_g - \frac{M_V}{I A_c}\,K = 0}$$

Assume: $M_V = e^{i\omega t}$; $s_g = H(\omega)\,e^{i\omega t}$

$$H(\omega) = \frac{1/A_c}{\left(1 - \frac{\omega^2}{\omega_r^2}\right) + i\,\frac{\sqrt{kI}}{A_c}\,\omega_b\,\frac{\omega}{\omega_r}}$$

So equ. is solved for single by $s_g = H(\omega)\,M_V$

For RANDOM M_V: It can be shown, that

$$s_{sg} = H(\omega)\,S_{M_V}$$

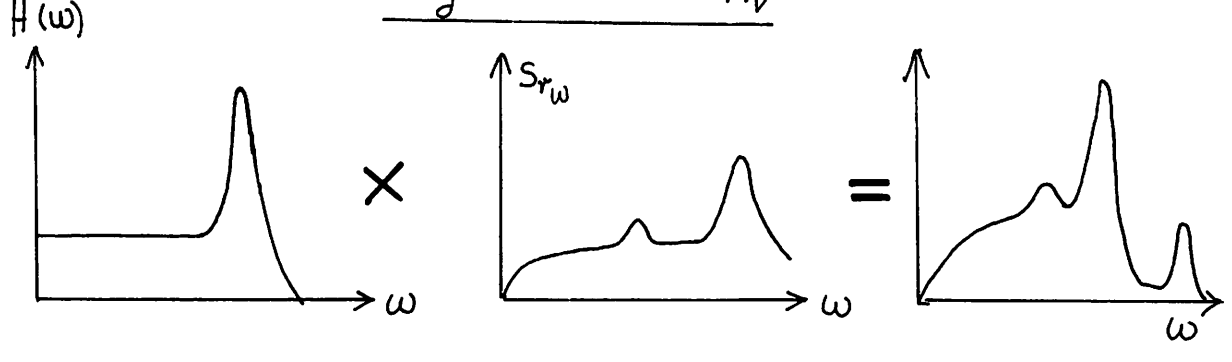

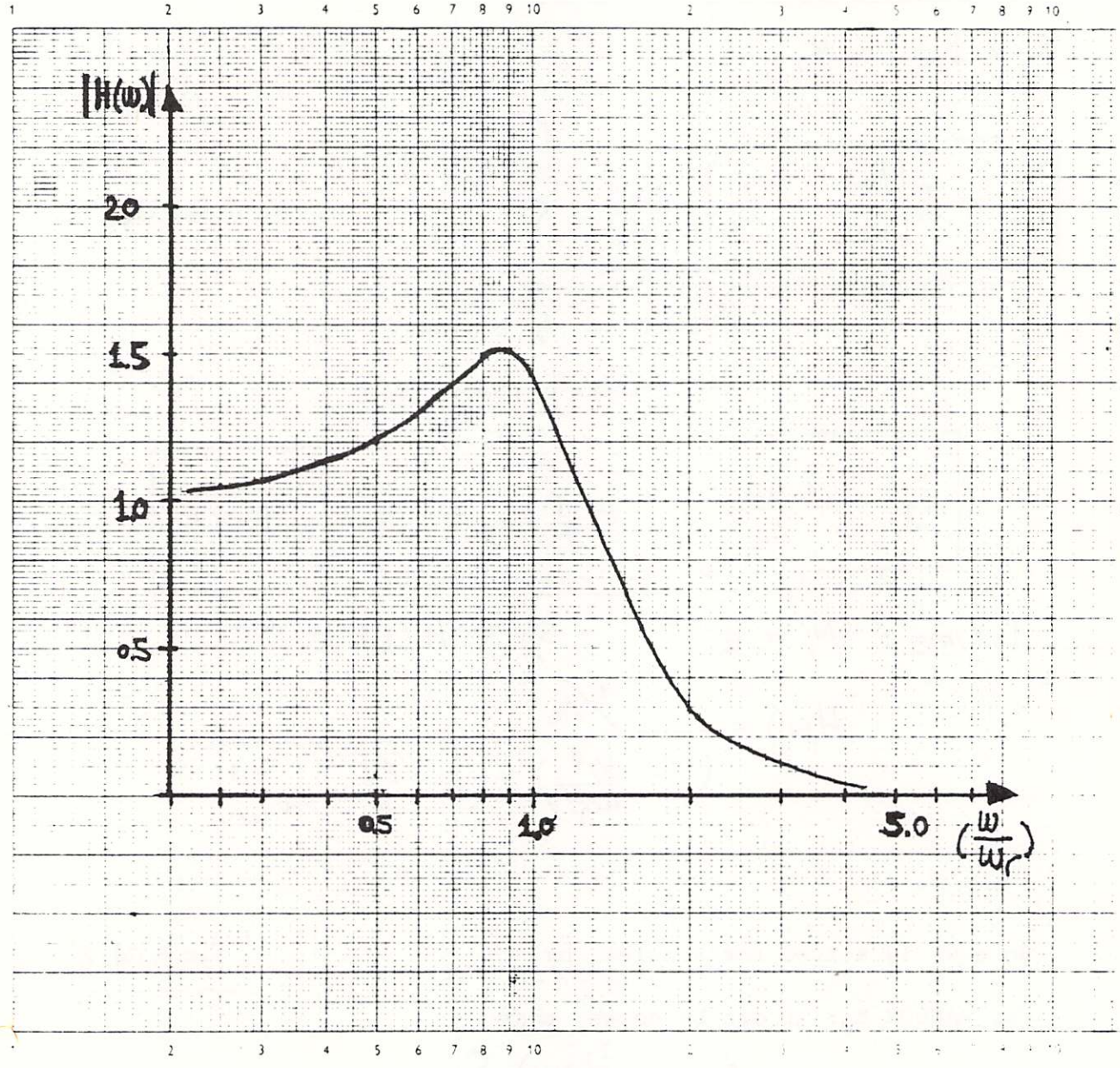
|H(ω)|
2.0
1.5
1.0
0.5
0.5
1.0
5.0
(ω/ω_r)

$S_s = H(\omega) \cdot S_M$ implies 2 resonance mech.:

1) inherent (born) in model $H(\omega)$

2) imposed from outside S_M

peak widths:

type 1) determined by model equation
(here by $\frac{I \omega_o}{A_c}$ if A_c real)

type 2) transfered as imposed

Another categorization:

A1) stemming from differential equation like above model

A2) stemming from periodic disturbing force

Type A2 only interesting for constant speed wind turbines, where peaks will be sharp and well defined, and often of constant strength under all conditions.

Type A2 will often be triggered by imposed random disturbances, like turbulence

Example next: Power spectra
high VS. low wind speed

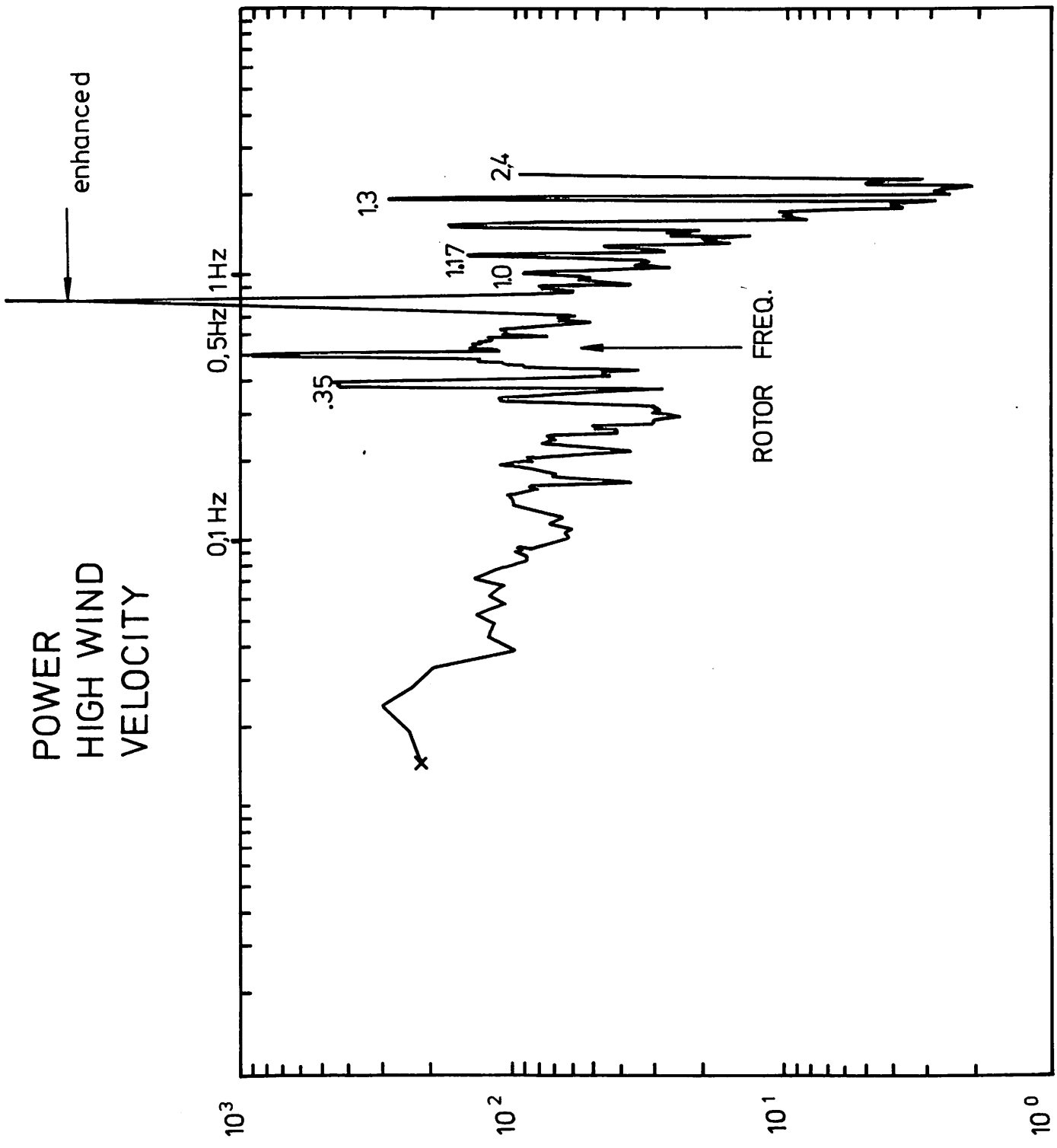
POWER
HIGH WIND
VELOCITY
enhanced
1 Hz
0,5Hz
0,1 Hz
1.3
2.4
1.17
1.0
.35
ROTOR FREQ.
10^{-3}
10^{-2}
10^{-1}
10^{0}

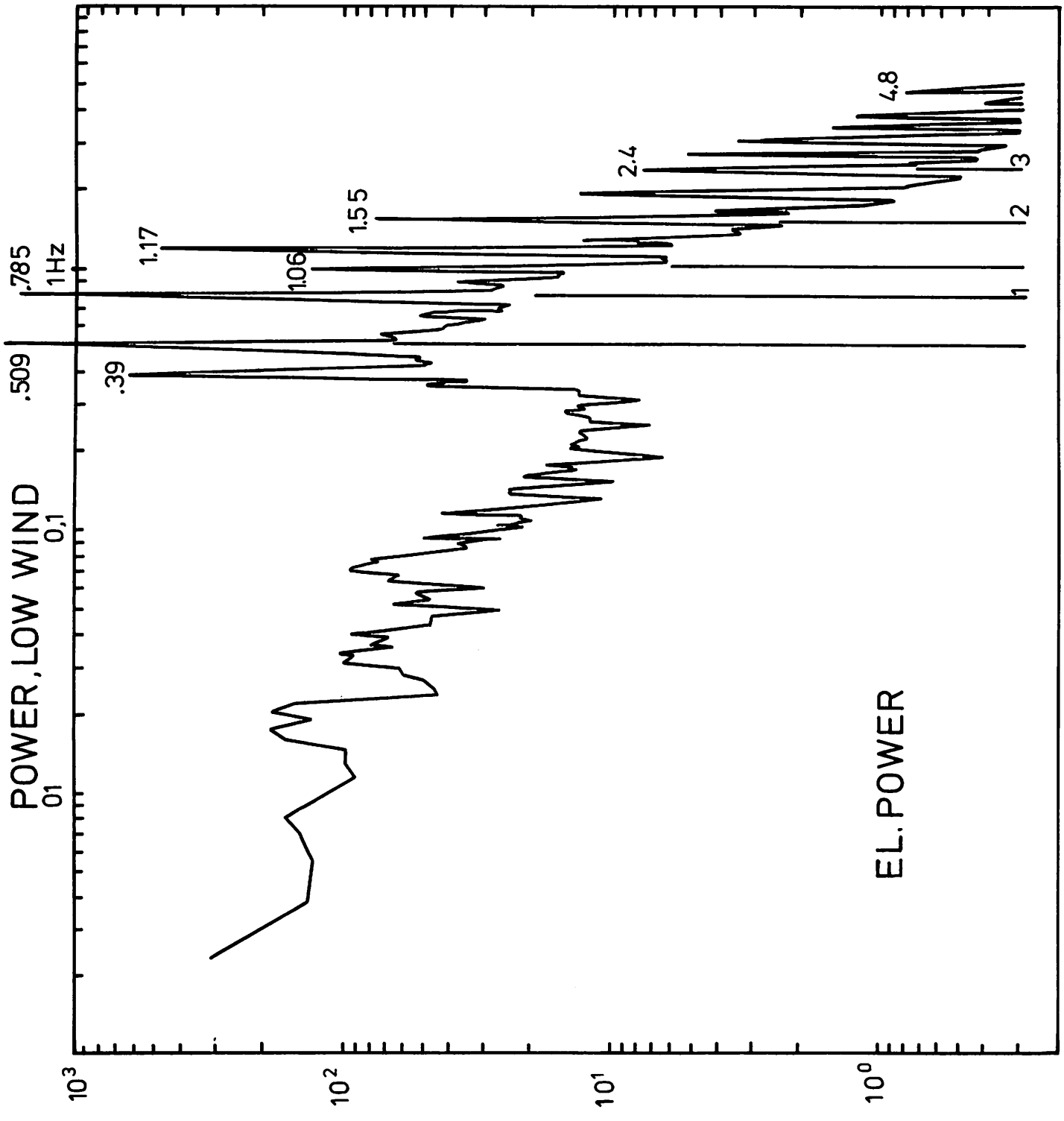
POWER, LOW WIND
01
0,1
.509
.785
1Hz
.39
1.17
1.06
1.55
2.4
4.8
1
2
3
EL. POWER
10^3
10^2
10^1
10^0

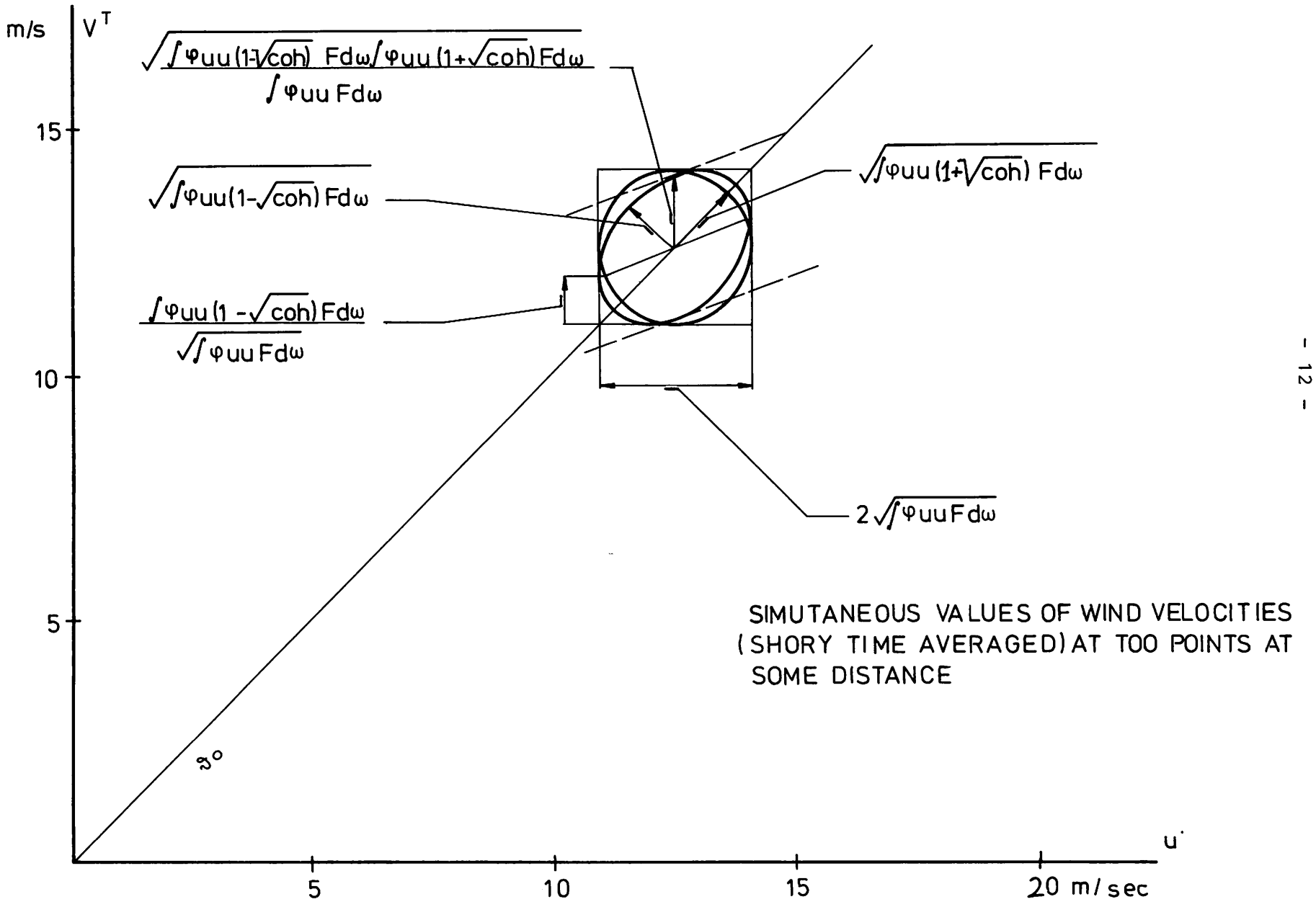
m/s
V^T
$\sqrt{\int \varphi_{uu}(1-\sqrt{coh})\,Fd\omega \int \varphi_{uu}(1+\sqrt{coh})\,Fd\omega}$ / $\int \varphi_{uu} Fd\omega$
$\sqrt{\int \varphi_{uu}(1+\sqrt{coh})\,Fd\omega}$
$\sqrt{\int \varphi_{uu}(1-\sqrt{coh})\,Fd\omega}$
$\int \varphi_{uu}(1-\sqrt{coh})\,Fd\omega$ / $\sqrt{\int \varphi_{uu} Fd\omega}$
$2\sqrt{\int \varphi_{uu} Fd\omega}$
45°
15
10
5
5
10
15
20 m/sec
u
SIMUTANEOUS VALUES OF WIND VELOCITIES (SHORY TIME AVERAGED) AT TOO POINTS AT SOME DISTANCE

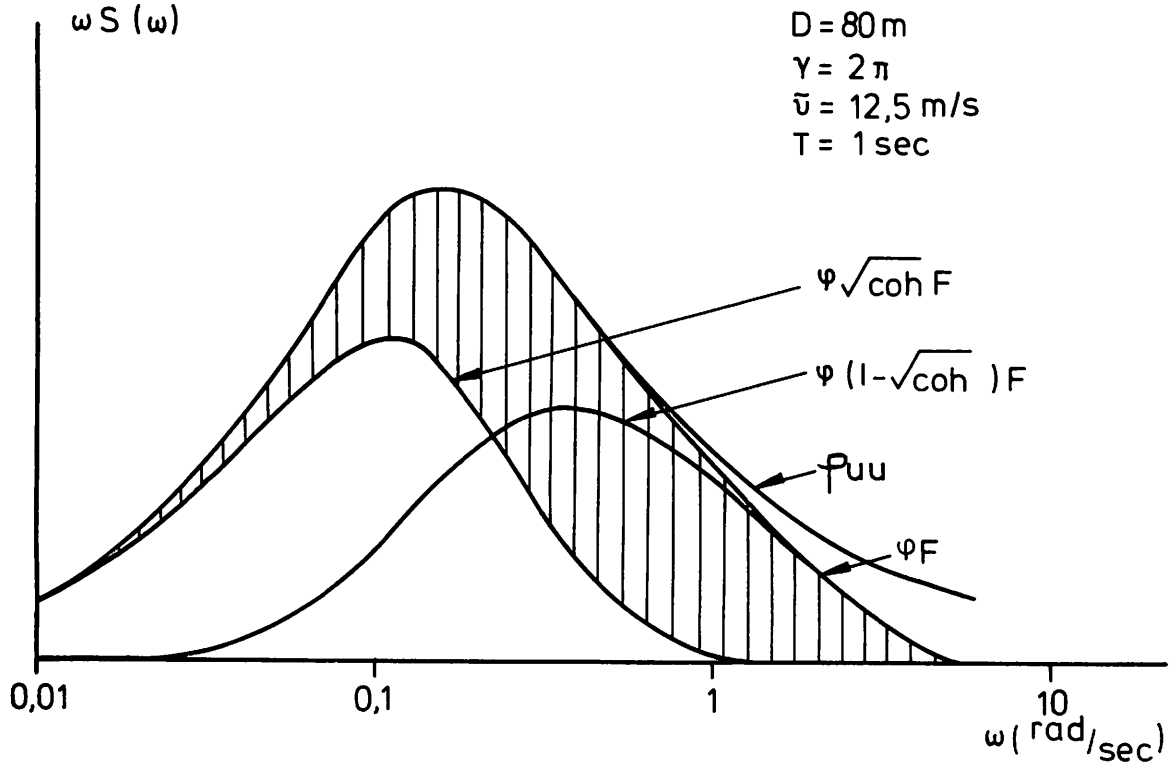

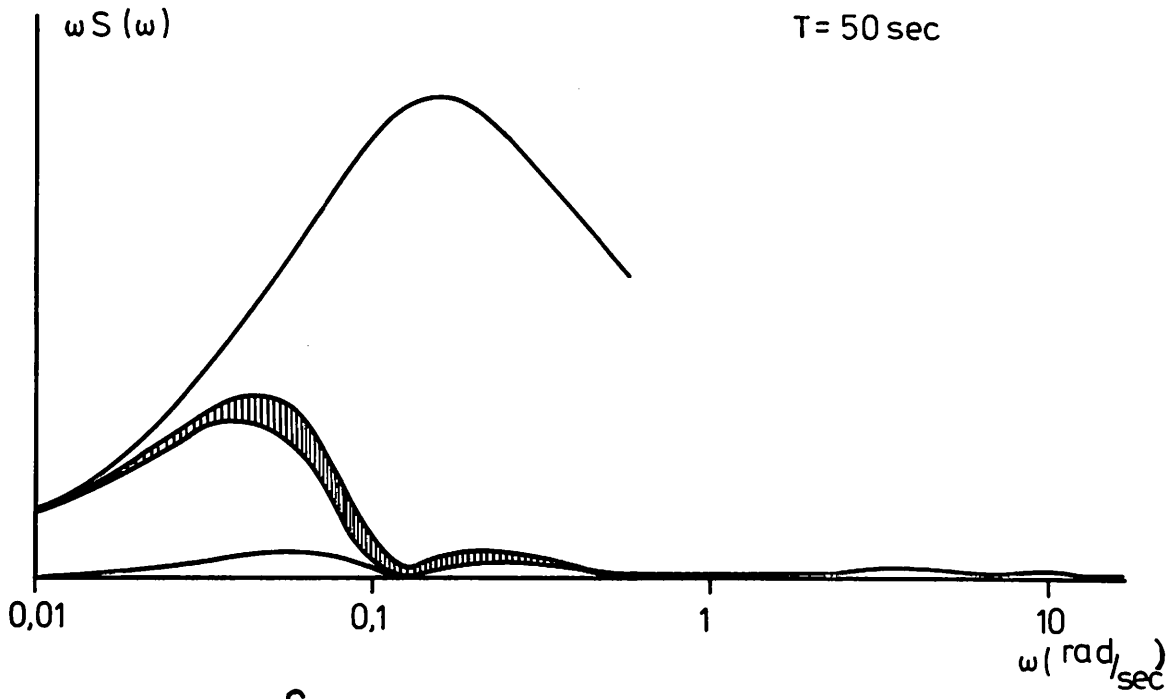

coh ~ 0: $(\sigma_v\ Tu)^2 \sim \int \phi uu\ F d\omega$

-- ~ 1: $(\sigma_v\ Tu)^2 \sim 2 \int \phi uu\ (1-\sqrt{coh})\ F d\omega$

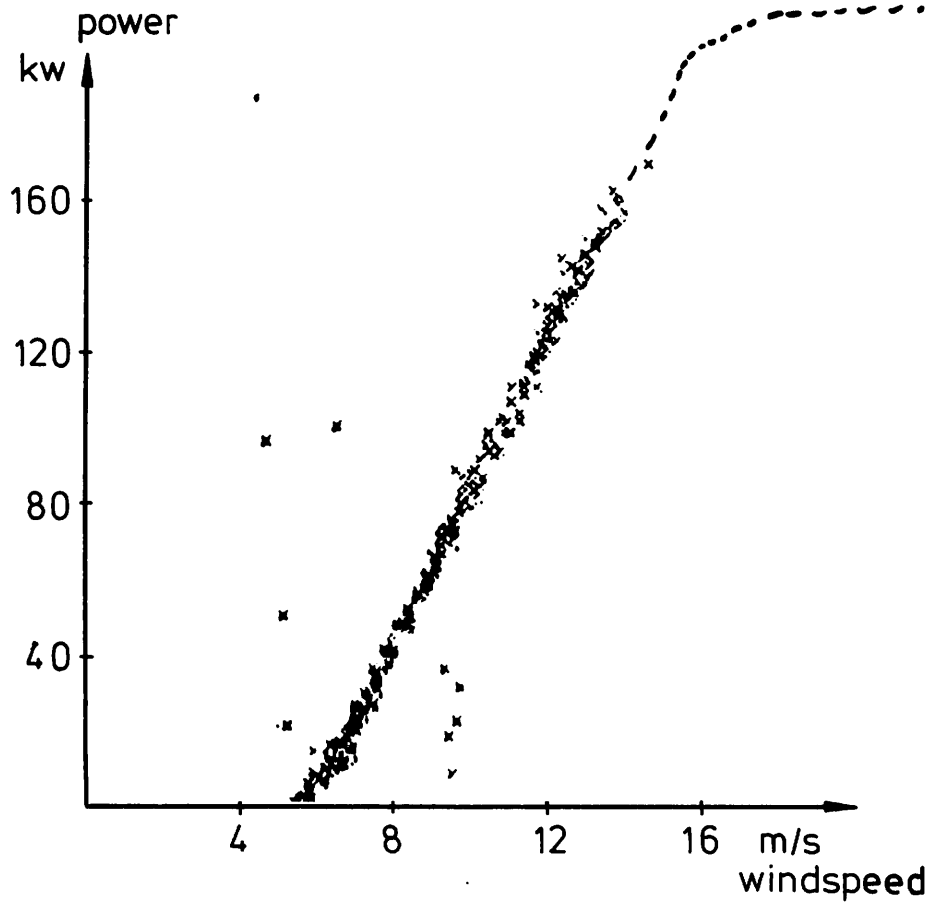

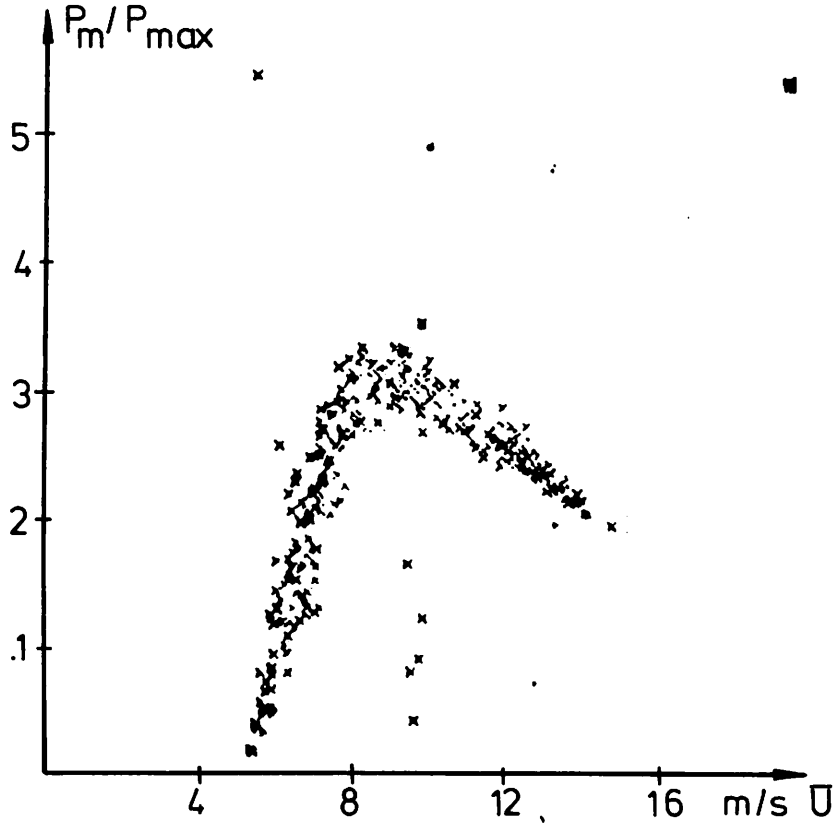

Power curve and efficiency for windspeeds up to ~ 14 m/s based on block averaged data (10MIN AV.)

A. JENSEN (Elkraft)

The electrical generation system for the 630 kW Nibe wind turbines

High-voltage distribution system

The electrical system has been designed with two generator-transformers, one for each unit, and a common transformer for the supply of anxilliary power for the two plants. The principle is shown in fig. 1.

As can be seen from fig. 1, there are three fields in unit A, one is used for the cable connection to the 20 kV grid, with surge arrestors and current- and voltage transformers for kWh-meters for total production and consumption. In the next field the cable to the anxilliary transformer is connected via withdrawable isolators with fuses. In this field too, the 20 kV-cable to unit B is connected. The third field contains the generatorbreakers, and current- and voltage transformers for the protection system. The breakers are of the SF_6 type.

These three fields, the generatortransformer and the anxilliary transformer are situated in a room separated by explosion-proof concrete walls and roof to safeguard against the consequences of possible transformer failure.

The lay-out of this room is shown on fig. 2 (unit A) and fig. 3 (unit B).

Low-voltage distribution system

Fig. 4 shows among other things the low-voltage distribution system. This consists of a total of four subsystems, two for each unit. Each unit has a subsystem in the bottom of the tower (i.e. 1st floor) and a subsystem in the nacelle. The subsystem in the bottom of the tower supplies power to the normal lighting system and via a 24 battery with charger

to the emergency lighting system. Furthermore anxilliary power to the relay protection, as well as power outlets for a welding transformer. Finally of course power to the sub-systems in the nacelle is taken from the "bottom" system.

The low-voltage distribution system in the nacelle supplies power to the electric motors in the hydraulic system, the µ-processor based control system, the fire protection system, the heating and ventilation system, and the lighting system. In the nacelle too, there are power outlets for welding transformers and other tools necessary for servicing the equipment in the nacelle.

Relay protection system

The generator and the generatortransformer are protected against electrical faults by a conventional relay protection system. The system protects against: thermal overload, short-circuits, over-voltage, under-voltage, negative sequence currents, earth-faults and reverse power from the grid.

Control system

The control system of the units are µ-processor based. In each nacelle is housed in a cubicle, the complete control system. Each control system controls and operates the following systems:

1) Blade-pitch angle

2) Yaw-movements

3) The generator-breaker.

In case of failure, the unit is shut-down automatically and an alarm is given, both on a display in the unit and via the remote grid-control system.

Communication and telephone system

The units are connected to the public telephone system, and telephones are placed in both units in the "bottom" of the tower and in the nacelle. Furthermore an intercom-system provides communication between the tower and the nacelle to ease operations during service and maintenance.

The units can be controlled from a controlroom situated in the southern part of Ålborg, about 15 kilometers away. From here commands can be given to start and stop the units i.e. put the µ-processor system in operation mode or vice versa. Also the generatorbreakers positions are shown, and 4 alarms are displayed in the controlroom.

Operation modes

The unit are designed for unattended operations utilising the automatic control system. The control system has four operating modes:

1."Cold shutdown"

2."Hot " "

3. Operation mode (available for powerproduction)

4."Emergency"shutdown

In mode 1, all systems are inoperative.

In mode 2, the yaw system is in operation to keep the nacelle in the direction of the wind.

In mode 3, the yaw system as well as all other systems are in operation.

Depending on the wind velocity the unit will generate power or will stand still. Mode 3 is the normal operation mode.

In case of failure in some system the operation mode is automatically changed to 4. Here all attempts to restart the unit are blocked, and a signal is given to the grid-control center in Ålborg.

In case of failure on the yaw system, the unit goes in mode 1.

Connection of tower and nacelle

The electrical connection of components in the tower with components in the nacelle is provided by cables, arranged so that the bundle can turn app. ± 4 turns from neutral. The numbers of turns is controlled by the µ-processor.

HIGH - VOLTAGE DISTRIBUTION

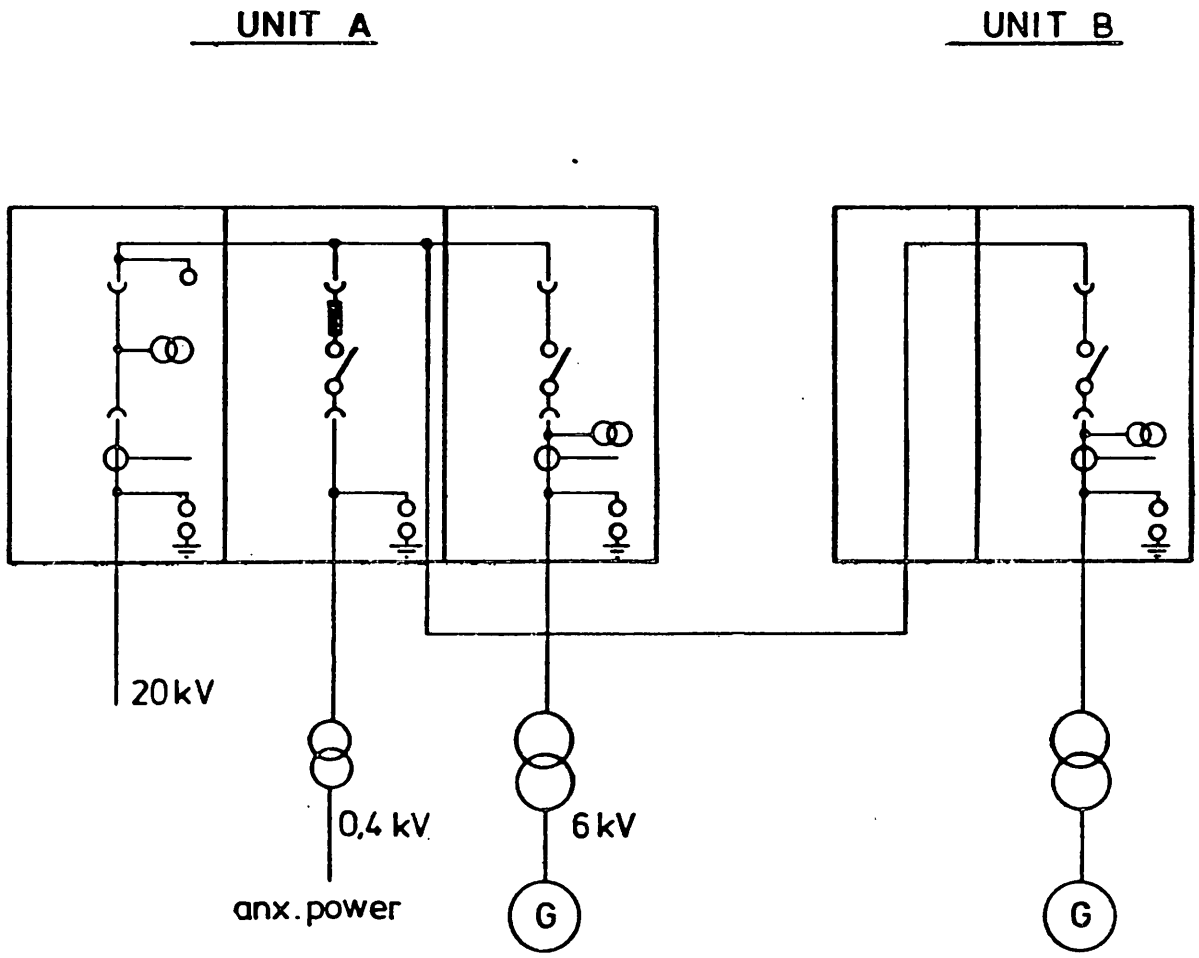

fig. 1

UNIT A

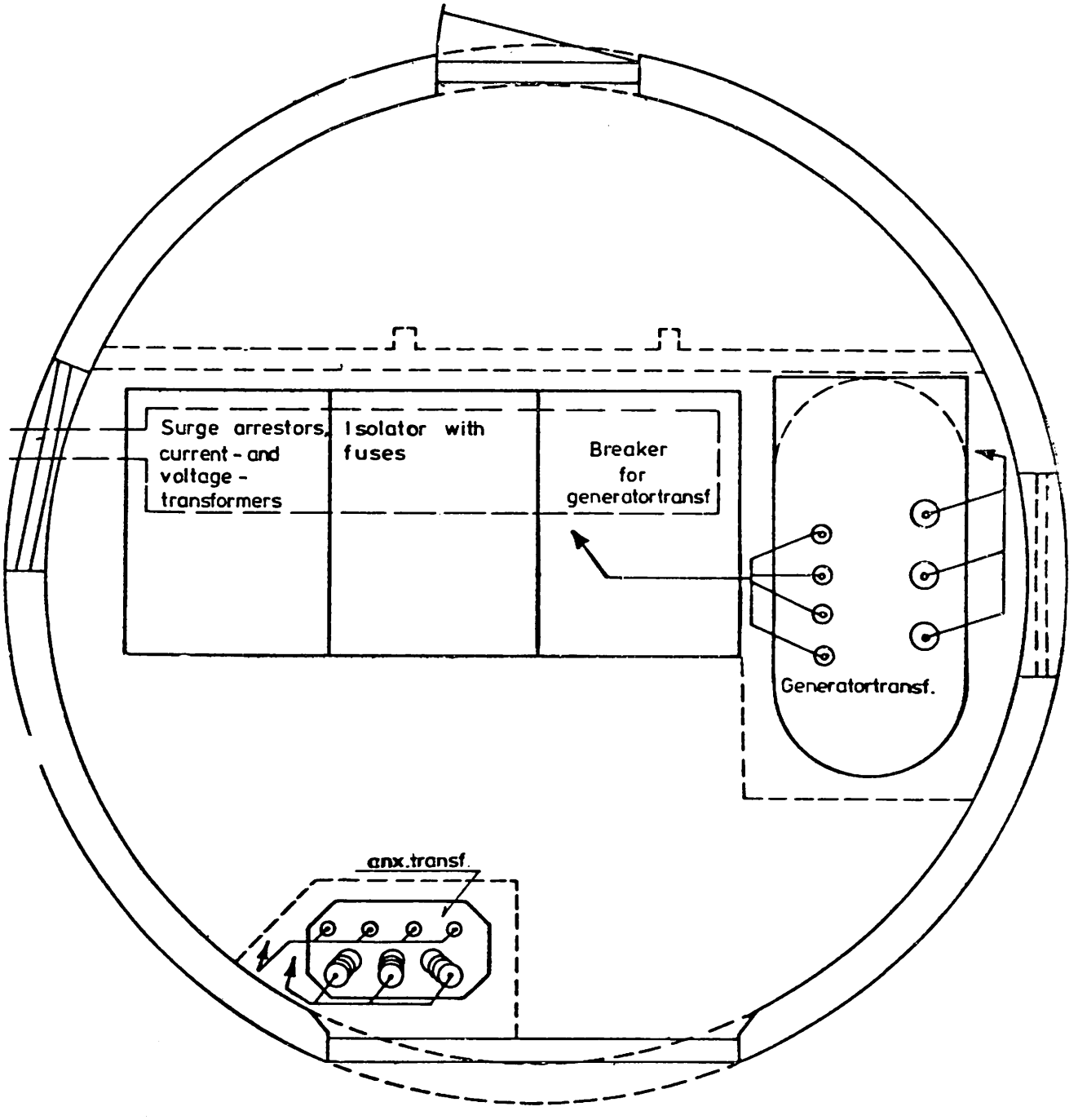
Surge arrestors, current - and voltage - transformers
Isolator with fuses
Breaker for generatortransf
Generatortransf.
anx.transf.

fig. 2

UNIT B

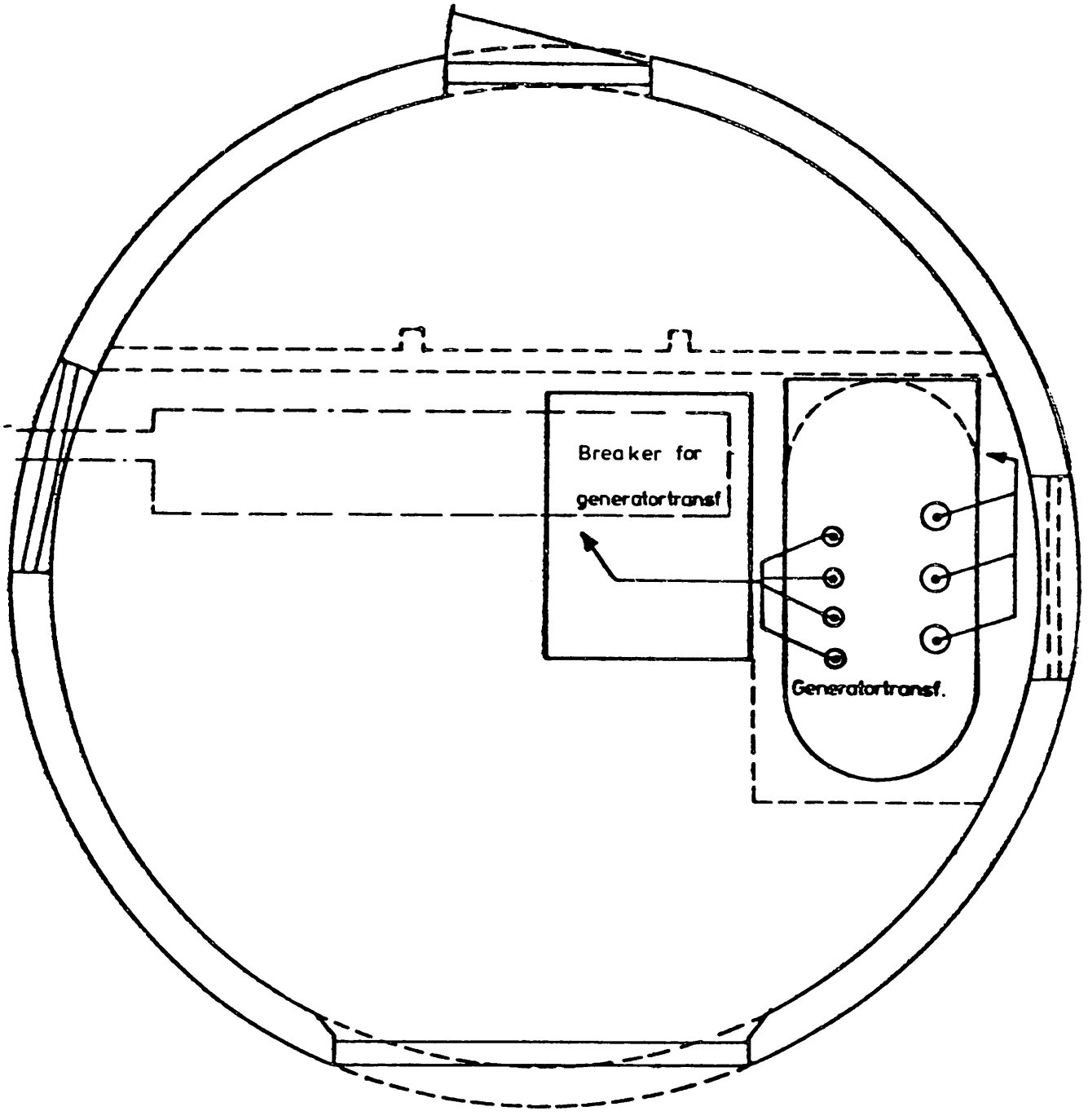

fig. 3

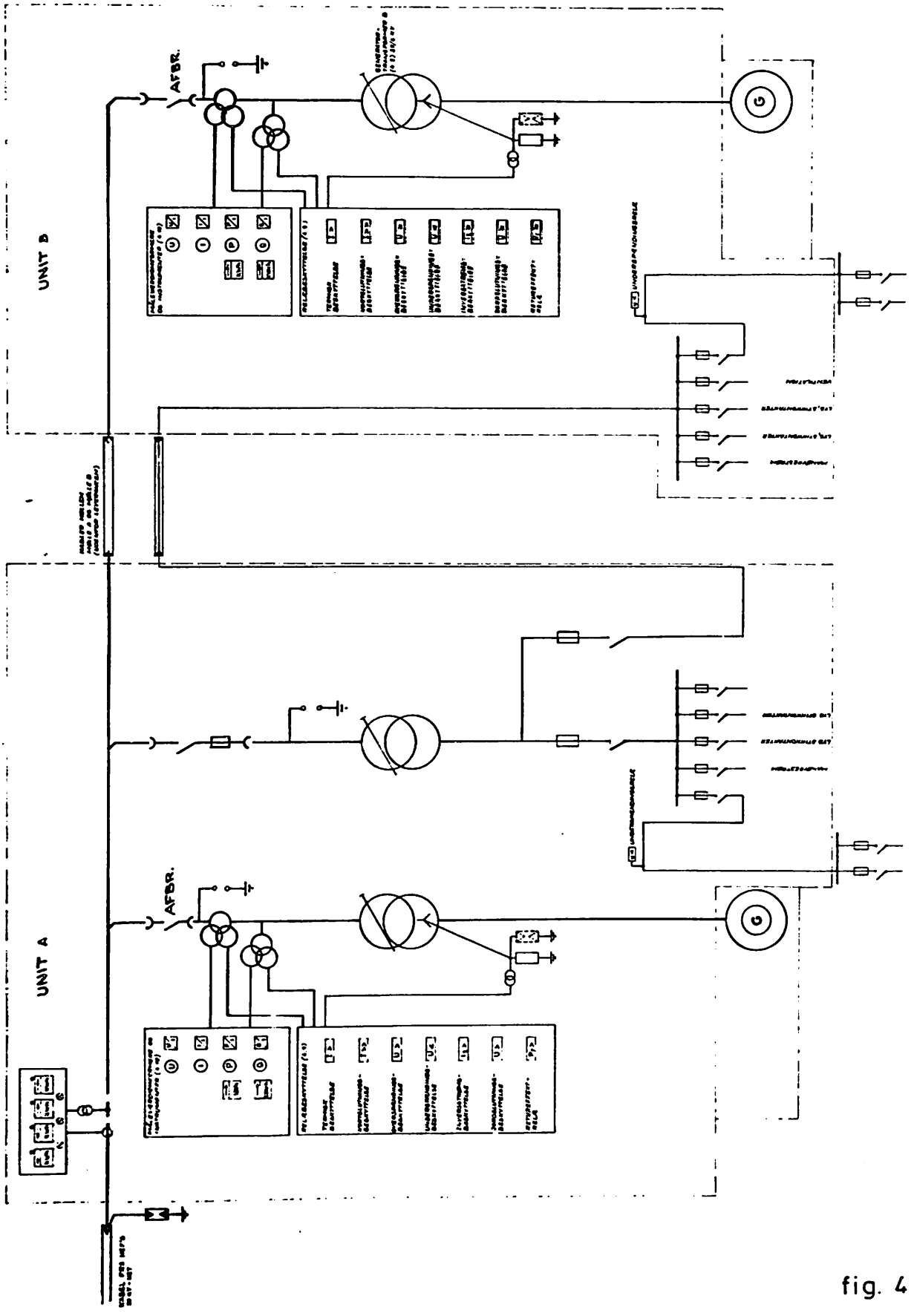

fig. 4

THE ELECTRIC POWER EQUIPMENT FOR THE WINDMILL IN TVIND.

by

Ulrik Krabbe

Laboratory of Electric Circuits and Machines

1979

I shall start to mention the Danish laws for schools of different kinds, built and run by nonprofit organizations. The laws allow any organization to build and run schools of different levels of education, and provided that certain formalities are fulfilled, they receive large state grants towards teacher's salaries and rents of buildings. Practically all folk high schools and private schools for children are subject to these laws.

The schools in Tvind near Ulfborg in Jutland are such schools. There are 3 sectors: A folk high school, a teacher's training college, and a school for children from the 8th to the 10th school year. The folk high school is specialized in arranging travels in foreign countries where the students for 4 months are studying the social and economic conditions of the country. All schools are boarding schools.

The schools are not connected with any political party, and have never in written form expressed their political ideology, but it is obvious that they are strongly influenced by Mao Tse Tung's philosophy.

The teachers have a joint economy, and since they live a very simple life, the school therefore gets sufficient capital for expansion and for the building of the windmill.

The decision to build a large windmill (54 m diameter) seems to be based on the following:

1) It fits with the philosophy, that theoretical learning should be combined with practical work with the hands.
2) It fits with the philosophy of decentralization.
3) Since they are good business people, they found that a windmill built by the students could be a good investment due to the expected rise in oil- and coal-prices.

When the project started there was no final design, and it has turned out, that the price of the mill became considerably higher than originally estimated.

The construction of the large windmill has no doubt been valuable publicity for the schools, partly as a result of frequent mention in the newspapers and TV-programmes, and also as a consequence of the thousands of visitors every week.

The project started in the spring of 1975. The first plan was to convert all the power into heat by water brakes in the bottom of the tower. This project was not realistic and was changed into a combination of a generator and eddy-current brakes at the top of the mill. However, it was found impractical to transport large quantities of water to the top of the mill, and therefore the project was finally changed to use of a synchronous generator connected to the shaft.

A design was made with a direct connected "pancake" generator with a rotor diameter of 4 m and 48 poles. (It was not planned for connection to the electric grid.)
The project was not quite unrealistic, even if the price was found somewhat higher than a gear and a 4-pole generator, but it was seriously evaluated. Before a decision was made for a direct connected generator, it was found possible to buy a second-hand gearbox at scrap-price. It was designed for a mine elevator of an iron-mine in the North of Sweden and was manufactured in the middle of the 60'es, but it never went into service. It weighed 18 tons and the price was 54.000 Sw. crowns. The rating is 1200 kW with good overload capacity.
At the same place was found a synchronous generator 2200 KVA 8 poles which had been working as a synchronous motor in a Swedish papermill. The price was 55.000 Sw. crowns. This cheap purchase influenced the future planning.

The school has a building area of more than 10.000 m^2, and in the winter all the power from the mill could be used for heating in connection with a planned 1600 m^3 hot-water reservoir, but in the summer there would be a surplus, and it was desirable to get it connected to the electric network.

There are 3 reasons why a direct synchronization to the grid is undesirable:

1) The grid is very weak. A 20 km 10 kv line and small transformers give a shortcircuit power of 5000 KVA which is considered too small for the 2200 KVA generator. It would be expensive but possible to reinforce the line, but
2) the gear ratio was fixed and the speed which corresponds to 50 cycles on the generator is the speed that gives the highest aerodynamic efficiency at a wind speed of 14 m/s. This would give too low an efficiency as a yearly average.
3) The third reason is the design of the wings. They are very flexible and it is desirable that there is a certain balance between the centrifugal forces which bend them in one direction and the windpressure in the opposite direction. The optimum nearly corresponds to the condition for highest aerodynamic efficiency, and a variable speed is the best solution.

For these reasons it was decided to connect the windmill generator with the grid through a frequency converter. It would be an advantage that the speed of the windmill could be varied and chosen freely also away from mechanical resonance frequencies.

Calculations based on the wind speed distribution showed that from a calculated annual production of 4,4 GWh, 40% could be delivered to the net, using a 400 kW frequency converter, provided that the supply to the net got the highest priority. Besides, 400 kW is a suitable size for a frequency converter using 2 x 6 thyristors at 380 Volt.

It is an advantage that the ease of control of the frequency converter gives possibilities for a flexible overall control system for the windmill.

The overall system.

The frequency converter is now in service, but the remaining load for the windmill is not ready. Fig. 1 shows the project.

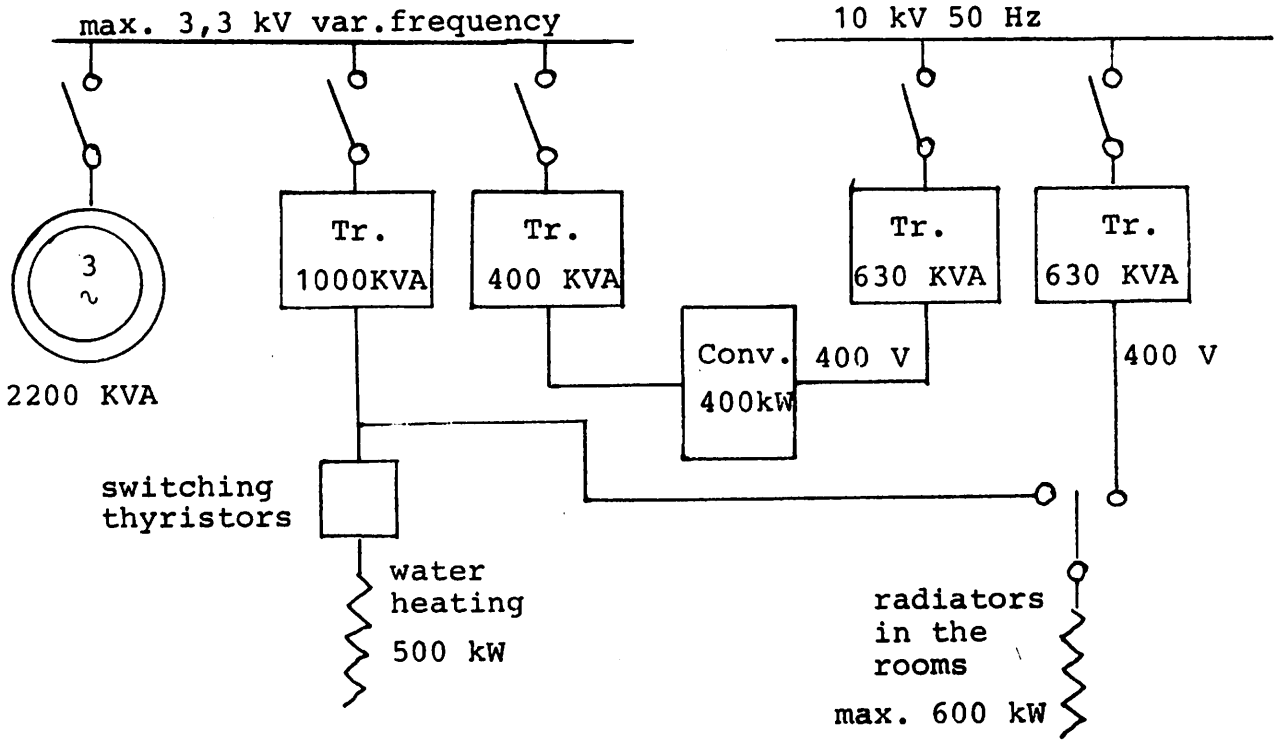

FIG. 1

The school buildings have partly central heating with oil-burners, and partly electric radiators in the rooms. For this reason there are three groups of loads:

1) The converter: 400 kW.
2) Heating elements for the hot-water central heating system: 500 kW.
3) Radiators with installed power: App. 600 kW.

The price, which the school can obtain for electric power, is approximately the same as it pays per kW from the oil-burners. On the other hand, when the school uses more power than the windmill can produce, it pays 2 - 2½ times as much per kWh. Therefore the water heating should get the lowest priority.

The control would be dependent on the wind speed. At low wind speed, the generator speed will be too low to give sufficient voltage for the radiators, and only the frequency converter will be in service. For higher wind power the radiators should be switched from the net to the generator and variations in power should be taken up by the frequency converter, and for even higher power (or in periods with 10 w loads on the radiators) the hot-water heating will be the power controlling devices. There may be periods when the windmill cannot get sufficient load, but on the other hand, the average wind speed is lower in the summer than in the winter. The control of load for hot water is planned using thyristors, for switching with zero voltage crossing on with the heating elements split into a reasonable number of groups.

The frequency converter.

The diagram in Fig. 2 shows the main circuit.

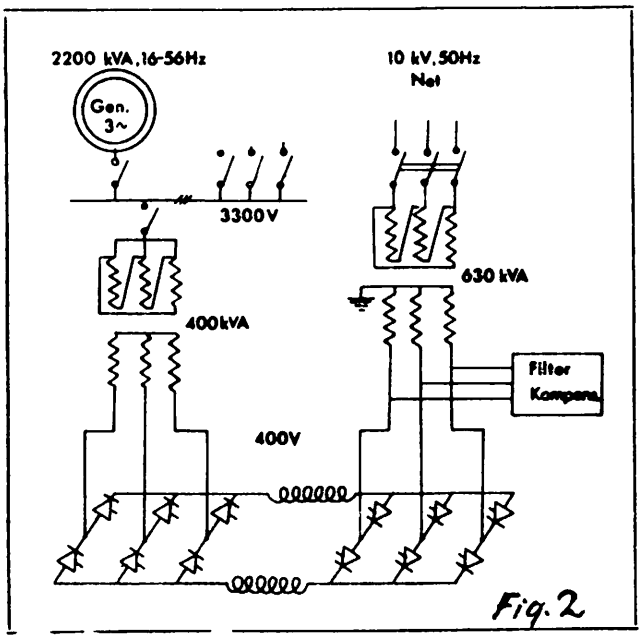

Fig. 2

In principle the design of the converter and the control method is the same as for high voltage DC transmission, except that 6-pulse circuits are used instead of 12-pulse circuits. The voltage from the secondary side can vary from 150 to 400 volt, and the frequency from 19 to 56 Hz.

The voltage is rectified by means of 6 thyristors, passes a DC reactor (with two windings to reduce the swing of the zero point in the rectifier side), and is connected to AC in another thyristor bridge.

The phase angle control is in principle a current control, with a current reference dependent on the frequency. Either the rectifier bridge or the converter bridge has the phase-angle-control active. The rectifier gets an increased firing angle when the current exceeds the reference and the converter gets a decreased firing angle when the current is below the reference. This means in practice that the converter control is active when the transformed generator voltage is below 340 Volt, and the rectifier control is active when the transformed generator voltage is above 340 Volt. The control system is made so that each rectifier bridge has its own current reference. The rectifier reference corresponds to 50 Amps DC more than the converter reference to avoid that the two thyristor bridges are controlled at the same time. This control system is similar to the system used for high voltage DC transmission and has the advantage that the voltage always is the highest possible to get lowest possible current losses and consumption of reactive power. The current reference is 1000 Amps when the frequency is above 36 Hz and falls linearly to zero at 19 Hz. This gives a reasonably good adjustment of the load torque to the torque from the windmill, when it has the highest aerodynamic efficiency.

Grounding.

From Fig. 2 it appears that the secondary of the generator transformer is not grounded, because a grounding of both

transformers would mean two 3-pulse systems with resulting higher harmonics.
However, since the generator voltage is 3,3 kV, no grounding means that the secondary of the generator transformer is also considered being a part of the high voltage system.
Therefore, to protect the electronic control, the ignition transformers had to be of a special design with an insulation level corresponding to the 3,3 kV.

Protection.

The most important types of faults considered when designing the frequency converter were:
1) Ground fault.
2) Drop-out of the net.

Both types will cause high currents and the electronic control system has to be fast acting.

Fault signals are given:
1) If the two current signals are uneven.
2) If one of the two signals exceeds a rated value.
3) If the line voltage deviates more than a certain percentage from the rated value.

All fault signals will stop firing of the rectifier thyristors.

If the voltage of the net vanishes, it means in practice a short circuit and the DC current will get a high rate of rise. The diode fuses will protect the thyristors, but diode fuses are expensive and it is desirable to make the control system so that the fuses are acting only when there are material faults in the system.

Even with an infinite fast electronic control it will in the worst case take a time corresponding to 150^{o} to get the DC voltage to zero and longest time is found at generator frequencies lower than 50 Hz.

Two precautions were made when designing:

1) The reactance of the DC choke was made larger than necessary for the smoothing to limit the rate of rise of the current.
2) In order to limit the time of getting zero DC voltage, the smallest delay angle for the rectifier was chosen to be 15^{o} - the highest angle was chosen to be 120^{o}, to get negative voltage for fast reduction of the current.

For the converter side the firing angle could vary between 90 and 150^{o} taking the overlap angle into consideration.

A computer programme showed that with a drop-out of the net under worst conditions it was possible to limit and reduce the current sufficiently fast to avoid fusing. However, no test has been made.

The phase-angle-control.

Fig. 3 shows a block-diagram for the whole system.

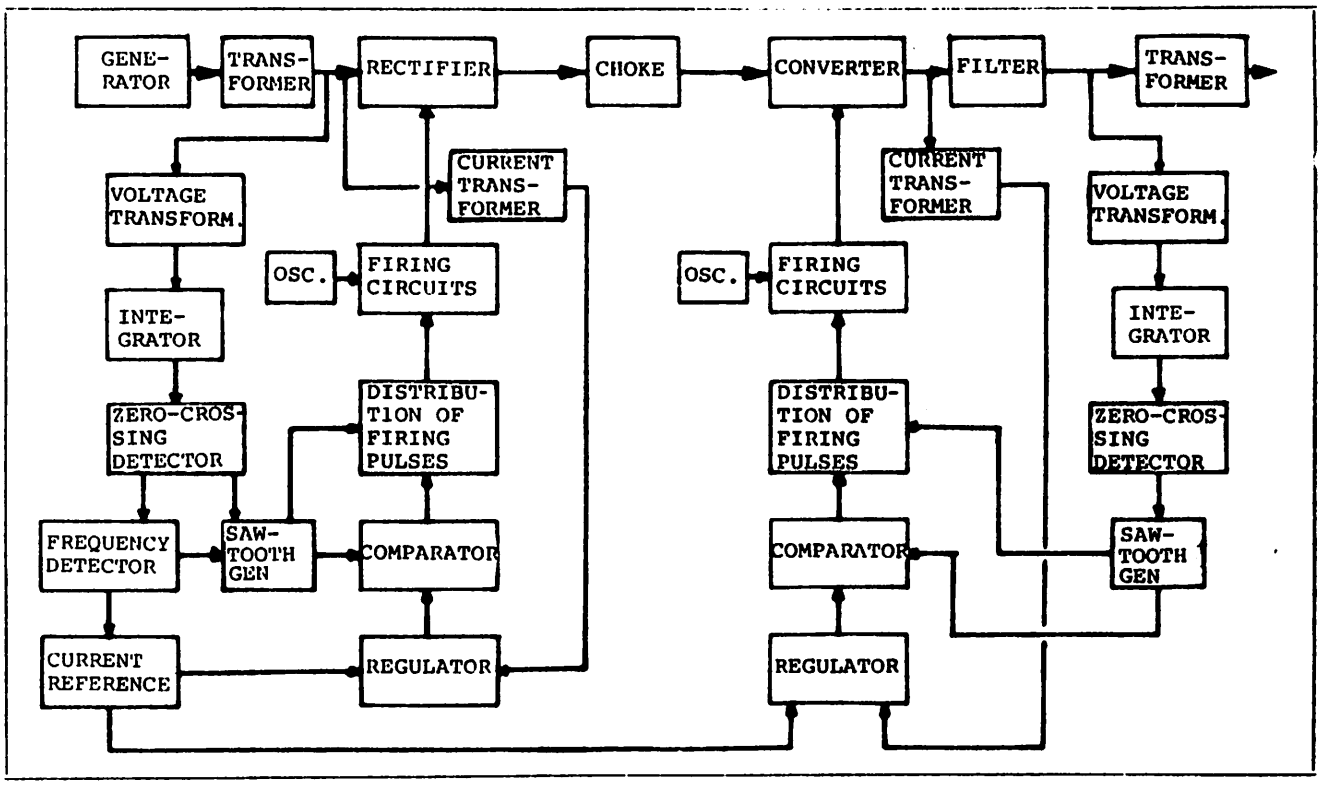

FIG. 3

A standard phase-angle-control system could not be used for the rectifier as a consequence of the large variation of voltage and frequency. The control system for the two thyristor bridges were made even and are based on sawtooth generators and comparators for comparison of sawtooth voltage and control voltage. The firing pulses have a length of 120^{o} and control a 20 kHz signal which is transformed by small ring-core transformers (with 3,3 kV insulation level) and rectified.

The automatic current control gets signals from the current transformers for each thyristor bridge, and PI control is used.

Filtering.

The filter has two purposes: To get rid of harmonics and give compensation for reactive power. The harmonics are a result of the rectangular current shape and give harmonics in the voltage caused by the impedance of the 10 kV line and transformers.

The voltage requirements on the 10 kV line were: No harmonics higher than 3% and a klirr factor of max. 4%. The filter consists of (on each phase) two series resonance circuits adjusted to the 5th and 7th harmonic. The two circuits together give a reactive compensation of 200 kVA.
The frequency converter was designed and built by 12 students during a special course given by The Laboratory of Electric Circuits and Machines at The Technical University of Denmark.

The price of the materials for the converter including electronic control, chokes, and capacitors was app. 80.000 Kr.

ELECTRICAL SYSTEMS FOR WIND POWER PLANTS

by

Hans-Inge Bengtsson

1. Power grid data and the WECS

NORDEL is the name of an agreement between the Scandinavian countries to have a common power grid and to buy and sell power between the countries. For this grid certain specifications have been set up:

Nominal frequency:	50 Hz
Frequency variations:	
Normally	± 0.1 Hz
At fault conditions	
- continuously	± 1 Hz
- rate of variation	0.5 Hz/s
At extreme fault conditions	
- during limited time	± 2.5 Hz
- rate of variation	1 Hz/s
Voltage variations:	
Normally	± 5 %
At fault conditions	- 15 %
	+ 10 %

The WECS must be constructed to withstand these variations without any damage to the machinery (shafts, gearbox etc.). The WECS must also withstand a short-circuit in the network and repeated reclosure attempts.

The WECS shall be disconnected from the network according to the following times:

internal electrical fault	< 0,2 s	
network fault	0,2 - 2 s	short-circuit
	< 5 s	earth-fault

2. Short-circuit power - voltage variation

The voltage variation on a critical busbar due to starting-up-transients and output-variations from the WECS must be kept within certain limits.
Figure 1 shows the Swedish norm for what is acceptable voltage fluctuations in a low-voltage system as a function of the disturbance frequency. The norm is based on the eyes sensitivity to light flickering.

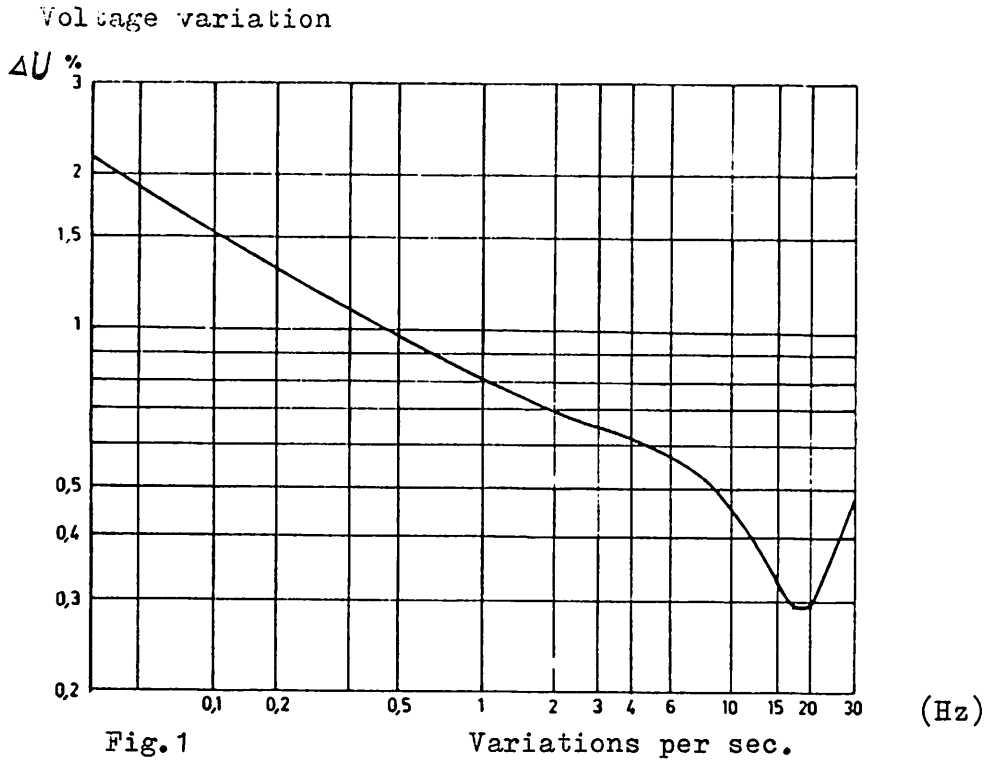

Fig. 1

The eye is most sensitive to voltage variations at 15-20 Hz. Here the ΔU-acceptance-level is as low as 0.3 %.
In the output from a WECS you often see variations with frequencies around 1 Hz depending on tower-shadow, gusty winds etc. Here the acceptance-level is 0.8 %. For occasional voltage fluctuations such as starting-ups a few times a day, the norm accepts a 2.5 % voltage fluctuation.

The short-circuit-power that is needed to limit voltage fluctuations depends on what kind of generator your WECS have:

A. Synchronous generator creates no problem with switching-in transients, provided that your phasing-in equipment works all right. In gusty winds you might however get a more or less out-of-phase switching, creating big transients and pulsating moments in the machine. In case you connect the synchronous generator unexcited to the network (so called "Russian phasing"), you get transients similar to those of an induction generator. The problem of how much short-circuit power you need depends on the whole WECS including wind-turbine-dynamics, power-train and generator and no guiding-value can be given without a complete study of the system. A very important factor is also the shape of wind gusts.

B. Induction generator. Here the switching-in phenomena are easier to predict. Figure 2 shows an oscillographic measuring when connecting a 360 kW induction generator to a network (76 MVA).

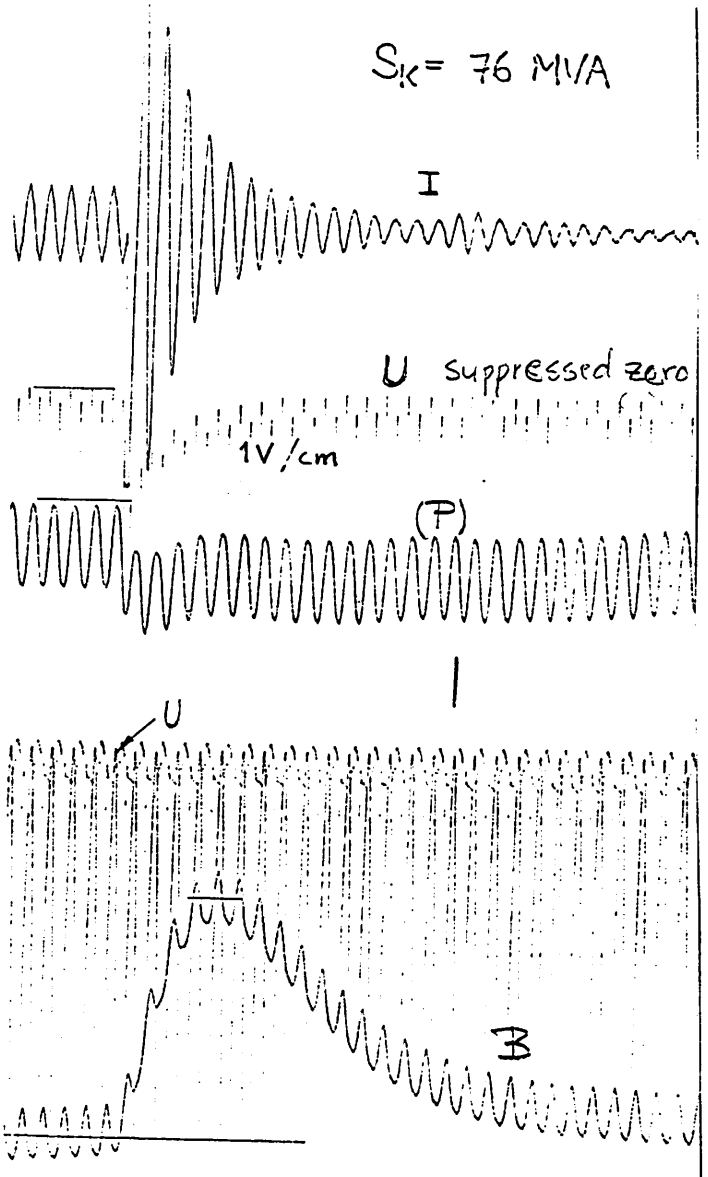

Fig. 2

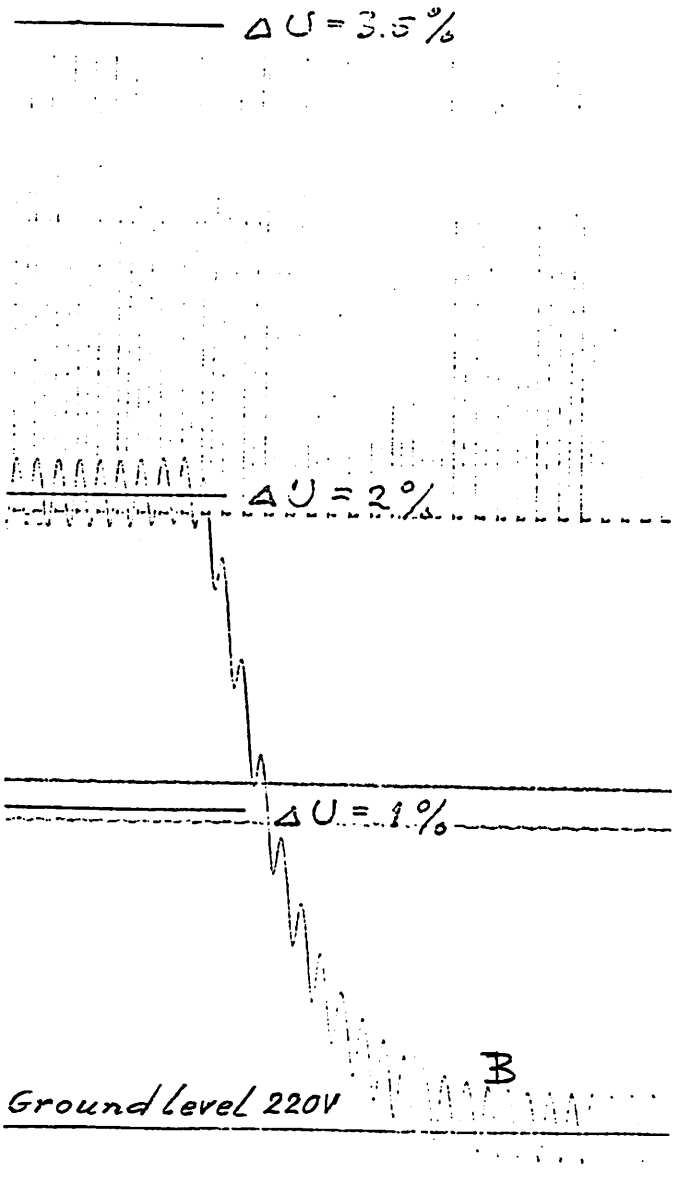

Fig. 3

You see the characteristic inrush current, which is damped after about 10 periods. Voltage drop is measured with suppressed zero-point to get a higher resolution.
The last curve shows the lighting from a 60 W glow-lamp measured with photo-cell. Maximum change in lighting occurs after 4-5 periods, because of the time-constant in the glow-lamp.
Figure 3 shows a comparison with the lighting change from a step-voltage-change.
Comparing the maximum lighting-change when switching-in the induction generator to nets with different short-circuit power, with what is accepted from a step-voltage tells us that a short-circuit-power of 50 x machine output would be enough. (See figure 4 below).

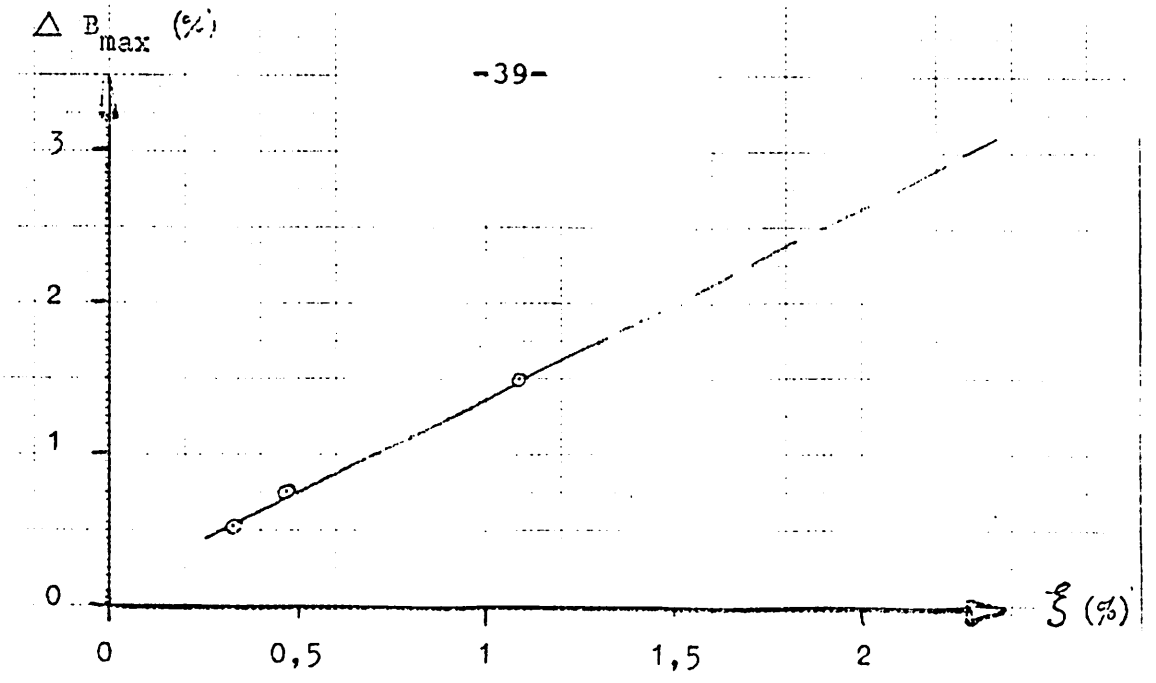

Fig 4. Lighting change versus ξ (ξ = $\frac{\text{rated machine output}}{\text{network short-circuit power}}$)

The voltage-drop acceptance-level is based on subjective measurement of what you feel as disturbing. Because the switching-in phenomena last for so short time, you might tolerate an even less short-circuit-power. The output-variations will in that case put a limit to what can be accepted.

3. Single-line diagram for a WECS

In figure 5 below is suggested a single-line diagram for a WECS with induction generator.
Depending on line-voltage, type of generator, short-circuit power and construction philosphy your scheme can have a little different appearance.
Some remarks:

- Local power feeding can be arranged either from the line-voltage or from the generator-voltage. For U > 24 kV it seems unpractical to have the feeding from the line-voltage.
- Transformer-breaker can be put on the upper- or lower-voltage side of the main transformer. This breaker works as a reserve for the generator-breaker.
- Capacitor battery for reactive power compensation is placed near the induction generator, but on the outer side of the generator-breaker.
- A reactor can be installed to limit big inrush current (if you have a very weak net).
  The reactor is then short-circuited after a short interval (e.g. < 1 s).
- Surge suppressors to prevent damage to generator and high-voltage apparatus.
- Help power feeding can eventually be arranged.

If you have a synchronous generator the capacitor battery shall be deleted. This is also the case with the reactor unless you use unexcited connection.
Normal protecting devices must of course be installed (not shown in the figure).

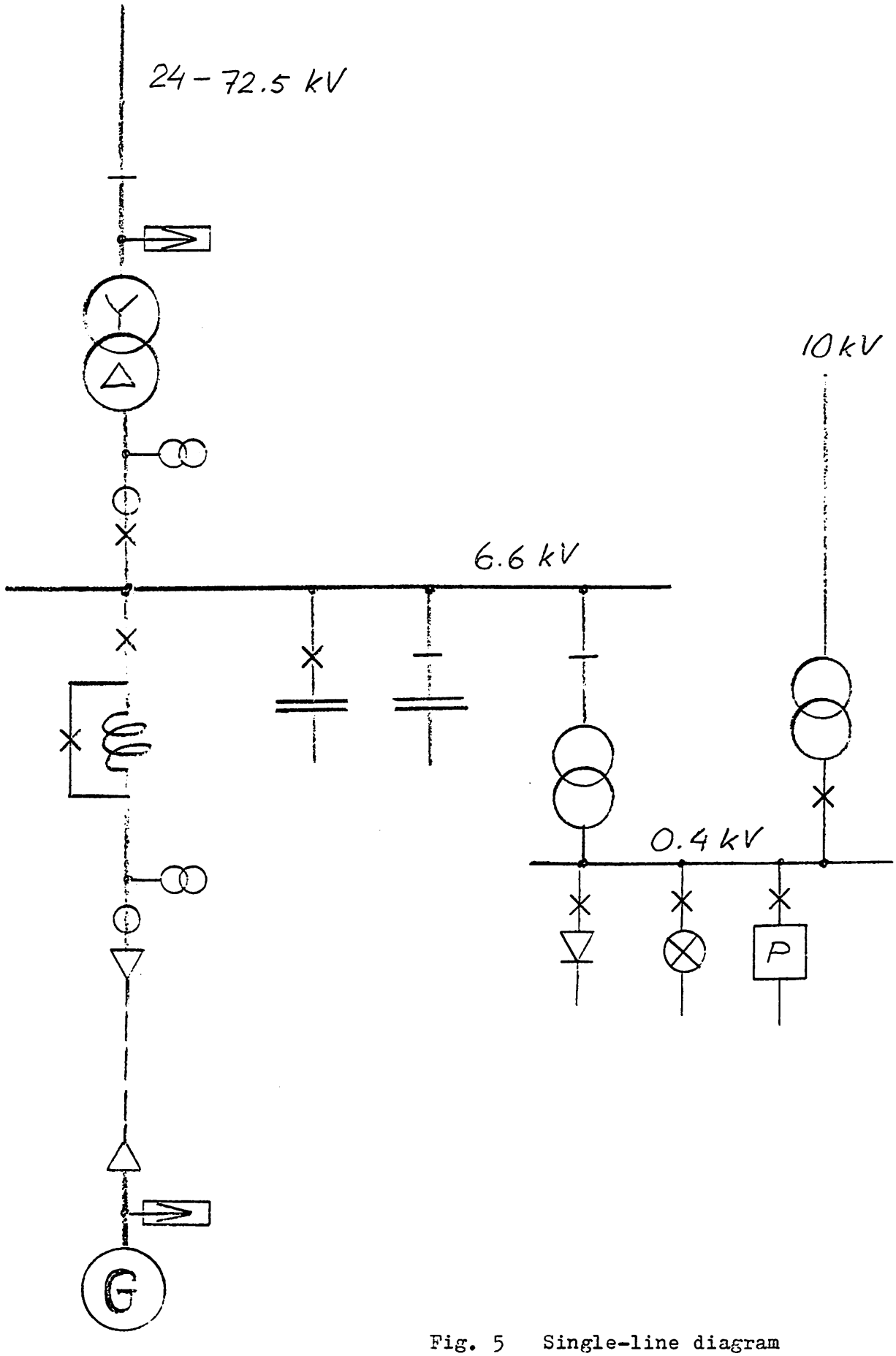

Fig. 5 Single-line diagram for a WECS

Generally the electrical system is quite conventional for a power production plant, except perhaps if you have a slipring transmission from the generator.
It is "only" the environment that is new to the apparatus. However the environment can come up with many funny surprises if you don't design your system carefully. You must analyse the consequences of things like:

- lightning protection
- vibrations and humidity in the nacelle
- long transmission lines for signals from nacelle to ground.

4. Group station of WECS-units

The location of a group station can be divided into two different problems:

- landbased
- off shore based

} group station

Off-shore based station

In figure 6 and 7 the electrical system of an off-shore based 100 MW group station with induction generators is shown.

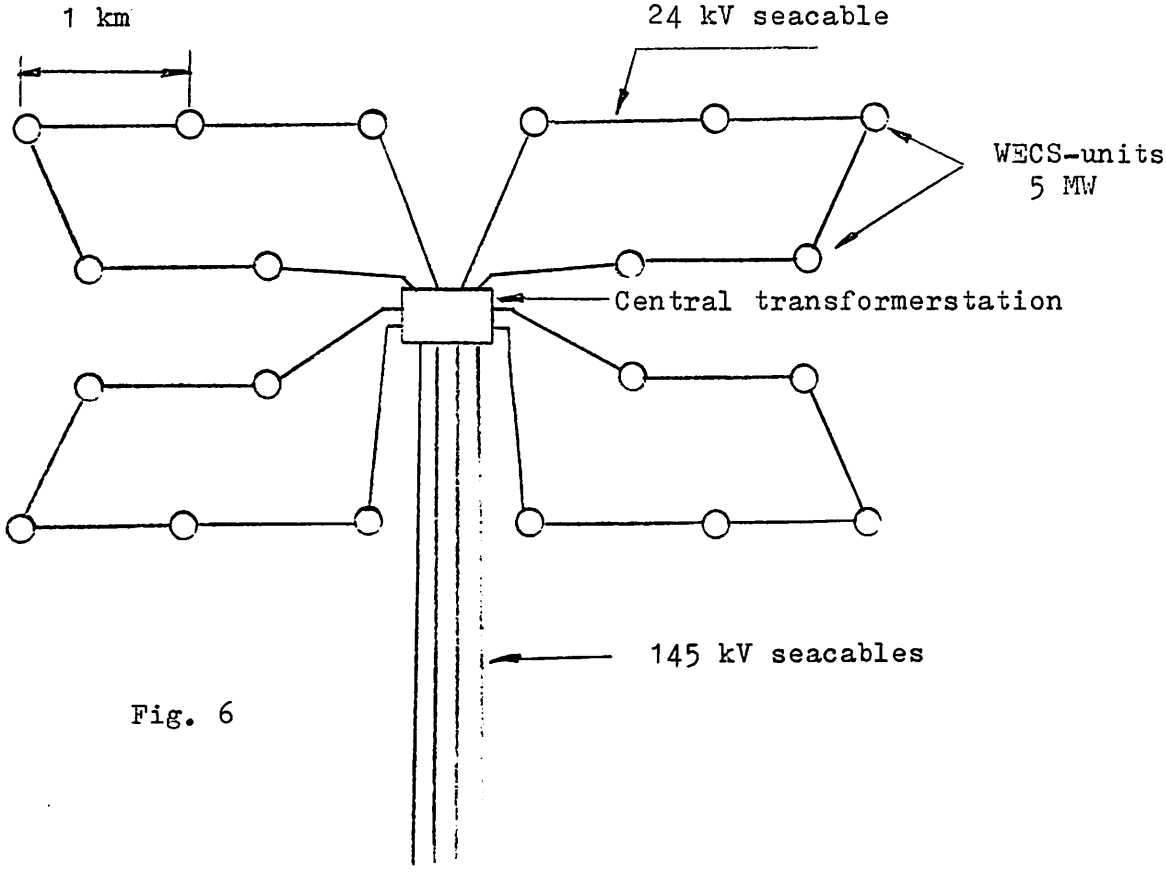

Fig. 6

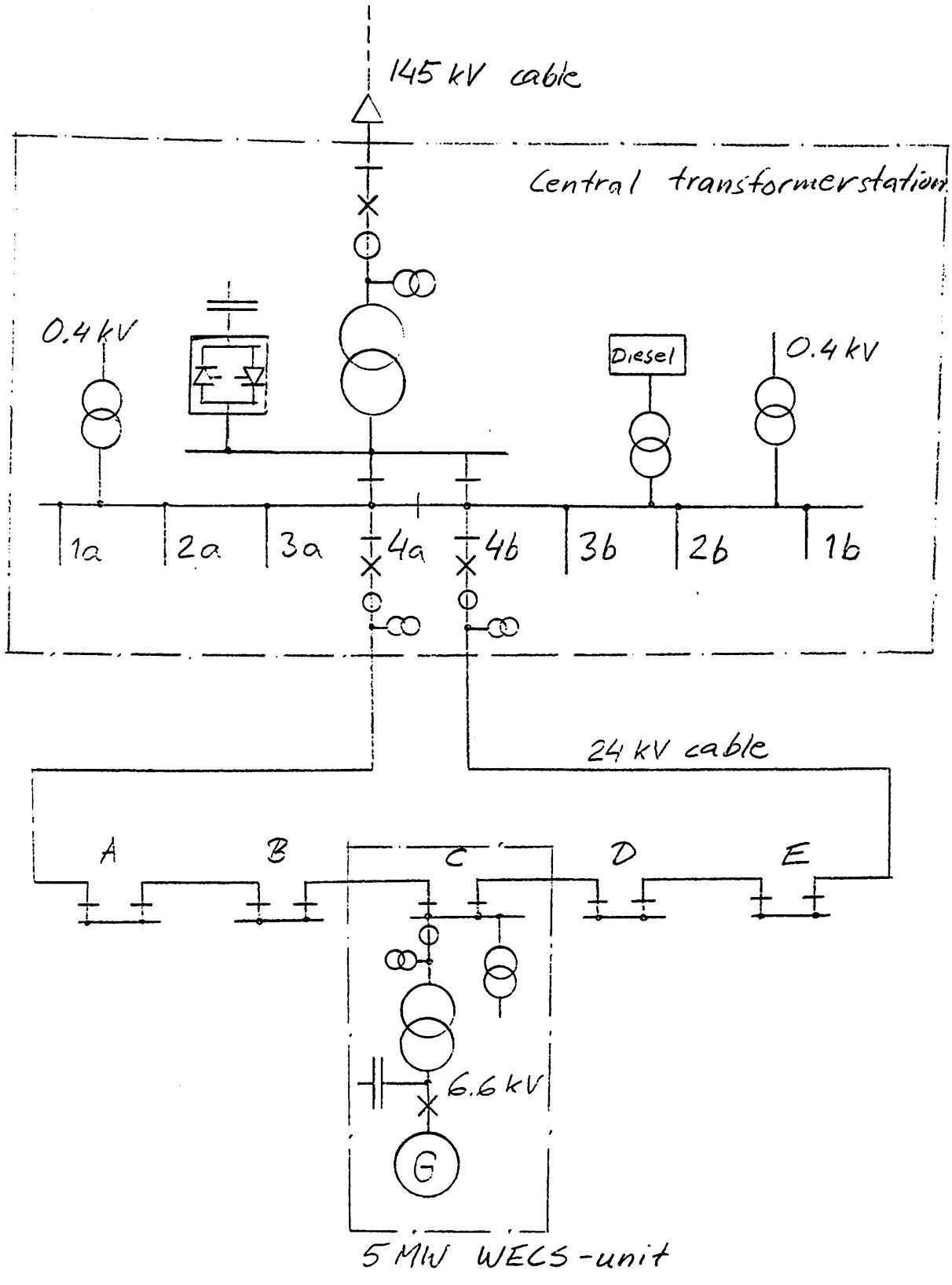

Fig. 7 Seabased group-station

A leading thought when designing the system must be to have very high reliability and redundancy, because it is sometimes impossible for weeks to go out on the station to do e.g. repair work.
This thought resulted in the ring feeding system. In this suggestion the station consists of 4 rings, each with 5 units à 5 MW. Normally the system is radially fed with the ring open somewhere. When something happens with a cable or WECS-unit, the faulty part is disconnected and the station can continue to operate. The units are connected to the central transformer-station via a 24 kV three-phase seacable. Power is transmitted to shore via three single-phase 145 kV seacables. One 145 kV cable is in reserve.
The thyristor controlled capacitor battery supplies the units with enough reactive power and stabilizes the voltage (not needed for synchronous generators).

If you have very long transmission lines ($>$ 50 km) it might be interesting to have a DC-transmission. This becomes however more interesting if you have bigger installed effect, say around 300 MW.
The control equipment must be very sophisticated. Remote control is assumed.

If you don't have too long distances a fibre optics transmission seems to be possible. The fibres are integrated with the cables. You get redundancy by having fibres in two or more of the 145 kV cables, and in the rings you have two separate signal ways.

A question that can be discussed is how much of control and operative action that can be done by a computer in the station, and how much that has to be done via remote control, but it is more a question of philosophy than of technique.

Landbased station

Also in the landbased version it can sometimes be impossible to get to the station within some days because of snow storm. Even in this case the ring feeding system seems attractive because of redundancy in local power and signal transmission. A radially fed system can however be sufficient if the costs are considerably lower. If the environmental and agricultural effects are very negative a cabled power transmission may be required. In that case the electrical system will be very similar to the off-shore version.

ELECTRICAL MEASUREMENTS ON THE WIND POWER PLANT IN KALKUGNEN, SWEDEN DURING OCTOBER 1977 - NOVEMBER 1978.

presented at the meeting of the
specialist group in Copenhagen
1979-04-04

by

Svante von Zweygbergk

Professor in Electrical Machinery

Chalmers Technical University
Gothenburg

Summary of measurements on the wind power plant with rigid hub in Kalkugnen made during October 1977 - September 1978.

The measurements have been carried out by staff at the Department of Electrical Machinery, Chalmers University of Technology, Gothenburg (CTH) and the Department of Electrotechnics, Lunds University of Technology, Lund (LTH).

1. Introduction

The wind power plant in Kalkugnen is equipped with an asynchronous generator (ASEA, MBK 250 S-4) connected to the 10 kV net by a transformer. The machine is marked 75 kW, 380/220 V, connection Y. The generator is 4-poled, the rated speed is 1540 r/min.
The measurements on the generator have been carried out at stationary operation and in transient condition. The purpose of these measurements has been to verify those at CTH made calculations and to create a realistic model for calculations on units in the megawatt range.

2. The aim of the measuring program

The wind power plant in Kalkugnen is built with the intention to give basic knowledge and experience concerning projecting of wind power plants in the megawatt range in Sweden. It was therefore important to shape those measurements, which were to be made in Kalkugnen, so that the behaviour of the wind power plant under normal conditions and under a number of unnormal operational cases was properly elucidated.

Extensive calculations with computers concerning the dynamic features of the wind power plant have been made at CTH. These calculations include following domains:

- Calculations of the phenomena of voltages, currents, power, torques and speed during 1, 2, and 3 phase short-circuits.
- Calculations of the above mentioned phenomena during sudden torque-pulses and sudden load changes and during connection in different phase positions.
- Calculations of the phenomena during on and off switching of compensating capacitances.

The measuring program was planned with the aim of as far as possible trying to verify these calculations. Measurements of short-circuit phenomena could not be made, not wishing to expose the wind power plant to the strains which are connected to short-circuit.

3. The measuring program, structure and motive

The measuring program includes:

3.1 Measurements at stationary operation

3.1.1 Simultaneous measurements of rms- values of voltage and current and of active and reactive power together with measurement of speed and torque and wind speed.

Because of the random variation of the wind it is difficult to define a stationary state of a wind power plant.

It is therefore necessary to measure during different periods at different wind speeds. An almost stationary state of a wind power plant may be considered to exist if the wind speed in a certain wind direction is almost constant during a period of several seconds.

Since the tower shadow might be expected of having a not insignificant influence on the output power it was also important to try to trace the influence of the tower shadow at the measurements.

3.1.2. Measurement of the instantaneous values of those in 3.1.1 mentioned quantities.

The moment of inertia of the wind turbine is several times larger than the moments of inertia of the anemometers used. Hence follows that a clear relation cannot be obtained between instantaneous output power and instantaneous wind speed. Not even at a constant value of the wind speed can a clear relation be obtained, since the wind speed varies over the swept surface of the wind turbine. In spite of this it is important to measure the instantaneous values of above mentioned quantities since it is probable that with a large enough statistic material one could obtain an acceptable relation between average values of output power and wind speed.

The diagram in appendix 1 shows the relationship between instantaneous output power and wind speed. The points in the diagram are plotted from several oscillograms taken with an UV-recorder.

3.1.3. Measurement of quantities in 3.1.1 during periods of strongly varying wind speed.

Measurements of this kind mostly aim towards getting an opinion of the gradient values of wind speed and torque. By calculating the stability of the system the assumption was made that the torque was varying either stepwise or

according to a harmonic function. In order to check this assumption it would be desirable to measure the real torque during periods of strongly varying wind speed. Unfortunally these measurements could not be done because the torque-meter, delivered by SAAB, failed to work during the measurement periods.

3.1.4. Temperature measurements on winding, plate unit and surroundings at stationary operation and at occasions of strong gusts.

By temperature measurements during a longer time an opinion is formed whether the generator is overdimensioned or underdimensioned and it is possible to calculate the life of the isolation.

We were, however, compelled to abandon this measurement because we were not permitted to drill holes in the bearing shield. The output power of the generator has only during very short periods exceeded the rated value, and this fact seems to indicate that the temperature of the winding has not reached very high values.

3.2. Measurements in transient conditions.

3.2.1. Measurement of the switching in transients of the generator.

At switching in of an asynchronous generator to the net by direct switching, current and torque reach very high values according to theoretical calculations. The duration of these high values increases with increasing difference between ultimate speed and switching in speed.

The first current peak at switching in depends on the switching in moment, but it might rise to 5 to 8 times the rated current,

which might lead to too large voltage drops on the net. The torque during the switching in might reach values of 4 to 5 times higher than the rated torque, which might involve large strains on the mechanical parts.

In a wind power plant the generator shaft is connected to the wind turbine by a mechanic gear. The rigidity of the system is of great importance for the switching in phenomenon because the oscillations in the shaft might jepardize the stability of the operation and generate exhausting phenomena in the mechanical parts. Measurements of switching in currents and voltage drop makes it possible to verify the assumed mathematical model of the electric system. Since the reactance calculation is uncertain at high currents it is important to make the measurement.

By measuring the switching in phenomenon it might be judged whether the system can be regarded as rigid or weak. It is therefore important to study the torque and speed phenomena after the switching in thoroughly.

The measurements showed clearly that the rotating system can be considered as a rigid system.

3.2.2. Measurements at switching in and off of load

A sudden switching in of a resistive load in series with the stator winding of the generator causes an increase of the electromotoric force of the generator and consequently also an increase of the maximum torque. It is conceiveable to parry gusts instantaneously by continuous or stepwise switching in of a suitable resistance. If such a method is applicable in practice the same maximum torque can be obtained with a smaller generator as with a larger type, which eventually brings about a higher efficiency at partial load. With

adequate dimensioning of generator and connection resistance (impedance) the inclination of the torque curve can also be regulated, which means that it might be possible to dimension the regulating system of the wind turbine for a longer time constant.

The measurements with in and off switching of resistances are intented to illustrate these conditions and to eventually discover such transients which have not been discovered at the calculations.

In order to reduce the risk of damages at occasional short-circuit when the resistance is switched in and off it is best to switch it into the zero point of the generator.

3.2.3. Measurements at switching in and off of compensating capacitors

The transient phenomena occurring at switching in and off of compensating capacitors to the generator terminals have been calculated at CTH. The calculations show that over-voltages as well as harmonics can be expected at these phenomena. It is probable that the measuring results shall differ from the calculation results depending partly on the characteristics of the capacitor switch used, and partly on the impedance characteristic of the net. It is, however, valuable to be able to establish how large the deviation can be.

These measurements ought to be carried out also at reduced short-circuit power of the net. It was therefore planned to connect two more transformers of the same kind in series with the existing net transformer.

These tests were not carried out during the time when the unit was equipped with a rigid hub, but they were made later when the flapping hub hade been installed.

4. Measuring equipment

There is a detailed description of the measuring equipment in those reports which have been published previously. In appendix 8 is a list of the instrument used.
The main instrument for recordings of all measuring signals was an UV-recorder with 12 channels.
The voltages were recorded by voltage transformers.
The currents were recorded by using either current transformers or measuring shunts.
The active and reactive power were measured by using multipliers installed by SAAB.
Transformation of the wind speed and the generator speed to DC-voltages took place in the equipment of SAAB.

The measurements with the UV-recorder and its peripheral equipment is described in part 6.

5. Summary of measuring results obtained with UV-recorder

Those in this part described measurements were made by staff at CTH. The measurements are recorded in monthly reports, appendixes 2,3 and 4.

5.1. Measurements in stationary operation

The average speed of the wind was about 15 m/s during the measuring period, the generator speed about 1530 r/min. The average values of the current, the electrodynamic torque, the active and reactive power were 125 A, 475 Nm, 73 kW and 48 kVAr respectively.

It should be noticed that the measured values of the current, the torque and the power oscillate. The period of the oscillations is about 0.4 seconds. The result of the measurements was that the amplitude variations of the current and the active power were about 15 per cent and about 8 per cent for the reactive power. These variations were probably caused by the tower shadow and partly by different wind conditions above and below the hub of the wind turbine.

The speed of the wind turbine was about 78 r/min during the measurements, which means that the propeller blade of the two-bladed propeller passed the tower 156 times per minute, which gives a period of about 0.4 seconds. No other unnormal oscillations in the unit beside the above mentioned could the noticed. Any torsional oscillations in the shaft of the wind turbine could not be detected with the measuring equipment used.

5.2. Measurements in transient conditions

5.2.1. Measurements of switching-in transients

The current, the voltage drop on the net and the generator speed have been given particular attention in connection with switching in phenomenon of the generator. The measuring results have been compared with the calculations. The difference between the measured and the calculated values of current and voltage is 2 respectively 8 per cent. When applied on the generator speed the difference is somewhat larger, but the measured and the calculated curves have the same character. This shows that the adopted calculation model is accurate enough.

Oscillations in the generator speed after switching in were damped after about 0.2 seconds. This shows that the rotating system can be regarded as rigid.

5.2.2 Switching in of resistive load

Switching in of resistive load gives a damped oscillation, however, of a very mild character. Two measurements were made the first at the generator speed of about 1513 r/min (65 A, 25 kW) and the second at 1525 r/min (76 A, 38 kW). In the first case the generator speed varied with 11 r/min and the current between 56 and 75 A. In the second case variations of 16 r/min for the speed were obtained. The current varied between 63 and 98 A.

In both cases the oscillations were damped after about 0.8 seconds. Switching in of resistive load does not affect the stability of the system.

6. Measurements carried out with measuring computer

These measurements were carried out by staff at LTH.

The actual measuring computer at LTH is a MY-16 manufacture. The computer is equipped with an analogue input which A/D transformer has a resolution of 8 bits. Moreover, there is a digital output of 8 bits and a number of control wires. A measuring interface constructed at the Department of Electrotechnics, LTH was used at the measurements in Kalkugnen. The measuring interface with its present construction has the possibility of sampling measuring data from nine channels by analogue switches. The input sensivity is $\pm$ 0.2 - $\pm$ 8 V resp. $\pm$ 0.2 - $\pm$ 80 V. One input is equipped with a linear reciever in order to recieve pulses from the speed rate control. The

maximum sampling frequency is about 3 kHz. The computer has a memory of about 5000 bytes. For storage of measuring data minidiscs are used.

The measuring computer is programmed in basic. Assembling routines are called for by the measuring interface for controlling. The basic program gives, after measuring is made, a possibility of studying the different measuring signals on the graphic screen. If the measuring results are to be preserved then they are transferred together with the rest of those for the measurement actual parameters to minidiscs.

The measuring results from measurements with the measuring computer are recorded in appendix 5.

7. Diagrams

Connection diagrams for the electric system of the wind power plant and for the measuring connections are recorded in aprendixes 6 and 7.

Instantaneous output power versus instantaneous wind speed

(The values are plotted from recorded UV-oscillograms)

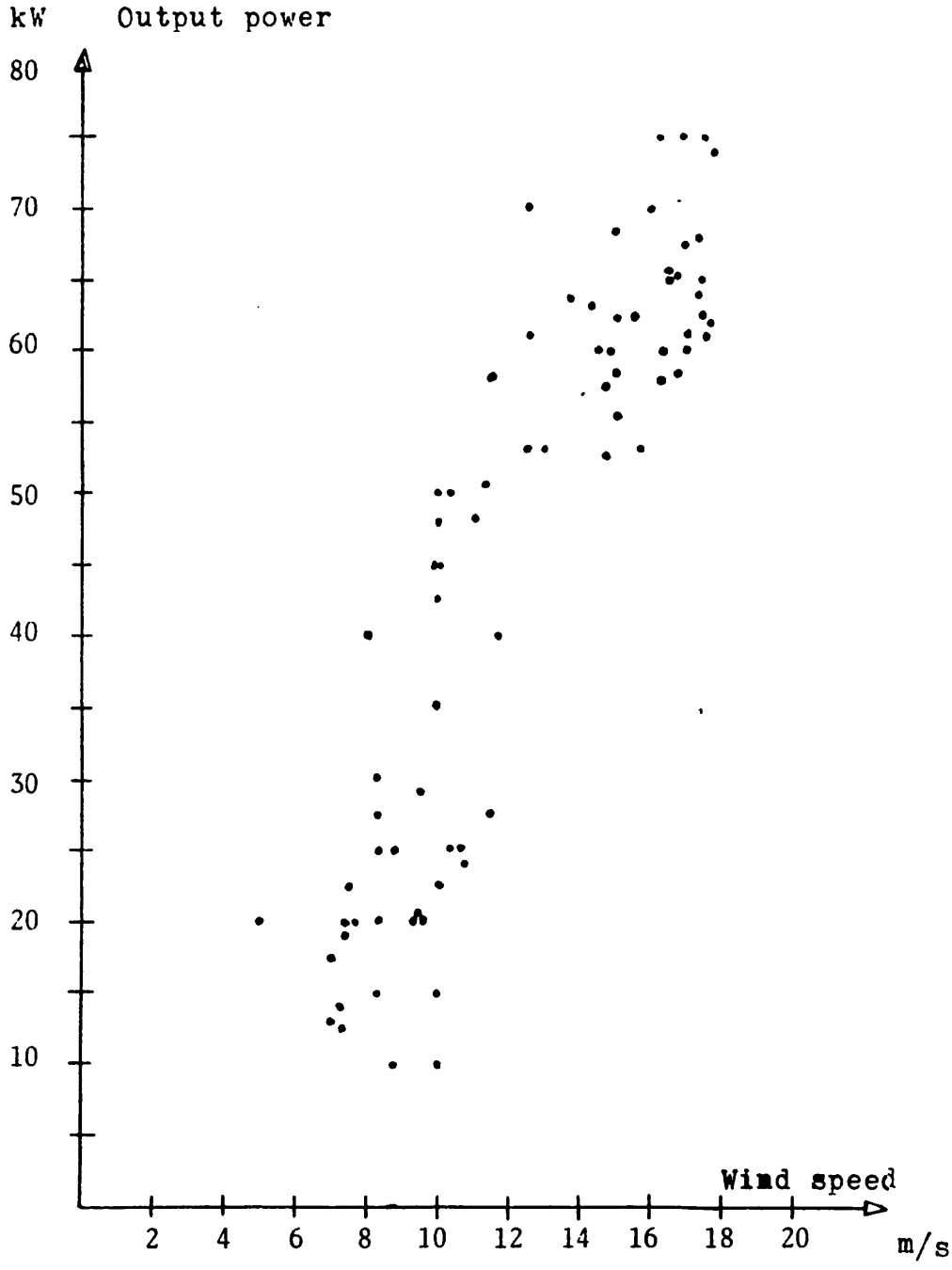

Measurements under steady state conditions
(Selected items from monthly report CTH - 780306)

Steady state condition is considered to prevail when the active power level is approximately constant. A registration of wind velosity, generator speed torque, current, active power, reactive power and voltage is presented on page 2 of this appendix.

Comments :

The wind velosity during the measurements was about 15 m/s. The generator speed was 1530 r/min, the average value of the torque 475 Nm ,the phase current 125 A_{RMS} , the reactive power 48 kVAr and the active power 73 kW. It is notable to observe that generator speed, torque, current, reactive and active power oscillate with a period of approximately 0.4 s. This cyclic variation could be transferred to the moment when one of two blades passes behind the tower. The blade will then be in a wind shade and, therefore, the torque will be reduced.

The wind turbine has two blades and a rated speed of 78 r/min. We expect a by-pass of 156 times/min.

The period of oscillation : 0.4 s.

$T = 0.4$

$f = 1/T = 2.5$

$2.5 \times 60 = 150$ times/min

It seems that there is correlation between the events.

The amplitude variation of the oscillations :

Evaluation of the oscillograms gives

- current 15 o/o
- active power 15 o/o
- reactive power 8 o/o .

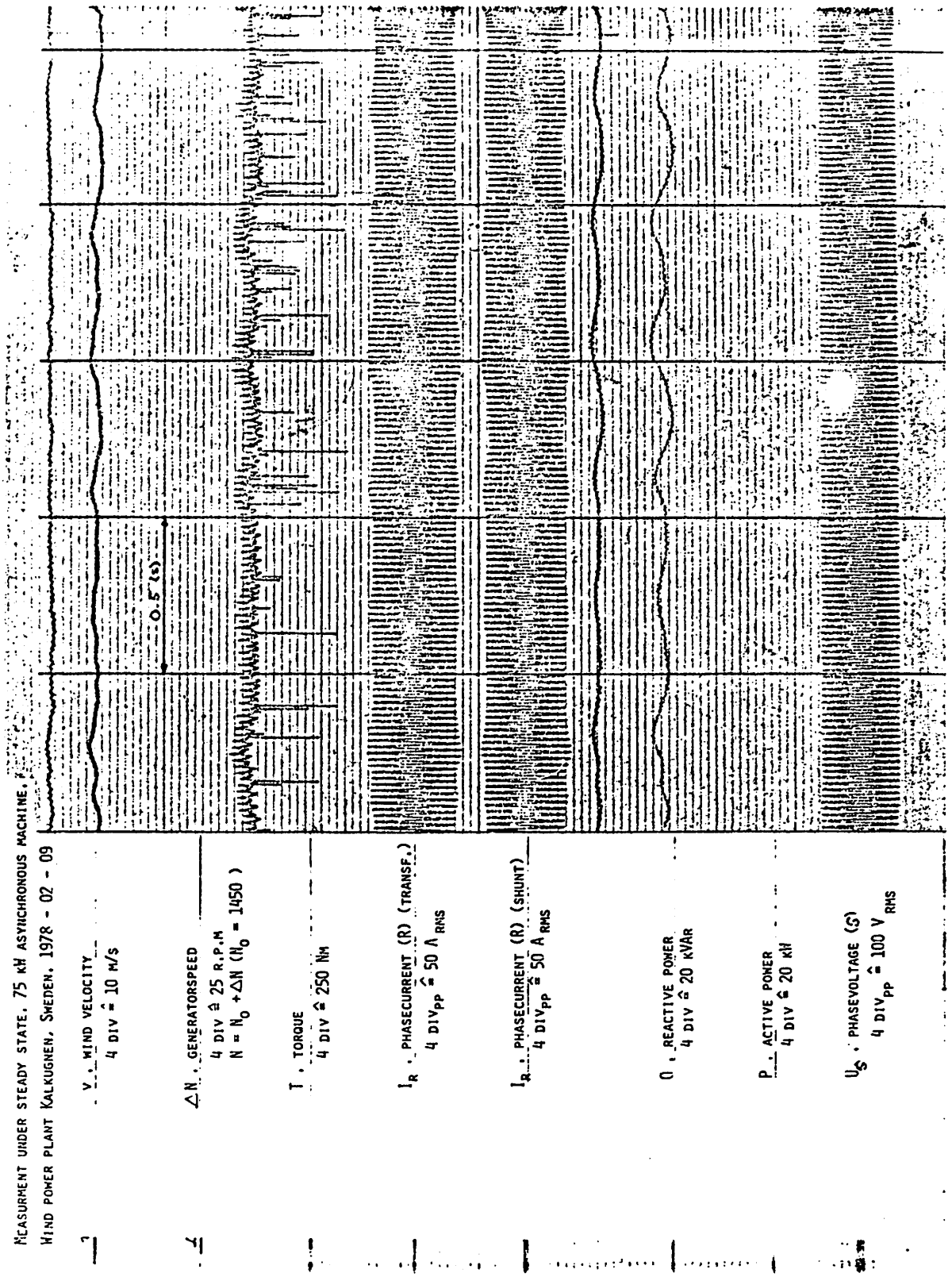
MEASURMENT UNDER STEADY STATE. 75 kW ASYNCHRONOUS MACHINE.
WIND POWER PLANT KALKUGNEN, SWEDEN. 1978 - 02 - 09
V , WIND VELOCITY
4 DIV ≙ 10 M/S
0.5 (s)
ΔN , GENERATORSPEED
4 DIV ≙ 25 R.P.M
N = N0 +ΔN (N0 = 1450)
T , TORQUE
4 DIV ≙ 250 NM
IR , PHASECURRENT (R) (TRANSF.)
4 DIVPP ≙ 50 ARMS
IR , PHASECURRENT (R) (SHUNT)
4 DIVPP ≙ 50 ARMS
Q , REACTIVE POWER
4 DIV ≙ 20 KVAR
P , ACTIVE POWER
4 DIV ≙ 20 KW
US , PHASEVOLTAGE (S)
4 DIVPP ≙ 100 VRMS

Measurements of switching-in phenomena

(Selected items from monthly report CTH - 780306)

When the generator is connected to the network the inrush current will be of a considerable value. The first peak amplitude depends on the circuitparameters of the generator and on the instantaneous value of the network voltage when switching-in. Since the circuit-breaker is rather simple there is no possibility to control the switching-in moment. Because of this, comparison between the measurements and the calculations with digital computer is difficult. However the calculations and the measurements seem to have rather good correlation.

Comments on the measurements :

On page 2 there is a recording af a phase current and a phase voltage during switching-in of the generator.

The maximum value of the switching-in current during the first half period is about 1100 A. The voltage drop is about 20 o/o. The calculated results are presented on p. 3 and 4. The calculations under approximately the sam conditions give : peak value of inrush current : 1100 A, voltage drop : 17 o/o.

On page 5 one can see the phase currents, a phase voltage and the generator speed. For example : Peakt value of inrush current in phase S is 1050 A. Voltage drop in phase S is 15 o/o. The calculations (p. 6 and 7) give inrush current 1030 A and voltage drop 15 o/o.

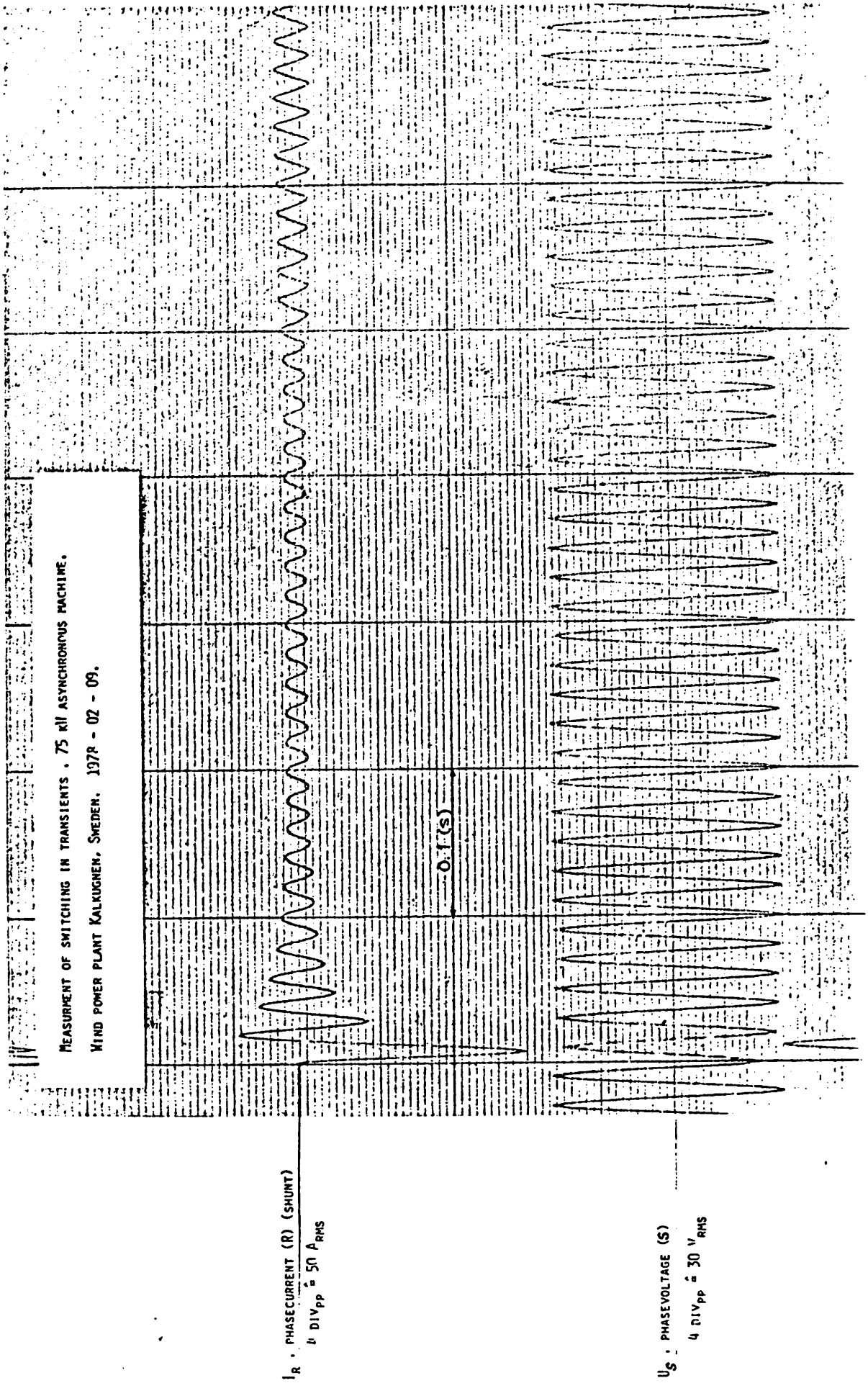
MEASURMENT OF SWITCHING IN TRANSIENTS . 75 kW ASYNCHRONOUS MACHINE.
WIND POWER PLANT KALKUGNEN, SWEDEN. 1978 - 02 - 09.
0.1 (s)
I_R . PHASECURRENT (R) (SHUNT)
1 DIV$_{PP}$ ≙ 50 A$_{RMS}$
U_S . PHASEVOLTAGE (S)
4 DIV$_{PP}$ ≙ 30 V$_{RMS}$

Appendix 3

Page 3

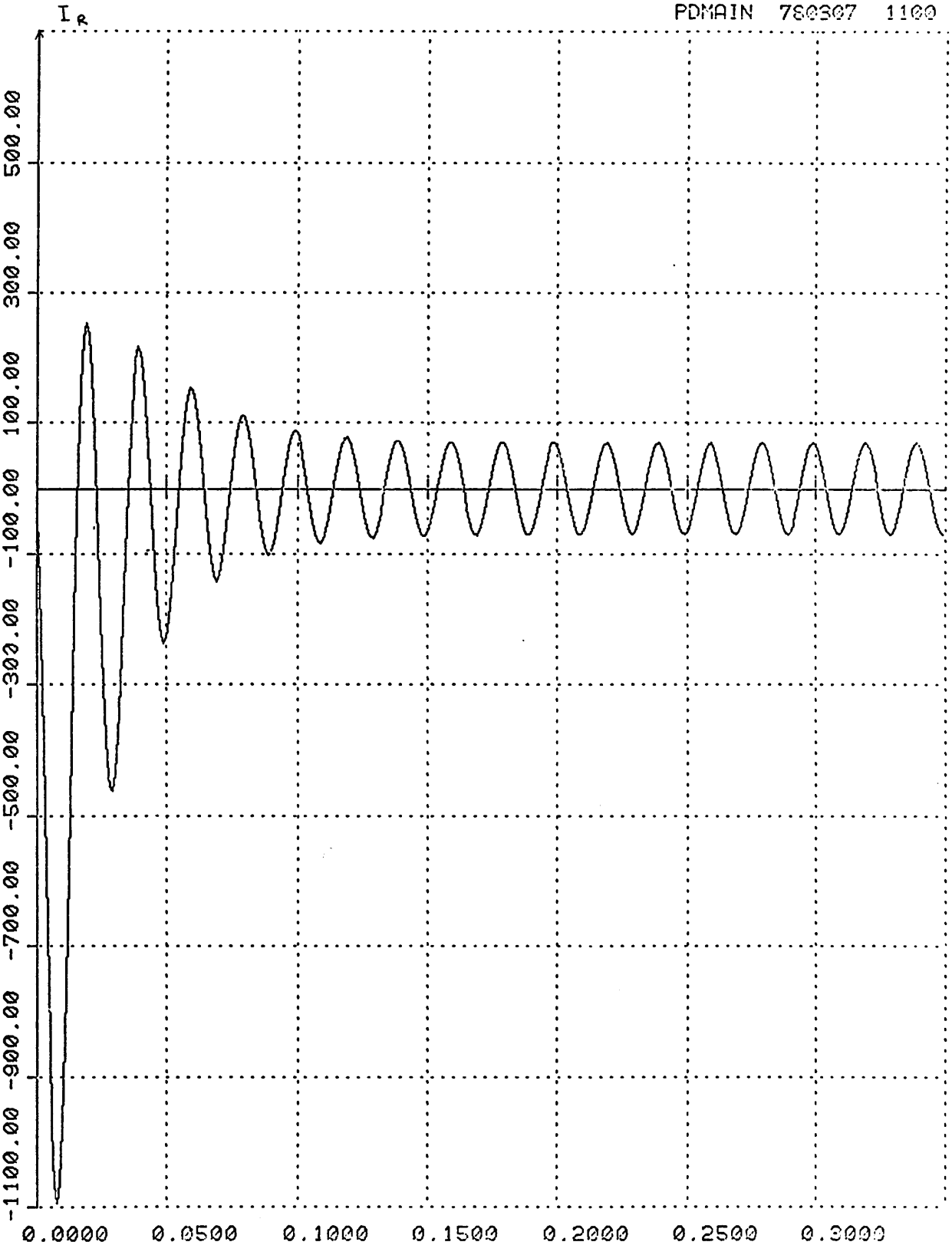

Appendix 3

Page 4

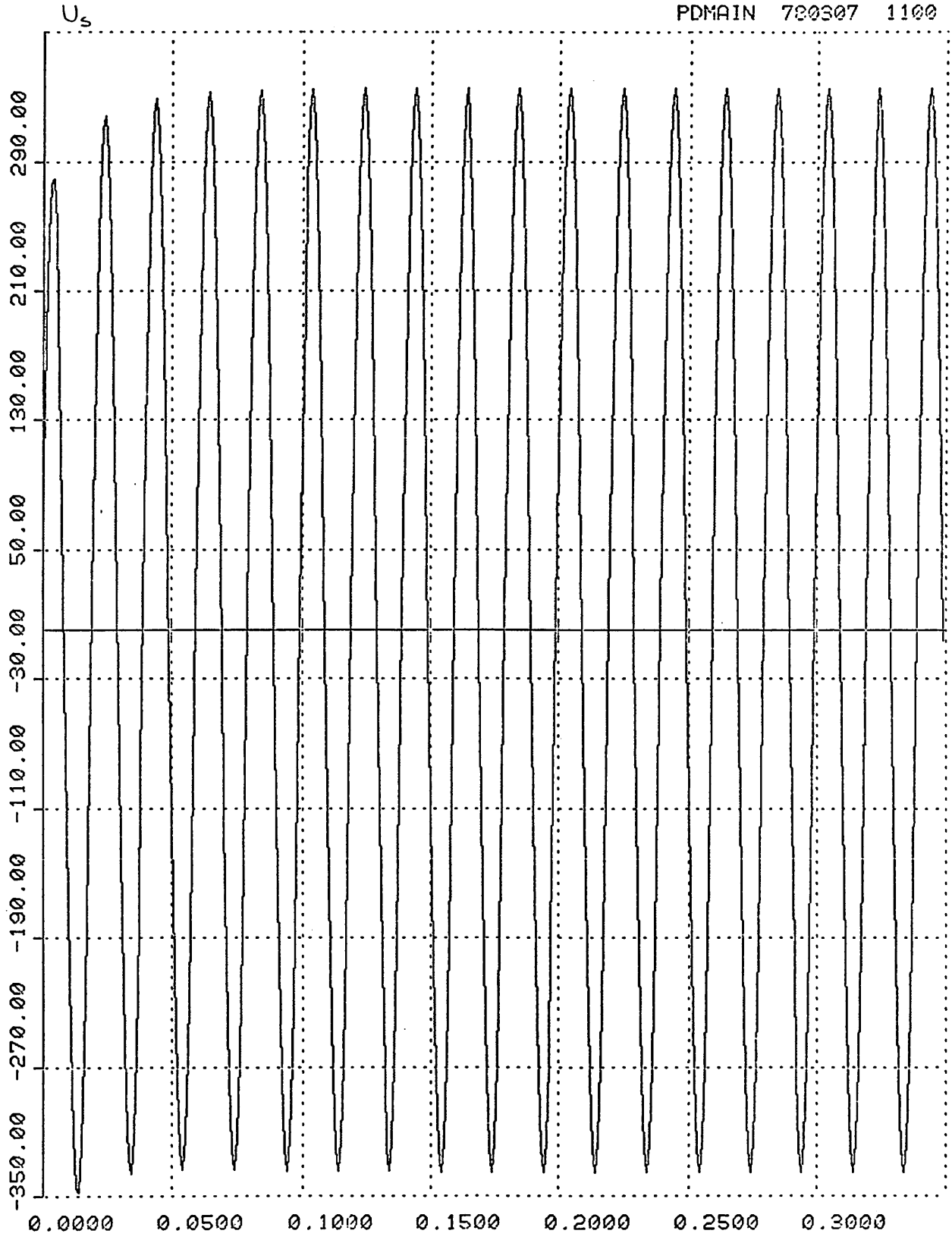

Report concerning measurements of the performance of the asynchronous generator in the wind power plant in Kalkugnen, Sweden

1. Introduction

This report concludes the first stage of the measurement program drawn up for the wind power plant in Kalkugnen and deals with connection of resistors in series with the stator circuit of the generator. The basics of the theory and measurement procedure are described.

Measurement of switching transients of the generator and steady-state operation are described in: Report concerning measurements of the performance of the asynchronous generator in the wind power plant in Kalkugnen, Sweden, PM-HJ-780306.

2. Terminal voltage control of wind-driven induction generators

The problems concerning operation stability of the wind-driven induction generators during the periods of varying wind velocity and gusts have hitherto been solved by regulating the angles of the turbine blades. The question is if inprovments of performance and economy can be obtained by extending the control system to the generator. In this connection the main problem is to prevent overspeeding which takes place when the prime mover torque exceeds the breakdown torque of the generator. The torque of an induction machine is a function of terminal voltage, see fig. 1. The figure shows induction machine torque - slip curves in both motor and generator regions with the terminal voltage as a parameter.

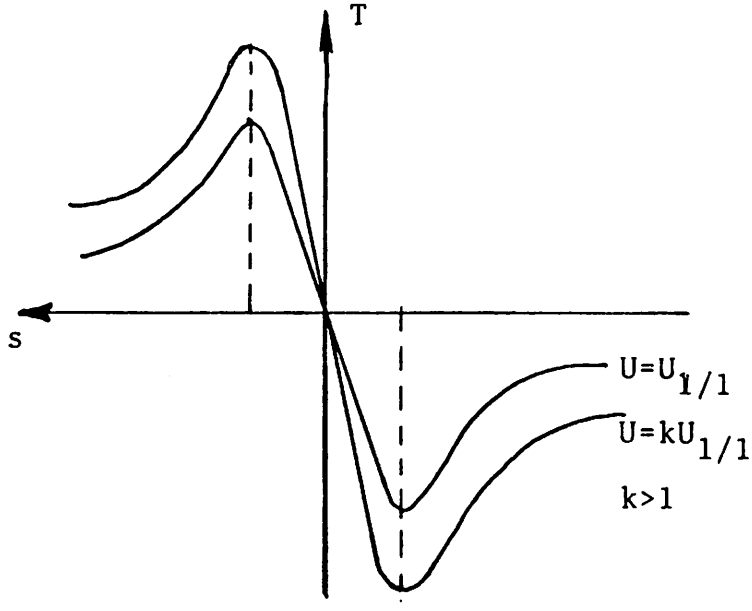

Fig. 1

Temporary rise of breakdown torque of the machine during gusts leads to improvment of operation stability. Control system on the turbine-side can have longer response time which is especially valuable when using large-scale generators with steep torque-slip curves at the point of rated operation.

Generally speaking the rise of terminal voltage has the following concequences:

- Maximum torque of the machine is increased

- When assuming a constant torque at the prime mover, generator speed and current are decreased.

The rise of terminal voltage can be achieved by connecting impedances in series with the stator circuit of the generator, see fig. 2. When this type of application is made the slip at breakdown torque is increased.

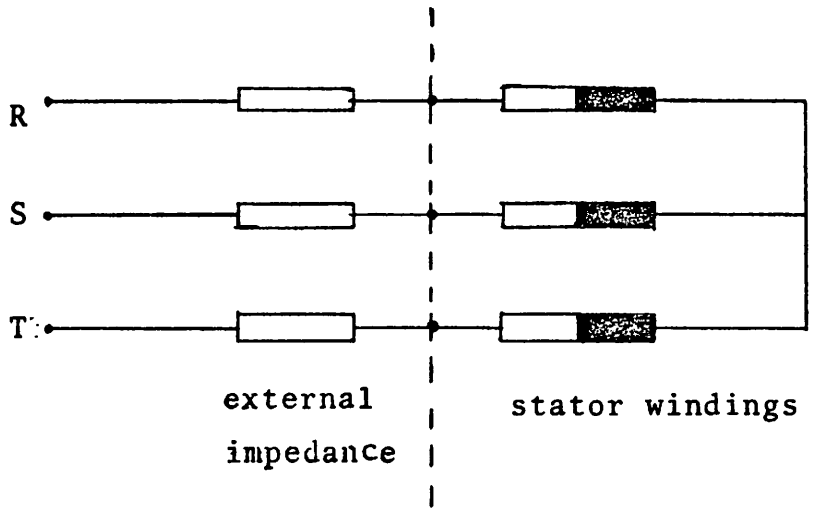

Fig. 2.

Connection of resistors in series with the generator, as shown in fig. 2, has been carried out in the wind power plant in Kalkugnen. In the following sections the measurement procedure and results will be described.

3. Description of the measuring circuit and the measuring quipment.

The external resistors and the shunts for current measurements have been installed in the neutral point of the generator, see fig. 3.
The resistors are normally shortcircuited by a contactor, which can be operated from the measuring room. All signals of interest are measured as described in PM-HJ-780306.
The UV-recorder which is provided for the registration is also used as a control device for the switching of the resistors.

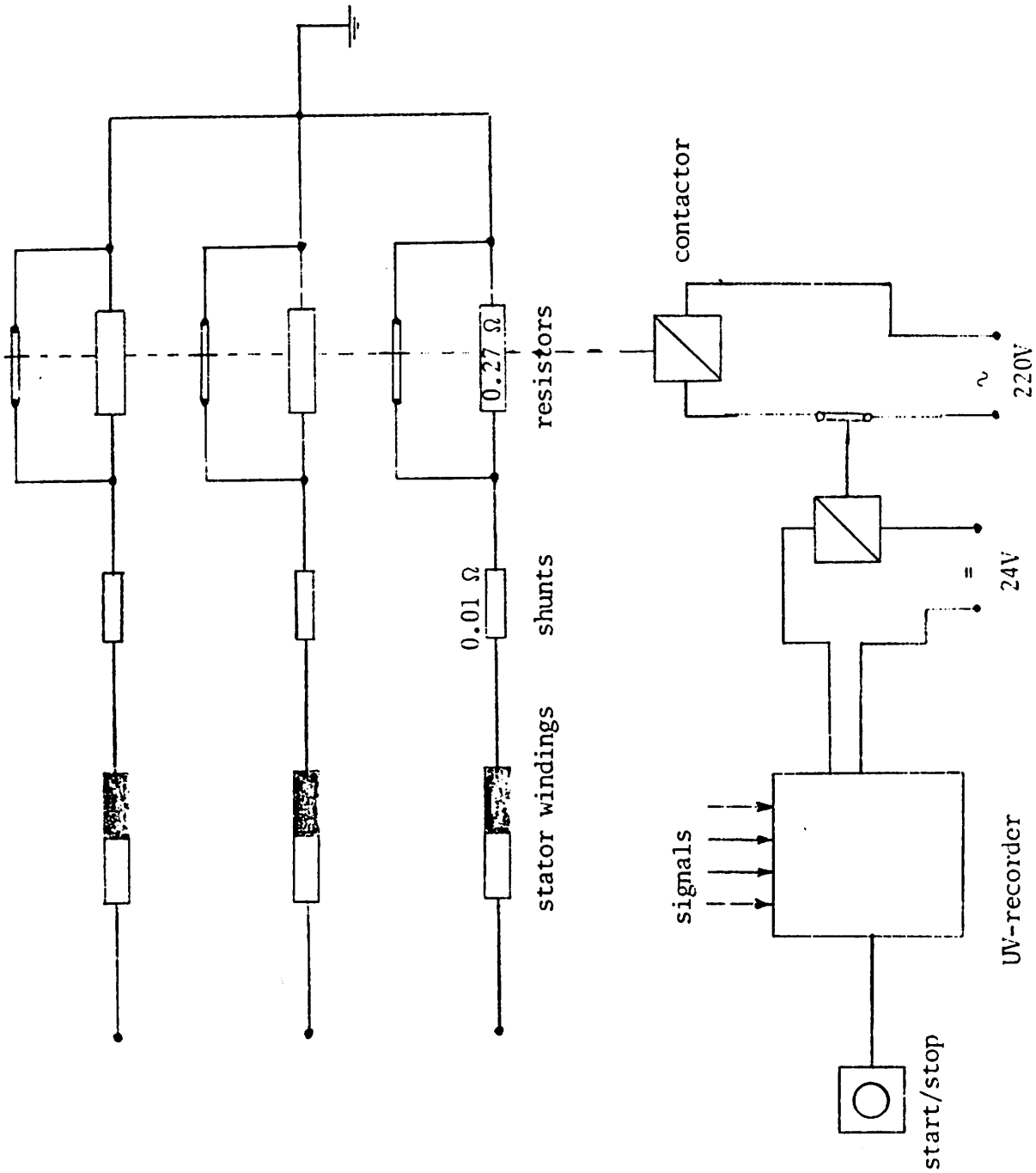

Fig. 3 The measuring circuit

The start of the process can be pre-setted with arbitrary delay in relation to the start of the registration. One of the advantages of this system is the possibility to record the signals both before and after the switching of the resistors.

4. Measurement conditions

The weather conditions were rather bad during the measurements. The wind velocity was about 5-7 m/s and therefore the power output of the generator was under the rated level. Rated output calls for wind velocity about 10 m/s.

5. Comments on the measurement results

The results of the measurements are presented on page 8-9.

The difference between the cases shown is the power output before switching of the resistors.
The graphs shows one phase current, the generator speed and the active power. (The torque signal was temporarily missing). An arrow indicates the start of the switching process.

Comments on page 8 :
Before the switching of the resistors the generator speed was about 1513 r/min, the phase current about 65 A and the active power output 25 kW.
As the oscillogram shows,the switching results in a damped oscillation. The maximum variation of the generator speed is about 11 r/min. The value of the current varies between 56 A and 75 A.
The period of the oscillation is about 0.12 s ($f \simeq 8$Hz) and the duration about 0.8 s.

Comments on page 9

In this case the active power output was slightly higher, namely 38 kW. The instant before switching, the generator speed was about 1525 r/min and the machine current 76 A.
The character of the process is the same as in the previous case. The max. and min. values of the current are 63 A and 98 A respectively, maximum change of generator speed is about 16 r/min. The period of oscillation is about 0.12 s (which gives a frequency of 8 Hz.) and the duration is 0.8 s.

Consider fig.4 which shows two operation points of the generator when the prime mover torque is assumed to be constant. Point 1 is the stable point before switching. Point 2 represents the stable operation point with resistors connected to the system.

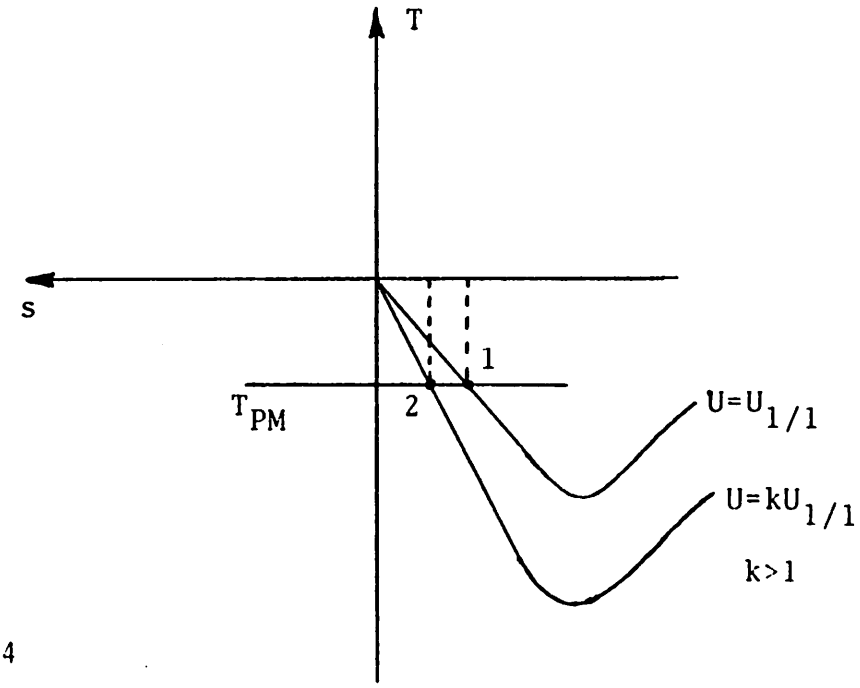

Fig. 4

Transition between these two points does not follow a straight line. Examination of the torque curve of the generator (see p. 10 - 12) shows the transient oscillation which results in swing of geerator speed.

It is fairly clear that switching of resistors does not affect the system stability.

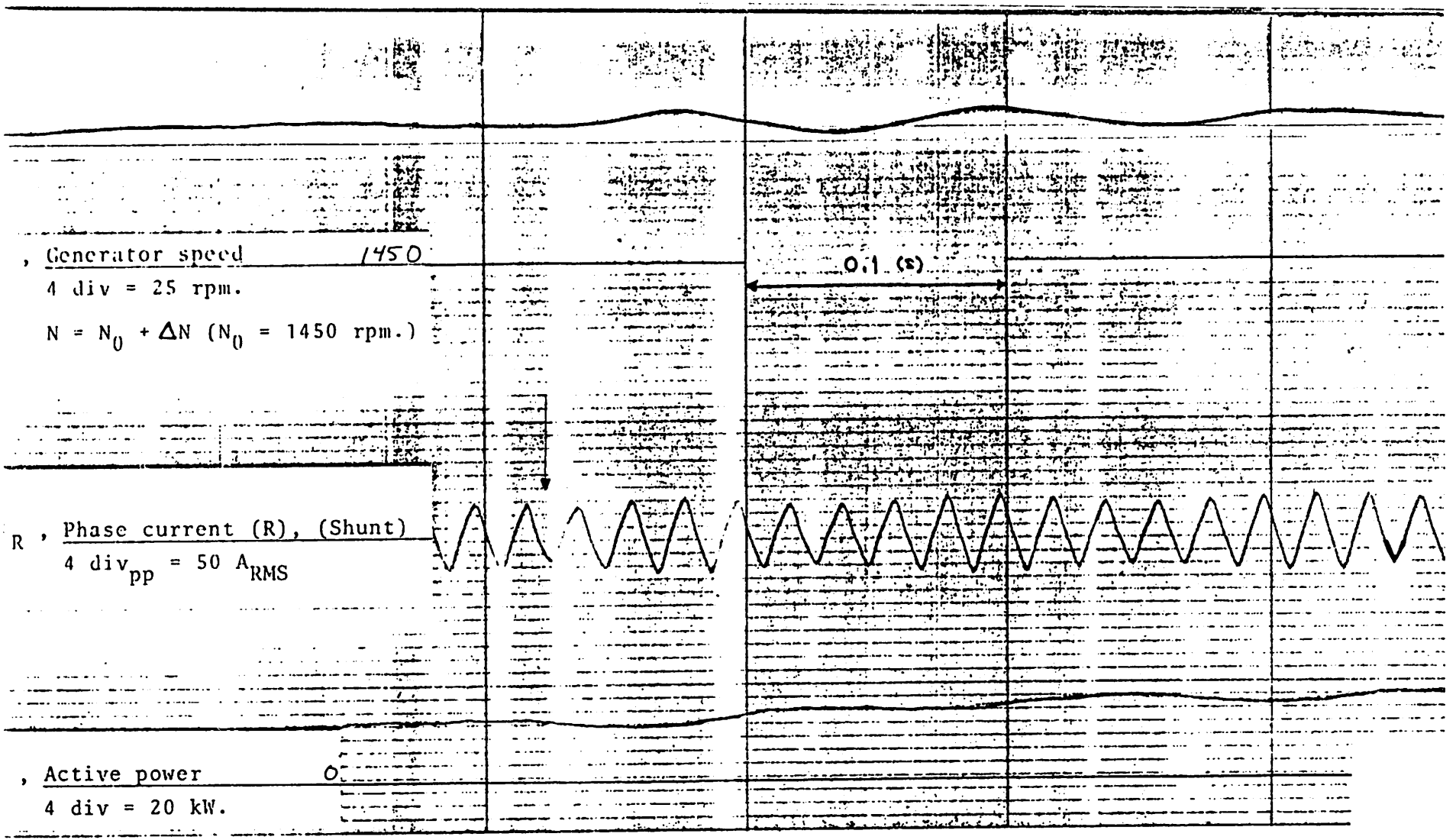

Measurement on 75 - kW asynchrononus machine.

Wind power plant, Kalkugnen, Sweden

Resistor switching 1978 - 03 - 15

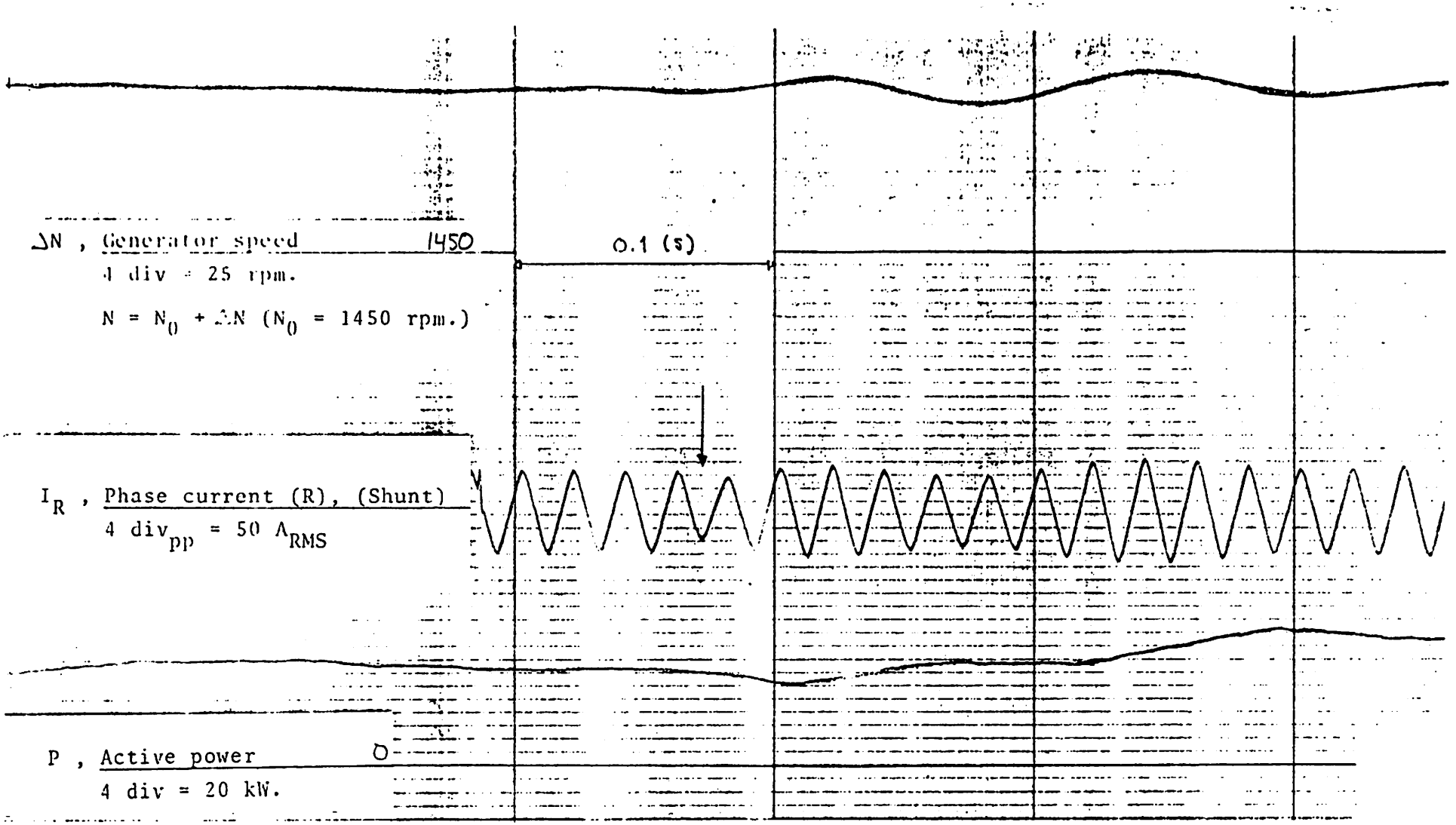

Measurement on 75 - kW asynchrononus machine.

Wind power plant, Kalkugnen, Sweden

Resistor switching 1978 - 03 - 15

PECAP

ELECTRICAL MACHINERY

CHALMERS

AT 1713 1/11 1977.

USER'S SYMBOLS:

I (1) = Ø

I (6) = ω

U (15) = Δ

I(1) = I_R (A)

I(6) = N (el.rad/s)

U(15) = T (Nm)

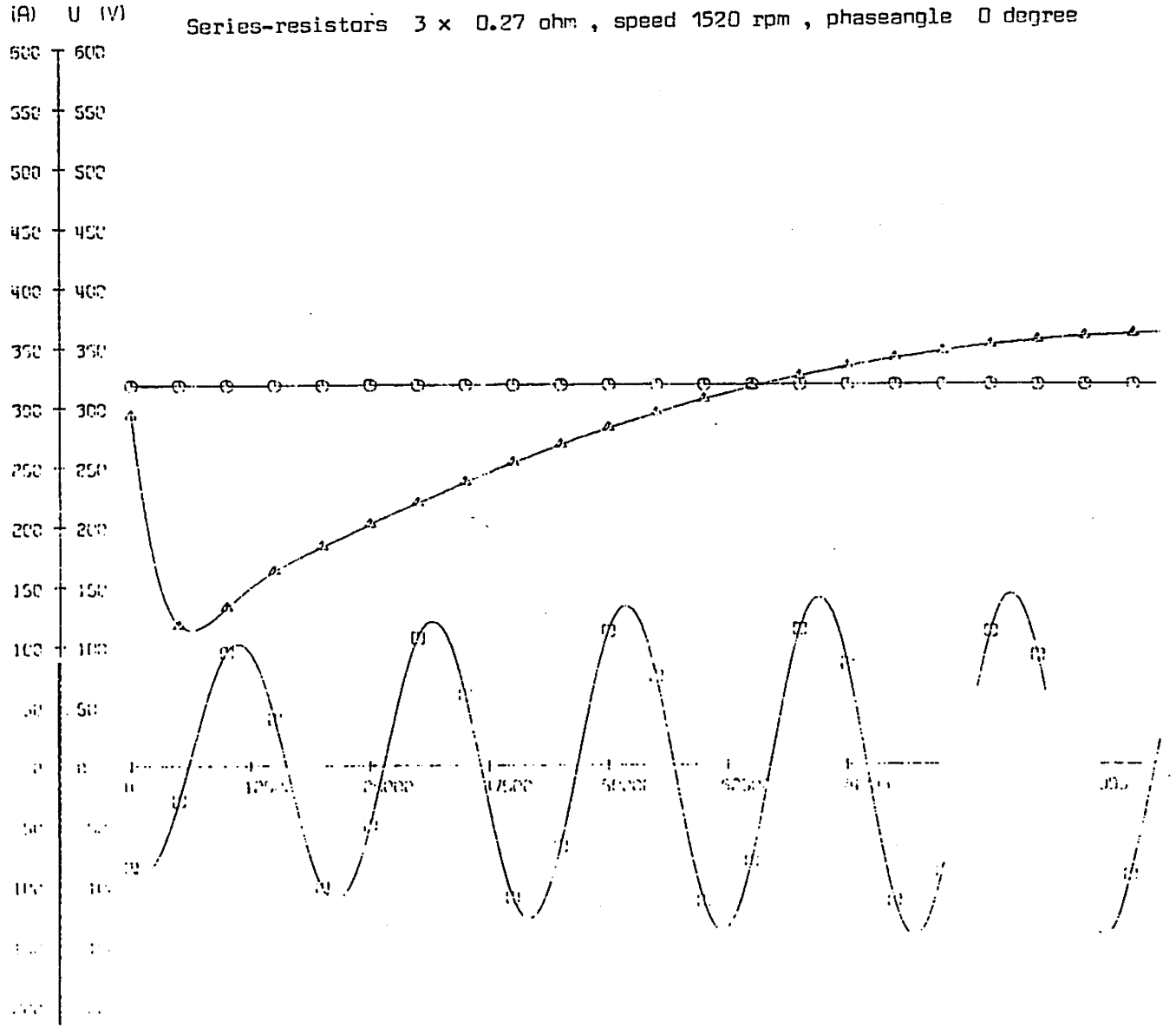

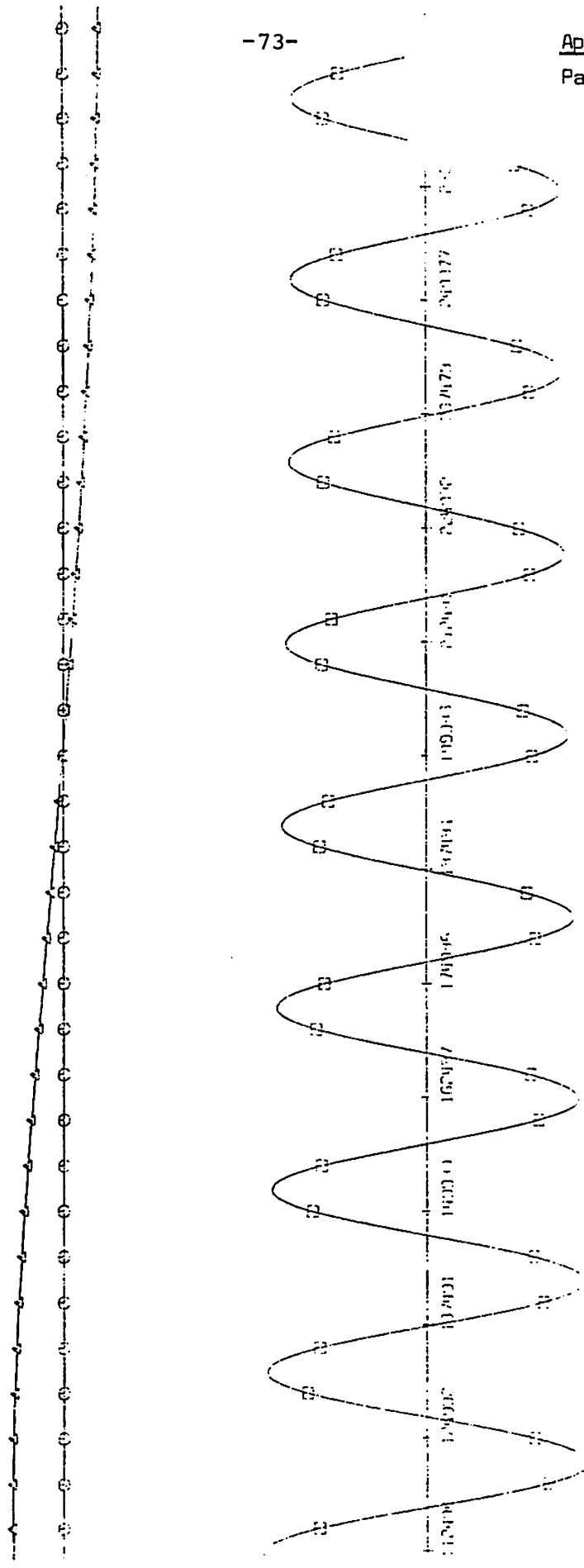

Results of measurements with measuring computer

(The measurements have been made by the staff of LTH)

The measured quantities are recorded by switching the generator into the network. The recorded quantities are : phasecurrent, torque , wind speed , reactive power and active power.

The calibration in y-direction is :

current	12.8	A/div
torque	125	Nm/div
wind speed	2.56	m/s /div
reactive power	6.4	kVAr/div
active power	12.8	kW/div

The torque-curve has its zero-line 8 division above the x-axis, and also the curve of active power.

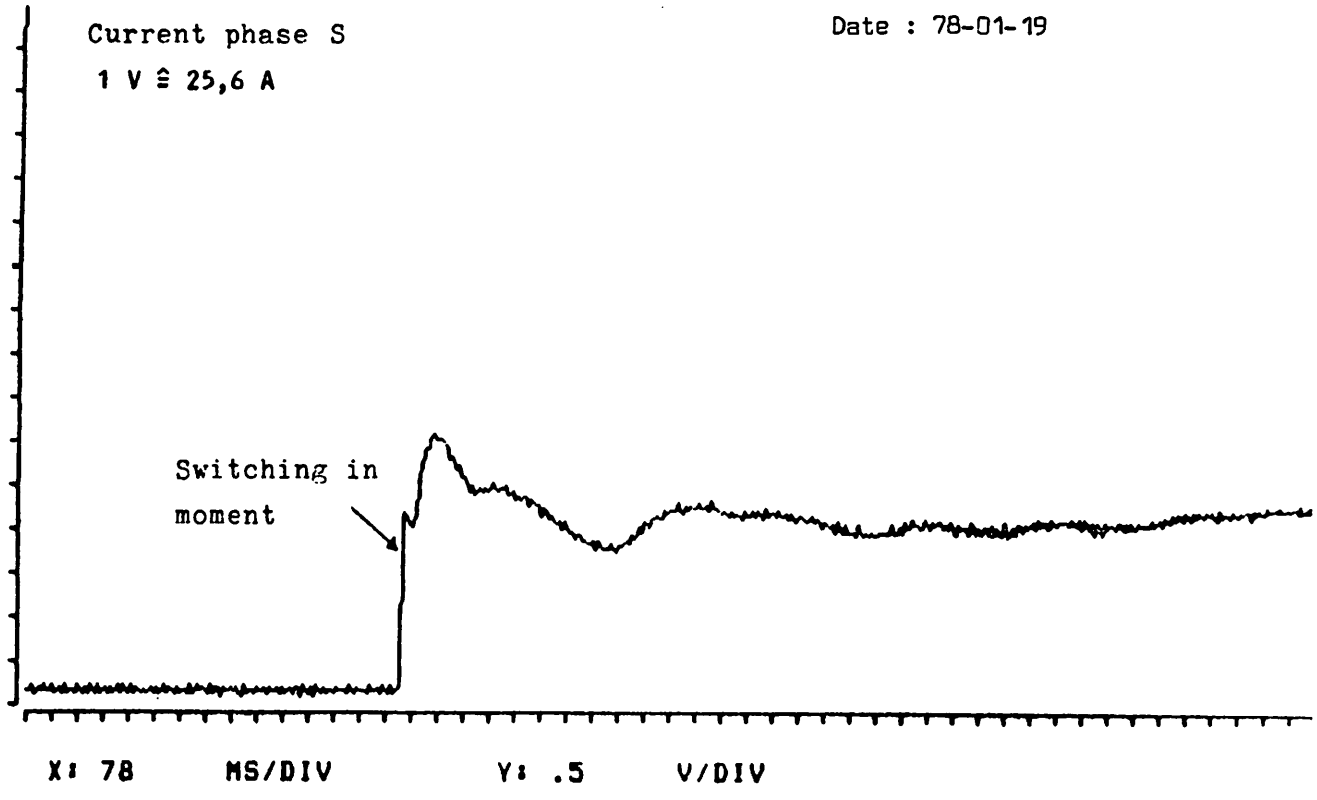
Current phase S
1 V ≙ 25,6 A
Date : 78-01-19
Switching in moment
X: 78 MS/DIV
Y: .5 V/DIV

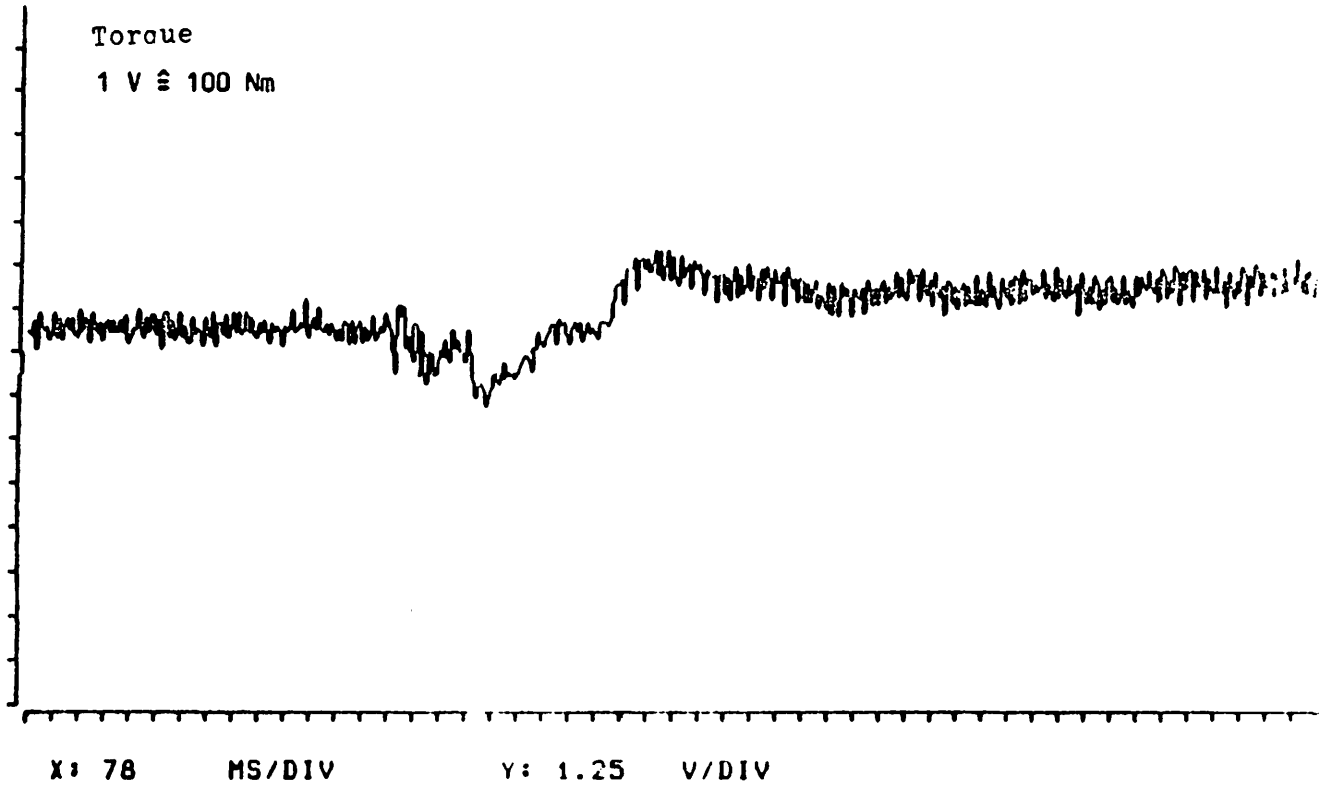
Torque
1 V ≙ 100 Nm
X: 78 MS/DIV
Y: 1.25 V/DIV

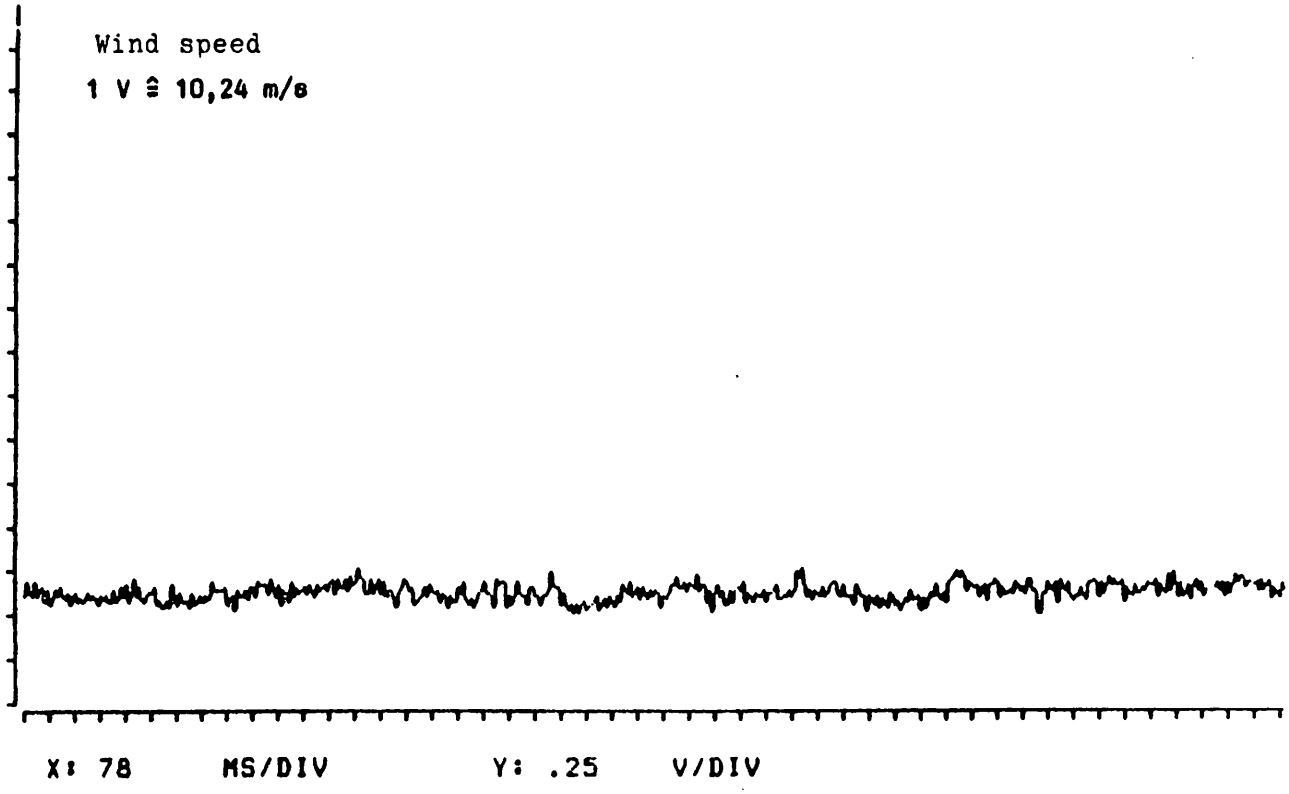
Wind speed
1 V ≙ 10,24 m/s
X: 78 MS/DIV
Y: .25 V/DIV

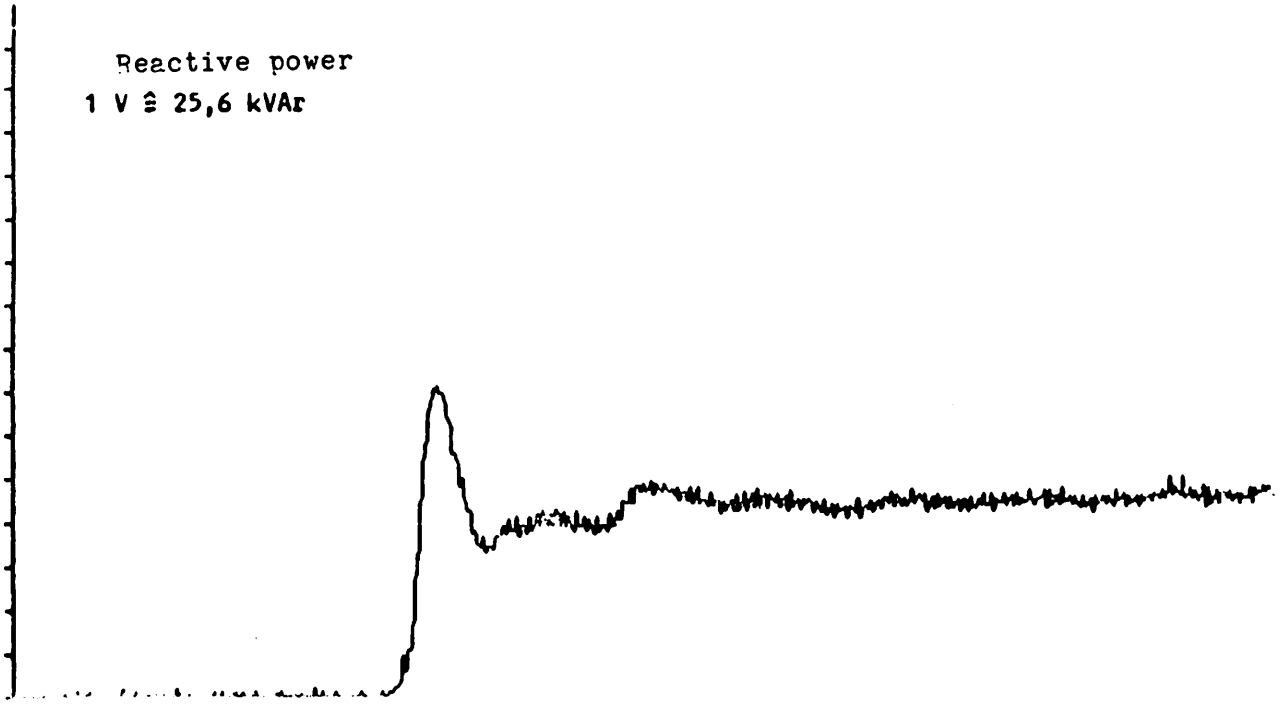
Reactive power
1 V ≙ 25,6 kVAr

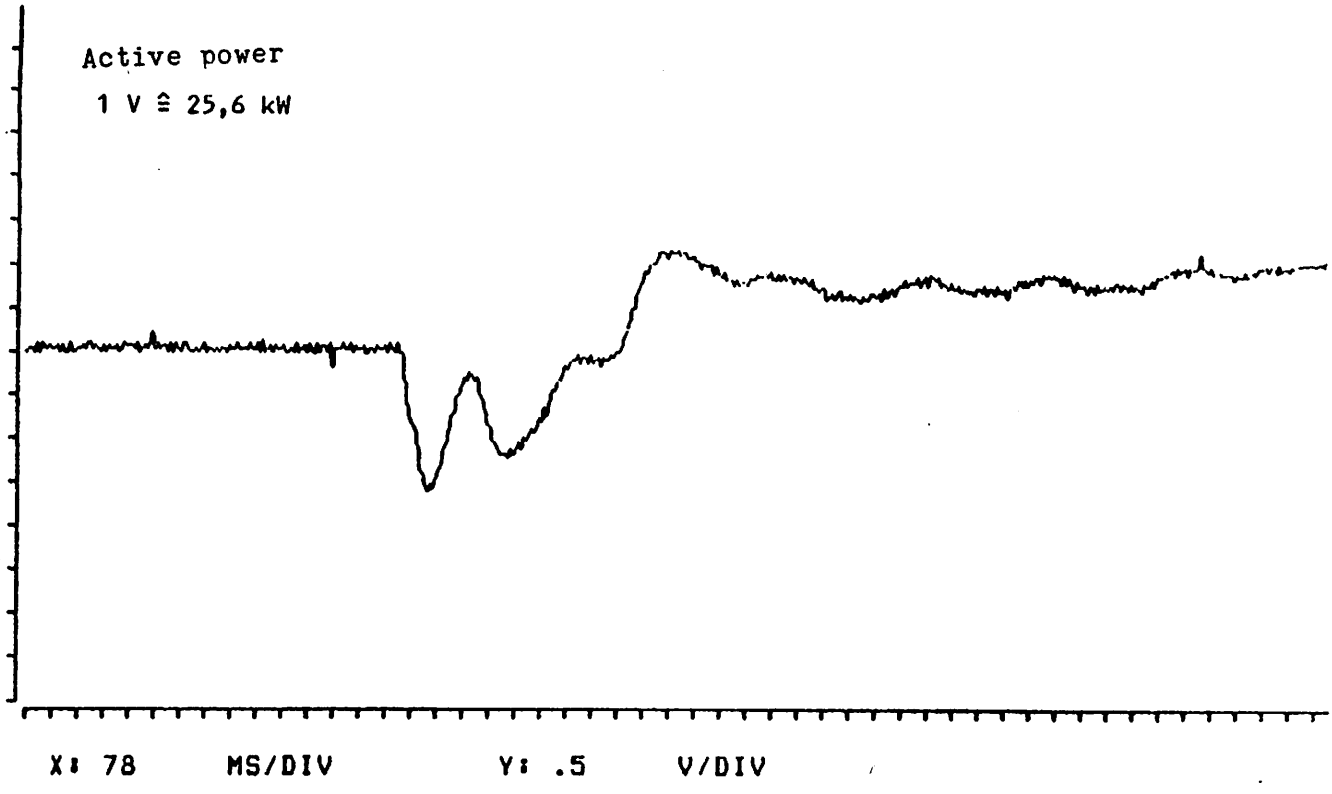
Active power
1 V ≙ 25,6 kW
X: 78 MS/DIV
Y: .5 V/DIV

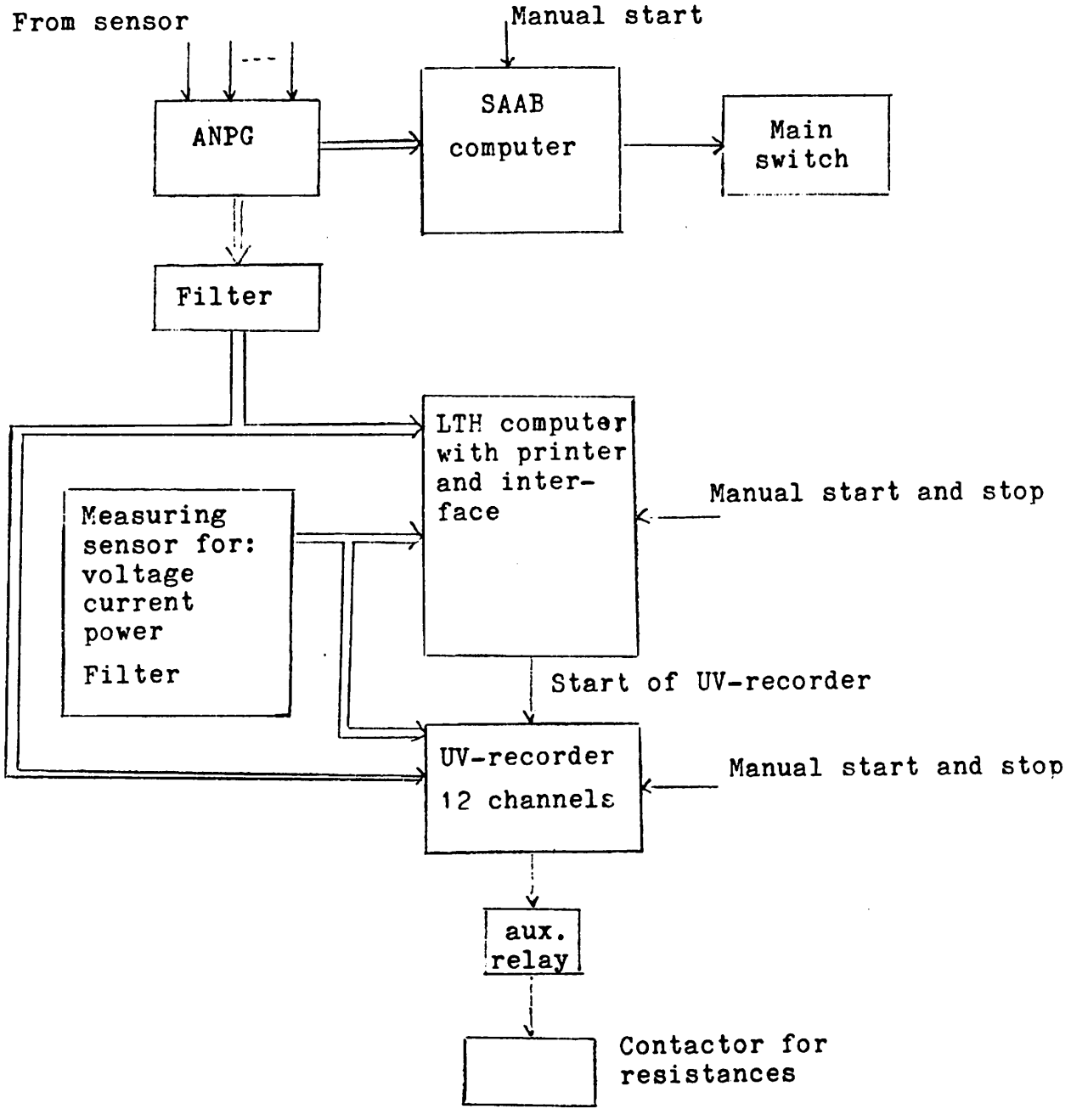

Principal connection of the measuring units

Appendix 7
Page 1

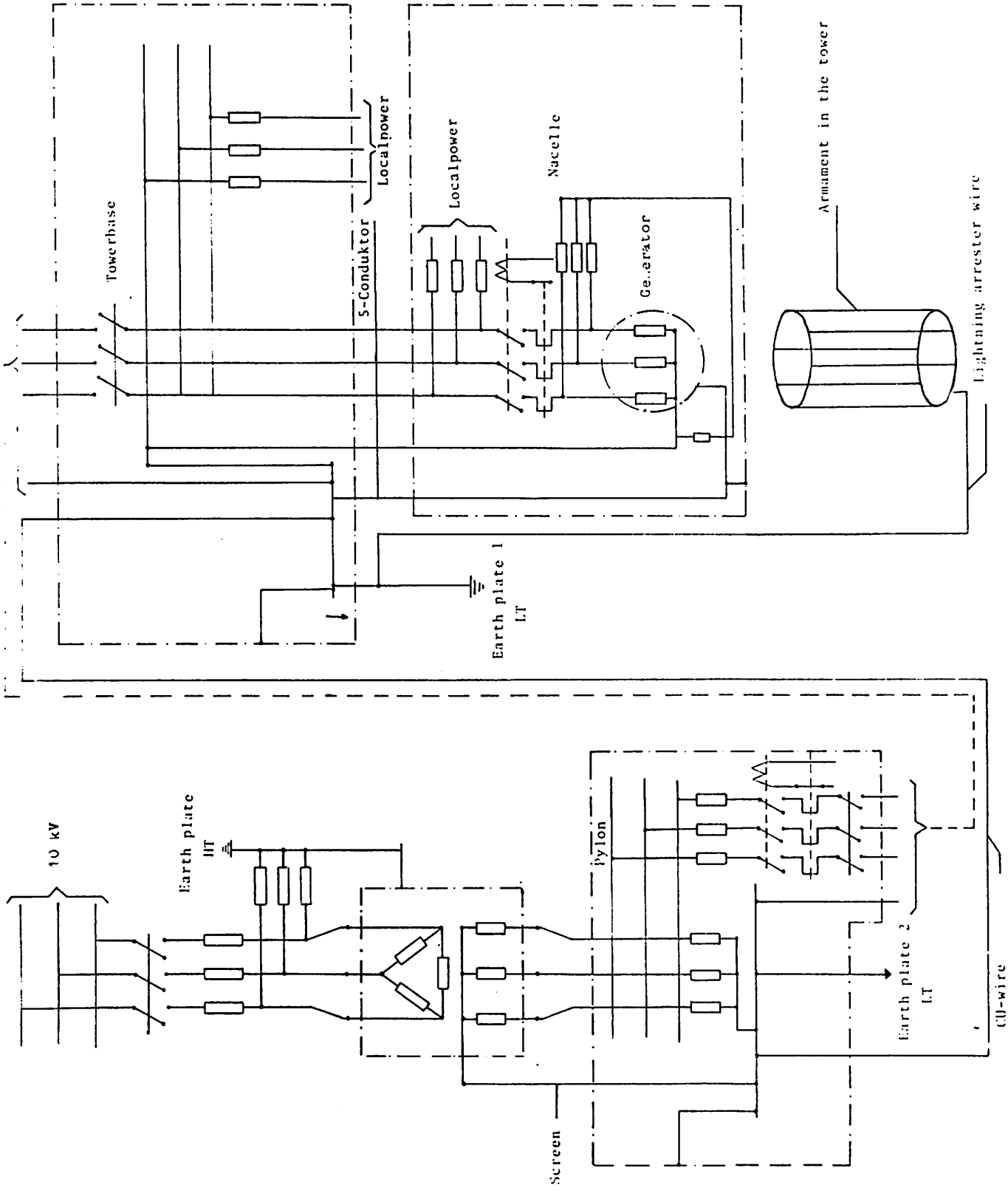

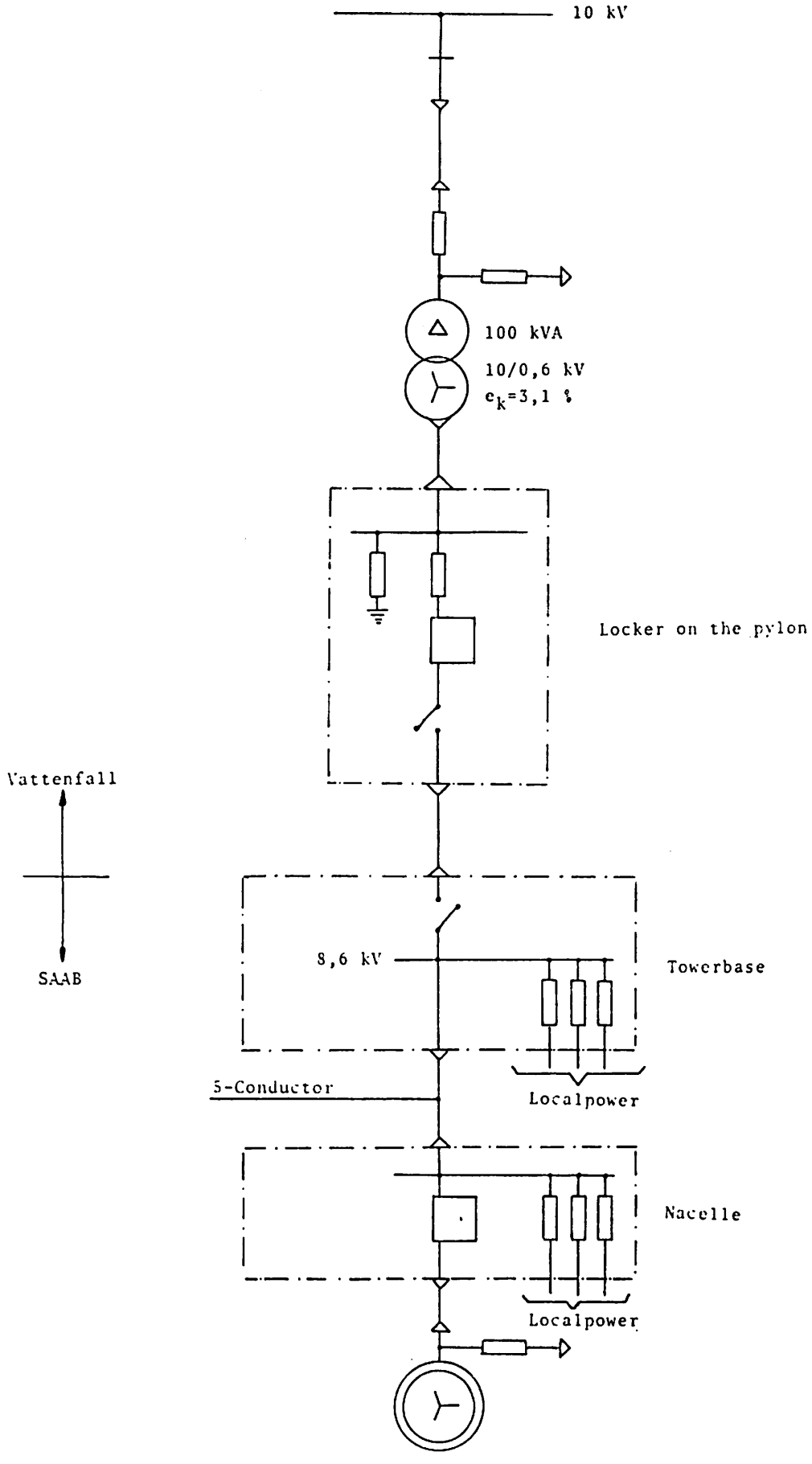
10 kV
100 kVA
10/0,6 kV
e_k=3,1 %
Locker on the pylon
Vattenfall
SAAB
8,6 kV
Towerbase
5-Conductor
Localpower
Nacelle
Localpower

LIST OF MEASURING EQUIPMENT

1. In the unit existing equipment.

   a) Current transformers 3

      600/1 A kl 0,5 10 VA

   b) Voltage transformers 3

      $200/\frac{100}{\sqrt{3}}$ V 30 VA

2. From ITH/CTH used equipment.

   a) Measuring shunts 3

      150 A 60 mV for connection in the zero point of the generator

   b) Current transformers 3

      100/5 A 30 VA for connection in the zero point of the generator

   c) Voltage transformers. 1

      for measurement of reactive power with electronic wattmeter

   d) Analogous instruments.

      Hall-wattmeter 3-phase 1

      Electronic wattmeter 1-phase 1

      RMS transformer 2

      Speed rate control 1

      UV-recorder 12 channels 1

      Temperature-meter, digital 1

      Slip-meter 1

   e) Measuring computer with printer and interface.

f) Peripheral equipment.

Oscilloscope + camera			1
Multimeter			2
Wattmeter	55 V	5 A kl 0,5	3
Voltmeter		kl 0,5	2
Amperemeter		5 A kl 0,5	3
UNIGOR-instrument		kl 1,5	1

g) External manoeuvring device.

Contactor

Impedances (Resistances)

Condensers

MEASURING SIGNALS GIVEN BY SAAB

1. Torque
2. Speed (pulse train respectively analogously)
3. Wind speed
4. Other electrical quantities if wished

U_{pow}, I_{pow}, P, Q and cos ϕ (cos ϕ is calculated)

Measurements on the wind power plant in Kalkugnen at phase compensation with shunt capacitors. 78-10-25

Introduction

The wind power plant in Kalkugnen is equipped with a standard asynchronous generator. This type of generator demands however, reactive power for its function. The reactive power is taken from the net to which the generator is connected. This causes unnecessary losses in the net and voltage drop. It would therefore be desireable to be able to produce reactive power in connection to the place where it is consumed. Statistically it is possible to generate reactive power with capacitor batteries (see ref. 1) which are connected to the generator terminals. This is usually called phase compensation.

In connection with phase compensation of the asynchronous generator in the wind power plant in Kalkugnen a series of measurements has been carried out. These intend to illustrate the conditions prevailing when the shunt capacitors are connected to the generator. The measurements show stationary as well as transient phenomena.

Description of the power circuit

The asynchronous generator used in Kalkugnen has following rated data:

type MBK 250 S-4 (ASEA)
rated power P_{2n} = 75 kW
rated current I_n = 145 A
rated voltage U_n = 380 V
rated speed n_1 = 1540 r/min

When the measurements were carried out the generator was connected to a 10 kV-net by three transformers (0,4/10 kV, S_n = 100 kVA) see fig. 1. The purpose of the two extra transformers was to soften the net, i.e. reduce the short-circuit power, so that the tendencies at measurements on transient phenomena should be strengthened.

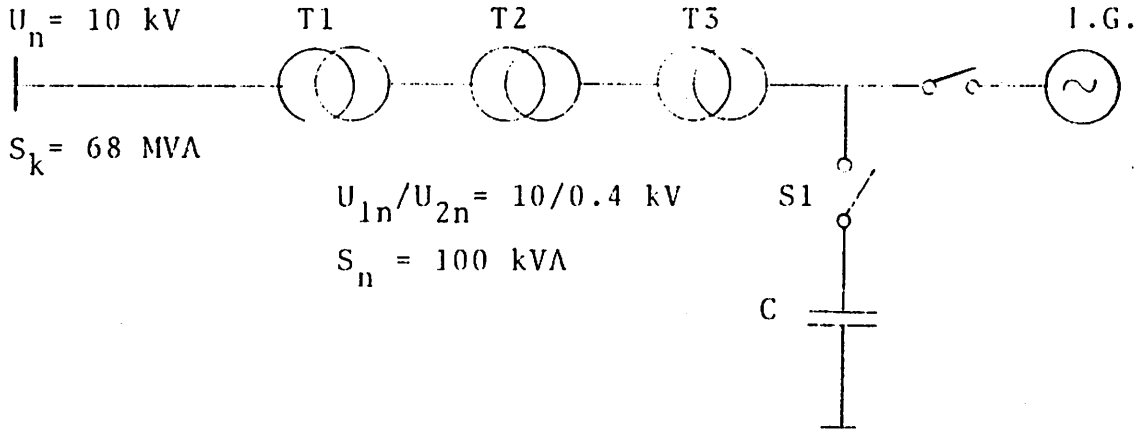

Fig. 1 The appearance of the power circuit

A Δ-connected shunt capacitor battery was placed according to fig. 1. The battery could be switched in and off aided by a hand manoevered switch (k2).

The capacitor battery was so dimensioned that the generator was almost fully compensated at rated operation. ($\because \cos \varphi \approx 1$ at rated operation). It was built up of 68 μF-capacitors connected so that it made a total of 1122 μF/phase (see fig. 2).

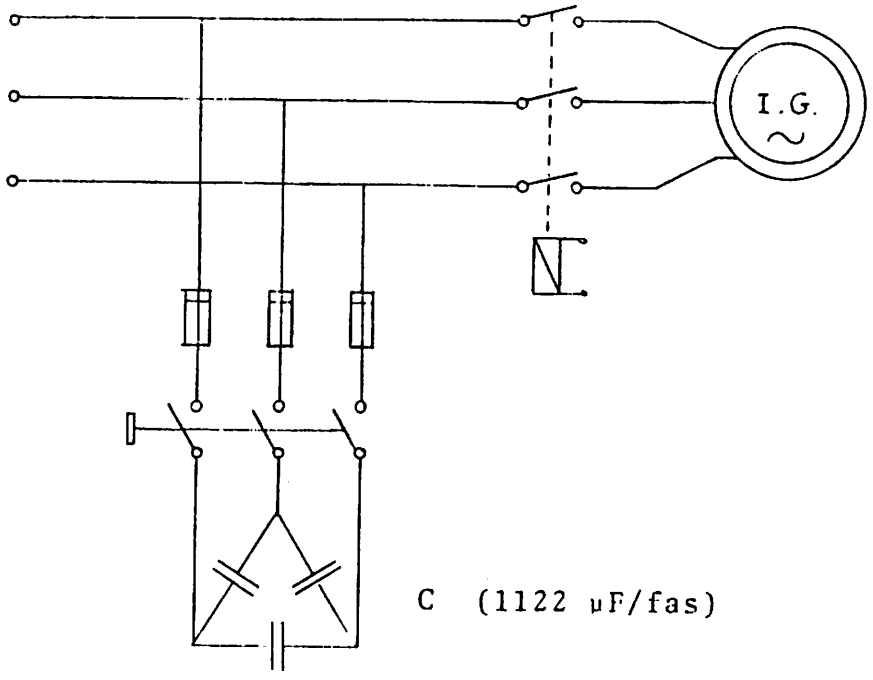

Fig. 2 The principal appearance of the capacitor battery

Description of measuring circuits and measuring equipment

For measuring of stationary voltages a digital voltmeter was used, it was connected to a connection plinth near the capacitor switch. The stationary currents were measured by using current transformer and amperemeter. The current transformers were placed in one and the same phase according to fig. 3 (I) for measuring af the net current, (II) the generator current and (III) the capacitor current.

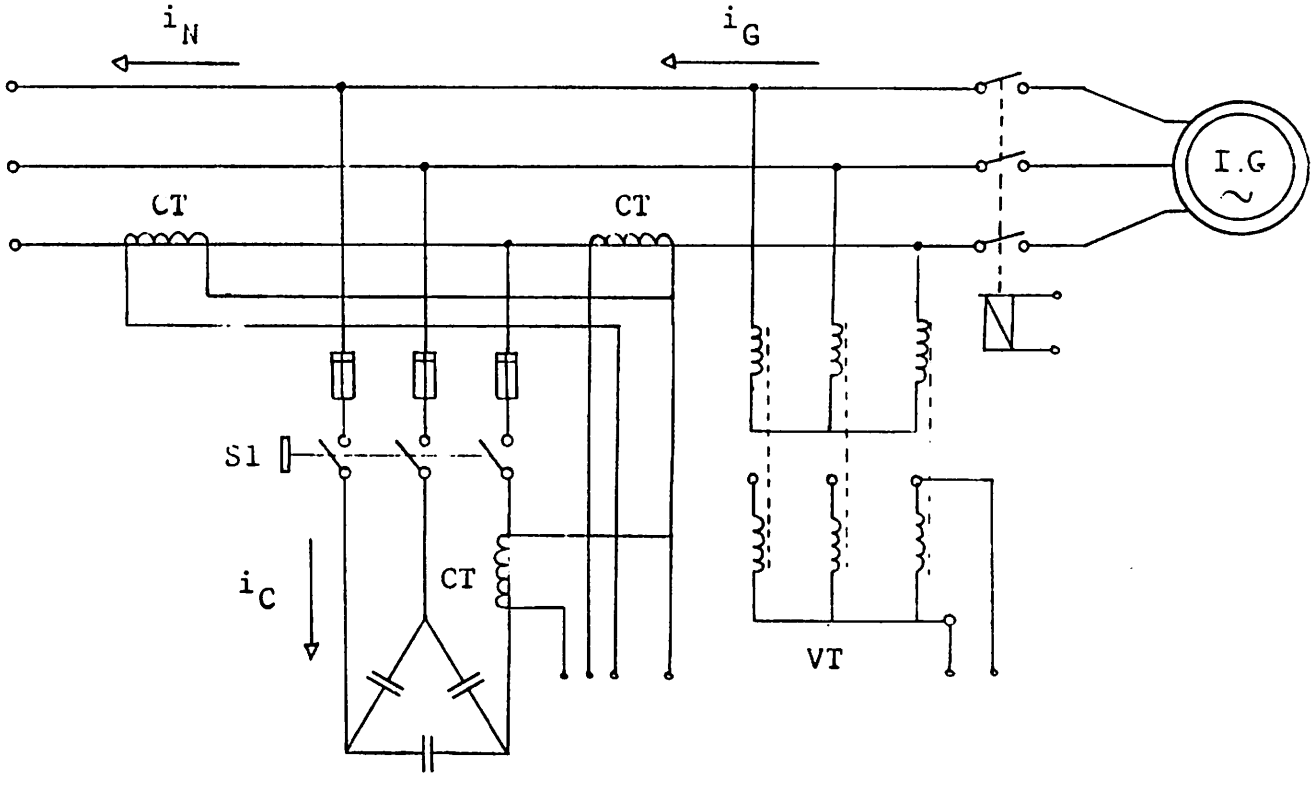

Fig. 3 The placing of the measuring transformers

The secondary circuits of the current transformers were loaded with an amperemeter and a measuring shunt of 0,01 ohm. The voltage over these shunts was amplified and recorded by using a multi-channel UV-recorder. The generator voltage was connected to the UV-recorder by a voltage transformer.

The above mentioned equipment made it possible to measure transient phenomena at switching in and off generator and capacitor battery. Upper limiting frequency of the loops of the UV-recorder was 1 kHz.

Other signals of intererest such as generator speed, wind speed etc. were obtained from sensors installed by SAAB.

The measuring equipment was placed in a building beside the wind power plant, where measuring cables were extended. Since the UV-recorder must be started before the phenomenon which is to be recorded, a remote control cable was drawn to the tower foot and further to the capacitor switch. This way the UV-recorder could be started some second before the manoeuvring of the capacitor switch.

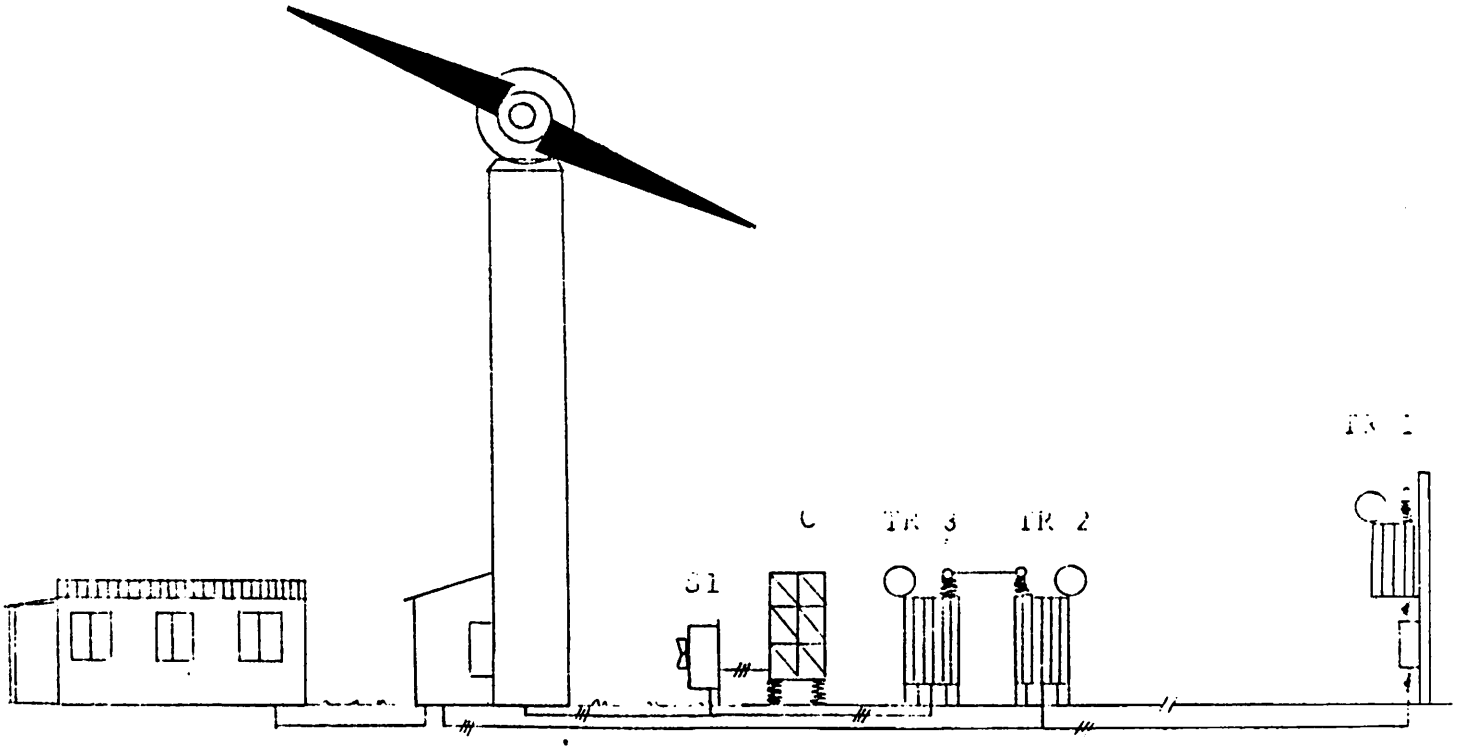

Fig. 4 Situation plan

Conditions

When the measurements were carried out the wind was rather gusty and the wind speed oscillated between 3 - 10 m/s. During most part of the measurements the wind speed was about 5 m/s, which caused a low output power from the wind power plant (5 - 15 kW). The wind power plant was at these measurements equipped with a new turbine hub of not rigid construction.

Stationary measurements

The voltage on the low voltage side of transformer T3 was measured under different conditions (see fig. 1).

I Capacitor battery not connected:
- a) Generator not connected U = 389 V
- b) Generator connected ($P_2 \simeq 10$ kW) U = 383 V

II Capacitor battery connected:
- a) Generator not connected U = 413 V
- b) Generator connected ($P_2 \simeq 10$ kV) U = 406 V

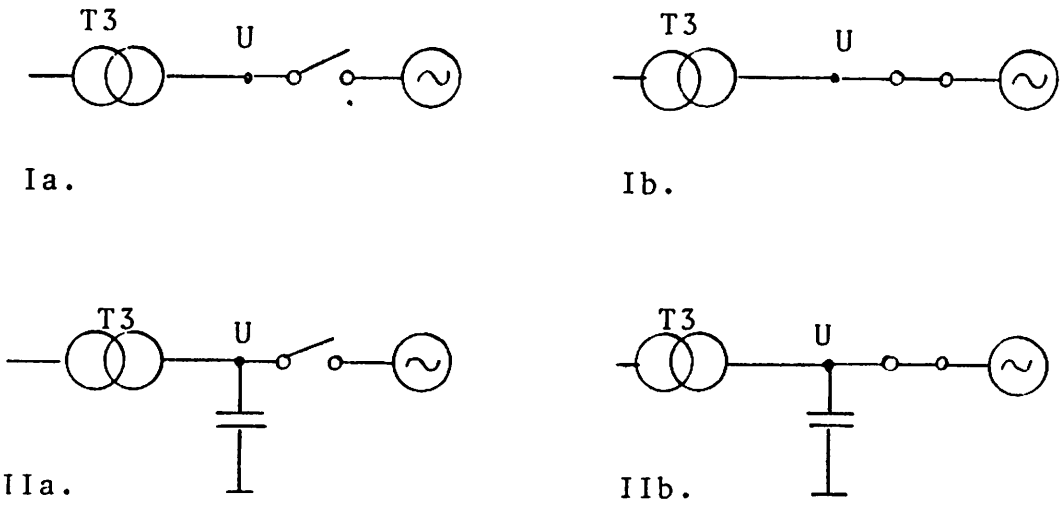

Fig. 5

Capacitor current according to case II a was $I_C = 84$ A/phase

Control calculation:

$$I_C = \frac{U}{\sqrt{3}\, X_C} \qquad X_C = \frac{1}{\omega C} \qquad (1:1)$$

$$I_C = \frac{U}{\sqrt{3}}\, \omega C \qquad (1:2)$$

$U = 413$ V $\qquad \omega = 100\ \pi$

$C = 1122\ \mu$F/phase

$\therefore I_C = 84.1$ A/phase

There is an oscillogram showing generator current, capacitor current and net current at stationary operation in appendix 1. The wind speed was about 10 m/s and the average value of the generator current was about 130 A at the time of recording. This means that the generator is close to rated operation ($i_n = 145$ A). Moreover, the oscillogram shows that the amplitude of the net and generator current varies with the period 0,4 s (f = 2,5 Hz). This phenomenon has been pointed out earlier in ref. 2 (PM HJ 780306). The generator current varies between:

$I_{Gmax} \approx 140$ A $\qquad I_{Gmin} \approx 120$ A

$\Delta I_G = 20$ A

$\therefore \pm 7{,}7$ % in relation to the average value 130 A

The currents are not sinusodial but contain some harmonics, where the 5 th harmonic is most apparent.

The oscillogram in appendix 2 shows a transient phenomenon at switching in of the capacitor battery, but it also shows the outlook of the stationary currents before and after the switching in.

The capacitor and the net current show most apparently their contents of the 5 th harmonic. Further it can be seen that the net current decreases when the capacitor battery is switched in but the amount of harmonics increases. The output power of the generator (P_2) was at this measurement about 40 A (the fundamental wave considered) at switching in of the capacitor battery.

Measurements on transient phenomena

These measurements were carried out in order to measure the switching transients and to compare these with computer calculations. When the wind power plant is switched to and off the net depending on the wind conditions, those transients which often may occur on the net must be considered.

At switching in of the uncompensated generator there was a voltage drop of about 20 % (see PM HJ 780306). The picture gets complicated when a capacitor battery is connected to the system. Three different ways of connecting a shunt capacitor battery to the wind power plant can be considered.

A. The capacitor battery permanently connected to the net

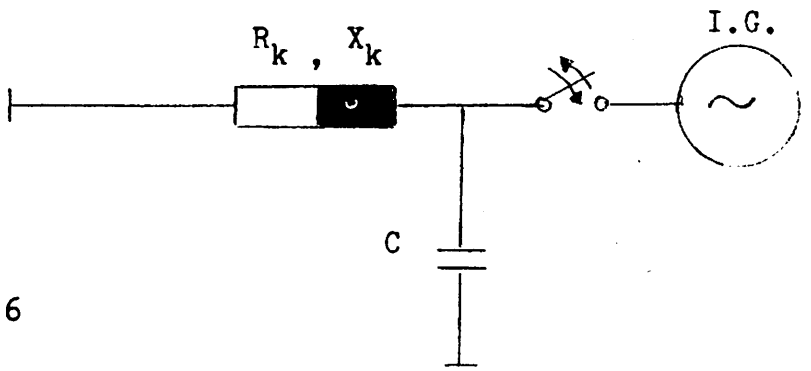

Fig. 6

The capacitor battery is here connected to the net all the time and supplies reactive power to the net when the generator is not connected. The voltage in the point to which the capacitor is connected will rise. Measurements gave 389 V without capacitor and 413 V with capacitor.

B. The generator is first connected to the net and then the capacitor battery is switched in

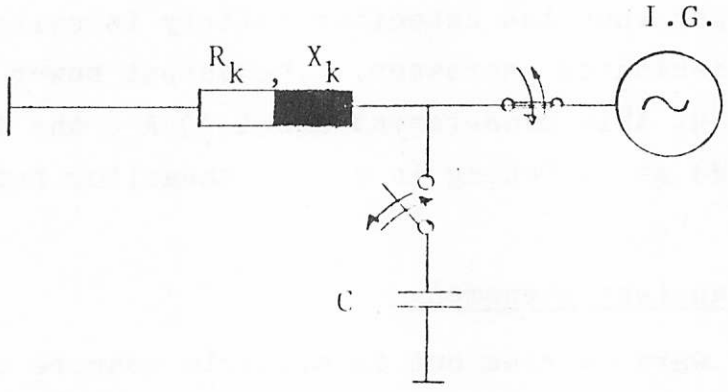

Fig. 7

With this method the capacitor battery is connected only when the generator is connected, i.e. it generates only reactive power during the time in which the wind power plant is operating. Two connecting transients are also obtained with this method.

C. The capacitor battery connected to the generator terminals at switching in

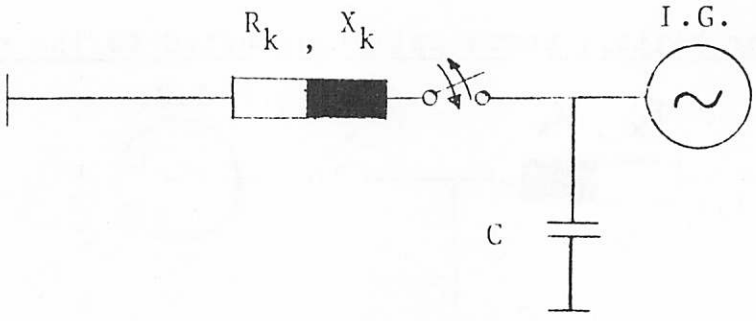

Fig. 8

This method may under certain conditions cause overvoltage on the generator. This phenomenon occurs when the generator is only loaded capacitively. See further chapter "Self-excitation of an induction generator" in ref. 1.

The carried out measurements illustrate the alternatives A and B

Comments to the transient measurements

The transient phenomena which occur when the capacitor battery is connected to the generator, when this is connected to the net, are shown in appendix 2 and 3. Appendix 2 shows capacitor current, generator current and the net current. It shows that there are transients in all three currents. The highest amplitudes are obtained in the capacitor current. The peak value of the current transients and the frequency of the damped oscillation which occur are determined by the short-circuit power S_k in the point and the power of the shunt battery Q_C. The amplitude of the transient also depends on the phase position of the voltage at the switching in moment.

Since the capacitor battery was switched in by using a hand manoeuvered switch there was no possibility of switching in at a beforehand fixed phase angle so the switching in moment was completely accidental.

In order to verify the calculations the phase angle of the voltage was read on the oscillogram and then the calculation was made.

Appendix 3 shows a switching in when the phase position of the voltage was about 200°.

On comparison with corresponding calculations following is obtained (see appendix 4, 5, 6, 7).

Current 1 pu = $\sqrt{2} \cdot 145$ A

Voltage 1 pu = $\frac{380}{\sqrt{3}}$ V

(The values given below apply for the first transient peak value.)

Parameters	Measurement (pu)	Calculation (pu)
u_G	1,26	1,22
i_C	1,3	1,4
i_G	0,70	0,77
i_N	0,62	0,64

The accordance concerning transient curve form is good. The harmonics which occur in the measurements do not exist in the calculated curves since the computer program only counts with sinusodial sources without harmonics.

Since it is difficult to estimate exact phase position at the switching in and since this affects the amplitudes, a comparison with calculations is only approximative.

Appendix 8 shows a switching off of the capacitor battery. A number of recordings showed that the switch off occurred in the zero passage of the capacitor current, why hardly any transients occurred.

Appendix 9 This measurement connects on to case A in the description. The capacitor is connected to the net and the generator is switched in. The wind speed was low at the measuring occasion for which reason the generator is near the no-load point after the switching in.

On comparison with corresponding calculation for switching in with the phase angle of the voltage of about 25^{o} the following results are obtained (see appendix 10, 11, 12 and 13) :

(The given values apply for the first transient peak value).

current 1 pu = $\sqrt{2}$ 145 A

voltage 1 pu = $\frac{400}{\sqrt{3}}$ V

Parameter	Measurement (pu)	Calculation (pu)
u_G	0,72	0,69
i_C	0,25	0,20
i_G	3,9	4,2
i_N	3,5	3,9

The oscillogram shows that all currents and the voltage contain much harmonics during some 15 periods after the switching in. Notice also the high frequency oscillation of the voltage at the switching in which is damped after some period.

Appendix 14 shows a switching in with contactor start, i.e. the first switching in failed. This occurred remarkably often during the measurements.

Appendix 15 This oscillogram shows the phenomenon at switching off the generator. The current is cut in the zero passage and any grave transients cannot be discovered.

The computer calculations enclosed in appendix are carried out by P. Druzynski.

Gothenburg, November 1978

/Hans Johansson/

References:

(1) P. Druzynski
Shunt-Compensation of Induction Generators
May 1978
Department of Electrical Machinery,
Chalmers University of Technology

Capacitor current (i_C)
1 div_{pp} = 10 A_{eff}

Generator current (i_G)
1 div_{pp} = 10 A_{eff}

Network current (i_N)
1 div_{pp} = 10 A_{eff}

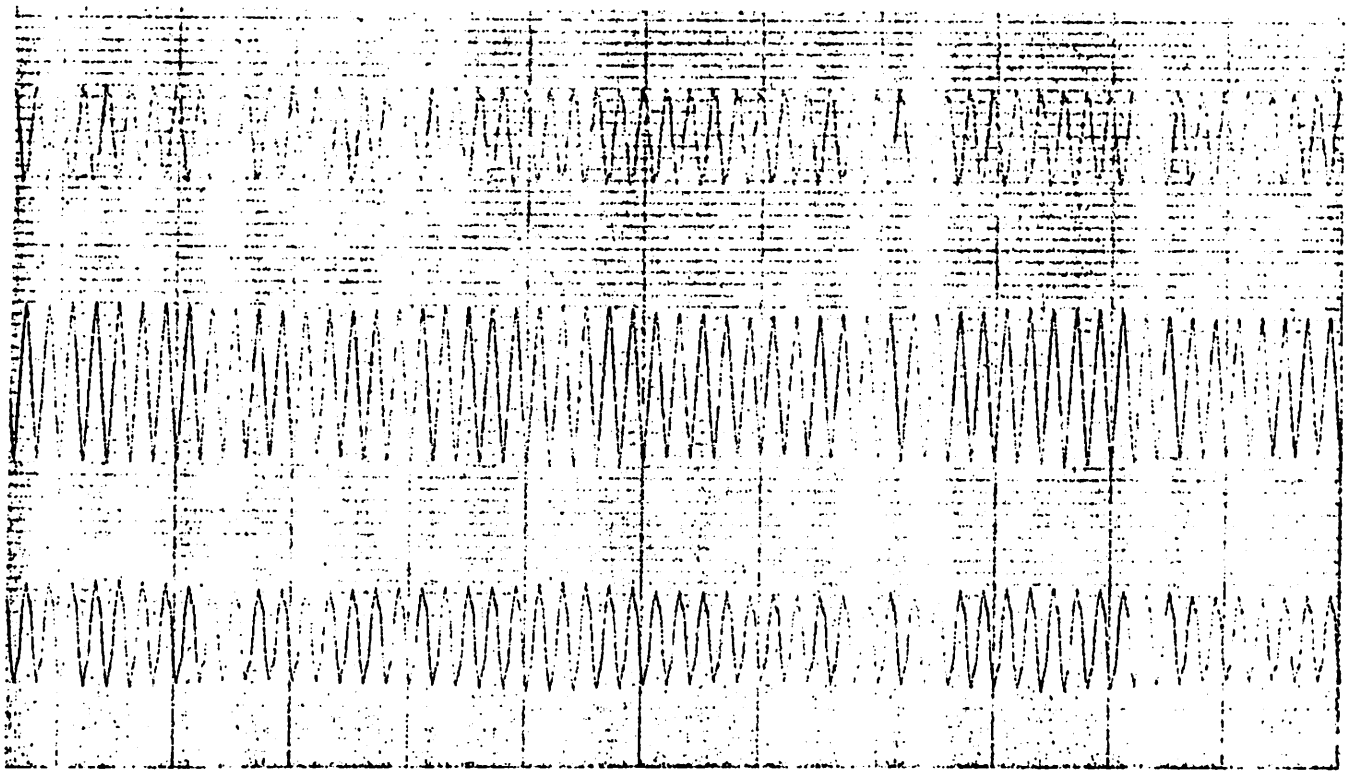

Measurments on the shunt-compensated asynchronous generator in Kalkugnen, Sweden.
Steady state condition. Wind velocity level, about 10 m/s. 1978-10-25.

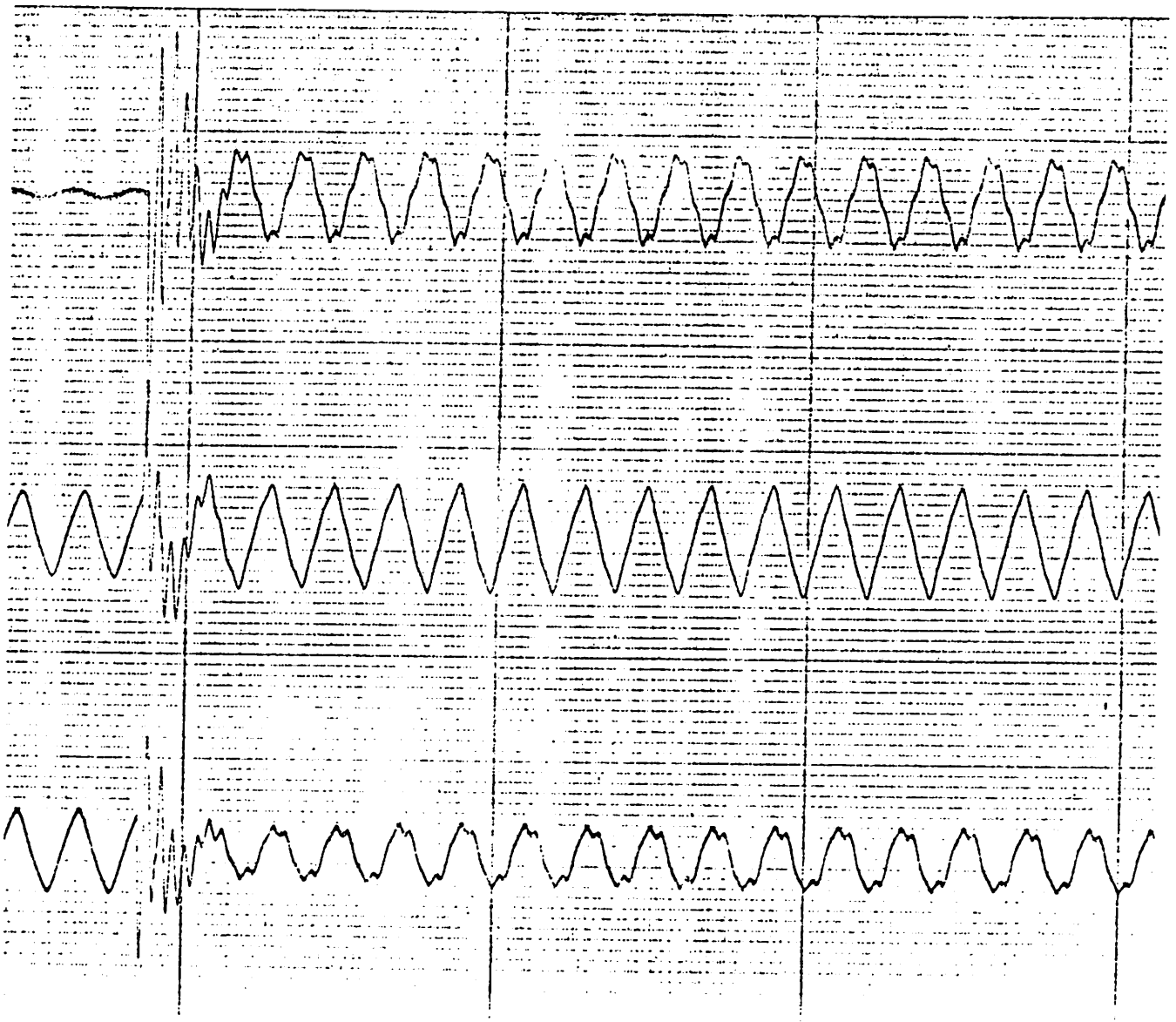

Current transients when switching a shunt - capacitor bank . C_s = 1122 uF Kalkugnen, Sweden 78-10-25

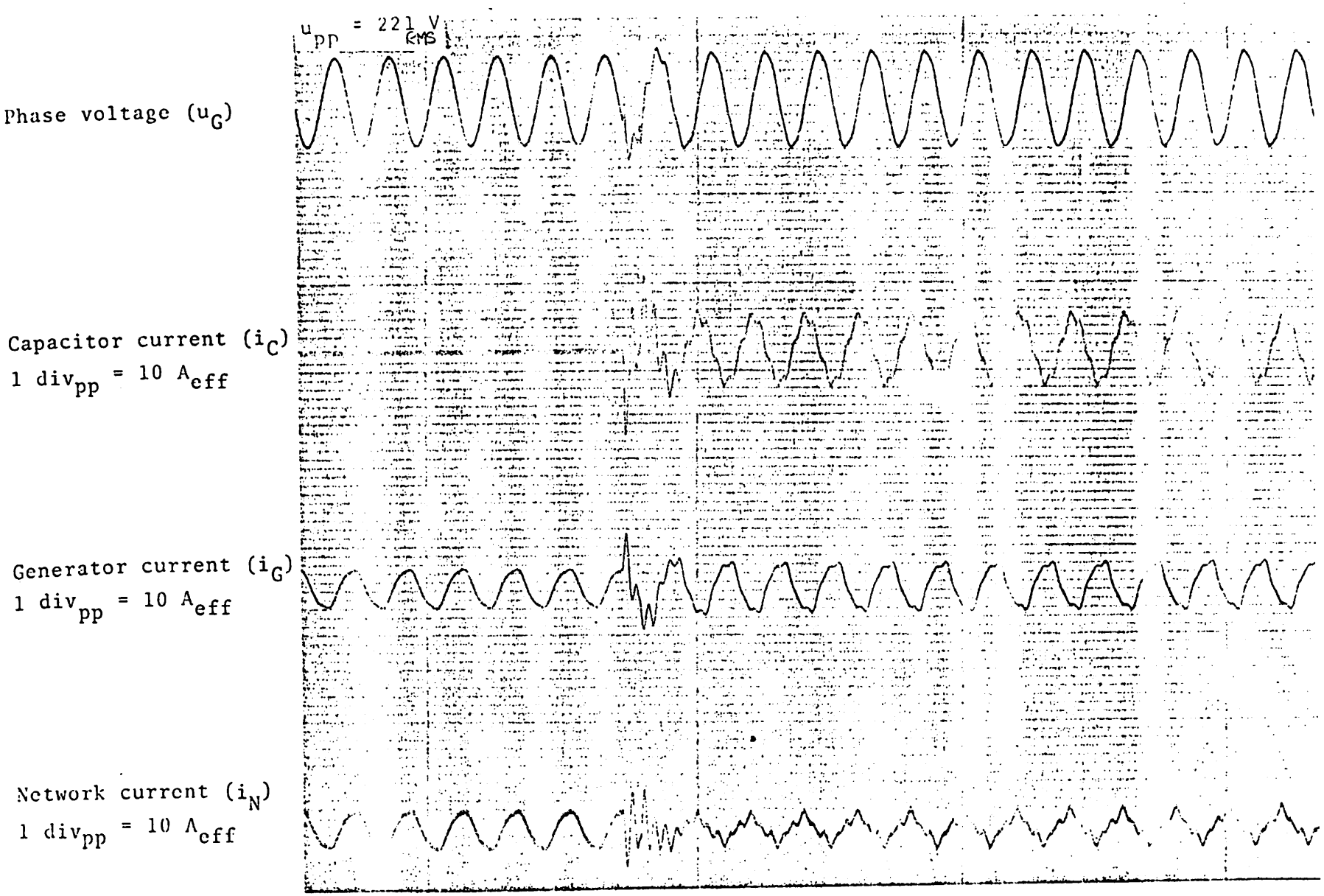

Voltage and current transients when switching a shunt capacitor bank, Kalkugnen Sweden 78-10-25

Appendix 4

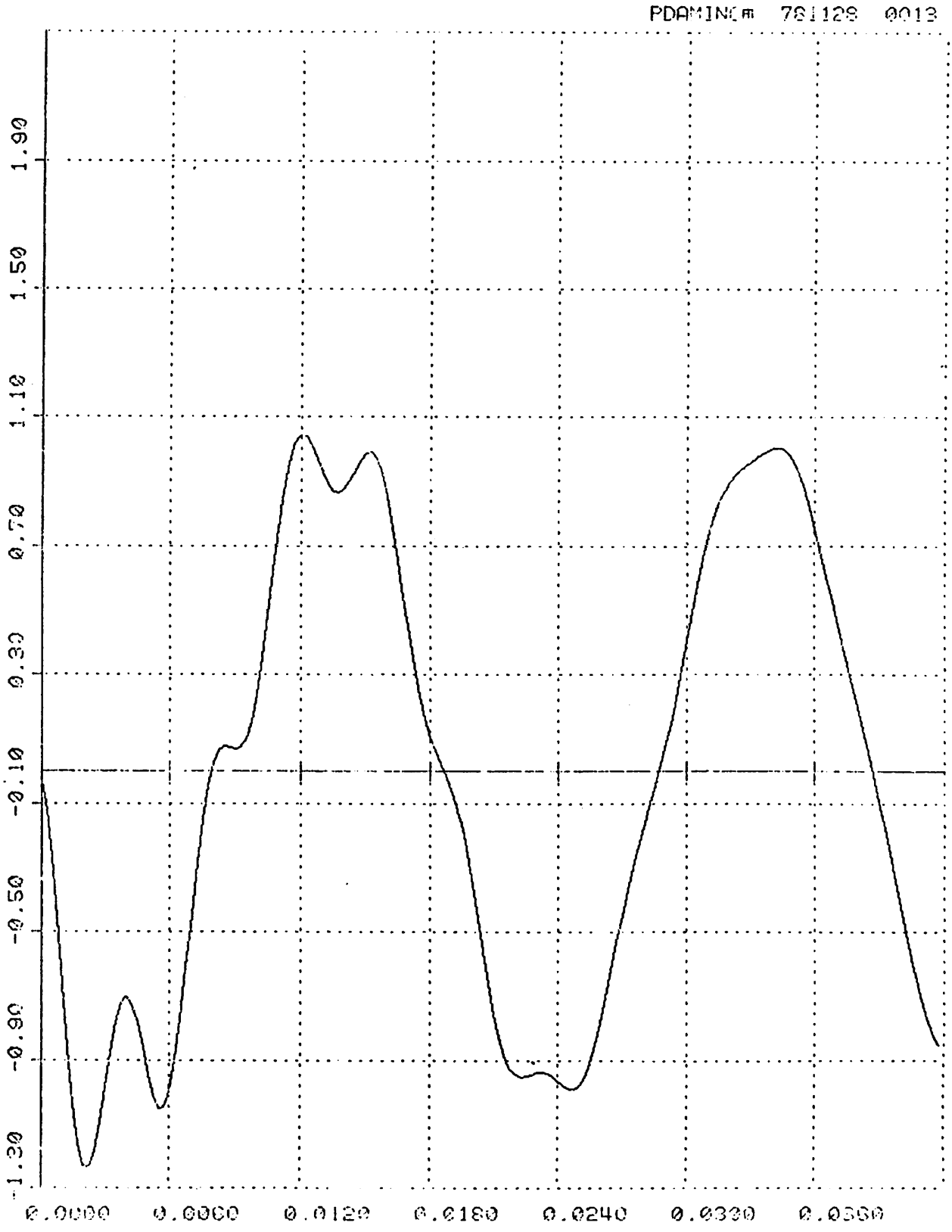

Capacitor voltage u_C , when switching a shunt capacitor bank.

Appendix 5

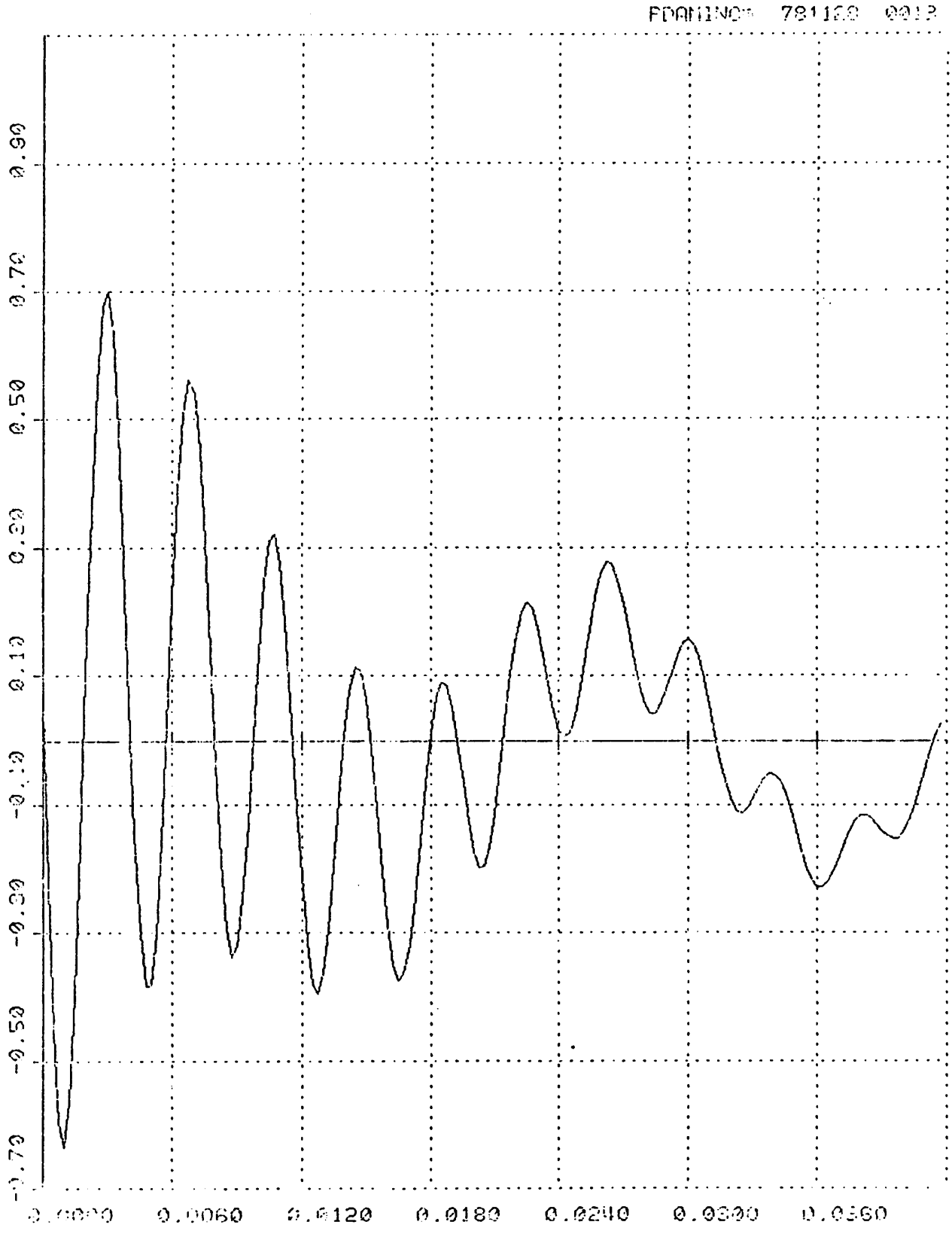

Network current i_N, when switching a shunt capacitor bank.

Appendix 6

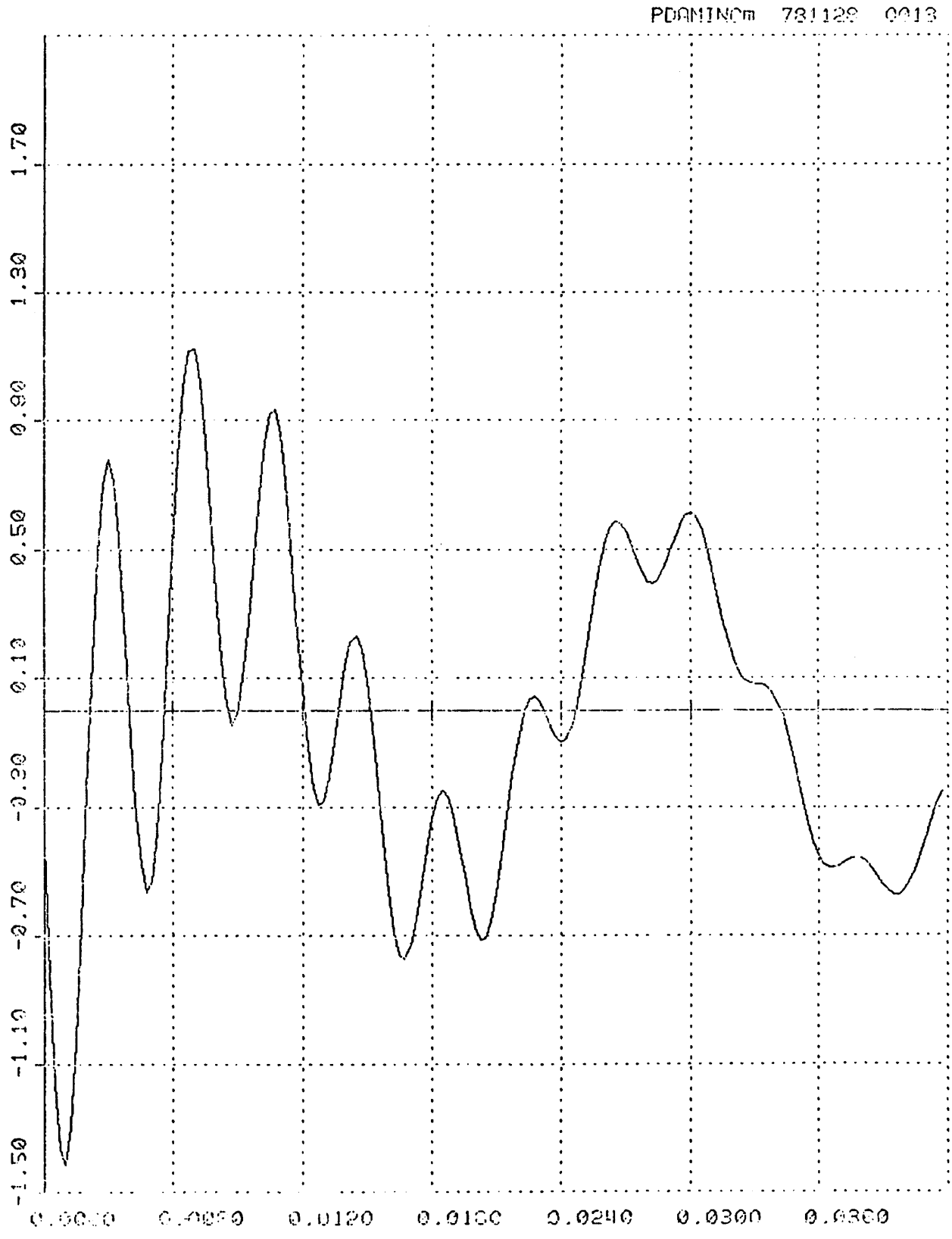

Capacitor current i_C, when witching a shunt capacitor bank.

Appendix 7

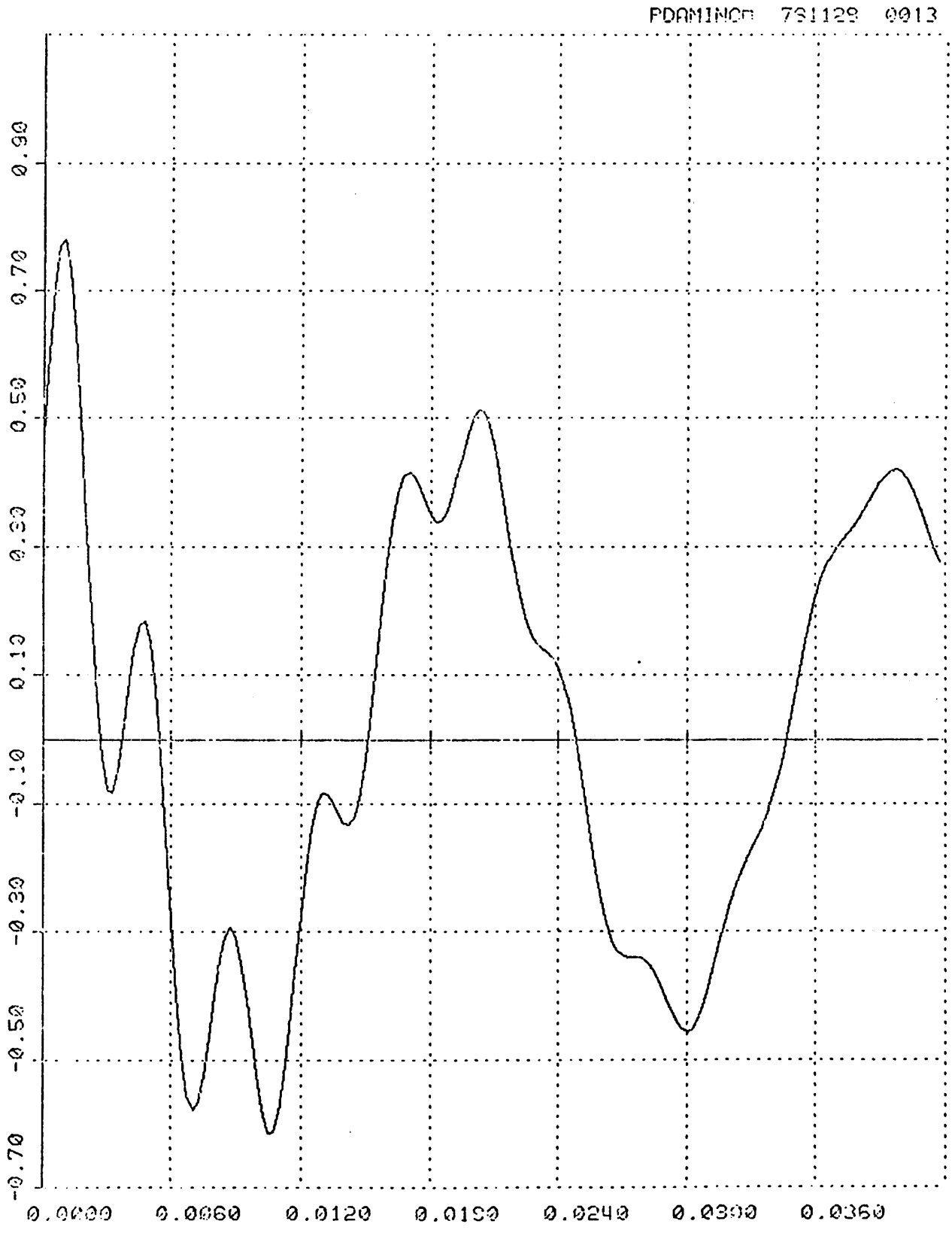

Generator current i_G, when switching a shunt capacitor bank.

$\varphi_{v_{t=0}} = 200^{o}$ 1 pu = $\sqrt{2} \cdot 145$ A

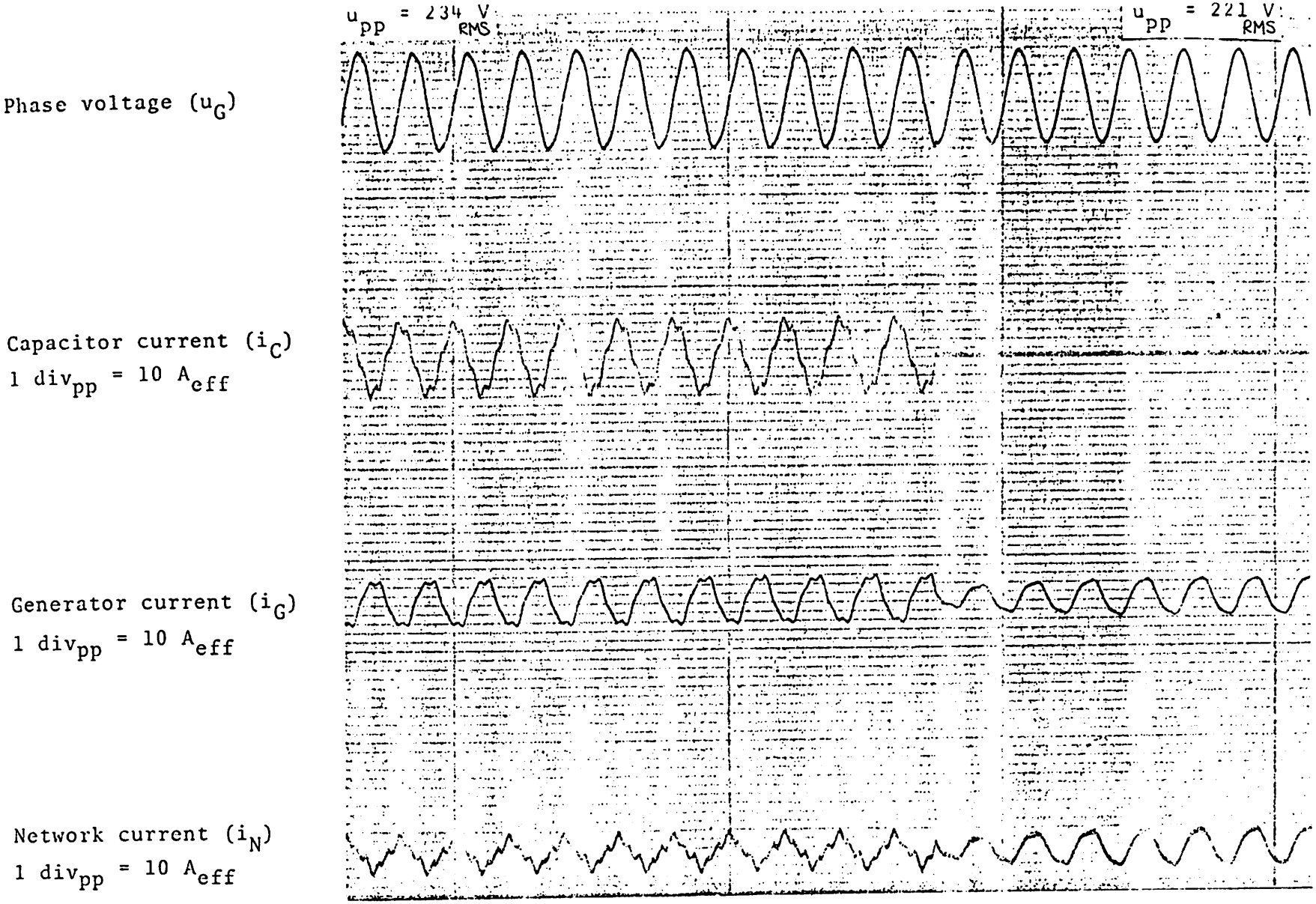

Voltage and current transients when switching a shunt capacitor bank, Kalkugnen Sweden 78-10-25.

Appendix 9

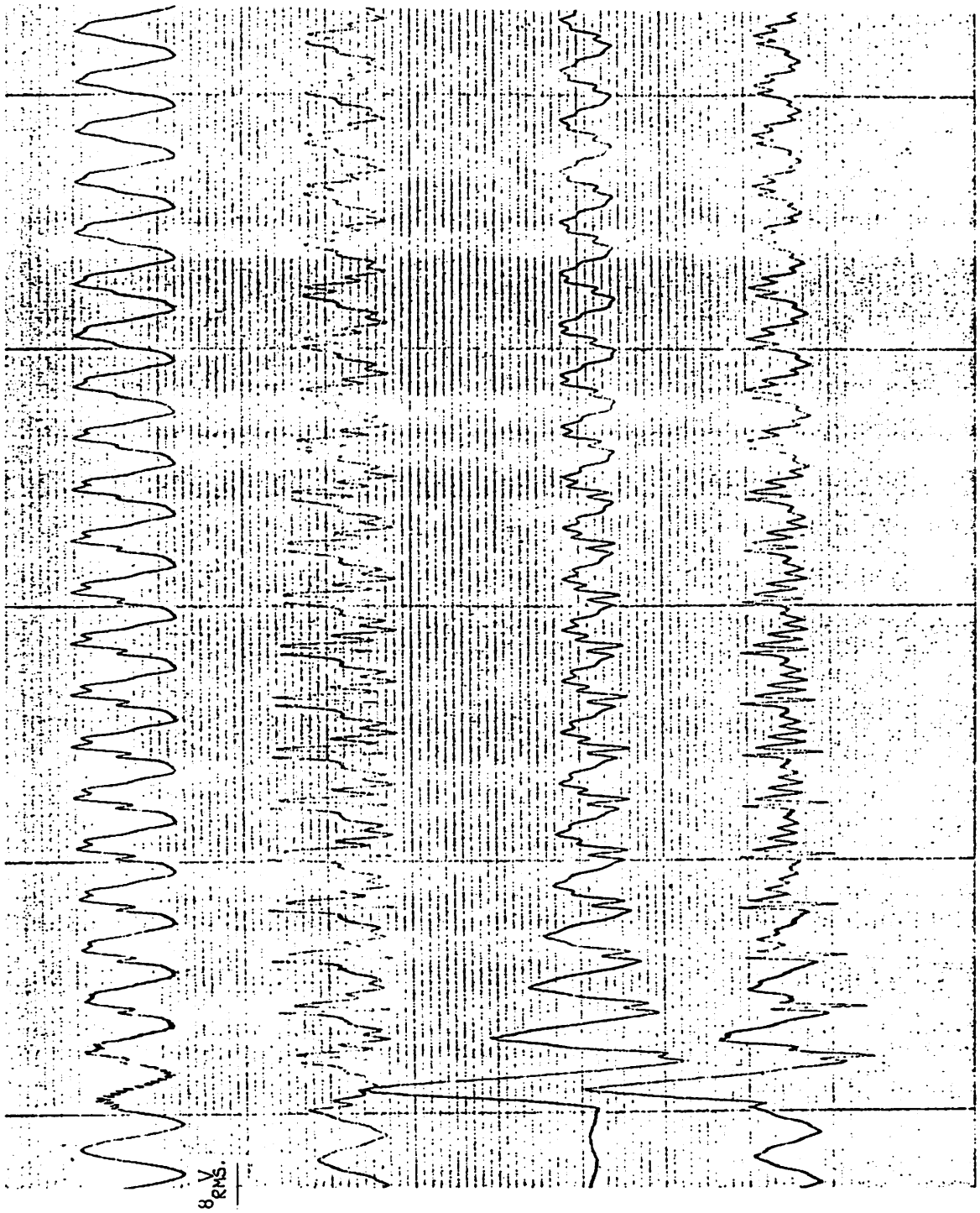

Voltage and current transients When switching an asynchronous generator to a system containing a shunt capacitor. Kalkugncn, Swedcn 78-10-25

Appendix 10

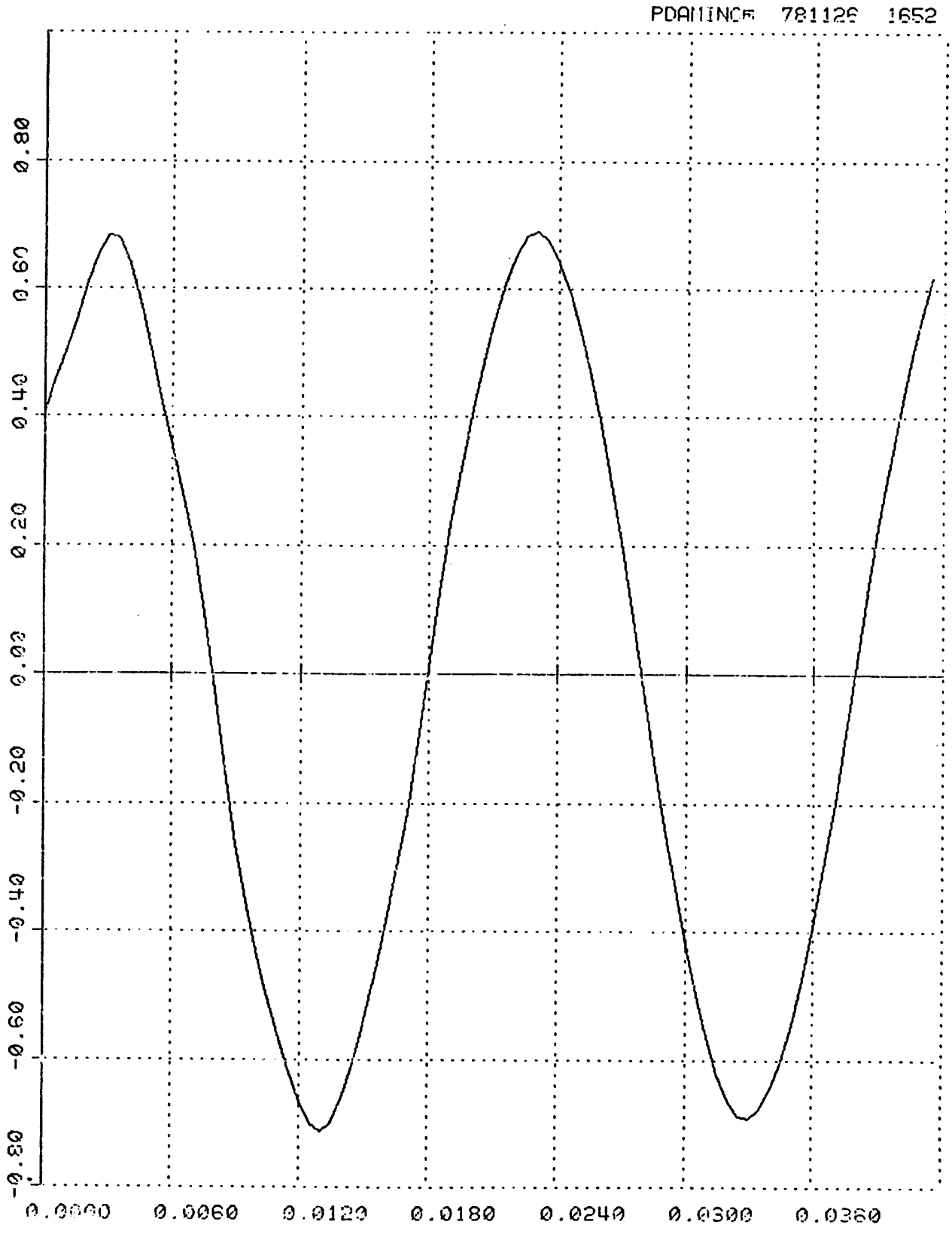

Capacitor voltage u_C, when switching the generator.

Appendix 11

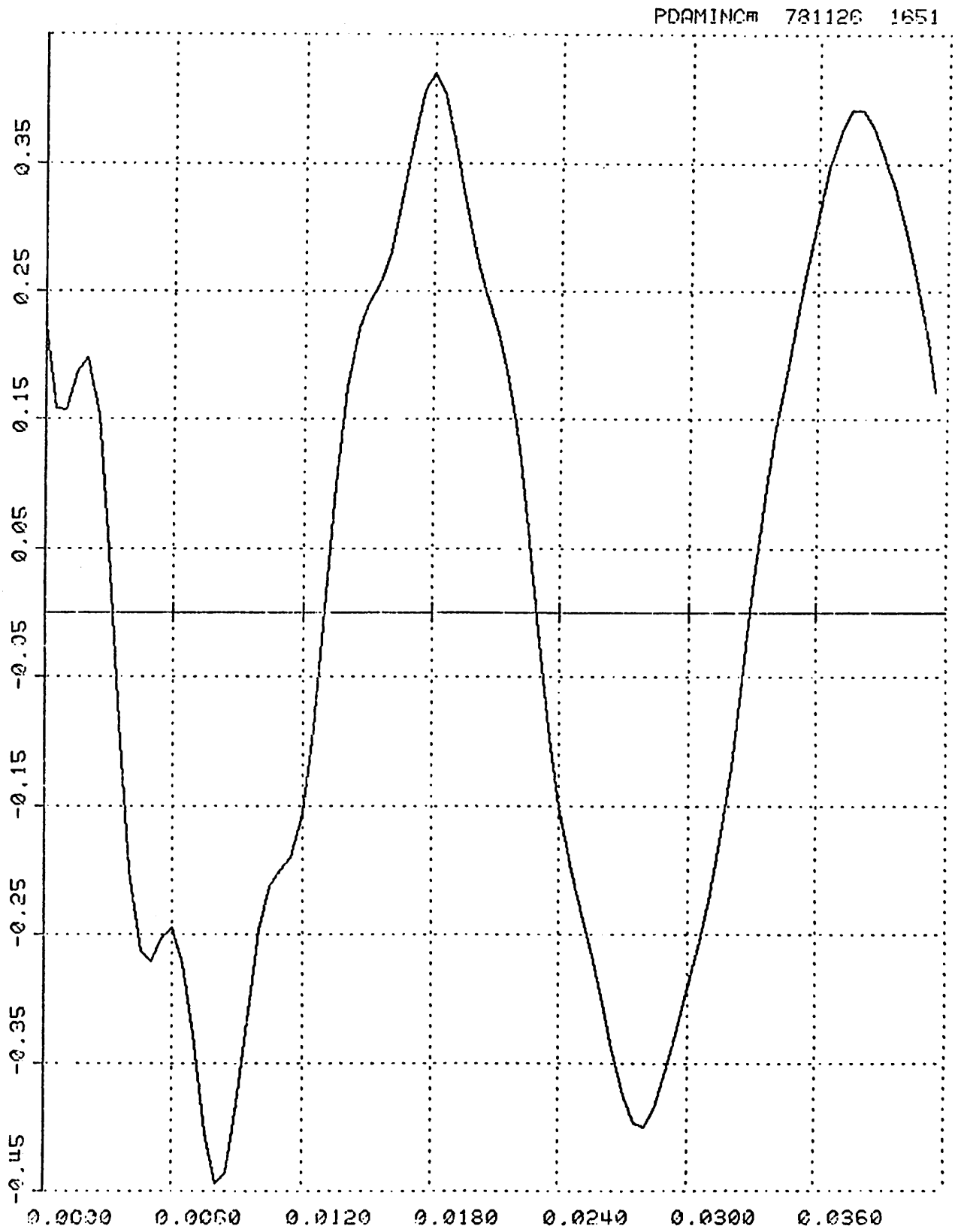

Capacitor current i_C, when switching the generator.

φ = 25° 1 pu = $\sqrt{2}$·145 A

Appendix 12

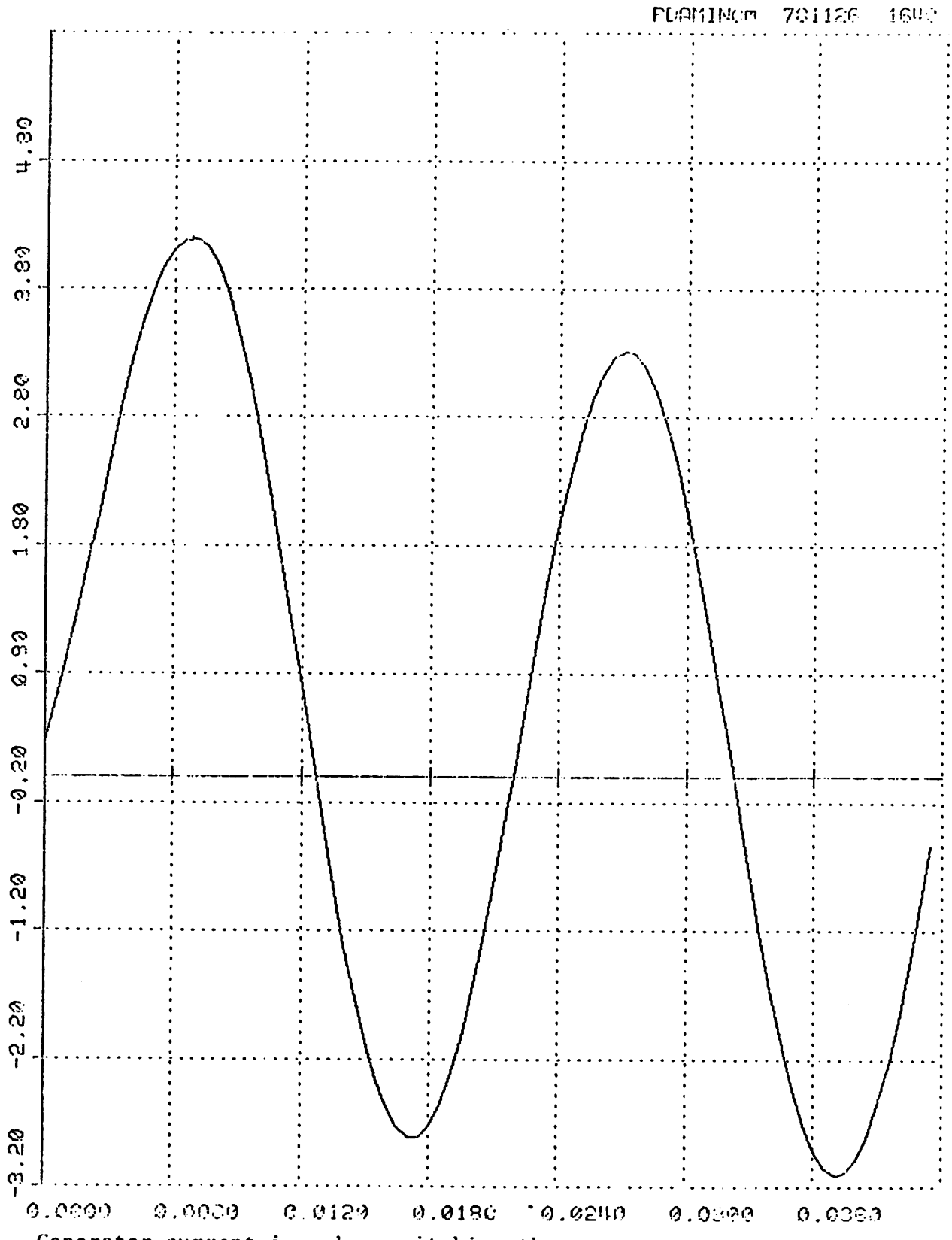

Generator current i_G, when switching the generator.

Control of a Variable Speed Wind Driven Converter Supplying Power to the Constant Frequency Line*)

W. Kleinkauf, Gesamthochschule Kassel (Part I)

W. Leonhard , Techn. University of Braunschweig (Part II)

Abstract

The first part of this investigation describes the control system for a large wind energy plant and discusses the operational behaviour at varying wind conditions.

The second part ist concerned with a detailed description of a variable speed alternator connected to the constant frequency line.

---

*) These investigations carried out for and on behalf of M A N were financed by the Bundesministerium für Forschung und Technologie

P A R T I

Control and Operational Behaviour of a Large Wind Power Plant

(1) Introduction

For the conversion of wind energy into electricity - in project GROWIAN - a horizontal axis machine with two rotor blades will be used. The blade pitch angles are variable /1.2/ . The hub height and rotor diameter measure 1oo m approximately. The rated power of 3 MW will be reached at a wind velocity of 12 m/sec. The generator of this plant is designed to operate in connection with a constant frequency line.

The existing utility grid consists today almost exclusively of thermal power plants, where it is possible to control the power output by changing the input of primary energy.

The primary energy of wind converters, however, is determined by the uncontrollable velocity of the wind, which is subject to long- and middle-term variations as well as short-term wind gusts. Accordingly, extreme power- and speed-variations are possible. To secure unimpaired functionning the dynamics of the wind-converters must be governed by a control-system, so that the properties of the turbine components as well as the demands of the grid are taken into account.

(2) Modes of Operation

Based on the general speed-power diagrams of a wind turbine for different wind velocities with optimal blade pitch angles shown in Fig.1 three modes of operation can be distinguished:

(a) Wind controlled operation

Here the operating characteristic corresponds to the maximum power curve P_{opt}. The speed must be kept variable (tip speed ratio λ = const). Working on the fixed frequency grid the optimal conditions can only be attained if the power generated

by the turbine is flowing through a converter matching the variable speed of the rotor to the speed of the generator, i.e. the frequency of the line. The adaption can be achieved on the mechanical side, e.g. by a step-up gear with variable ratio. On the electrical side a simular result can be achieved by combining a synchronous generator connected to a rectifier and feeding the DC power through an inverter to the grid.

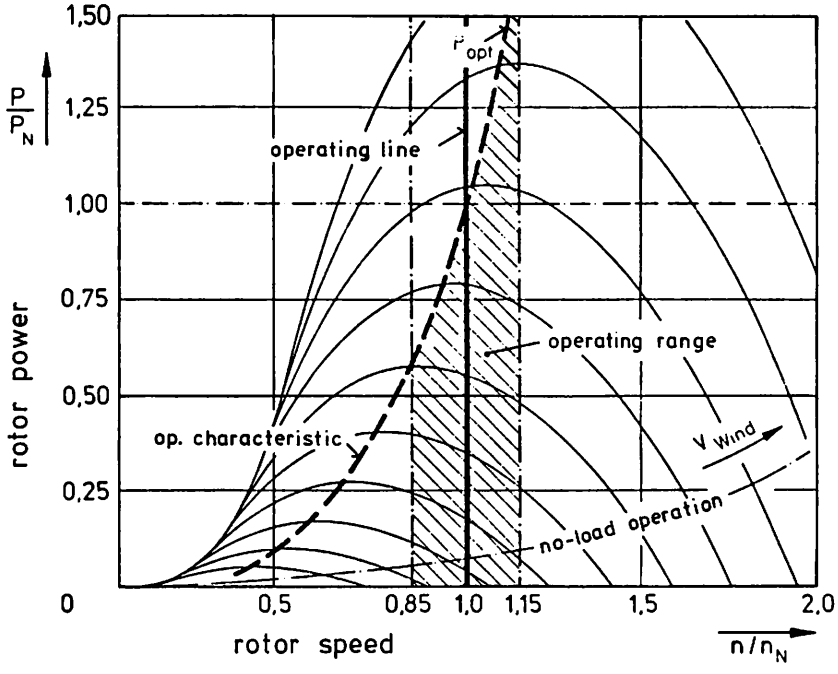

Fig. 1: Rotor power as a function of speed; wind velocity as parameter

(b) Grid controlled operation

Assuming a synchronous generator with DC-excitation rotor speed is given by the grid-frequency as constant (cf. Fig.1, operating-line, $n/n_N = 1$).

(c) Partially wind controlled operation

A limited speed range of the generator permits a partially wind controlled operation (cf. Fig.1, operating-range $0.85 < n/n_N < 1.15$).

The principal construction of a plant permitting this mode of operation is shown in Fig. 2. The turbine power is transmitted by a fixed ratio gear to the rotor of a double-fed generator. The stator of the generator is directly connected to a mains transformer. The three-phase rotor is fed through slip rings to the rotor windings. In steady state, the frequency of this current corresponds to the difference of rotor speed and grid frequency, thereby matching the mechanical section of the turbine to the demands of the grid. In order to keep the transmitted power of the converter reasonably low there should be a restriction of the deviation from the synchronous or rated speed (e.g. $\Delta n_{max} = \pm 15\% \; n_N$).

The choice of the mode of operation and thus of the components of the plant can be based on numerous criteria:
total efficiency of the wind converter, costs, effects on the grid, reliability, use of proved components, etc.
The particular characteristics of GROWIAN for wind controlled operation require the use of components, which either lead to several difficulties in connection with cost-effective realisation or have drawbacks regarding total efficiency, overload capacity, harmonics injected into the grid, etc.

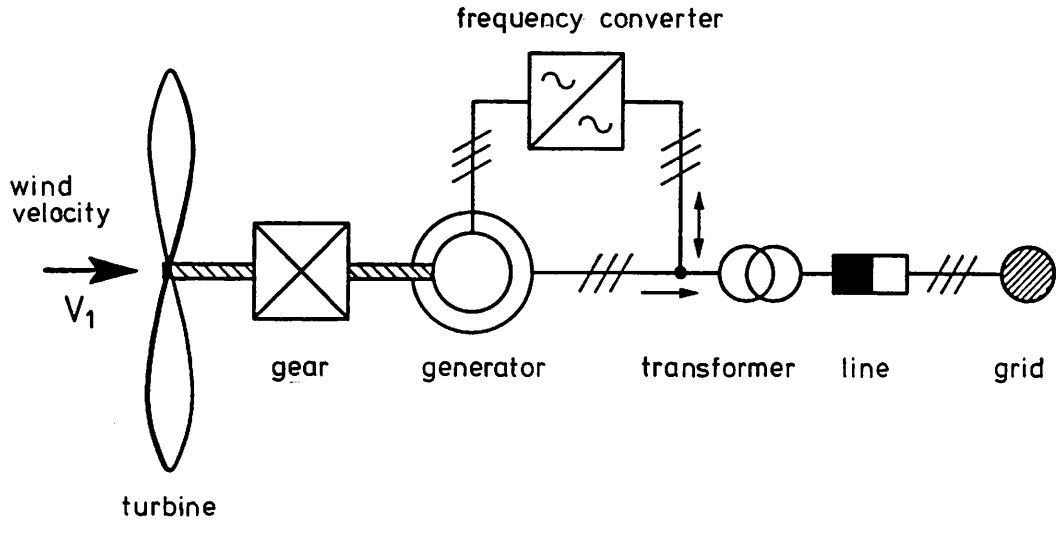

Fig. 2: Construction of the wind power plant with double-fed generator

If the mechanical blade is sufficiently fast so that problems of stability can be avoided the simple version employing a constant speed synchronous generator is most advantageous. Apart from this, however, the partially wind controlled plant with double-fed asynchronous generator is of particular interest. With respect to speed dynamics it constitutes a good compromise between wind- and grid-controlled system.
Fig. 3 shows typical reactions of controlled wind converters (rated power P_N = 3 MW) to a given wind velocity $V_1(t)$. These response plots result from a dynamic simulation, which will be discussed in more detail later on. In the case of the wind turbine with synchronous generator (dotted curve) the speed $n_i(t)$ remains constant while the power fed to the grid $P_i(t)$ is subject to severe fluctuations. The plant with double-fed asynchronous machine (solid curve) shows very smooth power output, because energy can be stored in kinetic form in the rotor experiencing speed variations when the velocity of the wind changes. The influence of wind gusts on the power output may be reduced or completly avoided depending on the control system employed.

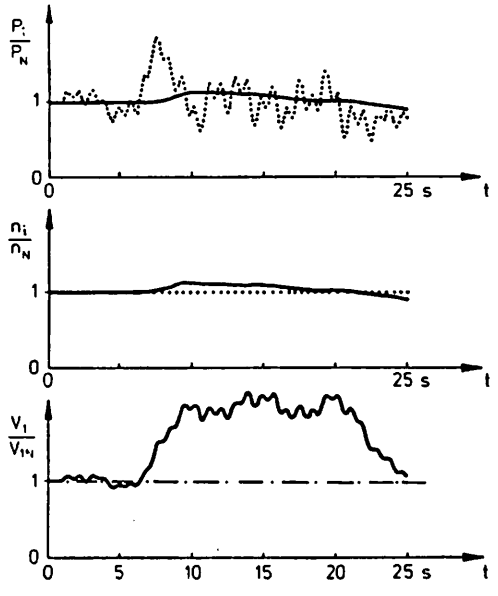

Fig. 3: Dynamic behaviour of wind converter
..... with synchronous generator
_____ with double-fed asynchronous generator

If a double-fed three phase machine is used the voltage or the reactive power can be controlled as is the case with a synchronous generator. The dynamic advantages gained by possible speed variation are believed to warrant the higher costs involved for the excitation

by frequency converter and the more complicated control system. Therefore, the type of plant shown in Fig. 2 was selected.

(3) Concept of Control

The main functions of the control system of the plant are:

(a) adjusting the wind rotor to the direction of the wind (yaw system)

(b) starting, no-load operation, shutting down and safety measures (supervisory control)

(c) active-power and speed control in connection with

(d) generator control.

Fig. 4 shows a diagram of the proposed control system. Essentially, the yaw axis works independently of the other control systems and therefore was not incorporated in this figure. For a short description of the concept the following will be based almost exclusively on a discussion of a control of active power and speed.

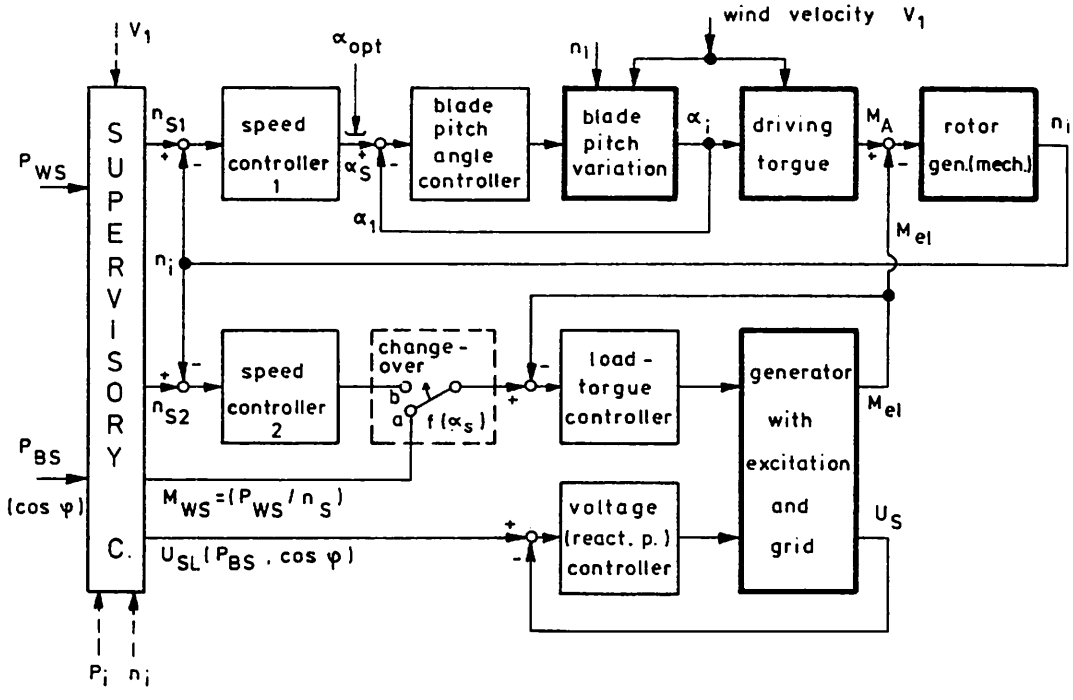

Fig. 4: Block diagram of control for GROWIAN

The heavy-faced blocks characterize the controlled plant containing the physical properties of the wind-converter, including:

- longitudinal behaviour of the blade depending on changes of the pitch angle including disturbances (controlled system "pitch-variation")
- formation of the driving torque M_A by the wind (controlled system "driving torque")
- influence of the rotating components' inertia on speed (controlled system "rotor, generator mech.") as well as
- electrical behaviour of the generator in producing the load torque and regulating voltage and reactive power (controlled system "generator with excitation and grid")

Longitudinal adjustment of the blades was assumed for the purpose of regulating the driving torque and this also makes it possible to vary shaft output torque and speed above rated wind velocity. Maintaining the load torque at a given reference value (controlling the output power for the grid) and the adjustment of voltage or reactive power forms part of the generator control function. These questions were analysed at the Techn. University of Braunschweig. Detailed results of these investigations will be presented in part II of this paper. For decoupling the control of active and reactive power the method of field orientation was chosen /3.4.5./. In the case of sudden gusts of wind the control of the generator performs speed transients into sub- and oversynchronous operation without changing the desired electrical values. The steady state active power control proper is effected by blade pitch variation.

The main features of active power and speed control can be divided into "necessary" and "desirable" characteristics.

Necessary features are:

(a) For all wind velocities $V_{1min} < V_1 < V_{1max}$ permitting operation of the plant the maximum speed deviation should not exceed $n_i = (1 \pm 0{,}15)n_N$.

(b) It should be possible to regulate setpoint power assuming sufficient wind velocities.

For optimization of power output the following characteristics are desirable.

Desirable features are:

(a) Wind controlled operation ($C_P = C_{Popt}$, λ = const.) should be possible within the range of acceptable speed fluctuations.

(b) For low wind velocity ($V_1 < V_{1N}$) it should be possible to adjust the blade pitch angle in such a way that optimal values of power output are obtained.

The block diagram of active power and speed control (cf. Fig.4) contains:

(a) a speed control loop (speed controller 1 in the upper section of the diagram, reference value $n_{S1} = n_N$) with subordinate control of the blade pitch angle. By means of the pitch angle (α = pitch angle, $\alpha = 0^0 \hat{=}$ feathered position) the driving torque and the speed of the turbine will be influenced;

(b) a control loop setting the load torque M_{el}, which is determined by supervisory control according to the active power required ($M_{WS} = P_{WS} / n_{S1}$). This constitutes an active power control loop;

(c) a change-over control section. At switch position "b" a change-over device makes it possible to superimpose a speed control circuit (speed controller 2) on the torque control circuit. This will occur when speed controller 1 is no longer in operation, e.g. if the reference value of the pitch angle below rated wind velocities has reached its optimal limit and remains constant. In a sense this corresponds to a change-over of the speed control circuit. In order to keep the generator within its operating speed range it is necessary to abandon power control in favour of speed control. Load torque and output power set themselves below the reference values in a manner allowing to attain reference speed n_{S2}.

In this way all the necessary requirements are fulfilled.

The following interventions permit realisation of the desired features:

(a) Partially wind controlled operation is possible if speed reference n_{S2} (cf. Fig.4) is given as a function of wind velocity predetermined by the supervisory control (e.g. simplified $n_{S2} / n_N = V_1 / V_{1N}$ in the range o.9 to 1.1).

(b) Optimal output blade pitch angle setting α_{opt} depending on wind velocity is made possible by limiting the reference value α_S as shown in Fig. 4 . For this purpose, a function generator computes the optimal value based on wind velocity; this is used limiting the speed controller 1 . Furthermore, this limit prevents overcritical blade pitch angles; hence the blade control is kept in the correct operating region. Appropriate safety margins should be observed when setting the blade angle.

In order to secure optimal operation of the plant, it is necessary to obtain the relevant wind velocity data. If difficulties should arise in measuring wind velocities optimal settings are not an absolute necessity; the control concept as such will not be endangered.

In order to gain data on the dynamic behaviour of the wind converter plant for different wind conditions the complete system shown in Fig. 4, was simulated by digital means. Many characteristics beside the usual electrical and mechanical responses had to be taken into account, especially those regarding the conversion of wind power an torque for adjusting the blades. The simulation is most accurate within a region close to the rated speed. Supervisory control which would be activated if a failure in the system occured was only used during simulation for providing reference values, but was not used otherwise. Thus, it is principally possible to reach critical states of operation.

Several transients obtained by simulation are shown in the following diagrams. The abbreviations used are listed at the end of the paper. Fig. 5 shows a simple wind characteristic; the diagram also indicates the time of switching over from wind to speed control so that the function of the control can be easily understood from these plots.

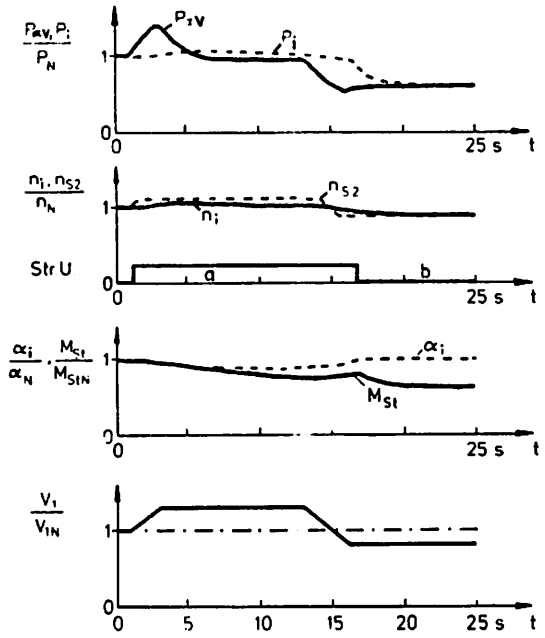

Fig. 5:
Dynamic behaviour of the wind converter based on limited fluctuations of wind velocity.

Fig. 6 shows the benaviour of the converter based on heavy fluctuations of wind velocity.

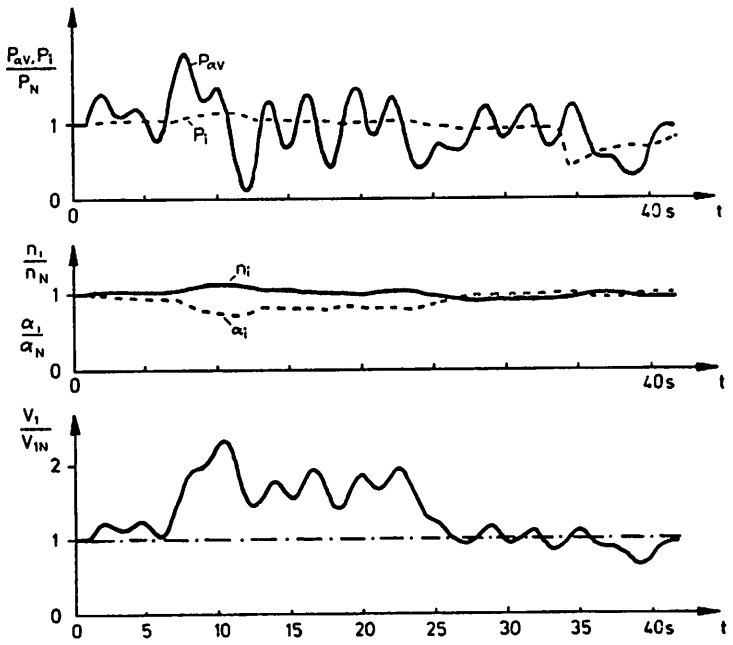

Fig. 6:
Dynamic behaviour of the plant based on heavy fluctuations of wind velocity

A very severe transient is caused by the wind gust as seen in Fig. 7 .

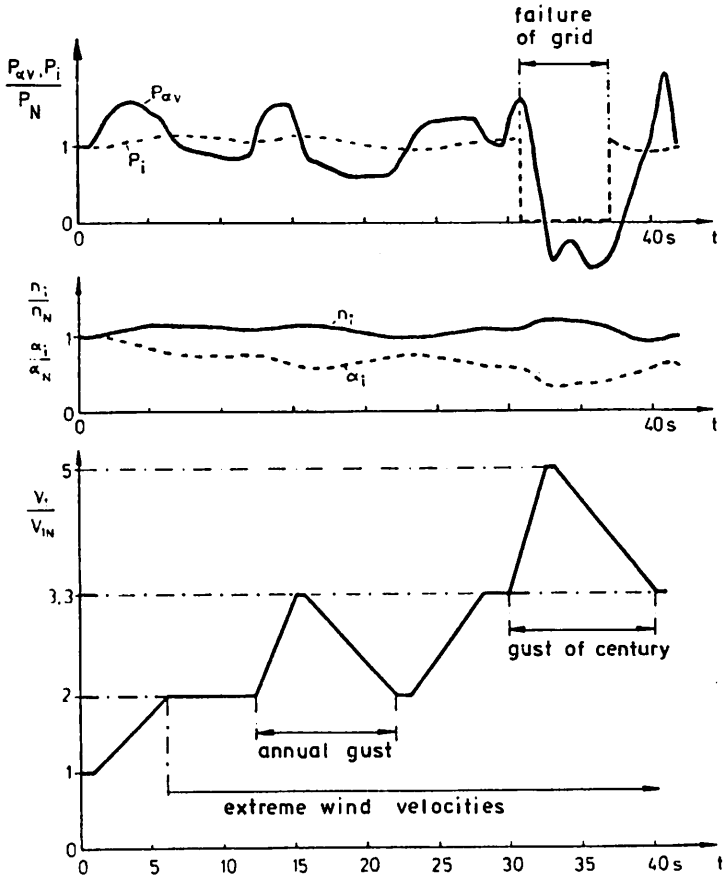

Fig. 7:

Dynamic behaviour of the plant at extreme wind conditions (gusts) and failure of the grid - without intervention of supervisory control -

(4) Conclusions

The investigations discussed in this paper show that a wind converter with double-fed generator can operate even under extreme wind conditions if a control system similar to the one described is used. The variable wind power plant is able to attenuate gusts to a very large extent. The electrical demands of the grid regarding reactive power and waveform of the alternating voltage can be met. Because of its good dynamic properties the plant could be used in a variety of situations. This is of great importance for the design of a pilot project.

Acknowledgement

These investigations were carried out in cooperation with Dipl.-Ing. S. Heier and students of the Department of Electrical Engeneering at the Gesamthochschule Kassel.

References

/1/ Hütter, U.: Der Einfluß der Windhäufigkeit auf die Drehzahlbestimmung von Windkraftanlagen. Stuttgart, Zeitschrift für Elektrotechnik Heft 6, 1948

/2/ Hütter, U.: Eine Windturbine mit 34 m Rotor-Durchmesser. Braunschweig, DFL-Mitteilungen, Heft 8/1978

/3/ Blaschke, F.: Das Verfahren der Feldorientierung zur Regelung der Drehfeldmaschine. Dissertation, TU Braunschweig, 1973

/4/ Leonhard, W.: Regelung in der elektrischen Antriebs-Technik, Stuttgart, B.G. Teubner, 1974

/5/ Leonhard, W.: Regelung in der elektrischen Energieversorgung. Vorlesung. Gedrucktes Manuskript, TU Braunschweig 1978

Symboles and rated values

α	blade pitch angle (α_N=94°)
λ	tip speed ratio
C_p	rotor power coefficient
M	torque
M_{St}	Operating torque at the blades (M_{StN}=135 kNm)
n	speed (n_N=18.5 1/min)
P	power (P_N= 3 MW)
$P_{\alpha V}$	power at the blades
V_1	wind velocity (V_{1N}=12 m/sec.)

Index:

A	drive
B	reactive
i	actual value
L	no-load operation
N	nominal, rated
S	reference, value
W	active

FIELD ORIENTED CONTROL OF A VARIABLE SPEED ALTERNATOR CONNECTED TO THE CONSTANT FREQUENCY LINE

W. Leonhard
Techn. University Braunschweig, Germany

Introduction

Electric power is today generated almost exclusively by synchronous alternators whose speed of rotation is tied to the frequency of the power grid. Operation at constant speed yields the best technical and economic results; for example, only one generator field winding with its associated power supply is required. However, there are cases where a certain amount of flexibility with regard to speed is necessary or desirable, for example if the machine is used to connect two grids of different and changing frequencies, for instance the supply network operated by the railroads in some European countries |2| and the public grid. Another possible application is wind energy convertors, such as the 3 MW, 100 m diameter wind power plant presently under consideration in Germany |4|. For a large mechanical structure like this, a fluctuating speed of rotation presents a convenient way of alleviating additional stresses caused by gusts; by allowing the high inertia rotor to perform limited speed excursions the mechanical blade control is given sufficient time to respond to changing wind conditions. When operating at constant speed, all the transient wind power would have to be absorbed by the generator, possibly endangering stable synchronous operation.

A wound rotor or squirrel cage induction generator can provide this desired degree of freedom, unfortunately at the expense of reactive current and with no means of controlling the terminal voltage. In order to combine the operational advantages of variable speed with the possibility of reactive power generation, a machine with symmetrical rotor windings - such as a wound rotor induction motor - and a variable voltage and frequency power supply for the rotor are required. Depending on the necessary speed range, a phase controlled cycloconvertor or a forced commutated invertor can be employed to feed slip-proportional power to the rotor. With suitable control the generator may be operated above or below synchronism and with positive or negative active and reactive power ; naturally , in steady state the active power is determined by the mechanical drive. Large machines of this type have been built for different applications |3| proving the scheme to be feasible.

In Fig. 1 and 2 a simplified schematic of a variable speed alternator and the available operating range in the speed-torque plane are shown. For simplicity a two phase rotor supply feeding two quadrature rotor windings through slip rings is assumed; in practice a standard three phase rotor design could be used instead.

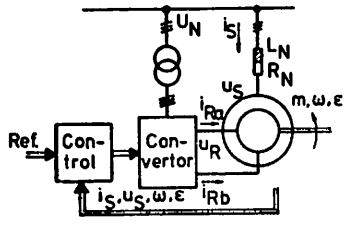

Fig. 1: Simplified schematic

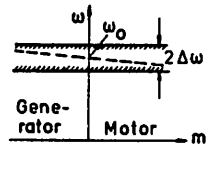

Fig. 2: Operating range

Fig. 3 describes the power flow for sub-synchronous and oversynchronous operation; with $\omega < \omega_o$ there is a recirculating power flow affecting efficiency. Also the reactive power and the line-side harmonics of the convertor need to be taken into account; however, these effects are not too serious as long as the slip-frequency, and hence, the power of the convertor are small.

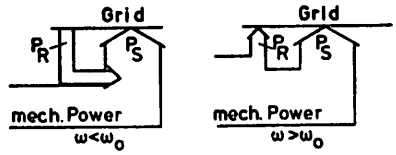

Fig. 3: Power flow

There are various ways of controlling a double-fed generator of this type; depending on the application, one or the other could be preferable. For use in a wind power station a sloped steady state speed-torque curve, as seen in Fig. 2, could be employed. In order to utilize the possibilities of influencing the torque by electrical means, fast response of the generator control is desirable.

In the following sections a control scheme is described which was first introduced for the control of induction motors |5, 6|. Since it is based on the magnitude and direction of a flux vector, established by direct or indirect measurement, it is called field-oriented control. The magnitude, frequency and phase of the input currents (in this case the rotor currents) are generated such as to give the rotor MMF-vector a prescribed orientation in relation to the main flux vector (which itself is a function of the rotor currents). The longitudinal component of the rotor current vector changes the terminal voltage, hence the reactive power, and through a substantial lag the magnitude of the main flux; the quadrature component of the rotor current vector immediately affects the torque and active power. This indicates a close analogy to the control of a compensated DC machine, which exhibits an almost ideal decoupled control structure.

Mathematical model of symmetrical double-fed machine with two-phase rotor

Assuming symmetrical stator and rotor windings with sinusoidal MMF-distributions, infinite permeability of the iron core, and neglecting slot and end effects as well as iron losses, the following vectorial differential equations may be derived to describe the general behaviour of the symmetrical double fed two pole machine |8|.

$$(R_N+R_S)\,\underline{i}_s + (L_N + L_S)\,\frac{d\underline{i}_s}{dt} + M\,\frac{d}{dt}\,(\underline{i}_R e^{i\varepsilon}) = \underline{u}_N(t), \quad (1)$$

$$R_R\,\underline{i}_R + L_R\,\frac{d\underline{i}_R}{dt} + M\,\frac{d}{dt}\,(\underline{i}_s\, e^{-i\varepsilon}) = \underline{u}_R(t), \quad (2)$$

$$\Theta\,\frac{d\omega}{dt} = m_m + m_{el} = m_m + \frac{2}{3}\,M\,\mathrm{Im}\left[\underline{i}_s\,(\underline{i}_R e^{j\varepsilon})^*\right], \quad (3)$$

$$\frac{d\varepsilon}{dt} = \omega\,, \quad (4)$$

where $\underline{i}_S(t)$, $\underline{i}_R(t)$ are complex (two dimensional) time-dependent vectors, composed of the instantaneous phase currents,

$$\underline{i}_S(t) = i_{S1}(t) + i_{S2}(t)\; e^{j2\pi/3} + i_{S3}(t)\; e^{j4\pi/3}, \quad (5)$$

$$\underline{i}_R(t) = i_{Ra}(t) + j i_{Rb}(t) = \left|\underline{i}_R\right| e^{i\xi(t)}. \quad (6)$$

$(\underline{i}_R e^{i\varepsilon})^*$ is the conjugate complex value of $\underline{i}_R e^{i\varepsilon}$. In steady state operation at constant speed, all currents are sinusoidal, but in nonstationary condition they may be arbitrary functions of time as long as $i_{S1} + i_{S2} + i_{S3} = 0$ holds at any instant, which is due to the isolated neutral of the stator winding. $\xi(t)$ is the direction of the rotor current vector in rotor coordinates.

There is an analogous definition for the voltages. The vector

$$\underline{u}_N(t) = u_{N1} + u_{N2} e^{j2\pi/3} + u_{N3} e^{j4\pi/3} = \frac{3\sqrt{2}}{2} U_{SO} e^{j\omega_o t} \quad (7)$$

describes the symmetrical three phase line voltages behind the effective grid impedance L_N, R_N; these voltages are assumed to be sinusoidal and of constant rated RMS value U_{SO} and frequency ω_o. Correspondingly,

$$\underline{u}_R(t) = u_{Ra}(t) + j u_{Rb}(t) \quad (8)$$

is the vector of the rotor voltage components supplied by the convertor; in steady state their fundamental frequency

$$\omega_R = \omega_o - \omega = s\,\omega_o \quad (9)$$

is proportional to slip speed. $\omega(t)$ is the angular velocity, $\varepsilon(t)$ the angular position of the rotor. $m_m(t)$, $m_{el}(t)$ are the mechanical and electrical torques respectively, both counted positive in the direction of rotation. Θ is the total inertia of the generator set. R_S, L_S, R_R, L_R constitute the stator and rotor impedances per phase, M is the mutual inductance and R_N, L_N represent the line impedance per phase.

Field oriented control

Considerable simplification is possible if the rotor currents can be regarded as being impressed by the convertors as a result of fast current control; this resembles the use of two independent current sources. Of course, this is only valid if the convertors have a sufficiently large frequency and voltage range. With this assumption equation (2) is of no relevance with regard to generator control as it is dealt with by the current control. With the stator leakage factor σ_s, the main inductance $L_h = M$ (assuming equal number of turns in stator and rotor),

$$L_S = (1 + \sigma_s)\, L_h, \text{ and } L_N = a\, L_S, \quad (10)$$

equ. (1) may be written as

$$(R_S + R_N)\underline{i}_s + L_h \frac{d}{dt}\left[(1+a)(1+\sigma_s)\underline{i}_s + \underline{i}_R e^{j\varepsilon}\right] = \underline{u}_N(t), \quad (11)$$

where the expression in brackets may be defined as a modified magnetizing current vector.

This current vector,

$$\underline{i}_{ms}(t) = (1+a)\,(1+\sigma_s)\,\underline{i}_s + \underline{i}_R e^{j\varepsilon} = \left|\underline{i}_{ms}\right| e^{j\mu(t)}, \quad (12)$$

is a measure of the stator flux rotating with frequency ω_{ms}, where

$$\frac{d\mu}{dt} = \omega_{ms}. \quad (13)$$

The $\underline{i}_{ms}$-signal may be constructed from the currents and the rotor position. ω_{ms} can deviate only temporarily from the line frequency ω_o.

Eliminating $\underline{i}_s$ from equ. (11, 3) results in

$$\frac{(1+a)L_S}{R_N + R_S}\frac{d\underline{i}_{ms}}{dt} + \underline{i}_{ms} = \frac{(1+a)(1+\sigma_s)}{R_N + R_S}\underline{u}_N(t) + \underline{i}_R e^{j\varepsilon}, \quad (14)$$

$$m_{el}(t) = \frac{2}{3}\frac{L_h}{(1+a)(1+\sigma_s)}\,\mathrm{Im}\left[\underline{i}_{ms}(\underline{i}_R e^{j\varepsilon})^*\right]. \quad (15)$$

Multiplying by $e^{-j\mu}$, i. e. referring all quantities to the field vector and splitting equ. (14) into real and imaginary parts yields two equations for magnitude and phase of the magnetizing current

$$\frac{L_N + L_S}{R_N + R_S}\frac{d\left|\underline{i}_{ms}\right|}{dt} + \left|\underline{i}_{ms}\right| = -cU_N \sin(\omega_o t - \mu) + \left|\underline{i}_R\right| \cos(\varepsilon + \xi - \mu), \quad (16)$$

$$\frac{L_N + L_S}{R_N + R_S}\left|\underline{i}_{ms}\right|\frac{d\mu}{dt} = cU_N \cos(\omega_o t - \mu) + \left|\underline{i}_R\right| \sin(\varepsilon + \xi - \mu), \quad (17)$$

with $c = \frac{3\sqrt{2}}{2}(1+a)\,(1+\sigma_s) \,/\, (R_N + R_S)$,

as well as an equation for the torque

$$m_{el} = -\frac{2}{3}\frac{L_h}{(1+a)(1+\sigma_s)}\left|\underline{i}_{ms}\right|\left|\underline{i}_R\right| \sin(\varepsilon + \xi - \mu). \quad (18)$$

The angular relations depicted in Fig. 4 indicate that $\varepsilon + \xi - \mu = \vartheta$ corresponds to the load angle;

$\left|\underline{i}_R\right| \cos\vartheta$, $\left|\underline{i}_R\right| \sin\vartheta$

represent the direct and quadrature axes components of the rotor current vector in relation to the magnetizing current vector $\underline{i}_{ms}$. All transformed quantities are constant in steady state when assuming sinusoidal rotor voltages.

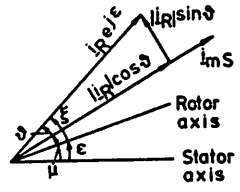

Fig. 4: Current vectors

Normalization of equ. (16 - 18) by rated RMS-quantities,

$$\underline{i}_{ms} = \frac{3\sqrt{2}}{2} I_{So}\, i_{ms}\, e^{j\mu}, \quad (18a)$$

$$\underline{u}_N e^{-j\mu} = \frac{3\sqrt{2}}{2} U_{So}\,(u_{Nd} + j u_{Nq}), \quad (18b)$$

$$\underline{i}_R e^{j(\varepsilon-\mu)} = \sqrt{2}\, I_{So}(1+\sigma_s)\, K_o\,(i_{Rd} + j i_{Rq}), \quad (18c)$$

$$T_S = \frac{L_N + L_S}{R_N + R_S} = \frac{1+a}{r_N + r_S} x_d \frac{1}{\omega_o}, \quad (18d)$$

$$S_o = U_{So}\, I_{So}, \quad (18e)$$

where x_d is the per-unit synchronous reactance and K_o the per-unit short circuit current, results in the following per-unit equations

$$T_S \frac{di_{ms}}{dt} + i_{ms} = (1+\sigma_s)\left[\frac{1+a}{r_N + r_S} u_{Nd} + \frac{2}{3} K_o\, i_{Rd}\right], \quad (19a)$$

$$\frac{1}{\omega_o}\frac{d\mu}{dt} = \frac{\omega_{ms}}{\omega_o} = \frac{1+\sigma s}{x_d i_{ms}}\left[u_{Nd} + \frac{2}{3}\frac{r_N+r_S}{1+a}K_o i_{Rq}\right] \qquad (19b)$$

$$\frac{m_{el}}{3S_o/\omega_o} = -\frac{2}{3}\frac{K_o X_d}{(1+a)(1+\sigma_s)} i_{ms}\, i_{Rq} \qquad (19c)$$

The normalized machine equations (19) are graphically presented in the right hand side of the block diagram, Fig. 5. The transformation of the rotor currents into field coordinates is clearly an extension of the usual d-q transformation with synchronous machines, where the rotor position serves as the frame of reference.

The inputs to the machine model are the two AC rotor currents of slip frequency, the line voltages and the mechanical torque.

The principle of controlling the generator in field-coordinates is as follows:

If the rotor currents i_{Ra}, i_{Rb} are sufficiently accurate copies of the reference currents i_{RaRef}, i_{RbRef}, i. e. if the error of the current control loops can be neglected, it is possible to cancel the machine-internal transformation $e^{j(\varepsilon-\mu)}$ by an external inverse coordinate transformation with $e^{-j(\varepsilon-\mu)}$ and thus gain immediate access to the direct and quadrature axes components i_{Rd}, i_{Rq}. For this purpose the sin and cos of the angle $(\mu-\varepsilon)$ of the magnetizing current vector in relation to the rotor must be measured or reconstructed from other quantities such as voltages, currents and rotor position. After this inverse transformation is accomplished, the remaining generator dynamics are straight forward as seen from Fig. 5. Since the magnetizing current i_{ms}, being a measure of stator flux and the utilization of the core, cannot be changed quickly anyway, it should be maintained at a constant value, for example through an inner flux control loop. To this a voltage or reactive power control loop may be superimposed. At the same time such a scheme simplifies the remaining control structure because of the ensuing linearization.

On the other hand, the quadrature component of the rotor current vector, which is subject to rapid change, may be employed to control the torque. For this purpose an internal torque- or active power-controller and a superimposed speed controller may be used to generate the quadrature current reference.

The main advantage of this control strategy is that the controllers, operating "in field coordinates", have to process DC variables in steady state. The conversion to AC is performed by the subsequent coordinate transformation which constitutes a modulation process, generating the AC current reference quantities.

If the assumption of impressed currents is valid and the modulation signals are correct, the generator completely loses its synchronous characteristics and resembles a compensated DC machine; it can no longer be pulled out of synchronism, neither does the machine require an additional damping winding as damping is achieved through the control.

While it is apparent that this type of two axes control is likely to have superior dynamic performance to most other control schemes, it may be argued that it is of considerable complexity and requires many control components such as sensors, multipliers etc. However, with the present development of microelectronics these obstacles may be overcome. For example, it has been shown that the coordinate transformation with cos $(\varepsilon-\mu)$, sin $(\varepsilon-\mu)$, and the controller functions, leading to the current references, may be carried out with one standard microprocessor augmented by an external arithmetic unit |9|.

Design of the inner current control loops

In the preceding section it has been assumed that the convertor with current control can be approximated by an ideal two phase current source; this assumption is now examined in more detail. When eliminating the stator current $\underline{i}_S$ in equ. (2) by the magnetizing current $\underline{i}_{ms}$, defined in equ. (12), we obtain

$$\frac{\sigma+a}{1+a}\frac{L_R}{R_R}\frac{d\underline{i}_R}{dt} + \underline{i}_R = \frac{1}{R_R}\left[\underline{u}_R - \frac{1-\sigma}{1+a}L_R\frac{d}{dt}\left(\underline{i}_{ms}e^{-j\varepsilon}\right)\right], \qquad (20)$$

$$\text{where } \sigma = 1 - \frac{1}{(1+\sigma_S)(1+\sigma_R)} \qquad (21)$$

is the total leakage factor of the generator and

$$\frac{\sigma+a}{1+a}\frac{L_R}{R_R} = \frac{\sigma+a}{1+a}T_R = T_R' \qquad (22)$$

is the transient time constant of the generator connected to the line; it varies between $T_R' = \sigma T_R$, i.e.

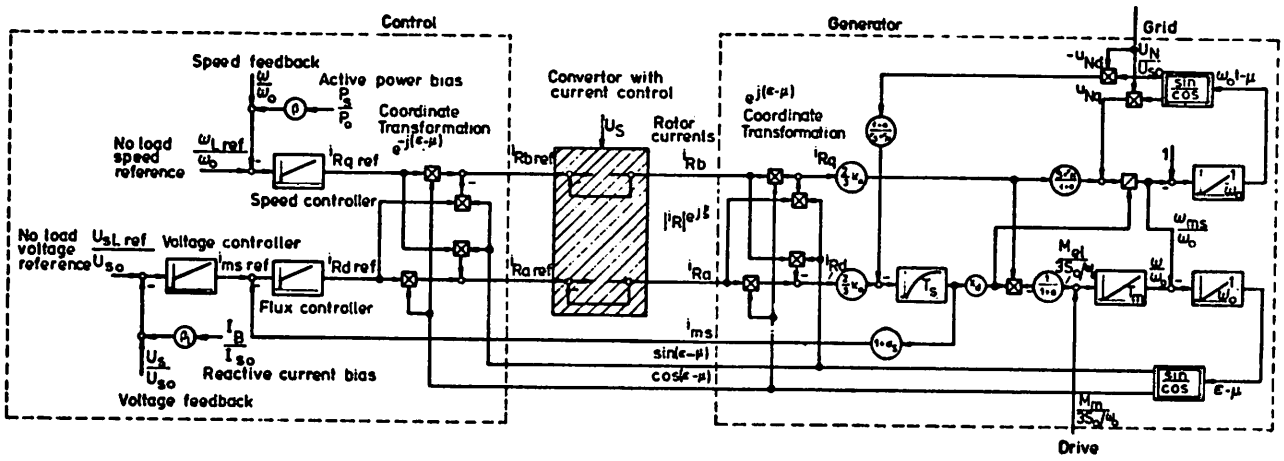

Fig. 5: Block diagram of control

short circuit value at zero line impedance (a = o) and $T_R' = T_R$ for open circuit (a >> 1).

The expression in the bracket in equ. (20) contains the rotor terminal voltage $\underline{u}_R$, supplied by the convertor, and a voltage induced in the rotor windings by the main field of the generator. By developping this second expression, we obtain

$$\frac{1-\sigma}{1+a} L_R \frac{d}{dt} (\underline{i}_{ms} e^{-j\varepsilon}) =$$

$$= \frac{1-\sigma}{1+a} L_R \left[\frac{d|\underline{i}_{ms}|}{dt} e^{j(\mu-\varepsilon)} + j(\omega_{ms}-\omega)\underline{i}_{ms} e^{-j\varepsilon} \right] \qquad (23)$$

If the magnetizing current is maintained at constant magnitude, this reduces to a voltage proportional to slip frequency $\omega_{ms} - \omega$. This indicates that the task of the current controllers may be greatly simplified by voltage feed-forward, i. e. by cancelling the slip dependent voltage, as seen from the single-phase diagram in Fig. 6. At low power this can of course only be approximated due to the delay of the convertor. The derivation of the feed forward signal presents no additional complication since $\underline{i}_{ms}$ is required for the field oriented control anyway.

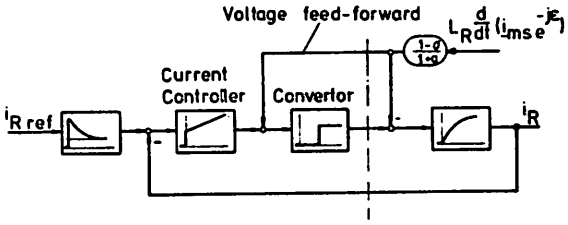

Fig. 6: Current control with voltage feed-forward

The remaining small lag of the current control loop may still be reduced by a corresponding lead-lag element at the reference input; this is also seen in Fig. 6.

Digital simulation of the complete system

In order to examine the function of the control scheme described and to achieve definite design specifications of the components, the whole system, including the 3 MW generator with the line, the convertor and the control was simulated on a digital computer [4] using proven partitioning methods [7]. The open-loop dynamics of the cyclo-convertor, which determines the integration step size, was first approximated by a linear lag element; after the various design parameters had been established, the convertor model was replaced by a more realistic one which included the actual phase controlled switching. Commutation transients were neglected as they do not affect the control. While the computing time increased by a factor of ten with the detailed convertor model, no change of the structure nor the parameters of the control was found necessary.

In Fig. 7 one of the many computed simulation results is shown. At this stage the control system included a voltage control loop with reactive current bias and an electric torque control loop; the superimposed speed loop was omitted for this test. The output voltages of the two six-pulse convertors were limited to the values established with the detailed analysis.

The generator is at first operating with synchronous speed at no load, hence the rotor voltages and currents are zero. At t = 0 the mechanical driving torque and simultaneously the electric torque reference were

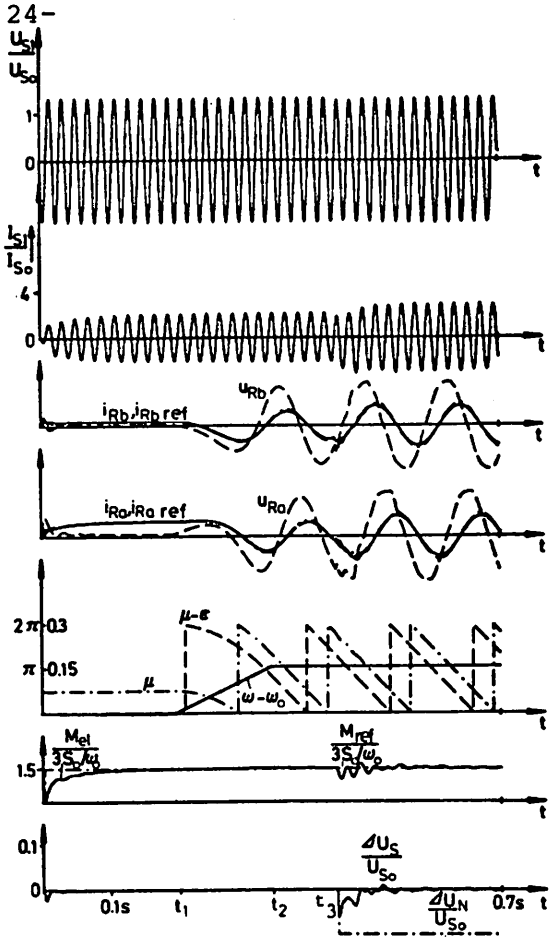

Fig. 7: Simulation results

changed by a step to 1.5 rated torque, which caused the rotor currents and the electric torque to build up quickly, having little effect on speed and terminal voltage.

Between t_1 and t_2 an unrealistically large increase in driving torque, simulating an excessive gust, was assumed; since the electric torque reference remained unchanged, the generator speed increased to the maximum specified, 1.15 rated speed. It is seen that there is a very rapid control action; the rotor begins to slip without noticeable effect on the electric torque and the stator voltages or currents. Finally, at $t = t_3$ a 10 % reduction of the line voltages is assumed which causes transients of the electric torque and the terminal voltage; there is a stationary increase in the stator currents.

The simulation results with the detailed convertor model are quite similar, proving that the control scheme can be expected to handle the required disturbances. The design work described is now followed up by laboratory tests with the aim of incorporating the higher level control functions into a microprocessor.

Summary

The paper describes the design of a control system for a variable speed-fixed frequency alternator with a low frequency rotor supply from a cyclo-convertor. The principle of field orientation is described, which permits fast decoupled control in direct and quadrature axes by providing immediate access to active and

reactive stator currents and, hence, to torque and voltage. The performance of the control is shown by digital simulation. The low power control functions can be performed by a microprocessor.

Acknowledgements

The digital simulations referred to in the paper were carried out by Dr. E. Schnieder and Dipl.-Ing.J.Hohlfeld at the Institute of control engineering, Techn. University Braunschweig.

|1| Lauffer, H.
Die Drehstrommaschine mit polradwinkelabhängig eingeprägten Läuferströmen
Archiv für Elektrotechnik 1968, S. 289

|2| Spinnler, W.
Netzkupplungsumformer für die Deutsche Bundesbahn
Siemens-Zeitschrift 1971,
Beiheft Bahntechnik, pg. 66

|3| Dirr, R., Neuffer, J., Schlüter, W., Waldmann, H.
Neuartige Regeleinrichtungen für doppelt gespeiste Asynchronmotoren großer Leistung
Siemens-Zeitschrift 1971, pg. 362

|4| Kernforschungsanlage Jülich
Statusreport Windenergie
JÜl Conf. 27, 1978
Teilbericht Regelungskonzept für GROWIAN,pg. 325

|5| Blaschke, F.
Das Verfahren der Feldorientierung zur Regelung der Asynchronmaschine
Siemens-Forschungs- und Entwicklungsberichte 1972 pg. 184

|6| Blaschke, F.
Das Verfahren der Feldorientierung zur Regelung der Drehfeldmaschine
Dissertation, Techn. University Braunschweig,1974

|7| Schnieder, E.
Digitale Nachbildung stromrichtergespeister Maschinen unter besonderer Berücksichtigung der wechselrichtergespeisten reihenschlußerregten Reluktanzmaschin:
Dissertation, Techn. University Braunschweig,1978

|8| Leonhard, W.
Regelung in der elektrischen Antriebstechnik
Teubner, 1974

|9| Claussen, U., Leonhard, W.
Microprocessor-controlled linear synchronous motor as positioning drive
Int. Conf. on electrical machines, Brüssel, 1978, paper L5/2

Power System Operation of a "Growian"

Hugo Mühlöcker, Siemens AG - E 111, Erlangen

1. Introduction

Operation of the Growian is planned for a medium-voltage power system of constant frequency with connection to a radial line. No detailed study has been made of operation in an isolated system, of operation in parallel with another individual generator or of the operation of several "Growians" in a power plant park.

The climatic conditions were based on those prevailing on the German North Sea coast.

The short circuit power arising in the medium-voltage system was taken as 100 MVA for the 10 kV level and as 150 MVA for the 20 kV level.

2. System requirements

The system requirements to be met by the "Growian" for operation under the conditions listed are as follows:

1. Provision of power supply at constant frequency.

2. Provision of uniform active power.
   Fig. 1 shows for the 100-kW-windmill Stötten that these two requirements will bring a lot of tasks for the regulating equipment.

3. Machine to cover its own reactive power requirements.

4. The harmonics generated by the "Growian" must be kept as small as possible and must under no circumstances interfere with existing centralized ripple control equipment.

5. It must be possible to operate the plant automatically.

6. The short circuit power supplied by the "Growian" must be sufficient to safely operate protective gear.

7. The Growian must be capable of operating with three-phase rapid enclosure in the medium-voltage system and under conditions of frequent system failure during stormy weather.

3. Operating modes of the machine set

On the basis of the wind velocity distribution given by meteorologists over a period of a year and on the basis of the wind turbine speed curve to be expected for these wind velocities, the following operating modes have been laid down for the wind turbine:

1. Standstill with blades stationary.

2. Spinning with the electrical machine switched off.

3. Load operation according to wind power available in a range of ± 10 % of the rated speed continuously and ± 15 % short time below the curve for the permissible continuous output of the electrical machine.

4. Load operation up to the maximum power output of the machine set by the system control centre.

5. Short time overload operation within the speed control range according to wind power available.

6. Overload operation above the speed control limit with the electrical machine supplying braking torque.

4. Properties of the electrical machine

(Fig. 2 speed variation curves, Fig. 3 operating diagram of the asynchronous machine)

As can be seen from the operating diagram a machine had to be selected as a generator which permits speed flexibility within a certain range. After the advantages and disadvantages had been considered, preference was given to double-fed asynchronous machine with a frequency converter in the rotor circuit against a synchronous machine with a frequency converter in the stator circuit. In operation within a given speed range, this machine can supply a constant frequency at the stator terminals. Hence, the vector of the magnetic flux in the stator rotates at a speed proportional to the frequency of the power system. By suitable

control of the converter frequency, a condition is produced whereby the sum of the frequency proportional to the mechanical speed and the frequency of the converter is always equal to the power system frequency. As a result of this type of excitation, the asynchronous machine behaves in a similar manner to a synchronous machine. This enables the requirements regarding constant system frequency and uniform active power to be met, since intermediate storage in the rotating masses takes place during speed variations.

Apart from the losses in the converter transformer, the converter and the rotor winding, the slip power in supersynchronous operation is fed to the power system via the converter and added to the stator power. In subsynchronous operation, the slip power is subtracted from the stator power. This produces the slip-proportional limit lines shown in the operating diagram for the active power supplied to the system.

By controlling the specific current loading in the rotor circuit according to magnitude and phase angle - this is done through the control setting of the converter - it is possible to set any required reactive current within the operating range independently of the active current in the stator of the machine. Requirement No. 3 is thus met fully.

To avoid the necessity of having to take the machine off the system every time short sharp wind squalls occur (overloading of the thyristors in the converter is not permitted), the switching-in of a short circuiting resistance in the rotor circuit for asynchronous operation is provided for when the machine exceeds the maximum operating speed. This has a braking effect on the machine and thus prevents sudden sharp increases in the speed which could endanger the whole plant. Fig. 2 shows a computer run for the speed variation following a big squall with and without braking effect of the generator. When the squall has died down, and the speed has returned to within the normal control

range, the machine can be synchronized with the converter again operative in the rotor circuit. During this period of overload operation, however, the power system must supply the magnetizing current for asynchronous operation of the machine. In this special case, the requirements regarding uniform active power and the supply of reactive power cannot be met simultaneously.

5. Arrangement of the power circuit

Fig. 4 shows the basic arrangement of a wind power plant of this kind. In accordance with German conditions, it is assumed that the plant is connected to the line of a rural radial system operating at 10 or 20 kV. Where possible, reference should, however, be given to connection to a ring-main system in view of the higher degree of security afforded. The system side transformer is provided to enable the power plant to be designed for a uniform voltage of 6.3 kV - which is a favourable value for machines of this size - independently of the particular medium-voltage system. The circuit arrangement for the rotor shows a slipring rotor whose starpoint is connected in the machine. The 3-phase terminals are connected to the converter via the sliprings. The converter transformer is connected to the same bus as the stator terminals and has 3 separate low-voltage windings, each of which supply a three-phase bridge. As a result of this multi-phase connection and the two transformers in series, the harmonics are reduced considerably. Moreover, the distortion factor of the system voltage, which mainly depends on the ratio of the system short circuit power to the converter power, is kept low owing to the type of machine selected with the relatively small converter power (slip power). Requirement No. 4 is thus met fully. If the selected upper speed limit is exceeded, the converter is separated from the rotor circuit and the rotor short circuited across a resistance.

The requirement relating to the supply of short circuit power on system short circuits cannot be met satisfactorily, since a high subtransient machine reactance has to be selected owing to the gear unit and the machine house design and because the converter voltage is too low to permit shock excitation on the occurrence of heavy voltage dip on the 6.3 kV bus. Because of this, provision is made for tripping by means of undervoltage protection on the 6.3 kV side.

6. Arrangement of the auxiliary system

In view of proposed operation in an area frequently affected by system failures, as stated under requirement No. 7, and because of conditions laid down by the authorities, e.g. regarding aircraft obstruction lighting, special attention must be paid to reliability of the auxiliary power supply. In addition to the incoming supply from the 6.3 kV bus, it would therefore desirable to have an external low voltage feed-in from another branch of the medium-voltage system. Furthermore, provision is made for a diesel generating set to cover the contingency of failure of the incoming feeder during periods when the wind turbine is at the standstill or only spinning. For protection, control and monitoring, batteries and rectifiers are provided both in the control stand of the machine house and in the switch house. To ensure the availability of a supply to essential loads, e.g. for aircraft obstruction lights for which authorities lay down the condition of 100 % availability, on total failure of the a.c. voltage and failure of the diesel generating set, inverters are provided which operate on these batteries in an instantaneous standby arrangement.
(Fig. 5 single line diagram auxiliary supply system.)

7. Control and monitoring

In planning the control and monitoring devices, it is assumed that the "Growian" operates fully automatically in accordance with requirement No. 5 and is provided only with superordinated monitoring and emergency shutdown control from a system control centre.

Consequently, the system control centre receives only group alarm signals, position indications for the medium-voltage breakers and power and voltage indications for the machine. Apart from emergency shutdown, only influencing of the active power and voltage by supervisory remote control acting on the local controllers is possible.

In the machine house a control room is provided for commissioning and supervisory work from which the machine can be started mechanically without it being possible to carry out excitation and paralleling.

The actual control room for the "Growian" is located in the switchhouse at the foot of the tower which all monitoring systems are brought together. From here it is possible to take the machine into any required operating state, either manually or automatically. Paralleling, however, is also carried out with an automatic paralleling unit in manual operation.

Both the automatic control and alarm signalling are subdivided into two separate groups in the control stand of the machine house and the switch house. The purpose of this is to minimize the number of cores that have to be taken over the pivot points between the machine house and the tower and, in the event of faults in these cables, to be able to supply and control the emergency systems in the machine house from the station battery.

The number of signals involved and the measured values for control have not yet been fixed in detail. However, it has already become obvious that the expenditure involved for a power generating plant of this capacity will be quite considerable. We must wait and see to what extent experience with a prototype plant will make it possible to simplify the system.
(Fig. 6 Supervision scheme)

8. Conclusion

It can be seen that the first five of the seven system requirements listed can be met. The last two requirements must be satisfied by providing special protective and auxiliary devices.

9. Special operating modes according to location

Where a high number of annual operating hours is involved, the presence of sea air with a high salt content calls for special cooling of the electrical machine. The cooling system must be of the closed-circuit type and the cooling air must be cooled in a secondary circuit. In the case of "Growian" this is done by an air/air cooler. Where a generating plant is located inland, this air/air cooler could be omitted and the machine could be operated with open-circuit cooling.

A possible interesting application for a wind power plant could be for a local isolated system with a synchronous machine driven from another primary energy source. Here, the wind power could, for instance, be used to reduce the fuel consumption of a diesel generating set. One could also consider air storage for a gas turbine or a pump plant for filling a storage reservoir in a hydroelectric plant. For applications of this kind, the present "Growian" concept could remain practically unchanged.

Pure isolated operation of a "Growian" is not likely to be considered, although it would be possible theoretically to start the machine set with the emergency diesel and to obtain the magnetizing current for the excitation build-up process from the diesel generator.

Where a large number of individual wind power plants of the "Growian" type are to be connected together to form a so-called power plant park, a packing density of about 9 plants per square kilometre could be expected. The spacing of the plants would be determined by aerodynamic considerations.

In regard to the rated current and short-circuit power on the medium voltage side, a rated current of 3000 A and a short-circuit power of 350 MVA can be calculated at 6.3 kV for the switchgear available today. Thus, with a connection of the Growians at this voltage level, it would be necessary to provide a common system feed-in via a 30 MVA transformer from the superordinated high-voltage system for each group of 9 plants. The so-called system transformers of the typical "Growians" could then be omitted. If the system transformers of the typical "Growians" were retained, the medium voltage level could be fixed at 20 kV. In this case, the number of "Growians" operating in parallel on a common medium-voltage bus with a feed-in voltage of 110 kV would be limited to 25 by the breaking capacity of the 20 kV breakers. For the system side contribution to the short-circuit power, a normal 110 kV system with a short-circuit power of 5000 MVA was taken as a basis.

However, this approximation does not take account of economic considerations or damping elements, nor does it make allowance for the different outputs available from the various wind power plants.

References

1. Seminary and state report Windenergy
on Oct. 23 and 24, 1978 at the
Nuclear Research Centre, Jülich

2. Operating experience with the 100-kW-wind-power-plant
of the Studiengesellschaft Windkraft e.V., Stuttgart,
July 1964

Fig. 1: Wind power variation curve
Fig. 2: Speed variation curves
Fig. 3: Operating diagram of the asynchronous machine
Fig. 4: Single line diagram main circuits
Fig. 5: Single line diagram auxiliary supply system
Fig. 6: Supervision scheme

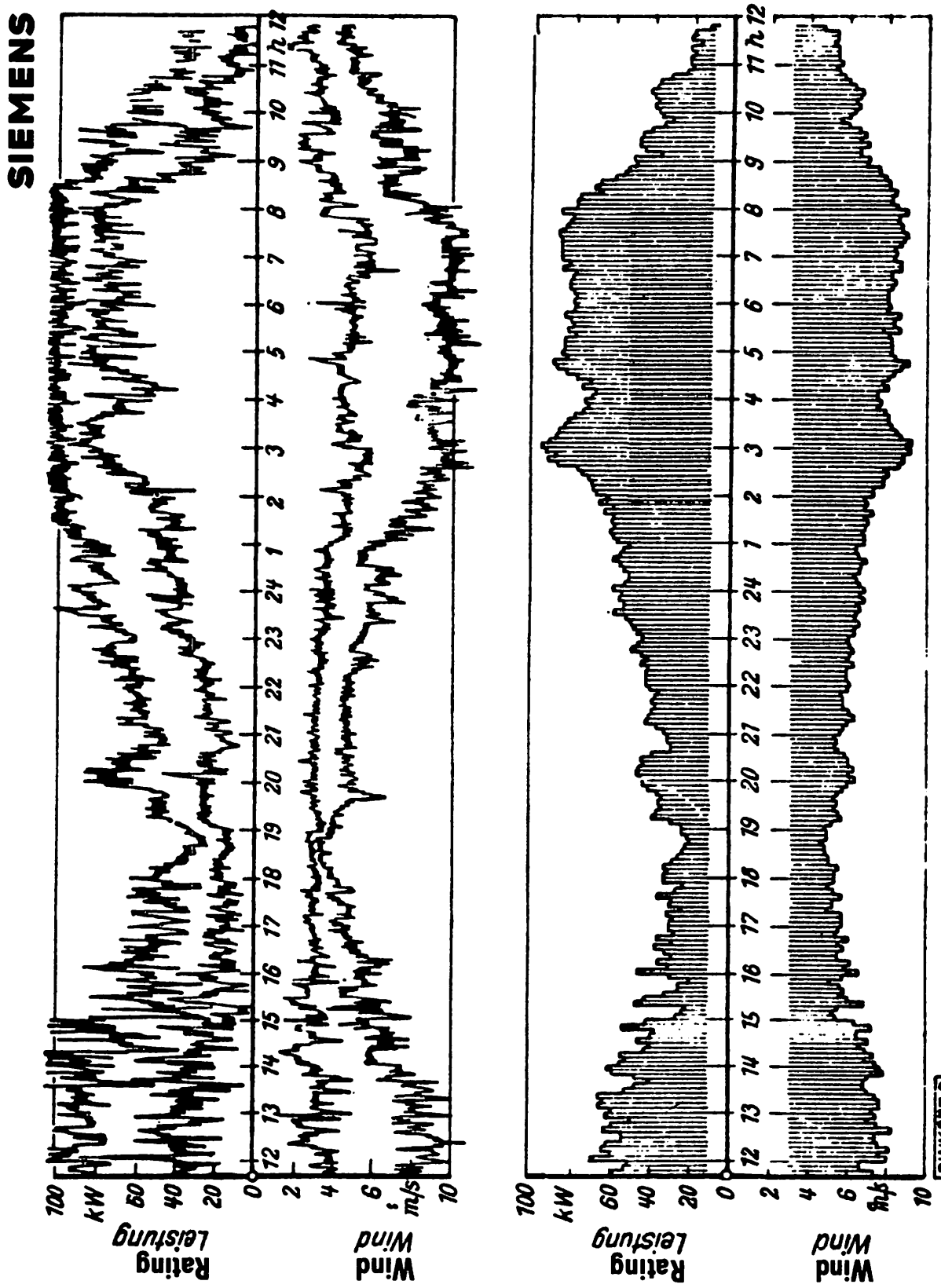

Output of 100 kW-wind-power plant

Fig. 1

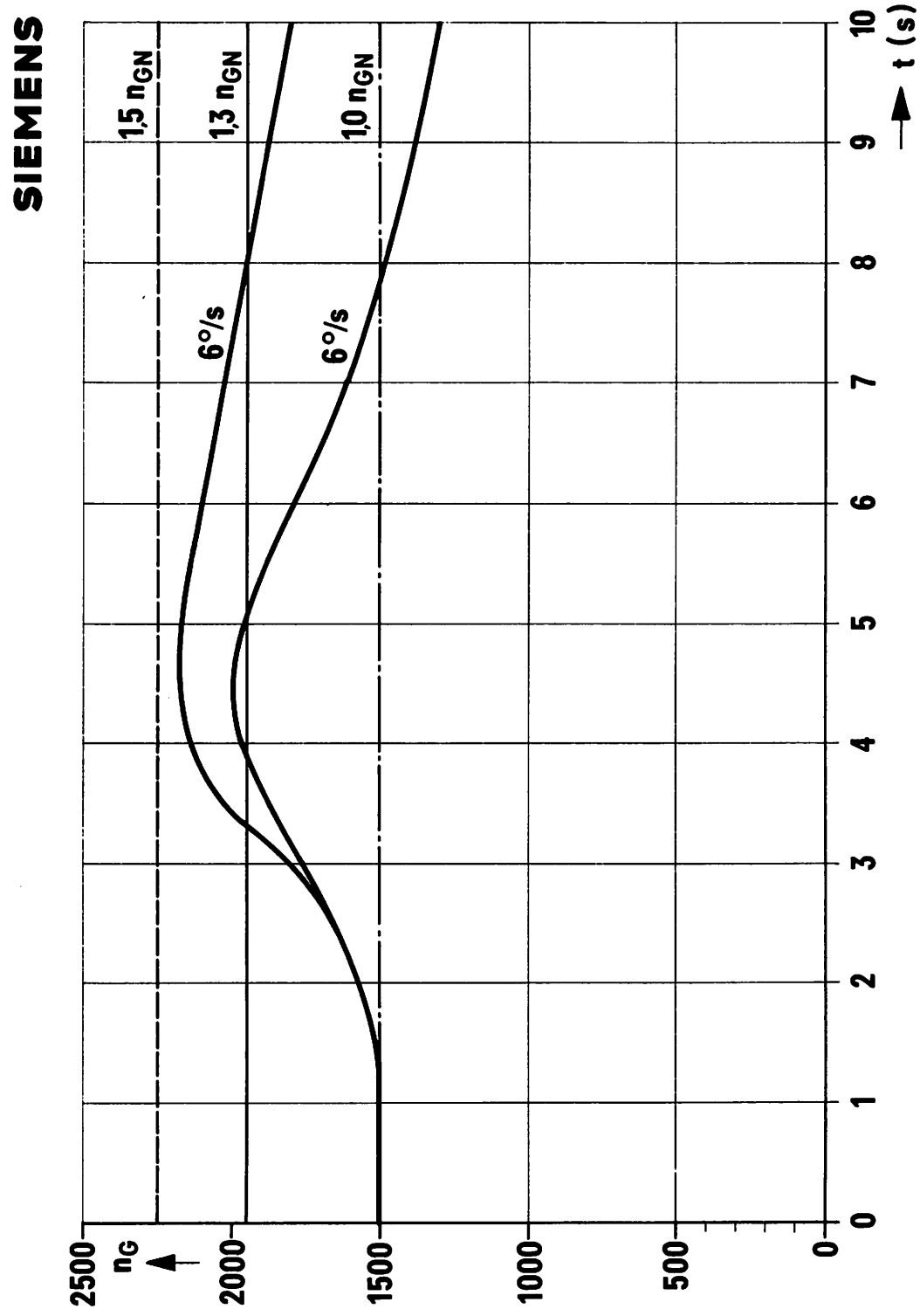

Fig. 2

Generator speed during load rejection

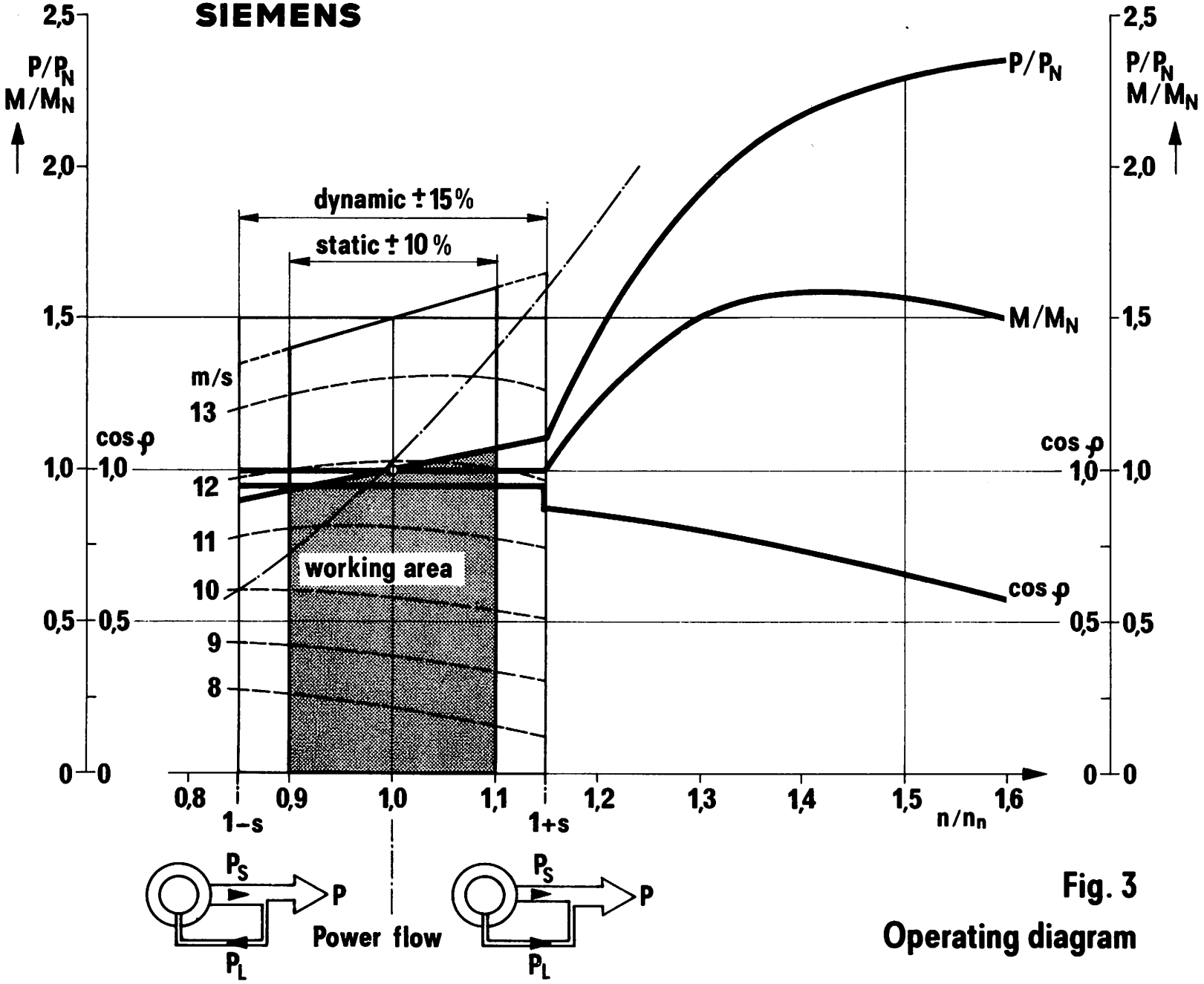

Fig. 3
Operating diagram

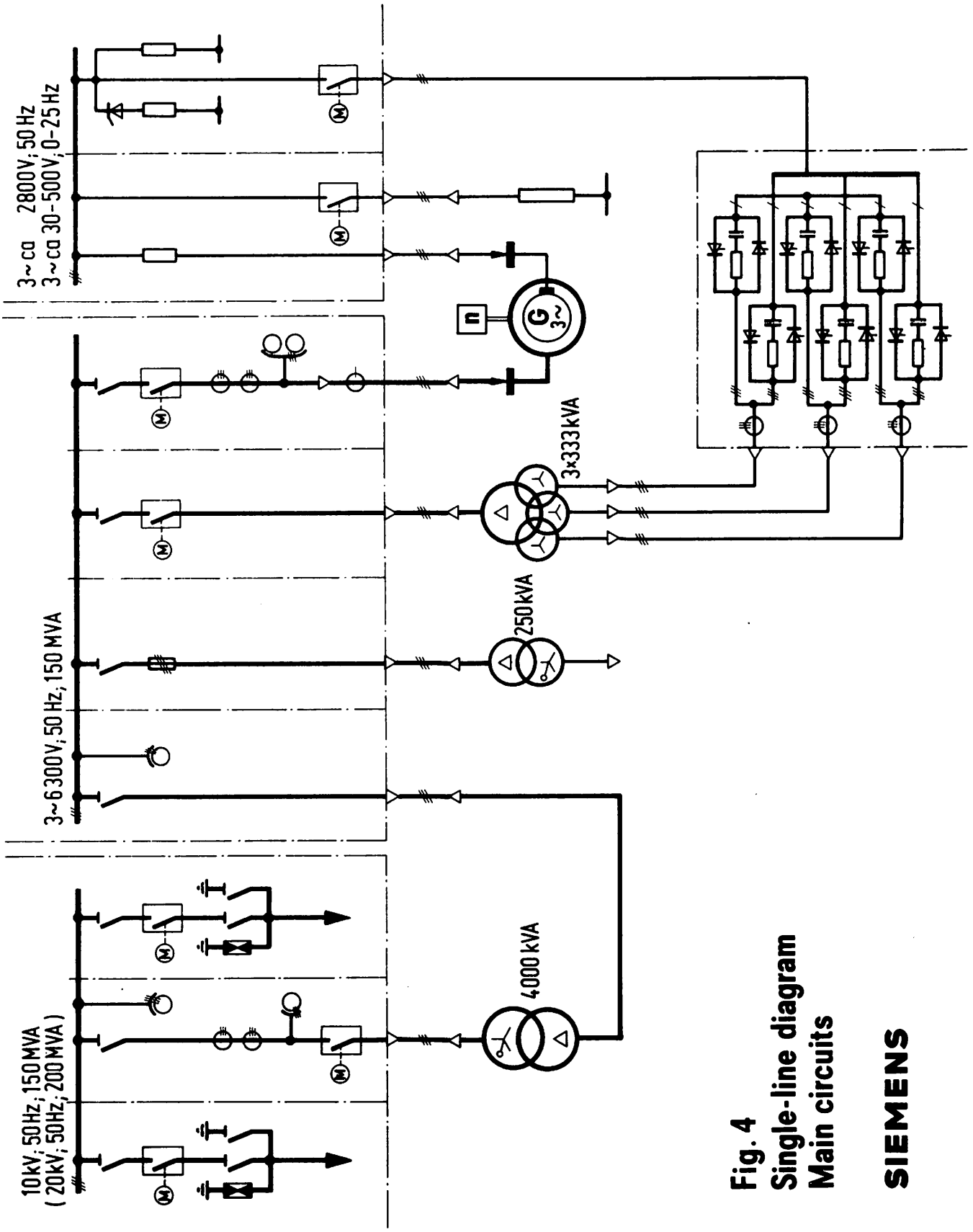

Fig. 4
Single-line diagram
Main circuits

SIEMENS

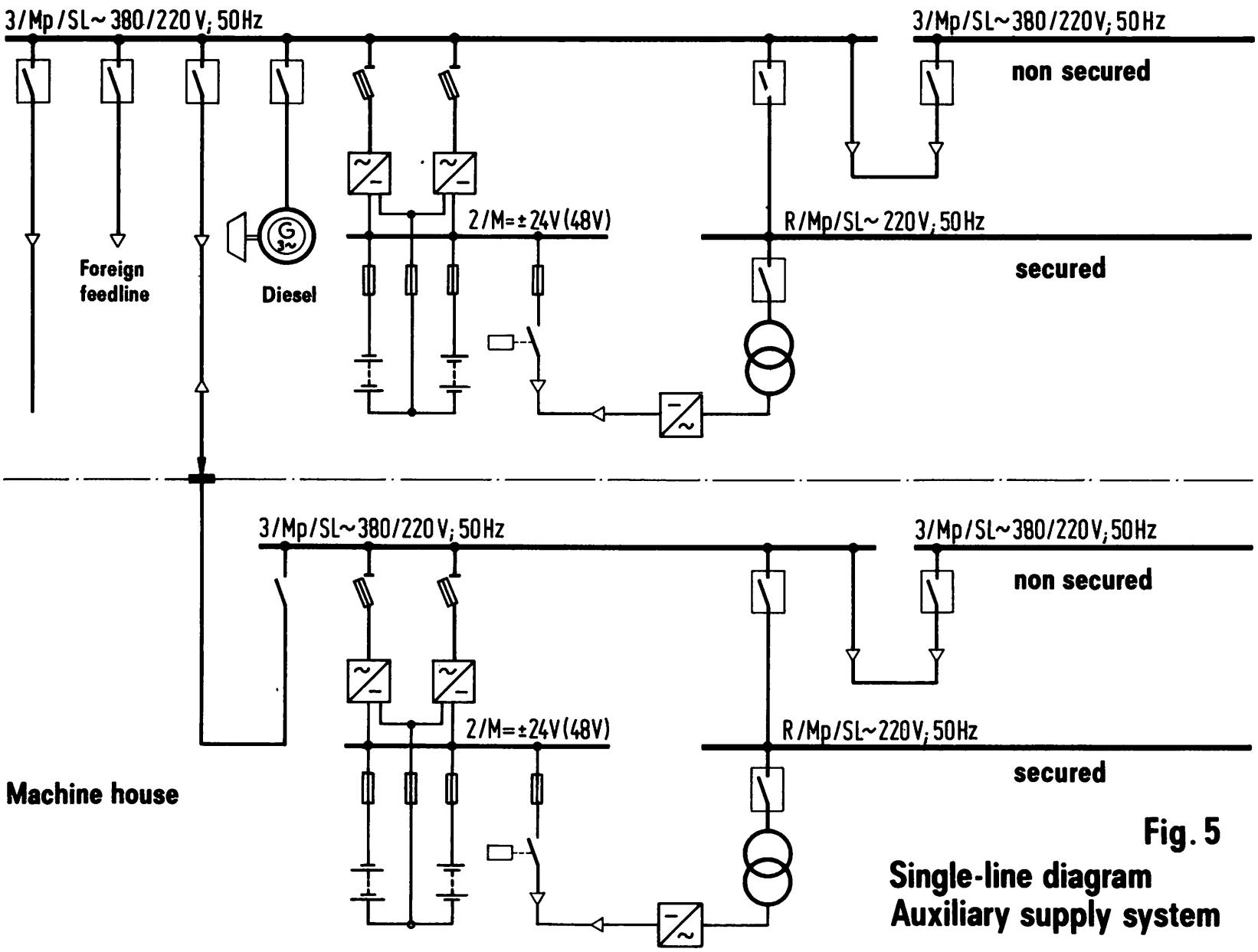

Fig. 5
Single-line diagram
Auxiliary supply system

SIEMENS

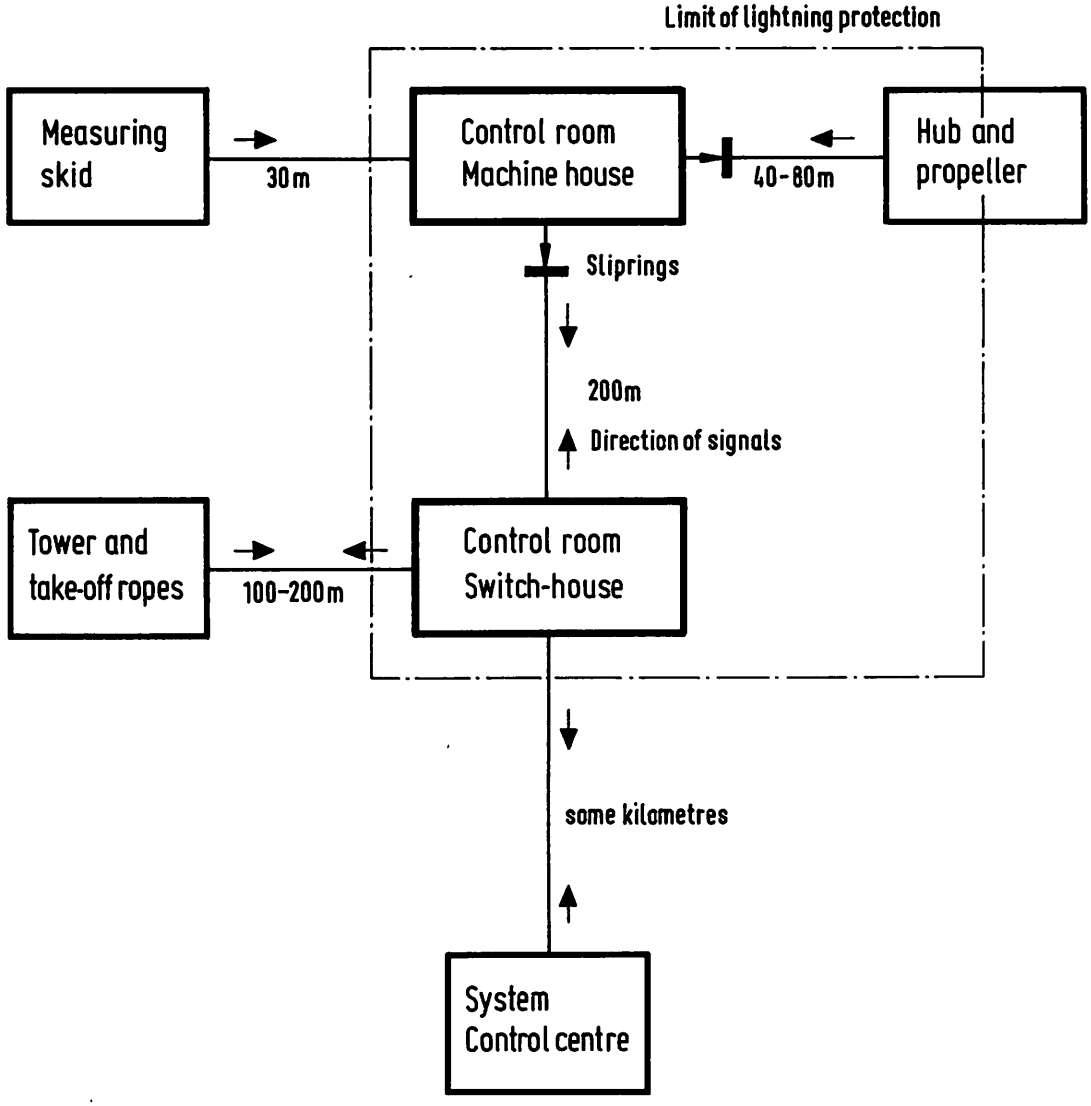

Fig. 6

Supervision schema

The report addresses the same material Bob Wolf talked about in the IEA Meeting

POWER TRAIN ANALYSIS FOR THE DOE/NASA 100-kW WIND TURBINE GENERATOR

Robert C. Seidel, Harold Gold,
and Leon M. Wenzel
National Aeronautics and Space Administration
Lewis Research Center

October 1978

Prepared for
U. S. DEPARTMENT OF ENERGY

SUMMARY

Progress in explaining variations of power experienced in the on-line operation of a 100-kW experimental wind turbine-generator is reported. Data are presented that show the oscillations tend to be characteristic of a wind-driven synchronous generator because of low torsional damping in the power train, resonances of its large structure, and excitation by unsteady and nonuniform wind flow. The report includes a dynamic analysis of the drive-train torsion, the generator, passive driveline damping, and active pitch control as well as correlation with experimental recordings. Experimental measurements of the system transfer function were made by disturbing the blade pitch angle. They compared well with the model dynamics up through the frequency of the first mode. Oscillations of power were experienced near the first-mode frequency and are explained as resulting from the first-mode resonance amplifying disturbances from, for example, blade asymmetries. Control of power about a set point used proportional-plus-integral feedback to the pitch actuator, and control gains were formulated for reducing disturbances up to frequencies less than the first mode. A fluid coupling installed in the high-speed shaft is one solution demonstrated for reducing the first-mode resonant amplification.

A predicted second-mode resonance at 3.5 hertz in the power train was not observed experimentally. A small effect of tower motion within the power train dynamics (an interaction not modelled) was observed experimentally. Experimentally observed variations in power at the two-per-rotor-revolution (2P) frequency were more than predicted. The larger 2P variation is suspected to be the impact of local turbulences not modelled. A wind feed-forward control scheme was employed, but failed to attenuate wind-speed-change effects as well as predicted because the anemometer measurement of wind speed used in the control was not well correlated with the wind speed at the rotor.

INTRODUCTION

A 100-kW experimental wind turbine-generator, designated the Mod-0, is being used to identify and solve technical problems associated with large wind turbines. It is located near Sandusky, Ohio and has been operating since November, 1975 under the federal wind energy program directed by the Department of Energy. The National Aeronautics and Space Administration, Lewis Research Center, has provided design and test.

Significant variations of power output are present when the Mod-0 is synchronized to a utility network (on-line). Some variations occur because of random

wind speed fluctuations that are too high in frequency for automatic compensation through the blade pitch mechanism. Further, blade passage through nonuniform winds such as wind shear and tower blockage produces high frequency periodic input disturbances. Because the generator assumes a torsion spring-like quality when on-line, a spring-mass resonance in the power train can result. This resonance can be destructive of structure and power quality.

The oscillation of parallel connected synchronous generators is a persistent problem even in current utilities. As discussed in reference 1, problems range from power variations of a single generator relative to a utility grid to regional oscillations for interconnected networks across the United States. Approaches to oscillations from wind turbine synchronous generators are given in references 2 to 5. The possible implementation of a slip coupling is discussed in reference 2. A slip coupling adds damping to the power train but at the cost of more complexity and reduced efficiency. In reference 3, transients accompanying wind gusts, with a compliant and damped shaft between the turbine and the generator, are calculated. A compliant shaft smooths the higher frequency power variations and damping prevents resonant oscillations with no steady power loss. However, construction of a suitably soft and damped shaft is not easily achieved. The use of a comliant shaft to lower the first resonance to below the turbine rotation frequency is analyzed in reference 4; and a method for increased generator damping through a variable excitation control is described in reference 5.

This study examines the nature of the power variations and evaluates, through analysis and test, several passive drive-train coupling elements and active pitch controls. Only torsional power-train dynamics are considered, and the analysis utilizes a linearization of the nonlinear system about an operating point. The wind turbine generator is modelled as one machine on an infinite bus with constant generator field excitation. The report does not include discussion of induction generators, fly wheel inertias, and active damping through variable blade pitch and generator excitor controls.

SYSTEM DESCRIPTION

An overall view of the Mod-0 wind turbine is shown in figure 1. It is a two-bladed, horizontal axis machine with a rotor diameter of 38.1 meters (125 ft). The axis of the downwind rotor is mechanically yawed normal to the wind. The blades are aluminum NACA 23000 series airfoils with a twist of 34^{o} from root to tip. The power train components, located inside the nacelle atop the tower, are shown in figure 2. The hub contains the hydraulic servo and bevel gears for collective pitch control. The low speed shaft supports the weight of the rotor through

For the dynamics study, the blade model was a single mass and torsion spring. The spring stiffness was sized to give the 2.47 hertz frequency calculated for the blade first inplane mode from structural studies (ref. 7). A nominal value of one-half of the rigid body moment of inertia was assigned to the blade tip and the remainder to the hub. The sensitivity of this approximation is discussed later.

A block diagram of the generator electrical model connected to an infinite bus is shown in figure 5. The generator model is the voltage-behind-subtransient-reactance model, E", of reference 8.

Control

An active generator exciter control is not modelled. Field tests showed the exciter response to be slow; hence a constant voltage is used. An active variable blade pitch angle control is modelled. The pitch actuator is modelled as a double lag at 1.5 hertz based on test measurements of the actuator response.

The static performance predicted for the blades is given in figure 6. For a power-train efficiency of 80 percent, a 125-kW rotor power input produces a 100-kW electrical power output. The blade pitch gain, the slope of the power-pitch curve, is shown at two wind speeds. The blade pitch gain of 42 kW/deg at the higher wind speed is about four times greater than the gain at the lower wind speed. To be conservative, that blade gain of 42 kW/deg for the higher wind speed is used in controller gain designs. The disturbance gain for wind speed changes can also be inferred from figure 6. In the high winds it is 56 kW/m/s (26 kW/mph). In a wind feed forward control scheme to be discussed later, the correction in pitch used for a change in wind speed can be obtained from these gains as (56 kW/m/s)/(42 kW/deg) = 1.34 degrees of pitch change per meter per second change in wind speed.

Model Equations

A list of the report symbols, detailed mechanical and electrical model equations, and FORTRAN computer program listings are presented in appendixes A, B, and C, respectively.

The power-train model has two nonlinear elements: the stiffness of the low speed shaft coupling, and the electrical generator. However, a linear analysis was used throughout the study. The low speed shaft was linearized at the operating point power level, and the generator equations became linearized by numerically perturbing the state variables (in both directions) around an operating point.

bearings mounted to the bedplate and is connected to the gear box through a spring-type coupling (not shown). The gear box is a triple mesh of gears that increases the 40 rpm rotational speed of the low speed shaft by a factor of 45. The high-speed shaft transmits the torque through a parallel set of five V belts, nominally having a 1:1 speed ratio. The generator is a four pole, 125 kVA, 480 volt, synchronous generator rated for 100 kW at a 0.8 power factor.

Three high speed shaft configurations were analyzed in the test program: a stiff steel coupling, a softer spring elastomeric coupling, and a fluid slip coupling.

A block diagram of the power control feedback loop is shown in figure 3. A transducer measurement of the power is compared with set point power and the error signal sent to a proportional plus integral structured controller. The controller commands a pitch angle through the pitch actuator.

MODEL DESCRIPTION

The primary goal of the power train modelling was to describe the transfer function of generator power-to-blade disturbances for on-line operation.

Drive Train

A block diagram of the power train mechanical elements represented as lumped masses connected by torsion springs is shown in figure 4. The values of stiffness, inertia, internal damping, and external damping used in this model are listed in table I. The stiffness and inertia values are from a normal modes analysis of the Mod-0 wind turbine reported in reference 6. The aerodynamic damping of blade inplane motion, parameter D1, was estimated from curves of rotor power at different speeds and is relatively small, especially considering it represents the inherent damping available from the wind. The external damping values represent viscous losses from friction, windage, etc. which are based on a measured 80 percent power train efficiency. The relatively larger internal or material damping values are estimates based on an assumed 0.05 damping ratio in the higher modes.

Two sets of values are given for the elastomeric shaft. The parameters labeled "stiff" are the parameters for the physical elastomeric shaft tested. The set labeled "soft-damped" are for an assumed shaft with an overly optimistic damping. Its lower stiffness corresponds to the stiffness obtained from bench tests rather than the stiffness measured in actual wind turbine test operation. The shaft was instrumented to enable recording its windup while rotating at 1800 rpm. The higher stiffness recorded is believed to be the result of internal binding of the elastomeric shaft steel supports.

The generator linearization was not particularly sensitive to the perturbation size for even a 20 percent change. System transfer functions and frequency responses were obtained using the programs of reference 9. In comparisons of experimental and analytical results, a few percent error may exist because the generator power and the generator torque were assumed proportional and were used interchangeably.

MODEL ANALYSIS

The analysis concerned primarily the transfer function of generator power-to-blade disturbances with different plant element dynamics and pitch control. Sensitivity studies were made for different blade tip inertias and generator electrical conditions.

Plant Dynamics - No Control

Frequency response magnitude plots of the transfer function of generator power-to-blade disturbances are shown in figure 7. Phase angle plots convey mostly redundant information and are not shown. Blade disturbances can result, for example, from angle of attack changes due either to changes in wind speed or pitch angle. Responses are shown for three high-speed shaft configurations: a stiff steel shaft, a soft-damped elastomeric shaft, and a slip coupling set to slip 2.3 percent at 100 kW. The responses are normalized to one at zero frequency and include no pitch control. The stiff steel shaft displays a large peak in the response at 0.69 hertz, a frequency very close to the one per rotor revolution (1P) frequency of 0.67 hertz. This resonance amplifies wind fluctuations and the periodic power variations due to, for example, any differences between blades. The peak is less with the slip and elastomeric couplings because of the damping the couplings provide.

From figure 7 it can be seen that the responses of the different configurations are about the same at the even multiples of rotor revolution frequency (2P, 4P, . . .). The largest difference occurs at the 2P frequency where the slip coupling response is about 50 percent lower than that of the stiff shaft. Thus it would be expected that the response to disturbances at frequencies above 2P would be nearly the same for all configurations.

The systems' first and second mode natural frequencies and damping ratios corresponding to the peaks in the magnitude response plot are listed in table II. It is seen that the different couplings affect primarily only the first mode damping ratio. The ratio increases from 0.097 for the stiff elastomeric coupling, to 0.10

for the stiff steel shaft, to 0.42 for the soft-damped elastomeric coupling, to 0.92 for the 2.3 percent slip coupling. Note that the damping ratio for the stiff elastomeric shaft is lower than for the stiff steel shaft, showing that a softer coupling lowers the resonant frequency but without enough damping may increase the resonant amplification.

As discussed, the blade tip moment of inertia was set to one-half of the blade's rigid body moment of inertia. System frequency responses with the slip coupling configuration for three blade tip inertias of 0.1, 0.5, and 1.0 of the rigid body inertia are plotted in figure 8. To keep the results comparable, the blade's natural frequency and damping ratio with the hub fixed and the total moment of inertia of the blade tip plus hub were held constant. It is seen that the second mode of the power train is sensitive to the tip mass. The smaller tip mass results in more peaking at a lower frequency.

In another sensitivity study, changes in the generator and electrical tie line conditions were investigated. The sensitivity analysis was for one machine on an infinite bus with no active exciter control. The conditions were changed one at a time from the power factor of 0.8 to 1.0, the power level of 100 kW to 10 kW, and from the external tie line reactance of 0.0103 per unit to 0.3 per unit. Results are considered for the stiff shaft configuration because of its initially low damping. The power train's first and second mode characteristics are listed in table III. The first mode damping ratio increases for increased power factor and decreases for decreased power. The sensitivity to all changes, however, is small.

Periodic Response

The periodic disturbances resulting from linear wind shear and tower blockage of the wind were calculated by the rotor aerodynamics program MOSTAB-WT (ref. 10). (In the MOSTAB program the blade is divided into 12 segments and allowed to move in the flap direction. The program assumes a rigid rotating hub with no blade torsional dynamics.) The time domain power variations calculated by MOSTAB for three different wind speeds are plotted in figure 9. In high winds the rotor power momentarily drops to less than half. The spectral components of the rotor power curves of figure 9 are plotted in figure 10. The curves have content only at the even multiples of rotor frequency (2P, 4P, . . .) which is the case for periodic disturbances to two symmetric blades.

A MOSTAB forcing function and the resulting responses in power output are shown in figure 11. The method used to obtain the power responses in the time domain was:

(1) Use MOSTAB to calculate the forcing function as a function of time.

(2) Take a Fourier transform of the forcing function.

(3) Multiply by the appropriate drive-train transfer function.

(4) Take an inverse Fourier transform of resulting product.

The responses obtained for the three high-speed shaft couplings appear similar. The output variation displays a 2P and a 4P component nearly equal in amplitude. The maximum excursion of power is about 7 kW from the mean.

The spectral magnitude components of the output power (from step 3 above) at the key (2P, 4P, . . .) periodic frequencies are plotted in figure 12 for the slip coupling configuration with no blade pitch control. These magnitudes are less than the MOSTAB disturbance given in figure 10 by the attenuation of the power train. Consistent with the time response description, the 4P components are as large as the 2P components.

Closed Loop Pitch Control

The proportional plus integral blade pitch controller was described in figure 3. System magnitude responses with closed loop pitch control are shown in figure 13 for the slip coupling configuration for a family of controller gains each having the proportional gain equal to one-half of the integral gain. For a given integral gain, that ratio nearly maximizes the damping ratio of the first mode. Depending on gain, the control attenuates disturbances to a value between 0.7 and 0.2 of their open loop value at a frequency of 0.1 hertz. At a frequency a decade lower the closed loop amplitude is about a decade lower because of the integral control action. All responses peak above the open loop amplitude before reaching the system first mode frequency. The peaking develops into a closed loop instability with sufficiently high gains at about 0.6 hertz. The effect of the control is not significant at the (2P, 4P, . . .) blade passing frequencies because the control bandwidth is less than the 2P frequency.

The effect of the controller with the stiff steel shaft is similar to results shown for the slip coupling if a filter set to notch out frequencies near the system first mode is used in the control. The notch filter used was a second order zero with a damping ratio of 0.1 (to cancel the system first mode) over a second order pole with a damping ratio of 1.0. Of course, the control does not remove the first mode resonance, which continues to exist, but the control does not excite this resonance. Without the notch filter the stiff high-speed shaft coupling is harder to control. For example, for system stability there can be no significant proportional gain and the integral gain must be low.

Wind Feed Forward Control

A wind feed forward control scheme using the wind speed signal as an open-loop input into the pitch angle control was investigaged as a means of attenuating the effect of wind speed changes. A schematic of the wind feed forward control is shown in figure 14. The anemometer used was insensitive to the wind direction and was located on the nacelle. It was about 4.6 meters upwind of the rotor and had about a 4.6-meter of air distance constant. These characteristics are modelled with an exponential lead and a lag. Figure 15, a cross plot of the data in figure 14, shows the pitch angle required to keep constant power for different wind speeds. The rated and low power curves shown have nearly the same slope, 1.342 deg/(m/s), thus one gain can approximate all power levels. The feed forward schedule is cut off for wind speeds below 8 m/s, and the output of the closed loop power control effectively biases the schedule up and down. A potential flaw in this scheme is that the wind speed measured by the relatively small anemometer may not be representative of the rotor average wind velocity.

The wind speed correction has dynamics because the signal must pass through the anemometer and pitch actuator dynamics. With an ideal measurement of the wind speed (one that is truly representative of the instantaneous blade average wind) and the assumed linear relation between wind speed and power, disturbances due to wind speed changes would be attenuated by the following factor

$$1 - \frac{e^{\frac{\text{distance upwind}}{\text{wind speed}}\, s}}{\left(\frac{\text{distance constant}}{\text{wind speed}}\, s + 1\right)(\text{actuator constant}\ \ s + 1)^2}$$

The frequency response magnitude of this expression is plotted in figure 16 for several wind speeds. It can be seen that the feed forward control theoretically should result in greatly reduced low frequency wind disturbance error and error reduction up to about 2 hertz.

RESULTS AND DISCUSSION

As part of the search for a better understanding of the Mod-0 power variations and the means to smooth them, experimental measurements of the power train dynamics were made and compared with model predictions. Measurements were made for the three high-speed shaft couplings, a range of controller gains, and with wind feed forward control. The transfer function of generator power output-to-rotor disturbance was the key relationship sought.

Transfer Function Measurement

To obtain data on the response of output power to rotor disturbances, the blade pitch angle was intentionally disturbed. In figure 17, a schematic block diagram of the setup used to disturb the blade pitch angle is shown. A signal from a random noise generator was summed into the pitch command. The resulting pitch disturbance provided data for transfer function measurements. About 25 minutes of data were recorded to achieve statistically good results for each test. The taped signals were either analog or sampled adequately to be nearly analog for frequencies of interest below 10 hertz. The reduction of data to its spectral content and transfer function relationships was performed using a spectrum analyzer (ref. 11).

For some tests in days of low winds, the generator was run as a motor driving the blades as a fan. Comparisons showed that whether the generator was run as a generator or as a motor did not significantly affect the transfer functions sought.

An example measurement of the transfer function of electric power output to pitch angle change is shown in figure 18. The data are most reliable near 0.5 and 2.0 hertz as indicated by the high coherence. That is, the output is attributable to the input and not to some other plant noise. Near zero frequency the coherence is low and the data are not reliable. The magnitude response does not hold a nearly constant value extending to zero frequency because wind speed changes compete with the test pitch disturbance. The action of the closed loop control is to suppress power changes. This occurred primarily at low frequencies where the wind's content is concentrated (ref. 12), and where the loop gain is highest because of the integral control. The coherence is also low near 0.7 and 1.3 hertz because of system 1P and 2P disturbances not related to the test disturbance. Beyond about 2.5 cps the coherence is generally near zero, and further results are reported to only 2.5 hertz.

There was no clear measurement of a system second mode resonance which the power train dynamic model would predict to be near 3.5 hertz. A second mode resonance would be indicated by a peak in the magnitude response accompanied by a phase shift of 180° and high coherence. In the sensitivity study, it was noted that the second mode peak decreased for increased inertia in the blade tip. However, it may not follow that the experimental nonobservance of a second mode can be used to increase the tip inertia because the cantilevered and tapered blade was represented by only a single mass.

Stiff steel shaft. - A transfer function measured in high winds with the stiff steel high-speed shaft (no slip coupling) and the corresponding model predictions are compared in figure 19. The vertical magnitude axis scale is linear to more clearly illustrate the large resonance. The resonant frequency, that frequency where the phase is -90° and the magnitude peaks, is seen to be 0.69 hertz which is also the calculated value. The experimental resonant peak is lower than that predicted by the model. The experimental first mode damping ratio is estimated to be 0.22 which is more damping than the calculated value of 0.10 (table II). Increased damping could result from slippage in the V belts. About 0.3 percent slip was found; but it was not very repeatable. A 0.3 percent viscous slip in the model results in a 0.2 damping ratio but lowers the calculated first mode frequency lower than the measured value. Alternative explanations include presuming the generator has more damping than calculated. It is more likely, however, that nonlinearities become important for large swings in power. Nonlinearities in a system may appear to decrease a resonance because power input at one frequency may shift upon output to different frequencies and thus be missed in the data reduction.

Stiff elastomeric shaft. - A measured and calculated transfer function with the stiff elastomeric high-speed shaft is shown in figure 20. A large first mode resonant peak, similar to the results with the steel shaft, is evident in the plot. The observed resonant frequency is 0.54 hertz which is also the calculated frequency. From the transfer function magnitude and phase characteristics, the first mode damping ratio is estimated to be 0.22, which is more damped than the calculated value of about 0.1. It is noted that experimentally, both the elastomeric and the steel shaft responses give a damping ratio of about 0.22. Slip in the V belts in the motoring mode where the elastomeric shaft test was run was much less than the 0.3 percent slip quoted for the steel shaft. The likely explanation for the greater apparent damping again being that, for large swings in power, nonlinearities in the system appear to reduce the resonant peak.

Slip coupling. - The calculated and measured system transfer functions for the slip coupling set to slip 1.5 and 4.7 percent at 100 kW are compared in figures 21 and 22, respectively. The predicted responses are in good agreement through the first mode resonance of about 0.5 hertz. Near 2 hertz there exists a difference of about 10 dB or a factor of 3. This is discussed next.

Tower interaction. - In previous transfer function magnitude comparisons the amplitude responses of the model were lower than the experimental data near 2 hertz. Because measurements of tower motion correlate well with power variations near that frequency it is believed that there is tower interation. Three accelerometers were mounted in perpendicular planes on the rear main bearing

support of the low speed shaft. Only the horizontal yaw results are reported; the other two planes were similar. To show the effect of tower motion on the power train, the path is broken into two parts. First, the response of tower acceleration-to-pitch is shown in figure 23, and then the response of power-to-tower acceleration is shown in figure 24. Judging from the coherences, this path is important only near 2 hertz where tower natural frequencies are excited. At 1.85 hertz it is interesting to note that "acceleration-to-pitch" (0.18 g/deg) times "power-to-acceleration" (107 kW/g) equals 19 kW/deg. This 19 kW/deg compares well with the direct value obtained from figure 21 of about 17 kW/deg measured (and 6 kW/deg calculated). Thus, with good coherence, the tower motion path accounts for the higher response magnitude. Fortunately, tower motion does not cause a serious problem for the Mod-0 because it occurs at a relatively high and well placed frequency in comparison with the major excitation forces.

Control gains. - The effect of the controller on the closed loop response of power-to-pitch command is shown in figures 25 and 26. Figure 25 was run at normal values of proportional and integral gain while in figure 26 the gains were increased by a factor of 6. Calculated responses are shown in both cases; it is noted that the analytical and experimental results agree well. The response with the high gain controller exhibits better low frequency attenuation but it is more resonant. The actual system was nearly unstable; it oscillated out of synchronism moments after completing the test tape. The model with that high gain was unstable. The phase response calculations are shown to only the frequency of instability. Obviously the control gain needs to be some compromise between attenuation at low frequency and amplification near the first mode.

Wind feed forward. - Operational data recordings of the slip coupling configuration were made with and without wind feed forward control. Comparisons varied because of wind differences between runs and it was difficult to isolate the effect of the feed forward control. A comparison of the coherences of the responses of "power-to-the measured wind speed" is shown in figure 27. The argument for wind feed forward is that it should decrease any relation between wind and power. It is seen that in both cases the coherence is mostly low and the transfer function data are not reliable. The coherence with feed forward showed a lower relation at the very low frequencies but a generally higher relation up to 1 hertz. This would indicate that the feed forward as implemented was increasing rather than decreasing power excursions resulting from unsteady wind conditions over a broad frequency range. This is attributed to the single, relatively small wind speed sensor not being a reliable indication of the instantaneous average wind over the circle of area swept out by the blades.

Power Time History

Sample time history traces of Mod-0 power variations about a 100-kW set point are shown in figures 28(a) and (b). The power dropped below the set point sometimes because there was not enough wind. In circled areas labeled "over power", the power peaked to near 150 kW. In the figure 28(a), the case without wind feed forward, the overshoot was apparently in response to a gust of wind. It is noted that control action subsequently reduced the power level although the wind speed remained high. In figure 28(b), the case with wind feed forward, the power overshoot occurred in response to a drop in the measured wind speed! Apparently, the feed forward control over-corrected because the measured drop in local wind was not representative of the blade average wind speed. Unlike the model calculations of figure 11, the power exhibits oscillations at a frequency of 2P fading in and out. The 2P oscillations have at times about a 20-kW zero-to-peak amplitude for both low and high winds. This 20-kW (maximum) amplitude compares poorly to a predicted (mean) amplitude of only 1.2 kW in a 8.9 m/s wind from figure 12.

Spectral Analysis of Power

A frequency domain spectral analysis of generator power measurements is shown in figure 29. The peak at the odd 1P multiple exists because, as was found, the blades were not pitched the same by a difference of 1.7^{o}. The source of the peaks labeled "X" at 2.56 hertz and at twice that frequency has not as yet been identified. There are peaks at the even multiples of the blade passing frequencies (2P, 4P, . . .). The 2P peak differs qualitatively from the others in that it is much broader. This may suggest that nonlinear or higher order couplings exist. Another possibility is that the flow field has random local distortions over only part of the blade area and lasting only a few revolutions so as to modulate the periodic power around the 2P frequency. The buildup around the 2P peak was observed "real-time" during the data reduction. It appeared to be random, lending support to assumed unsteady local wind turbulence.

In figure 30, the frequency content in the peaks of the spectrum of figure 29 are compared with model predictions. The experimental peaks are not a single frequency as in the analytical case. The effective content of the broad peaks was calculated as the square root of the sum of the squares of individual analyzer readings. The analytical points were values from figure 12 divided by the square root of two to convert zero-to-peak sinusoidal amplitude to root mean square power. The comparison shows good agreement at the 4P and 6P frequencies, but there is much more content in the experimental data at 2P and 8P. The 8P content

was small enough and at a high enough frequency to be insignificant. The average 2P output power content, about 4 kW rms, is about four times that predicted and is discussed further.

Power oscillation at the 2P frequency has just been shown higher than that predicted using input from MOSTAB for a fixed hub applied as a schedule to the power train torsional model. An insight is that the 2P power correlates well with the blade flatwise bending moment (a nontorsional moment and not in the model). Transfer function data between power and blade flatwise bending moment, from experimental data recorded during normal operation are shown in figure 31. Because the coherence is high near the 2P frequency, it can be concluded that the 2P power variations result probably from a forcing function and not some unknown torsional resonance. A 2P forcing function not considered in the MOSTAB calculations is nonlinear wind shear. The MOSTAB calculations assumed a linear wind shear of plus and minus 15 percent of the hub wind speed. This linear shear causes little net aero-torque variations as blade differences cancel. However, a quadratic shear with power portional to wind speed would increase the aero-torque variations. A calculation that does not include inertial effects from flap dynamics shows quadratic shear could about double the 2P spectrum content (add a 7.5 kW sinusoid to the 2P rotor input or 1.3 kW rms to the 2P generator output). Another possible source of 2P power variation not considered in the MOSTAB calculations are random local turbulences.

CONCLUDING REMARKS

1. Oscillation of electric power near the one-per-rotor-revolution frequency (1P) was evident during early on-line tests of the Mod-0 with the stiff high-speed shaft. This was found to result from a torsional power-train resonance near the 1P frequency having only a 0.10 damping ratio. The resonance-amplified 1P noise resulting from nonsymmetric blade-pitch settings. The control system (when without a first-mode notch filter implemented) further increased the oscillation. The frequency of the first mode depends upon the power-train torsional spring rate. To shift the resonant frequency away from the 1P frequency and to add damping to the system so as to reduce the amplification, different high-speed shaft couplings were studied. The calculated damping ratio of the first mode increased to 0.42 for a soft-damped elastomeric coupling and to 0.92 for a fluid coupling set to slip 2.3 percent at 100 kW. Experimental measurements of the system transfer function compared well with linear-model dynamics up through the frequency of the first mode. In particular, the ability of the slip coupling to damp the first mode in comparison with the stiff shaft was demonstrated experimentally.

2. Although the model predicted a significant resonance from the second mode of the power train, there was no clear measurement proving its existence.

3. A small tower motion was observed experimentally. However, tower motion was not part of the power-train model.

4. The measured power content near the two-per-revolution (2P) frequency was broadband and had some four-times-greater content than predicted. The larger 2P power may result from local turbulences acting over only part of the blade area.

5. In a sensitivity analysis, dynamics of the power-train model (with constant generator excitation) were not significantly affected by small variations of the generator and electrical parameters of power level, power factor, and tie-line reactance.

6. Closed-loop pitch controller proportional-plus-integral-feedback gains were formulated that could attenuate low-frequency disturbances but only up to frequencies less than the system first mode. Excessively high gains drove the system toward instability at about 0.6 hertz.

7. Analysis of a wind feed-forward control scheme using a wind-speed signal to command pitch indicated virtual elimination of low-frequency wind effects and attenuation to frequencies well beyond the system first mode. But the large advantage predicted was not seen, on the average, experimentally because the measured wind speed did not represent the instantaneous wind speed past the rotor blades.

APPENDIX A

SYMBOLS

C	torque conversion, N-m/P.U.
D	external damping, N-m/(rad/sec)
d	direct axis
d	internal damping, N-m/(rad/sec)
E	rms EMF, P.U.
E_{FD}	field EMF, P.U.
F	torque, N-m
I	rms current, P.U.
J	inertia, N-m/sec^2
j	imaginary number
K_1, K_2, K_d	constants
k	spring rate, N-m/rad
P	rotor frequency
q	quadrature axis
R	resistance, P.U.
R_g	gear ratio
r	reference axis
r_a	armature resistance, P.U.
s	Laplace variable, sec^{-1}
T	time constant, sec
T_b	blade torque, N-m
T_e	electrical torque, N-m
V	voltage, P.U.
v	wind velocity, m/s
X	reactance, P.U.
X_{xd}	constant

x synchronous reactance, P.U.

x_{ad} mutual armature damper circuit reactance, P.U.

Y admittance, P.U.

β angle between V_∞ and V_a, rad

β pitch angle, deg

δ angle between quadrature and reference axis, rad

δ'' angle between E'' and reference axis, rad

θ angle between reference axis and I_a, rad

λ_D stator rms subtransient flux linkage, P.U.

φ angle between I_a and V_a, rad

Subscripts:

a armature

d direct axis

e external

IC initial condition

q quadrature axis

r reference axis

t terminal

x conjugate direction to r axis

0 open circuit

1 first blade

2 second blade

3 hub and low speed shaft

4 gear box and high-speed shaft

5 first pulley and "V" belts

6 second pulley and generator

∞ infinite bus

Superscripts:

' transient

'' subtransient

^ summed impedance

APPENDIX B

MODEL

Mechanical Model

The differential equations of the mechanical model of the Mod-0 power train shown in figure 5 are listed below for a perturbation about an operating point.

$$J_1\ddot{\theta}_1 = F_1 - D_1\ddot{\theta}_1 + T_b$$

$$J_1\ddot{\theta}_2 = F_2 - D_1\dot{\theta}_2$$

$$J_3\ddot{\theta}_3 = F_3 - F_1 - F_2 - D_3\dot{\theta}_3$$

$$J_4\ddot{\theta}_4 = R_gF_4 - F_3 - R_gD_4\dot{\theta}_4$$

$$J_5\ddot{\theta}_5 = F_5 - F_4 - D_5\dot{\theta}_5$$

$$J_6\theta_6 = -F_5 - D_6\theta_6 - \left[\left(T_e - T_e\right)_{IC}\right]C$$

where the forces F_i between the inertias are

$$F_1 = k_1(\theta_3 - \theta_1) + d_1\left(\dot{\theta}_3 - \dot{\theta}_1\right)$$

$$F_2 = k_1(\theta_3 - \theta_2) + d_1\left(\dot{\theta}_3 - \dot{\theta}_2\right)$$

$$F_3 = k_3(\theta_4 - \theta_3) + d_3\left(\dot{\theta}_4 - \dot{\theta}_3\right)$$

$$F_4 = k_4(\theta_5 - R_g\theta_4) + d_4\left(\dot{\theta}_5 - R_g\dot{\theta}_4\right)$$

$$F_5 = k_5(\theta_6 - \theta_5) + d_5\left(\dot{\theta}_6 - \dot{\theta}_5\right)$$

Generator Model

The differential equations for the generator model shown in the figure 7 block diagram are listed next.

$$T_e = E''_d I_d + E''_q I_q$$

$$T''_{q0}\dot{E}''_d = -E''_d - (x_q - x'')I_q$$

$$T''_{d0}\dot{\lambda}_D = -\lambda_D + E'_q + (x'_d - x_\ell)I_d$$

$$T'_{d0}\dot{E}'_q = -E'_q(1 + K_d) + X_{xd}I_d + K_d\lambda_D + E_{FD}$$

$$E''_q = K_1 E'_q + K_2\lambda_D$$

$$I_d = Y\left[-\hat{R}(V_{\infty d} - E''_d) + \hat{X}''(V_{\infty q} - E''_q)\right]$$

$$I_q = -Y\left[\hat{X}''(V_{\infty d} - E''_d) + \hat{R}(V_{\infty q} - E''_q)\right]$$

where

$$\hat{R} = r_a + R_e$$

$$\hat{X}'' = x'' + X_e$$

$$V_{\infty d} = -V_\infty \sin(2\theta_6 + \delta_{IC})$$

$$V_{\infty q} = V_\infty \cos(2\theta_6 + \delta_{IC})$$

$$Y = 1\Big/\left[(\hat{R})^2 + (\hat{X}'')^2\right]$$

$$K_1 = (x'' - x_\ell)/(x'_d - x_\ell)$$

$$K_2 = 1 - K_1$$

$$K_d = (x_d - x'_d)(x'_d - x'')\Big/(x'_d - x_\ell)^2$$

$$X_{xd} = (x_d - x'_d)(x'' - x_\ell)/(x'_d - x_\ell)$$

Model electrical parameters are given in table IV. The external tie line resistance and reactance values listed are for the Mod-0 Plum Brook Station location. The following four parameters listed were estimated as follows.

$$x'' = (x''_d + x''_q)/2$$

$$T''_{d0} = T''_d(x'_d/x''_d)$$

$$T'_{d0} = T'_d(x_d/x'_d)$$

$$x_\ell = x_d - x_{ad}$$

INITIAL CONDITIONS

The assumed known initial variables were not model states but the machine power, the power factor $\cos \varphi$, and voltage of the infinite bus V_∞. An initial condition phase diagram is given in figure 32. The model values derived are in the direct-quadrature axis which is a rotated mirror image of the reference bus axis.

An estimate of current I_a is

$$I_a \cong \text{machine power}/(V_\infty \cos \varphi)$$

The power into the infinite bus is the machine power minus the transmission line ohmic loss.

$$\text{bus power} = \text{machine power} - R_e I_a^2$$

The current I_r in phase with this power is

$$I_r = \text{bus power}/V_\infty$$

The derivation of the I_x component follows. The coordinates of V_a from figure 32 (or p. 161 of ref. 8) using complex arithmetic are

$$V_a = V_\infty + I_a(R_e + jX_e)$$

$$V_a = V_\infty + (I_r + jI_x)(R_e + jX_e)$$

$$V_a = (V_\infty + I_r R_e - I_x X_e) + j(I_x R_e + I_r X_e)$$

The angle β between V_a and V_∞ is

$$\beta = \tan^{-1}(\text{Imag } V_a/\text{Real } V_a)$$

$$\beta = \tan^{-1} \frac{I_x R_e + I_r X_e}{V_\infty + I_r R_e - I_x X_e}$$

The power factor angle φ between I_a and V_a is the arc cosine of the power factor.

$$\varphi = \cos^{-1} (\text{power factor})$$

From figure 32

$$\varphi = \beta - \theta$$

where θ is the angle of I_a with the reference or

$$\theta = \tan^{-1}(I_x/I_r)$$

Thus

$$\tan \varphi = \tan(\beta - \theta) = \frac{\tan \beta - \tan \theta}{1 + \tan \beta \tan \theta}$$

which after substitution for θ and β can be solved for I_x.

$$I_x = -V_\infty \pm \sqrt{\frac{V_\infty^2 - 4(-X_e + R_e \tan \varphi)\left(-I_r^2 X_e + I_r\right)(V_\infty + R_e I_r)\tan \varphi}{2(-X_e + R_e \tan \varphi)}}$$

The sign of the quadratic used was that for the minimum I_x (a negative number).

From figure 32 the F'' and E_{qa} vectors with respect to the reference axis are

$$V_a = V_\infty + I_a(R_e + jX_e)$$

$$E'' = V_a + I_a(r_a + jx'')$$

$$E_{qa} = V_a + I_a(r_a + jx_q)$$

These variables are related to the model d-q axis. The electrical angle δ between the q and r axes is

$$\delta = \tan^{-1}(\text{Imag } E_{qa}/\text{Real } E_{qa})$$

The angle δ'' of the E'' vector to reference is

$$\delta'' = \tan^{-1}(\text{Imag } E''/\text{Real } E'')$$

From figure 32 geometry

$$E''_q = |E''| \cos(\delta - \delta'')$$

$$E''_d = - |E''| \sin(\delta - \delta'')$$

$$I_d = - |I_a| \sin(\delta - \theta)$$

$$I_q = |I_a| \cos(\delta - \theta)$$

The other initial conditions can be found by setting the state equations to zero. The λ_D state equation and the E''_q equation are two equations in two unknowns.

$$-\lambda_D + E'_q + (x'_d - x_\ell)I_d = 0$$

$$K_1 E'_q + K_2 \lambda_D - E''_q = 0$$

with solutions

$$E'_q = E''_q - K_2(x'_d - x_\ell)I_d$$

or using the definition of K_2

$$E'_q = E''_q - (x'_d - x'')I_d$$

and

$$\lambda_D = E'_q + (x'_d - x_\ell)I_d$$

The E'_q state equation solved for E_{FD} is

$$E_{FD} = E'_q(1 + K_d) - X_{xd}I_d - K_d\lambda_D$$

The set of numerical values for the figure 32 nominal operating point and parameters of table IV are listed below.

Machine power, P.U.	≈0.8
Power factor	0.8
V_∞, P.U.	1
$I_a(r,x)$	(0.7953, -0.5898)
$V_a(r,x)$	(1.0098, -0.0054)
$E_{qa}(r,x)$	(1.6517, 0.8411)
$E''(r,x)$	(1.1188, 0.1225)
δ, rad	0.4710
δ'', rad	0.1090
T_e, P.U.	0.8176
I_r, P.U.	0.7953
I_x, P.U.	-0.5898
E''_d, P.U.	-0.3985
E''_q, P.U.	1.0525
θ, rad	0.6381
I_d, P.U.	-0.8865
I_q, P.U.	0.4411
E'_q, P.U.	1.0565
λ_D, P.U.	0.9546
E_{FD}, P.U.	2.8694

APPENDIX C

COMPUTER SUBROUTINES

Computer subroutines written in FORTRAN generated the initial conditions and state derivatives for a linear analysis package. These subroutines are listed in figures 33 and 34.

The FORTRAN symbols which are unlike the report symbols are defined below.

$Z(1) = \theta_1$	$Z(11) = \theta_6$
$Z(2) = \dot{\theta}_1$	$Z(12) = \dot{\theta}_6$
$Z(3) = \theta_2$	$Z(13) = E''_d$
$Z(4) = \dot{\theta}_2$	$Z(14) = \lambda_D$
$Z(5) = \theta_3$	$Z(15) = E'_q$
$Z(6) = \dot{\theta}_3$	$Z(16) = T_e$ (lagged at 10 Hz)
$Z(7) = \theta_4$	$Z(17) = \beta$
$Z(8) = \dot{\theta}_4$	$Z(18) = \dot{\beta}$
$Z(9) = \theta_5$	Z(19) = controller state
$Z(10) = \dot{\theta}_5$	

CD1 = D_1, etc.	K11 = k_1
D1 = d_1, etc.	R1 = R_g
DLT = δ''	TM = $T_{e\ IC}$

The F vector is the derivative of the Z vector. For example, $F(1) = \dot{\theta}_1$ and $F(2) = \ddot{\theta}_1$. Other constants are

B = 2/0.112 servo damping

CONVRT (in-lb/P.U.) = torque high speed shaft

Gain (in-lb/P.U.) = transducer gain $\frac{10}{150}$ V/kW $\times$ servo gain (9.4 deg/V)

$\times$ blade gain (42.5 kW/deg) $\times$ convert (5869 in-lb/P.U.)

$\times$ speed ratio R_g (45 rpm/rpm

REFERENCES

1. Symposium on Adequacy and Philosophy of Modeling: Dynamic System Performance. 1975 Winter Meeting. IEEE, N. Y., 1976.
2. Wind Turbine Project. New York Univ., Engineering Research College, for Office of Production Research and Development, War Production Board, W.P.B.-144, Washington, D.C., Jan. 31, 1946.
3. Johnson, Craig C.; and Smith, R. T.: Dynamics of Wind Generators on Electric Utility Networks. IEEE Trans. Aerosp. Electron. Syst. Vol. AES-12, no. 4, July 1976, pp. 483-493.
4. Mirandy, L. P.: Rotor/Generator Isolation for Wind Turbines. AIAA Paper 77-372, Mar. 1977.
5. Barton, Robert S.: Mod-1 Wind Turbine Generator Analysis. Wind Turbine Structural Dynamics. NASA CP-2034, 1977, pp. 167-178.
6. Sullivan, T. L.; Miller, D. R.; and Spera, D. A.: Drive Train Normal Modes Analysis for the ERDA/NASA 100-Kilowatt Wind Turbine Generator. NASA TM-73718, 1977.
7. Chamis, C. C.; and Sullivan, T. L.: Free Vibrations of the ERDA-NASA 100 kW Wind Turbine. NASA TM X-71879, 1976.
8. Anderson, P. M.; and Fouad, A. A.: Power System Control and Stability. Vol. 1. The Iowa State University Press, 1977.
9. Seidel, Robert C.: Computer Programs for Calculation of Matrix Stability and Frequency Response from a State-Space System Description. NASA TM X-71581, 1974.
10. Hoffman, John A.; and Holchin, Barry W.: Modifications to MOSTAB for Wind Turbine Applications. MRI-2711, Mechanical Research, Inc., 1974.
11. Instruction Manual for the Model O-FFT 400, OMNIFEROUS Fast Fourier Transform Analyzer System. Nicolet Scientific Corporation, Northvale, N.J., 1976.
12. Lumley, J. L.; and Panofsky, H. A.: The Structure of Atmospheric Turbulence. Interscience Publishers, 1964.

TABLE I. - MECHANICAL PARAMETERS

(a) SI units

Station subscript	Inertia J, N-m-sec^2	Stiffness k, N-m/rad	Internal damping d, $\frac{\text{N-m}}{\text{(rad/sec)}}$	External damping D, $\frac{\text{N-m}}{\text{(rad/sec)}}$
1	31 930	7 682 968	33 895	3051
3	64 686	[a]558 477$\sqrt{\text{kW}}$	2 260	114
Four 2.3 percent slip	2 859	0	131	.113
Four steel	1 154	75 474	21	.113
Four elastomeric (soft-damped)	1 154	654	366	.113
Four elastomeric (stiff)	1 154	3 054	122	.113
Five slip	.1.69	20 337	17	.07
Five no slip	.86	20 337	17	.07
6	.11	------	---	.18

(b) U.S. customary units

Station subscript	Inertia J, lbf-in-sec^2	Stiffness k, lbf-in/rad	Internal damping d, $\frac{\text{lbf-in}}{\text{(rad/sec)}}$	External damping D, $\frac{\text{lbf-in}}{\text{(rad/sec)}}$
1	282 600	68 000 000	300 000	27 000
3	572 520	[a]4 943 000$\sqrt{\text{kW}}$	20 000	1 010
Four 2.3 percent slip	25 300	0	1 160	1.0
Four steel	10 210	668 000	186	1.0
Four elastomeric (soft-damped)	10 210	5 790	3 240	1.0
Four elastomeric (stiff)	10 210	27 039	1 080	2.0
Five slip	15	180 000	150	.62
Five no slip	7.6	180 000	150	.62
6	24.2	-------	---	1.6

[a]Linearized about steady state. Curve fit to stiffnesses of low speed shaft plus Falk coupling plus gears.

TABLE II. - SYSTEM RESONANCES - NO CONTROL

Configuration	First mode		Second mode	
	Natural frequency, cps	Damping ratio	Natural frequency, cps	Damping ratio
2.3 Percent slip at 100 kW	0.430	0.920	3.495	0.063
Elastomeric (soft-damped)	.516	.420	3.533	.058
Elastomeric (stiff)	.582	.097	3.522	.056
Stiff steel	.689	.104	3.540	.056

TABLE III. - POWER TRAIN (STIFF SHAFT) SENSITIVITY TO ELECTRICAL FACTORS

Variable	First mode		Second mode	
	Natural frequency, cps	Damping ratio	Natural frequency, cps	Damping ratio
Nominal[a]	0.689	0.104	3.54	0.0558
Power factor = 1	.713	.192	3.55	.0551
$X_e = 0.3$	.641	.080	3.50	.0537
Power = 11 kW (no change in k_3)	.570	.067	3.49	.0684

[a]Nominal conditions are power factor = 0.8, external reactance, $X_e = 0.0103$, power = 103 kW.

TABLE IV. - ELECTRICAL PARAMETERS

T''_d, sec	0.0085
T''_{q0}, sec	0.062
T'_d, sec	0.145
T''_{d0}, sec	0.011
T'_{d0}, sec	1.942
x''_d, P.U.	0.128
x'_d, P.U.	0.165
x_d, P.U.	2.21
x''_q, P.U.	0.193
x_ℓ, P.U.	0.05
x_{ad}, P.U.	2.16
x", P.U.	0.1605
K_1, P.U.	0.961
K_2, P.U.	0.039
K_d, P.U.	0.696
X_{xd}, P.U.	1.965
r_a, P.U.	0.018
R_e, P.U.	0.00466
X_e, P.U.	0.01031
V_∞, P.U.	1
Base kilovolt-amperes, kVA	125
Base voltage, V	480
Base ohms, ohms per phase wye	1.843

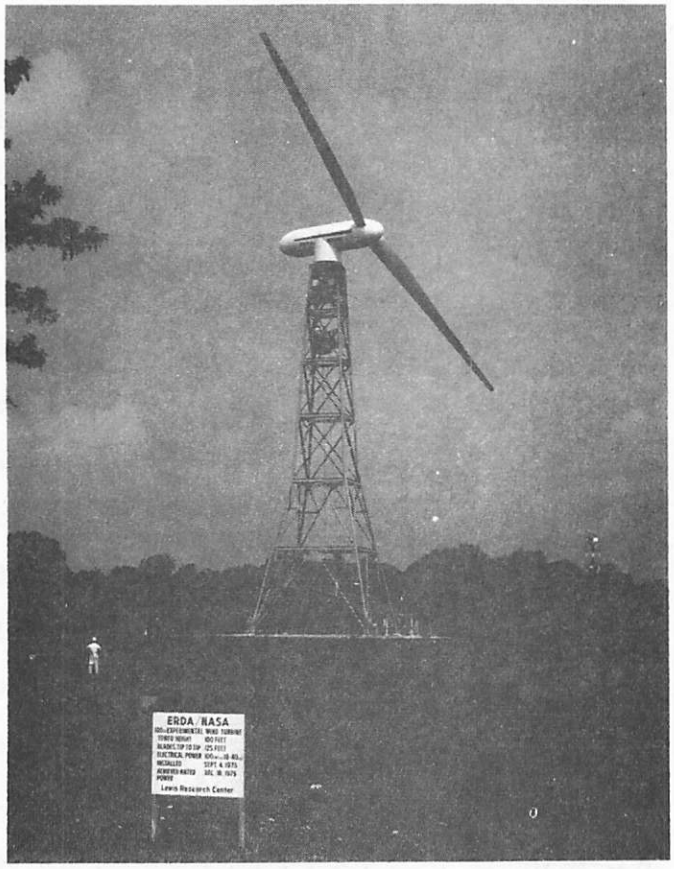

Figure 1. - Mod-0 100-kW wind turbine generator.

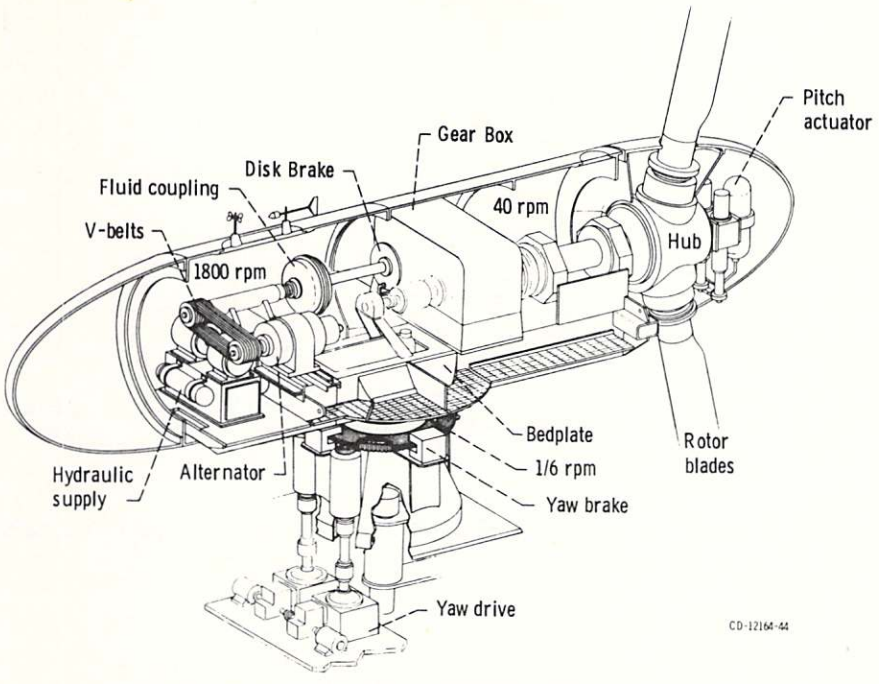

Figure 2. - Mod-0 turbine generator schematic of nacelle interior.

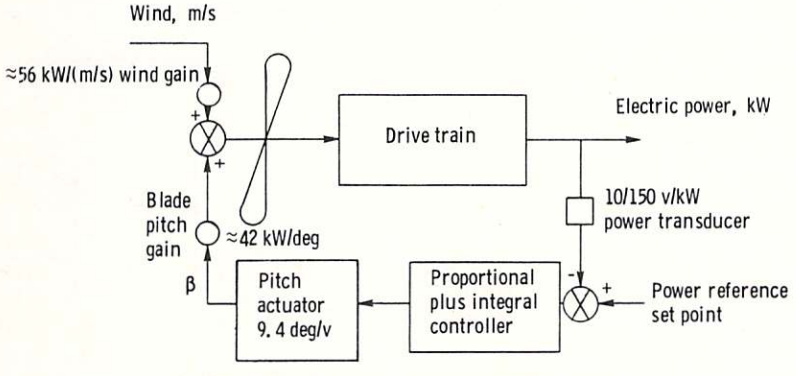

Figure 3. - Block diagram of closed loop power control.

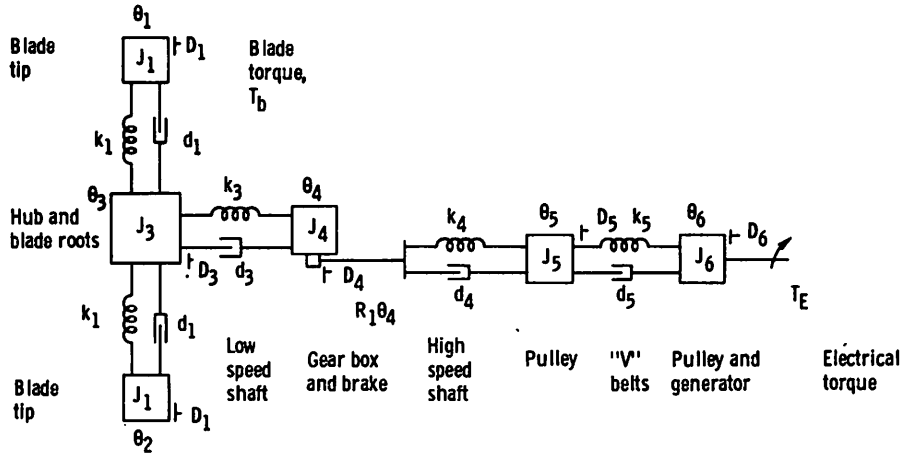

Figure 4. - Block diagram of simplified power train model showing inertial masses and torsional springs and dampers.

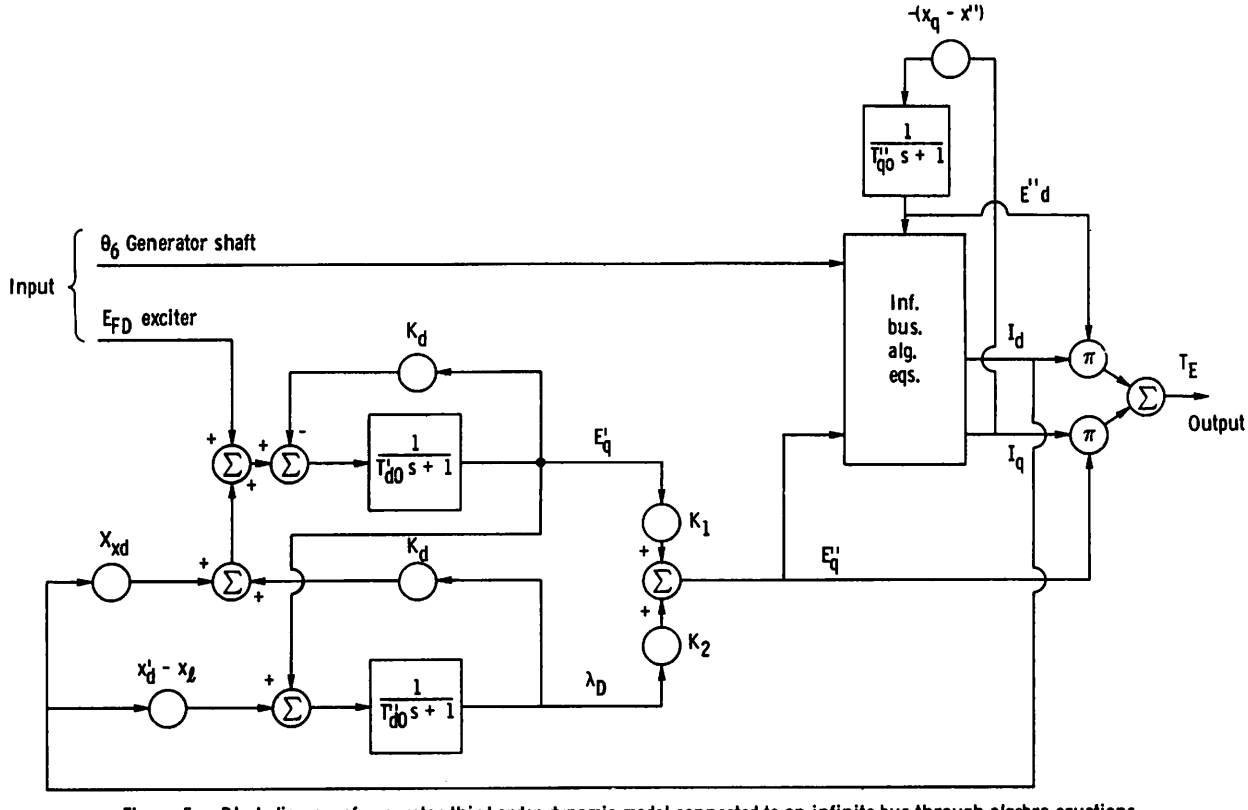

Figure 5. - Block diagram of generator third order dynamic model connected to an infinite bus through algebra equations.

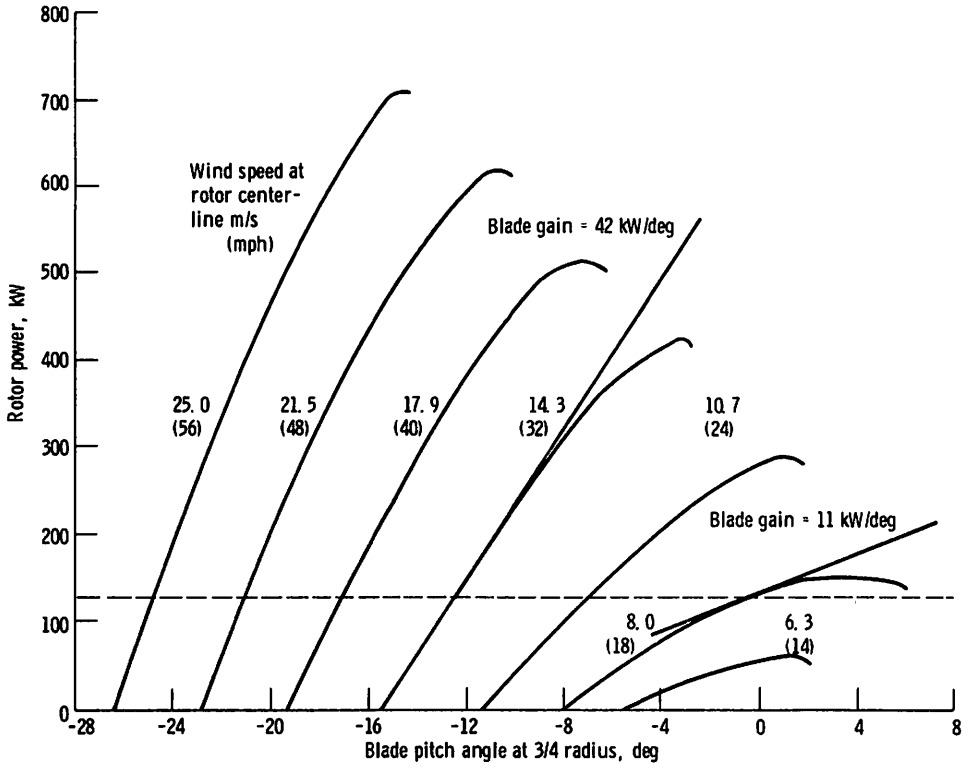

Figure 6. - Rotor performance map. Operating point tangents show blade gain at two wind speeds.

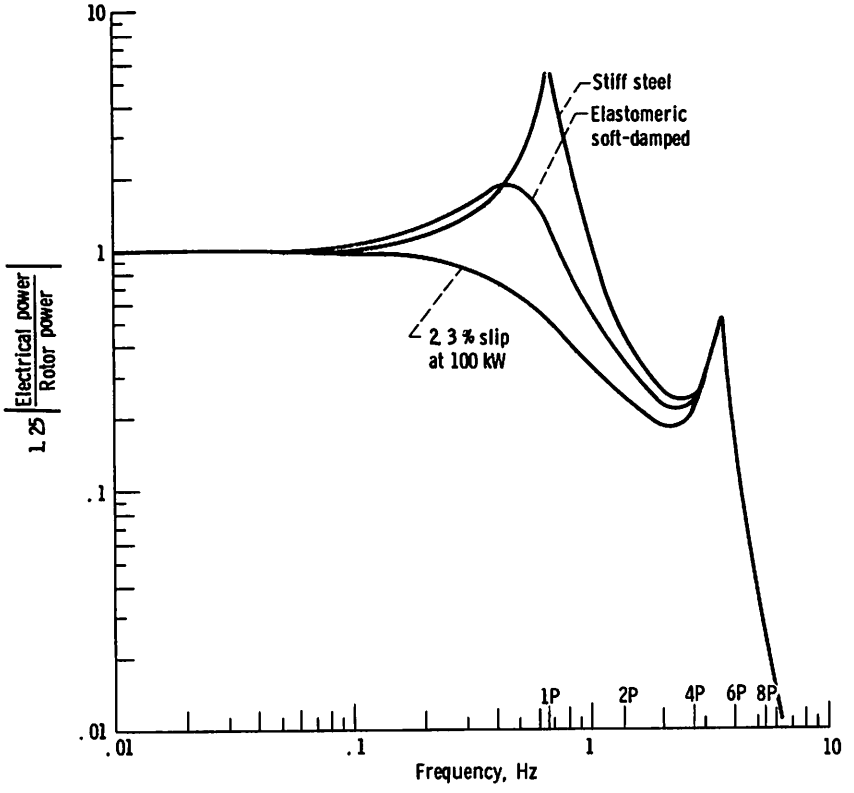

Figure 7. - Power train frequency response magnitude comparisons for three high speed shaft configurations.

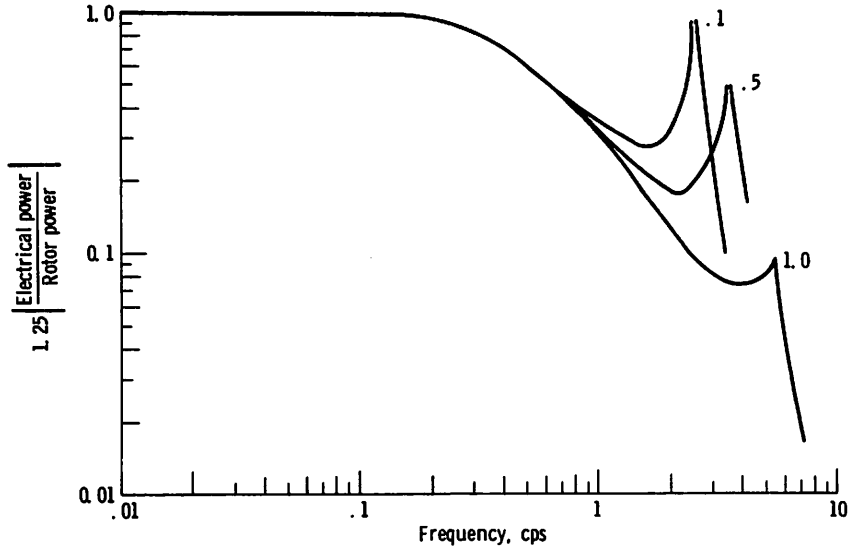

Figure 8. - Sensitivity study showing second mode variation in system frequency response magnitude comparisons for three blade tip masses given as fraction of blade rigid body moment of inertia. Slip coupling in high speed shaft slip rate of 2.3 percent at 100 kW.

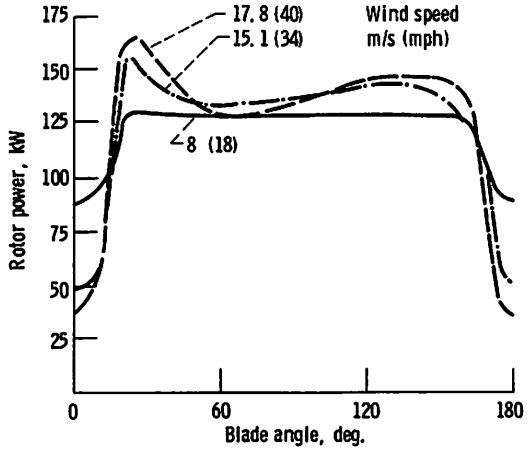

Figure 9. - MOSTAB rotor power versus blade azimuth for one-half revolution. Tower blockage assumed to reduce free stream velocity 28 percent over 30-degree arc. Blades vertical at 0^0 and 180^0.

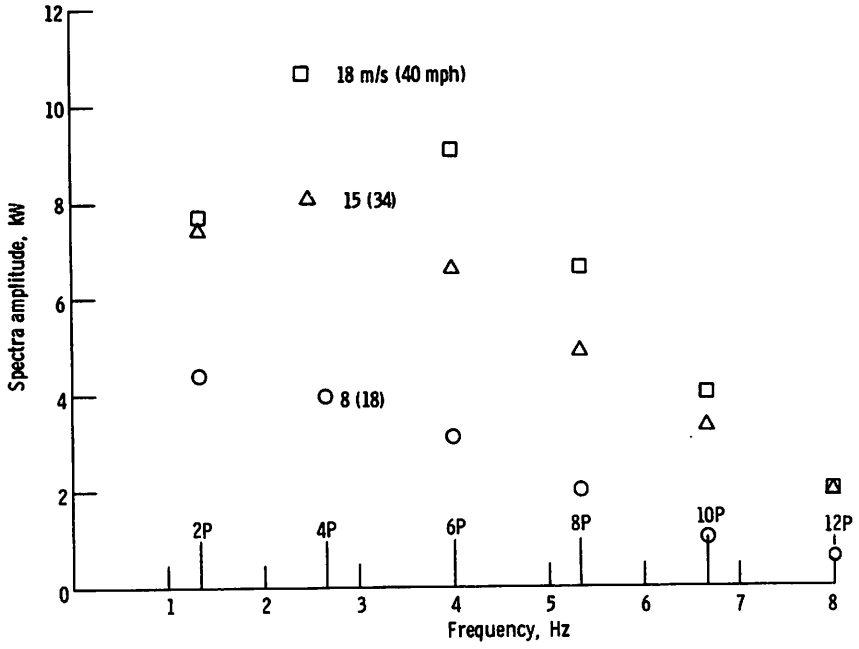

Figure 10. - MOSTAB rotor power zero-to-peak sinusoidal spectral components for three wind speeds.

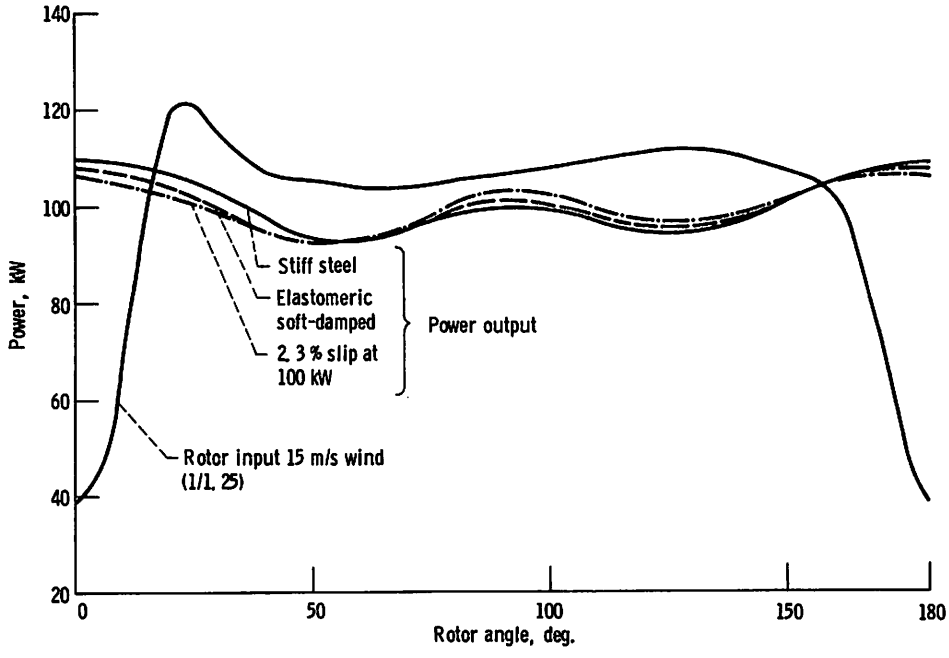

Figure 11. - Time response comparisons of power output with three high speed shaft configurations to MOSTAB rotor power input.

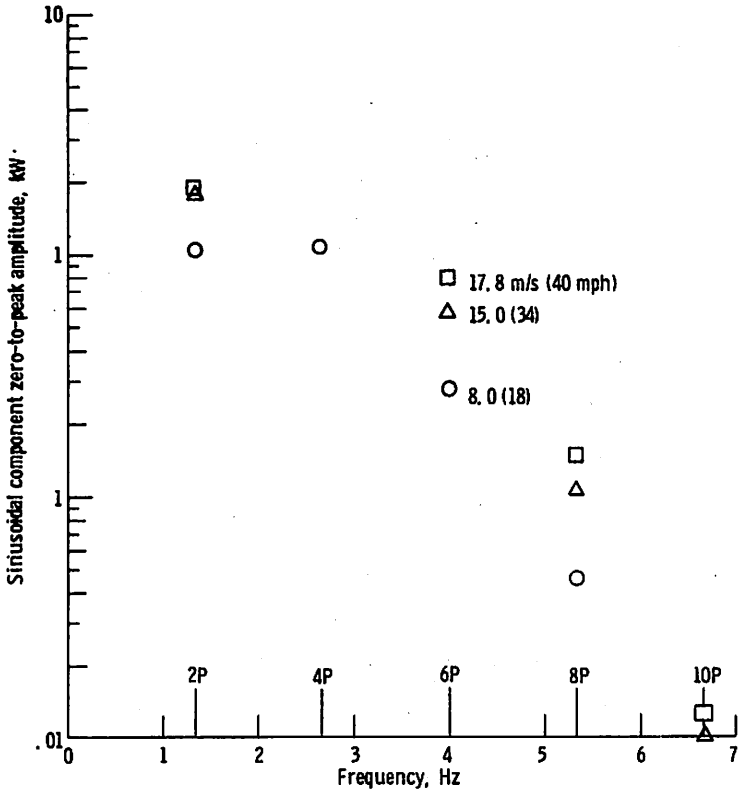

Figure 12 - Calculated spectral content of power output (with 2.3 percent slip at 100 kW in slip coupling) in response to MOSTAB rotor power input for three wind speeds.

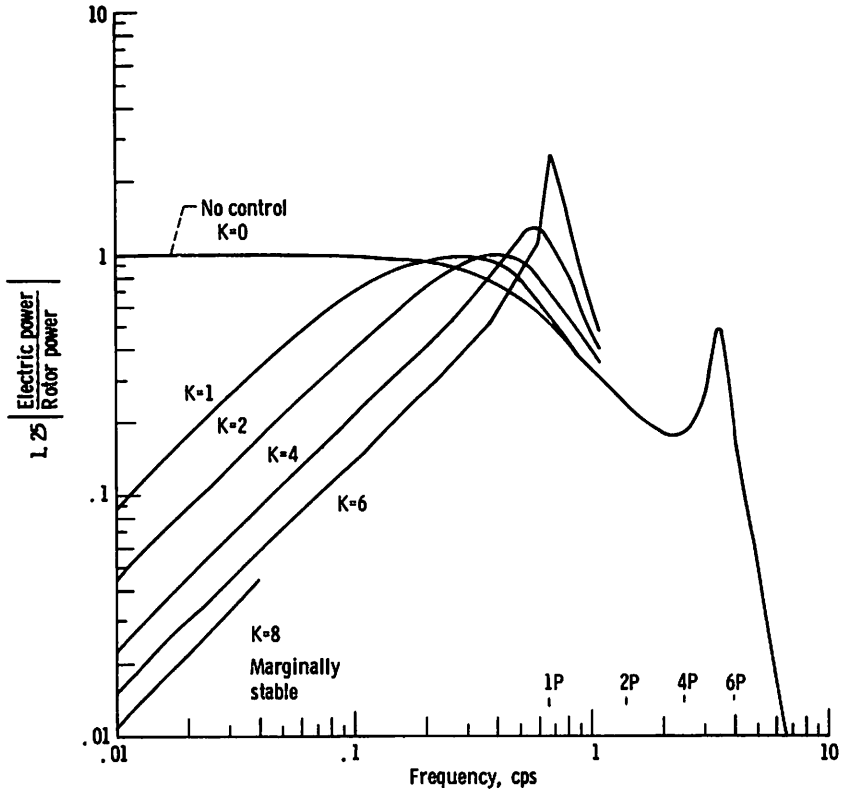

Figure 13. - Closed-loop frequency response magnitude comparisons for various pitch controller gains K with controller 0.027 K[(1/s) + 0.5]. Plant has slip coupling with slip rate of 2.3 percent at 100 kW.

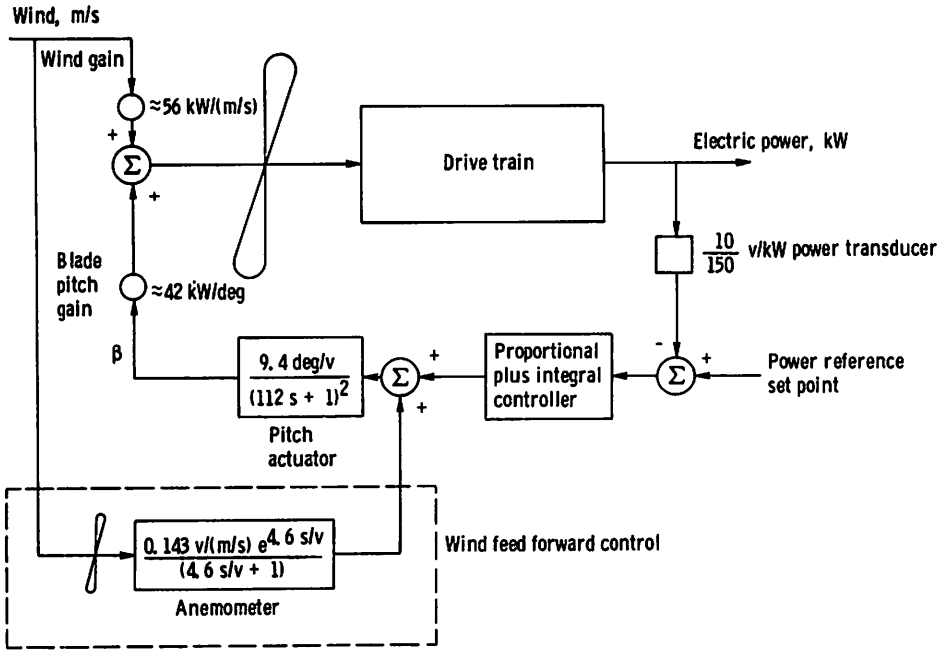

Figure 14. - Block diagram of closed loop power control and wind feed forward control.

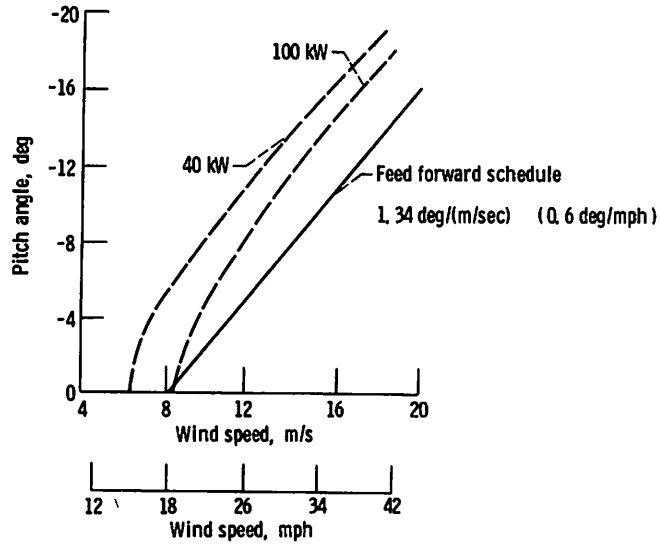

Figure 15. - Derivation of wind feed forward gain as slope of straight line approximation to curves of constant power in pitch angle versus wind speed.

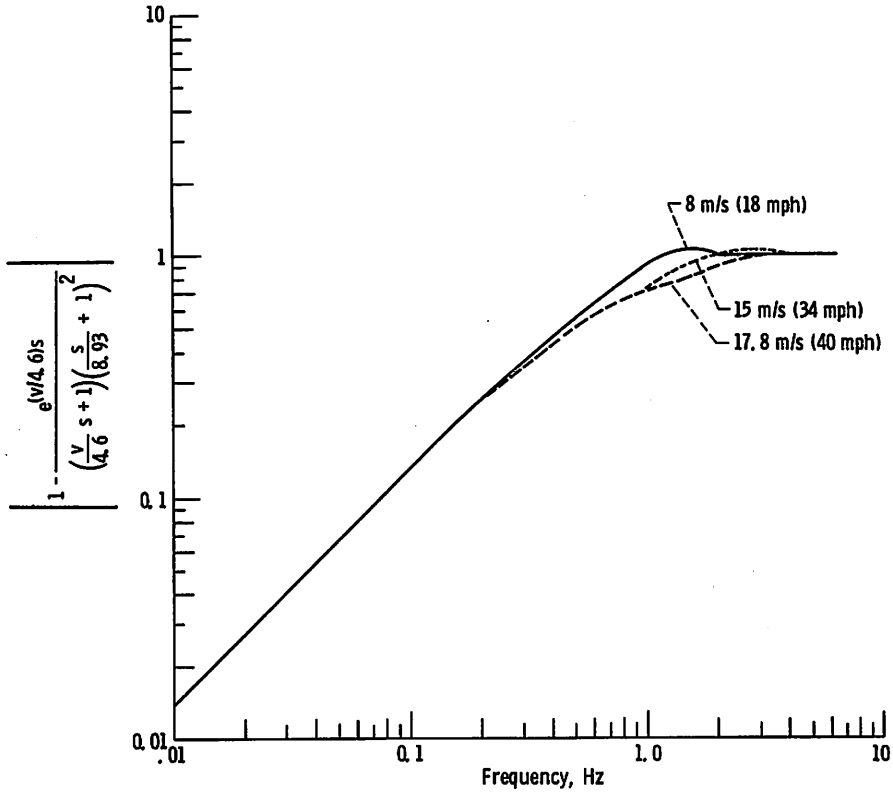

Figure 16. - Frequency response magnitude plot of theoretical attenuation of disturbances due to wind speed changes with wind feed forward control for three wind speeds.

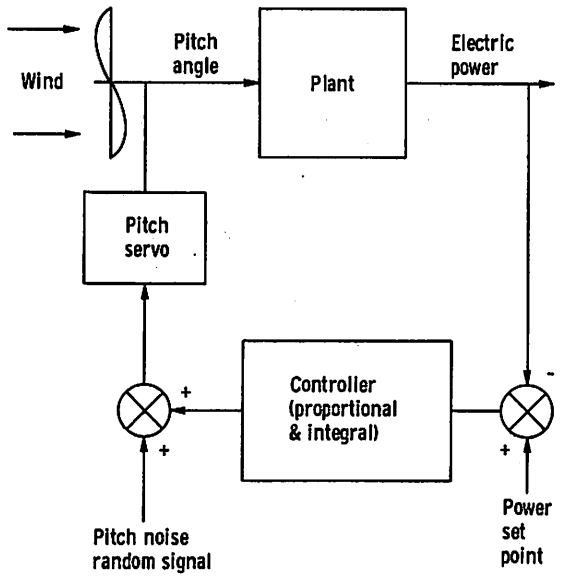

Figure 17. - Block diagram of pitch disturbance test for experimental frequency response.

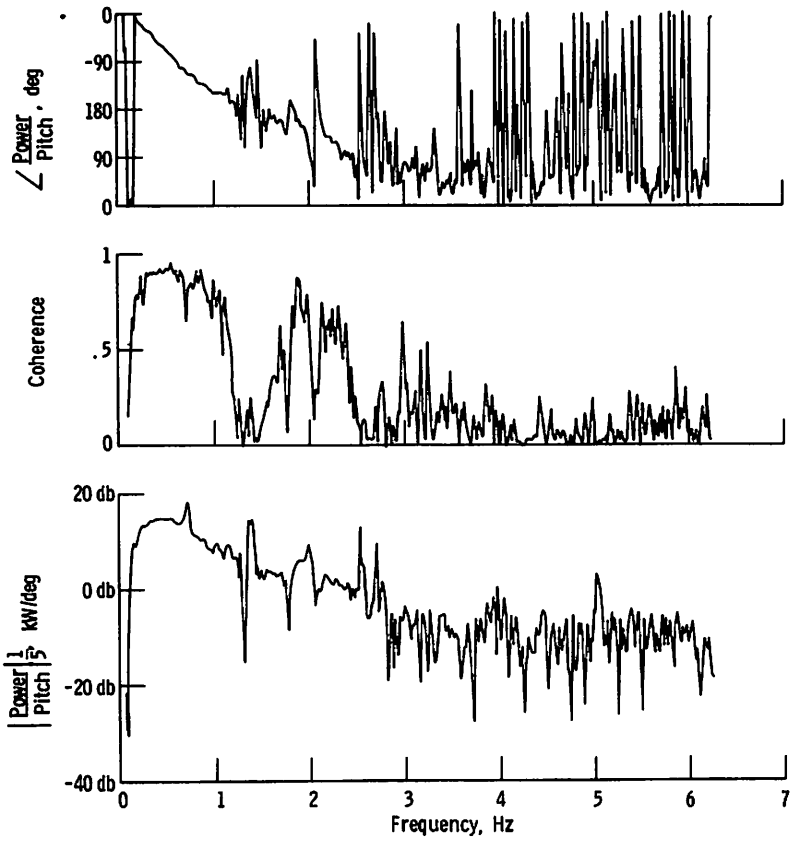

Figure 18. - Experimental phase, coherence, and magnitude frequency response plot of electric power-to-blade pitch angle. 1.05 percent slip at -70 kW. 0 db = 5 kW/deg.

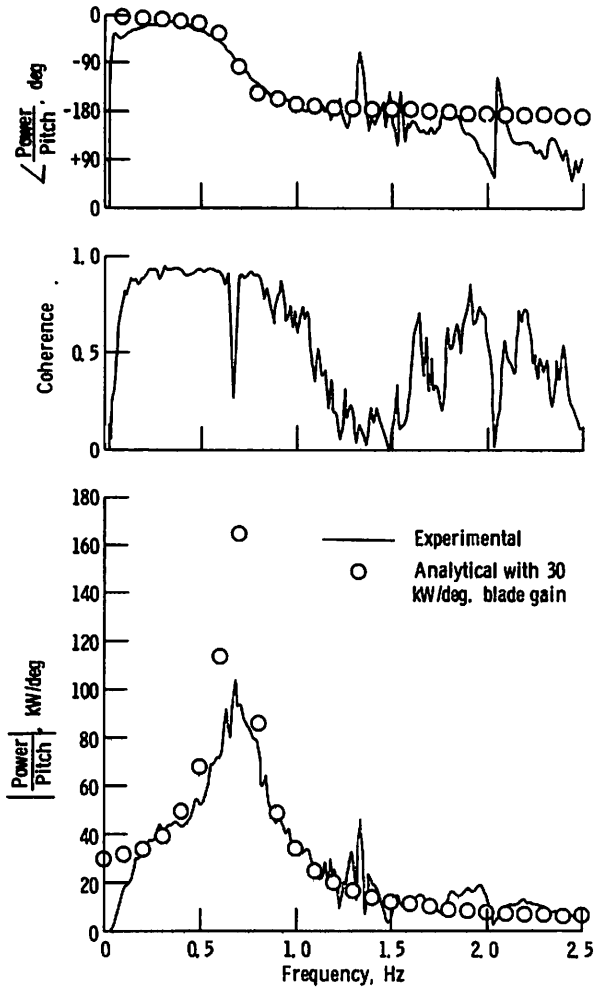

Figure 19. - Transfer function of electric power to blade pitch angle for steel high speed shaft. +70 kW.

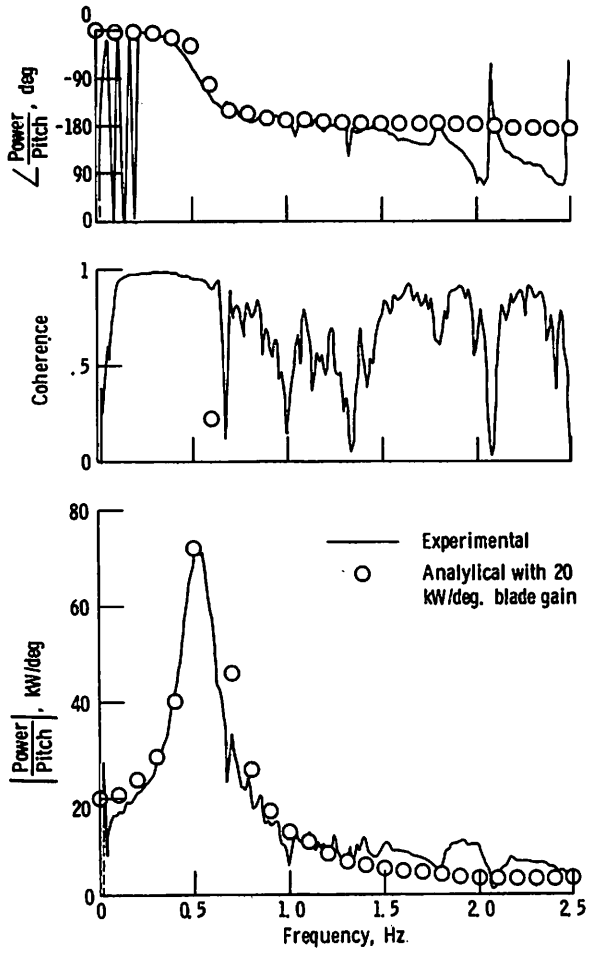

Figure 20. - Transfer function of electric power to blade pitch angle for elastomeric high speed shaft. -50 kW.

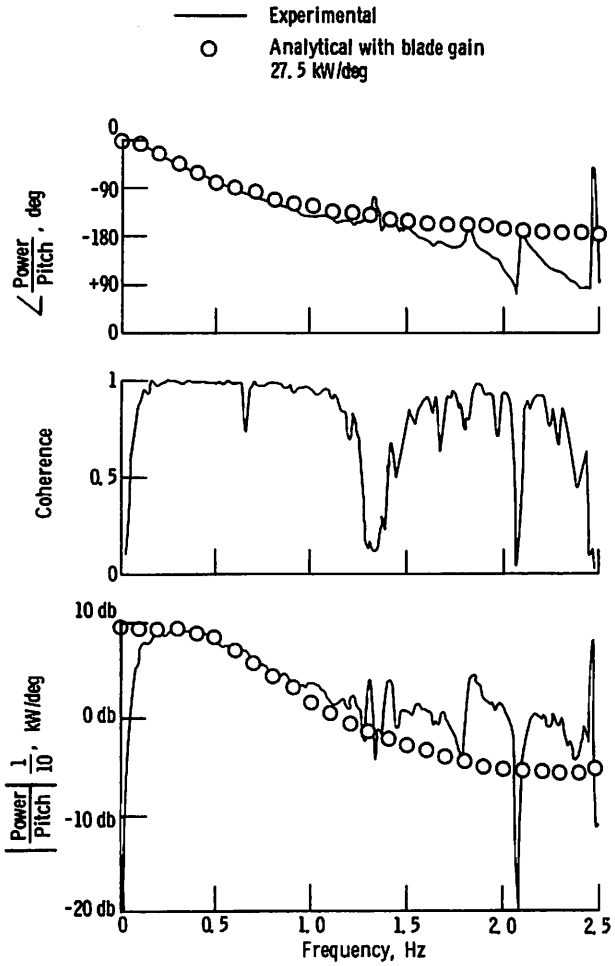

Figure 21. - Frequency response of electric power to blade pitch angle. 1.05 percent slip at -70 kW. 0 db = 10 kW/deg.

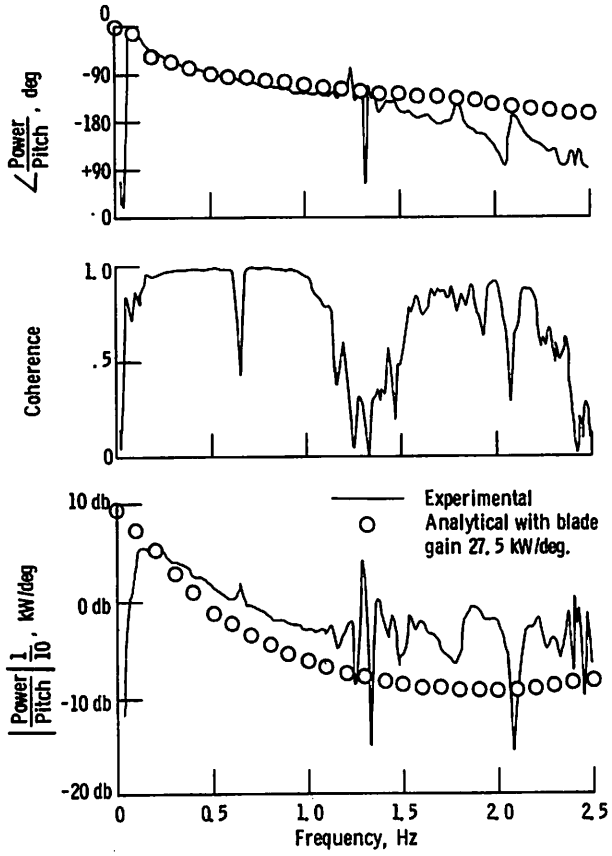

Figure 22. - Frequency response of electric power to blade pitch angle. 3.0 percent slip at -70 kW. 0 db = 10 kW.

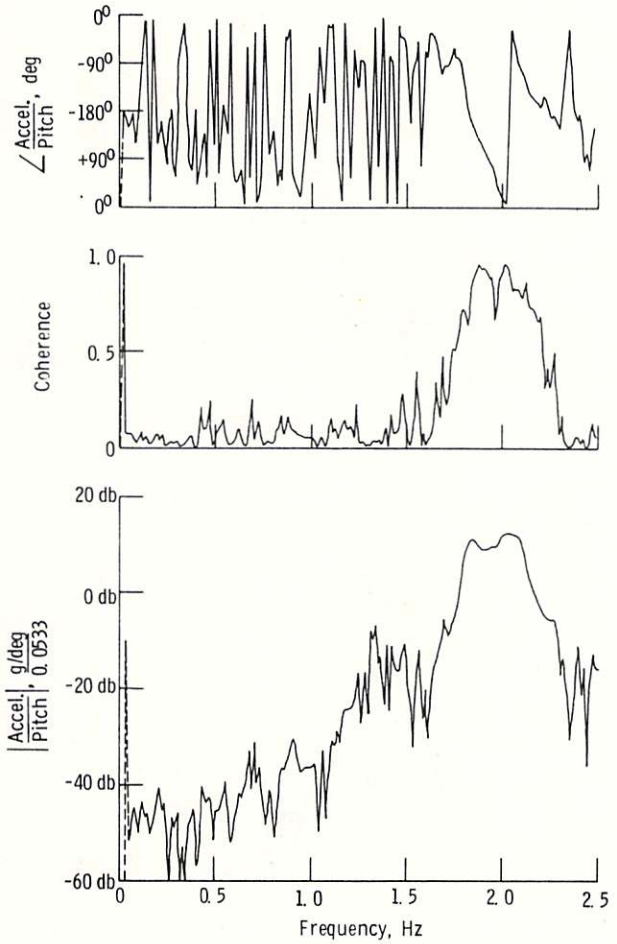

Figure 23. - Transfer function of horizontal acceleration of main bearing to pitch change. 1.05 percent slip at -70 kW. 0 db = .0533 g/deg.

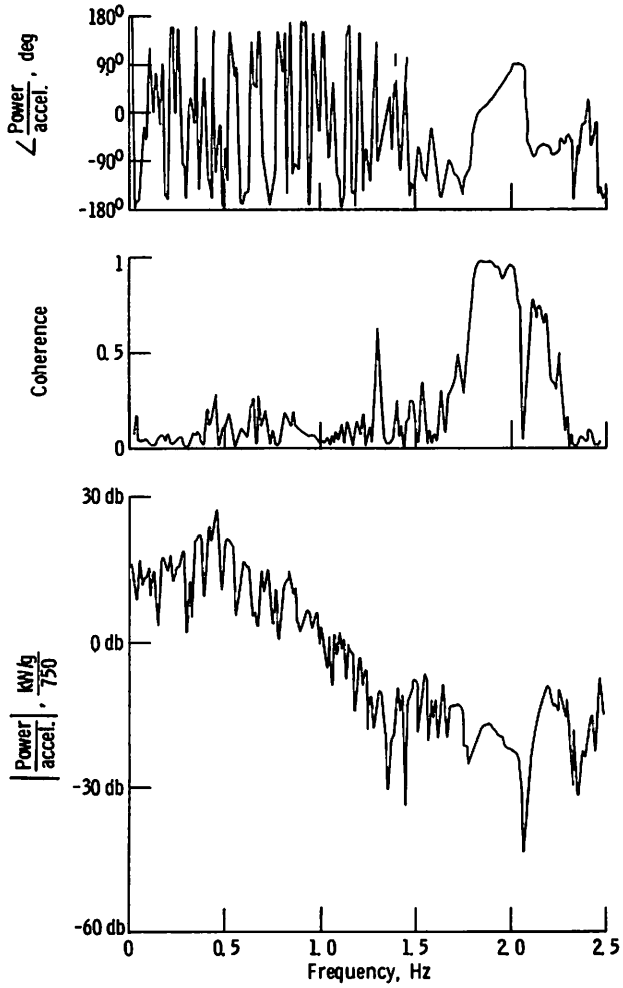

Figure 24. - Transfer function of electric power to horizontal acceleration of main bearing. 1.05 percent slip at -70 kW. 0 db = 750 kW/deg.

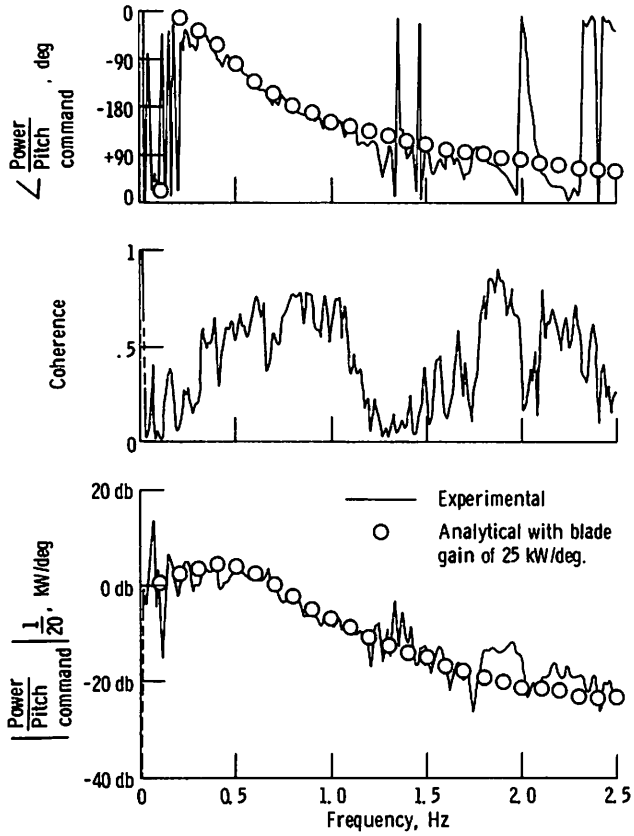

Figure 25. - Transfer function of electric power to blade pitch angle command with nominal control gains of proportional = 0.025 v/v and integral = 0.034 v/v/s. 1.2 percent slip at 50 kW. 0 db = 20 kW/deg.

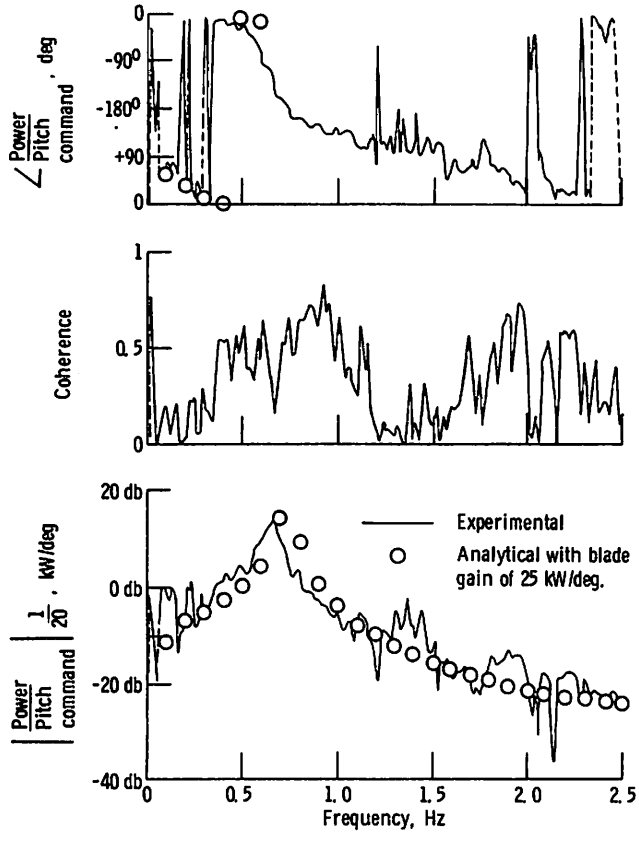

Figure 26. - Transfer function of electric power to blade pitch angle command with high control gains of proportional = 0.137 v/v and integral = 0.186 v/v/s. 0.75 percent slip at +50 kW. 0 db = 20 kW/deg.

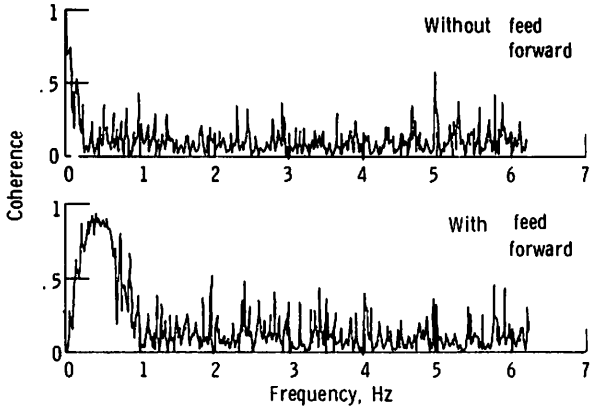

Figure 27. - Coherence between generator power and wind speed without and with feed forward control. Fluid coupling slip of 2.3 percent at 100 kW. Proportional control gain of 0.027 v/v and integral control gain of 0.027 sec.

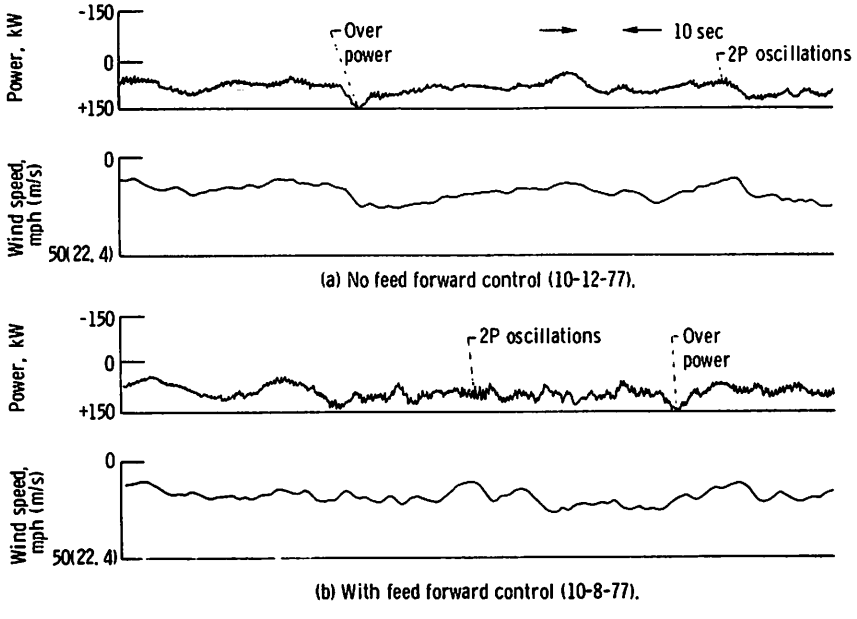

Figure 28. - Time history traces of power and measured wind speed with and without feed forward control. 2.3 percent slip at 100-kW. Proportional control gains of 0.027 v/v and integral control gain of 0.034 sec. Over power and 2P oscillations noted.

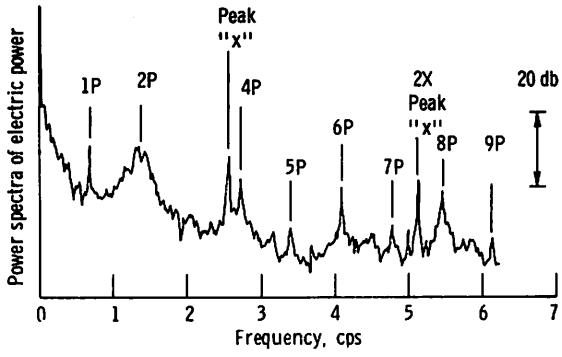

Figure 29. - 12-12-77 Spectra of generator electric power. 2.3 percent at 100-kW. Proportional control gains of 0.027 v/v and integral control gain of 0.034 sec. No wind feed forward control.

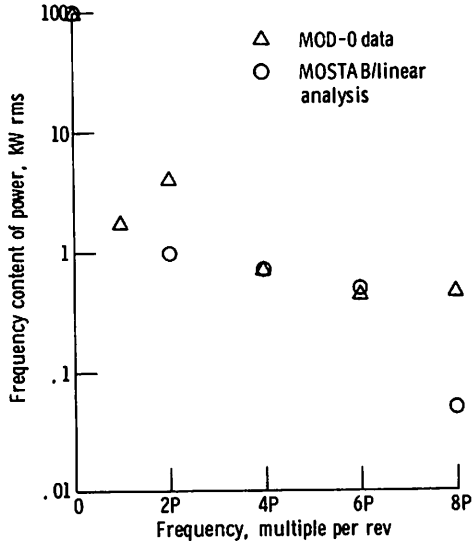

Figure 30. - Comparison of analytically predicted and measured frequency content of peaks in generator power.

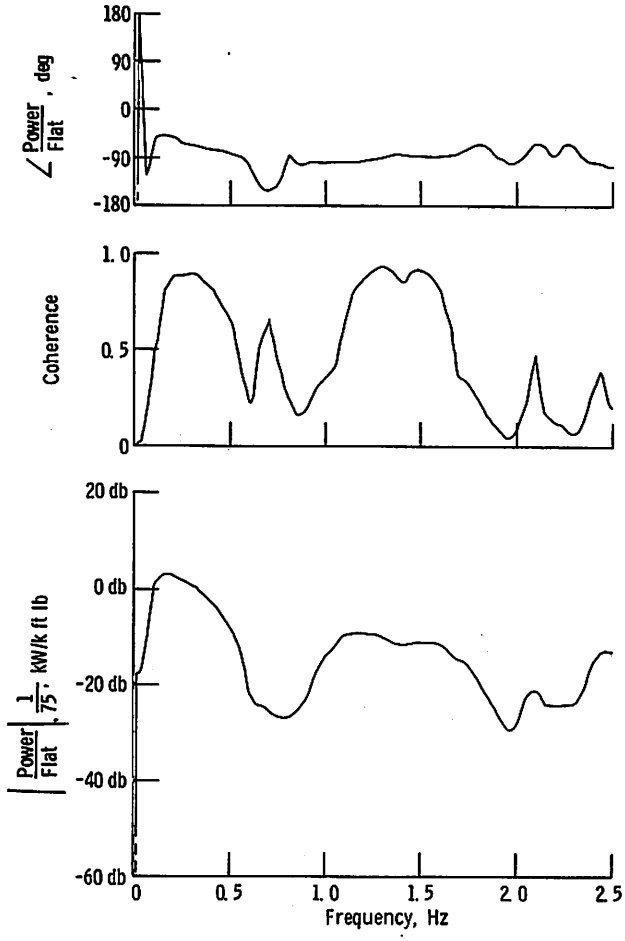

Figure 31. - Transfer function of electric power to blade flatwise bending moment with free yaw and 300 psi brake pressure. 1.5 percent slip at 100 kW. No induced pitch noise. 0 db = 75 kW/k ft lbs.

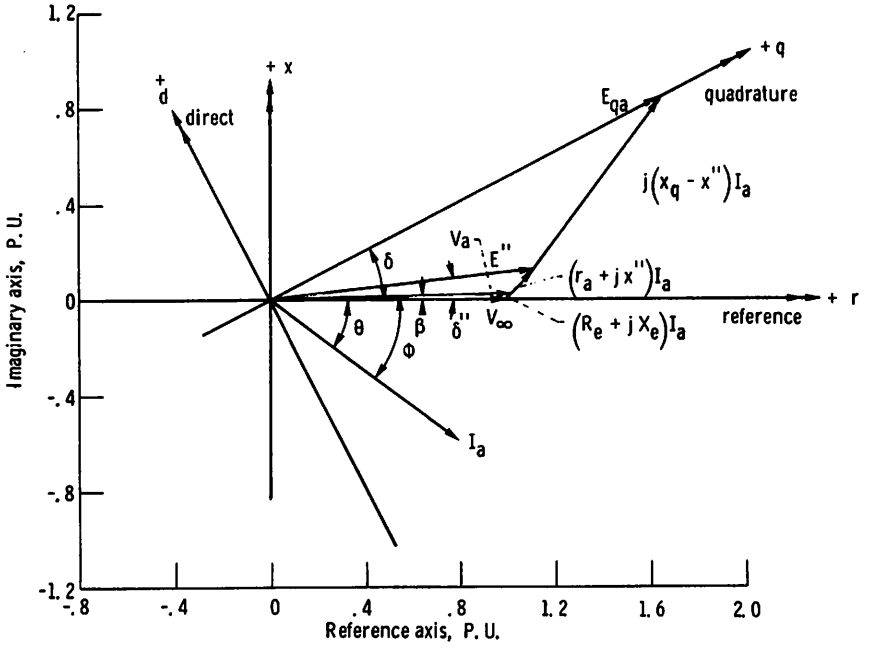

Figure 32. - Phase plot of generator initial conditions for power = 0.8 P.U., power factor = 0.8, and V_∞ bus voltage = 1.0 P.U. Imaginary number j shown as used in FORTRAN computer program with complex arithmetic.

```
C** MOD-0 INITIAL CONDITIONS
      SUBROUTINE CNSTS(Z,POWER)
      IMPLICIT REAL(I-L)
      COMPLEX IA,VA,EPP,EQA
      DIMENSION Z(1)
      COMMON/GEN/K1,K2,KD,XXD,XQXPP,XPDXL,Y,R,X,EFD,TM,K3,DELTA,VINF
      DATA XPPD,XPD,XD,XL/.128,.165,2.210,.05/,XQ,XPPQ/1.064,.193/
      DATA PF,RA/.8,.018/,RE,XE,VBUS/.0046012,.010307,1./
C**  GENERATOR CONSTANTS
 100  XPP=(XPPD+XPPQ)/2.
      XPDXL=XPD-XL
      K1=(XPP-XL)/XPDXL
      K2=1.-K1
      KD=(XD-XPD)*(XPD-XPP)/(XPDXL*XPDXL)
      XXD=(XD-XPD)*(XPP-XL)/XPDXL
      XQXPP=XQ-XPP
      R=RA+RE
      X=XPP+XE
      Y=1./(R*R+X*X)
      VINF=VBUS
C**  FIND IX AS PER PG 161 OF ANDERSON
      TTHEE=TAN(ARCOS(PF))
 200  IR=(POWER-RE*((POWER/(VINF*PF))**2))/VINF
      SQR=SQRT(VINF**2-4.*(-XE+RE*TTHEE)*(-IR*IR*XE+(VINF+RE*IR)*TTHEE*IR))
      IX1=(-VINF+SQR)/(2.*(-XE+RE*TTHEE))
      IX2=(-VINF-SQR)/(2.*(-XE+RE*TTHEE))
      IX=AMIN1(IX1,IX2)
C**  TERMINAL CONDITIONS
      IA=CMPLX(IR,IX)
      VA=VINF+IA*CMPLX(RE,XE)
      EQA=VA+IA*CMPLX(RA,XQ)
      EPP=VA+IA*CMPLX(RA,XPP)
      DELTA=ATAN2(AIMAG(EQA),REAL(EQA))
      DLT  =ATAN2(AIMAG(EPP),REAL(EPP))
      EPPD=-CABS(EPP)*SIN(DELTA-DLT)
      EPPQ=+CABS(EPP)*COS(DELTA-DLT)
      THETA=ATAN2(IX,IR)
      ID=-CABS(IA)*SIN(DELTA-THETA)
      IQ=+CABS(IA)*COS(DELTA-THETA)
C**  GENERATOR STATES
      EPQ=EPPQ-(XPD-XPP)*ID
      ED=EPQ+(XPD-XL)*ID
      EFD=EPQ*(1.+KD)-XXD*ID-KD*ED
      TM=EPPQ*IQ+EPPD*ID
      Z(13)=EPPD
      Z(14)=ED
      Z(15)=EPQ
      Z(16)=TM
C**  LOW SPEED SHAFT STIFFNESS
      K3=0.0494368*SQRT(ABS(TM*125.))
 300  RETURN
      END
```

Figure 33. - Subroutine CNSTS Fortran listing.

```
C**  MOD-0 STATE EQUATIONS
      SUBROUTINE HPRC(Z,F)
      IMPLICIT REAL(I-K)
      DIMENSION Z(1),F(1)
      COMMON/GEN/K1,K2,KD,XXD,XQXPP,XPDXL,Y,R,X,EFD,TM,K3,DELTA,VINF
      DATA K11,K5/.66E8,1.8E5/,R1,CONVRT,D,OMEGAS/45.,5869.,17.9,60./
      DATA J1,J3,J4,J5,J6/.2826E6,.5752E6,25300.,15.,24.2/
      DATA CD1,CD3,CD4,CD5,CD6/.27E5,1.01E3,1.,.62,1.6/,GAIN/7933096./
      DATA D1,D3,D4,D5/3.E5,2.E4,1100.,150./,HZ10/62.83/
      DATA TPPQ0,TPPD0,TPD0/.002,.011,1.042/
C  STIFF HSS:  J4=10214,K4=6.68E5,D4=186,J5=7.57
50    F1=K11*(Z(5)-Z(1))+D1*(Z(6)-Z(2))
      F2=K11*(Z(5)-Z(3))+D1*(Z(6)-Z(4))
      F3=K3*(Z(7)-Z(5))+D3*(Z(8)-Z(6))
      F4=K4*(Z(9)-Z(7)*R1)+D4*(Z(10)-Z(8)*R1)
      F5=K5*(Z(11)-Z(9))+D5*(Z(12)-Z(10))
      F(1)=Z(2)
      F(2)=(F1-CD1*Z(2))/J1+GAIN*Z(17)/J1
      F(3)=Z(4)
      F(4)=(F2-CD1*Z(4))/J1
      F(5)=Z(6)
      F(6)=(-F1-F2+F3-CD3*Z(6))/J3
      F(7)=Z(8)
      F(8)=(-F3+F4*R1-CD4*R1*Z(8))/J4
      F(9)=Z(10)
      F(10)=(-F4+F5-CD5*Z(10))/J5
      F(11)=Z(12)
      DLTA=Z(11)*2.+DELTA
      VINFD=-VINF*SIN(DLTA)
      VINFQ=+VINF*COS(DLTA)
      EPPQ=K1*Z(15)+K2*Z(14)
      ID=Y*(-R*(VINFD-Z(13))+X*(VINFQ-EPPQ))
      IQ=-Y*(X*(VINFD-Z(13))+R*(VINFQ-EPPQ))
      TE=EPPQ*IQ+Z(13)*ID
      F(12)=(-F5+(TM-TE)*CONVRT-CD6*Z(12))/J6
      F(13)=(-Z(13)-XQXPP*IQ)/TPPQ0
      F(14)=(-Z(14)+Z(15)+XPDXL*ID)/TPPD0
      F(15)=(-Z(15)*(1.+KD)+XXD*ID+KD*Z(14)+EFD)/TPD0
      F(16)=HZ10*(TE-Z(16))
      F(17)=Z(18)
      F(18)=-D*Z(18)-OMEGAS*(Z(17)-(Z(19)*R1+(TM-Z(16))*BP))
      F(19)=TM-Z(16)
100   RETURN
      END
```

Figure 34. - Subroutine HPRC Fortran listing.

1. Report No.	2. Government Accession No.	3. Recipient's Catalog No.
NASA TM-78997		

4. Title and Subtitle	5. Report Date
POWER-TRAIN ANALYSIS FOR THE DOE/NASA 100-kW WIND TURBINE GENERATOR	October 1978
	6. Performing Organization Code

7. Author(s)	8. Performing Organization Report No.
Robert C. Seidel, Harold Gold, and Leon M. Wenzel	E-9413
	10. Work Unit No.

9. Performing Organization Name and Address	11. Contract or Grant No.
National Aeronautics and Space Administration Lewis Research Center Cleveland, Ohio 44135	
	13. Type of Report and Period Covered
12. Sponsoring Agency Name and Address	Technical Memorandum
U.S. Department of Energy Division of Distributed Solar Energy Washington, D.C. 20545	14. Sponsoring Agency ~~Code~~ Report No. DOE/NASA/1028-78/19

15. Supplementary Notes

Final report. Prepared under Interagency Agreement E(49-26)-1028.

16. Abstract

Progress in explaining variations of power experienced in the on-line operation of a 100-kW experimental wind turbine-generator is reported. Data are presented that show the oscillations tend to be characteristic of a wind-driven synchronous generator because of low torsional damping in the power train, resonances of its large structure, and excitation by unsteady and non-uniform wind flow. The report includes dynamic analysis of the drive-train torsion, the generator, passive driveline damping, and active pitch control as well as correlation with experimental recordings. The analysis assumes one machine on an infinite bus with constant generator-field excitation.

17. Key Words (Suggested by Author(s))	18. Distribution Statement
Wind turbine Power train Dynamics	Unclassified - unlimited STAR Category 44 DOE Category UC-60

19. Security Classif. (of this report)	20. Security Classif. (of this page)	21. No. of Pages	22. Price*
Unclassified	Unclassified		

* For sale by the National Technical Information Service, Springfield, Virginia 22161